Ollscoil na hÉireann, Corcaigh

National University of Ireland, Cork

Modelling the Role of Hydrogen in Future Energy Systems Aligned with the Paris Climate Agreement

Thesis presented by

Duncan Mathews, BE, ME

https://orcid.org/0000-0003-2564-9642

for the degree of

Doctor of Philosophy

University College Cork

School of Engineering and Architecture

Head of School: Dr. Alan Morrison

Supervisors: Dr. Paul Deane & Prof. Brian P. Ó Gallachóir

2026

Table of Contents

Declaration

This is to certify that the work I am submitting is my own and has not been submitted for another degree, either at University College Cork or elsewhere. All external references and sources are clearly acknowledged and identified within the contents. I have read and understood the regulations of University College Cork concerning plagiarism and intellectual property.

Acknowledgements

First and foremost, I would like to express my deep gratitude to my primary supervisor, Dr. Paul Deane, who patiently reeled me in from my excessive side-quests. If I have absorbed even a small fraction of Paul's kindness through this undertaking, it will have been time well spent even to the exclusion of all else.

I owe significant thanks to Prof. Brian Ó Gallachóir and everyone else at University College Cork who played a role in supporting and administrating my funding from the Irish Research Council. I express my sincere gratitude to the Irish Research Council itself (now Research Ireland) and ElectroRoute for funding this research. I also wish to extend my thanks to Dr. Maarten Brinkerink for his collaboration and facilitation of my building on his work in other directions. To Aisling Murphy for her administrative problem-solving wizardry and to the many others with the Energy Policy and Modelling Group others for their energy, support and camaraderie.

To Energy Exemplar for their support of this work through the provision of an academic PLEXOS license and in particular to Siobhan Short for her kind encouragement and facilitating me in presenting some of this work at Xcelerate Conferences. I also wish to extend my thanks to the anonymous reviewers of my journal paper submissions whose constructive feedback improved this work.

Because no good work arises without entertaining discussions about the benefits of vertically integrated utilities, I especially wish to acknowledge my former ElectroRoute comrades, Brian Larkin, Niamh Troy and Devasanthini Devaraj. You guys are the hammer to my sickle.

To my former ScholarLee Mardyke housemates, the future Dr. Rui Gonçalves and future Dr. Tiago Cortez: The Google Scholar homepage encourages us to "stand on the shoulders of giants", I hope you will make do with standing on the shoulders of a procrastinating dwarf instead. Thank you both for your enthusiastic energy when working next to one another late into the evening.

To my family for enabling my education and putting a roof over my head during the continued housing emergency in Ireland. A special acknowledgment is due to Badger and Moose for their priceless companionship throughout the years, and finally, most importantly to Dr. Rachel Georgel – per autismum ad astra una.

Executive Summary

The Paris Agreement forms the backbone of the global efforts to limit atmospheric warming to well below 2°C above pre-industrial levels thereby reducing the future impact of climate change. Under the Paris Agreement, signatory parties have agreed to submit ambitious Nationally Determined Contributions that detail their plans for significant greenhouse gas emissions reductions and mitigation. In this context, hydrogen has long been championed as a versatile energy vector with the potential to decarbonise a wide range of end uses. However, hydrogen's history is marked by cycles of surging and waning enthusiasm, with periods of high expectation consistently followed by slow deployment and a subsequent loss of confidence. These hype cycles are more than a historical curiosity - they exacerbate uncertainty regarding the scope and timing of hydrogen's future role leading to challenging planning problems for policymakers and system planners.

Integrated assessment and energy system models are helpful tools that can alleviate uncertainty and inform policy around the optimal role of hydrogen in a future decarbonised global energy system. However, these tools exhibit limitations, such as spatio-temporal resolution constraints, that are particularly pertinent to the modelling of Hydrogen. Addressing these limitations and improving the foundational methodologies of these modelling tools is essential to provide the quantitative evidence needed to guide effective policy in this uncertain environment. This thesis develops and applies novel contributions to the modelling of electrolytic hydrogen in future systems aligned with the Paris Agreement. Regarding data inputs for energy systems modelling, this thesis provides a foundational contribution by demonstrating that the low round-trip efficiency of hydrogen-based long-duration energy storage provides an error propagation mechanism that significantly magnifies biases in widely used meteorological datasets for renewable power resource modelling.

Through developing and validating a framework for a high resolution 256 region global electricity and hydrogen model to be soft linked to integrated assessment model scenarios, this thesis provides an "engine" with which to generate coupled hydrogen and electricity models based on future scenarios aligned with the Paris Agreement. This allows the supplementation of low spatio-temporal resolution

integrated assessment models and ensures hydrogen's potential as a storage medium or energy vector is technically represented in the model. This framework is leveraged to provide evidence-based insights on the economic penalties of different policy pathways. Specifically, this work considers a scenario in which hydrogen's "false dawns" results in policymakers being surprised by a significant emergent role for hydrogen in the future. In this case, this thesis quantifies the costs of reactively planning for hydrogen's integration with the power sector versus a proactive, integrated approach. In addition, the cost of forcibly isolating the electrolytic hydrogen sector from the electricity sector versus the proactive, integrated approach is also quantified. The frameworks and analysis presented in this work contribute to addressing key modelling gaps identified in the literature and highlight the costs of sub-optimal policies in the face of uncertainty. Principally, this thesis explores the "Energy System Modelling Trilemma" and its implications for hydrogen in energy systems models. The trilemma is introduced in this thesis to describe the challenges of balancing computational tractability, spatio-temporal resolution and model scope. Overall, it is aimed to facilitate more robust, quantitative debate around hydrogen's role in deep decarbonisation scenarios.

Units And Abbreviations

°C	Degree Celsius
AC	Alternating Current
AEMO	Australian Electricity Market Operator
AR6	6^{th} Assessment Report
BECCS	Bioenergy with Carbon Capture and Storage
CAPEX	Capital Expenditure
CCGT	Combined Cycle Gas Turbine
CCS	Carbon Capture & Storage
CdTe	Cadmium Telluride
COP	Conference of Parties
CRU	Commission for Regulation of Utilities
DC	Direct Current
DNI	Direct Normal Irradiance
EGS	Enhanced Geothermal Systems
EJ	Exajoule
ENTSO-e	European Network of Transmission System Operators for Electricity
ERAA	European Resource Adequacy Assessment
ESM	Energy System Models
ESOM	Energy System Optimization Models
GFS	Global Forecasting System
GHI	Global Horizontal Irradiance
GW	Gigawatt
GWh	Gigawatt-hour
H2	Hydrogen

IAM	Integrated Assessment Model
IEA	International Energy Agency
IPCC	Intergovernmental Panel on Climate Change
IRENA	International Renewable Energy Agency
K	Kelvin
LCOE	Levelized Cost of Energy
LCOH	Levelized Cost of Hydrogen
LCOS	Levelized Cost of Storage
LDES	Long-duration energy storage
LHV	Lower Heating Value
LOHC	Liquid Organic Hydrogen Carriers
m	Meter
MBE	Mean Bias Error
MW	Megawatt
MWac	Megawatt (Alternating Current) Rating
MWh	Megawatt-hour
MWp	Megawatt Peak Rating
OCGT	Open Cycle Gas Turbine
OPEX	Operational Expenditure
P2G2P	Power-to-Gas-to-Power
P2X	Power-to-X
PECD	Pan-European Climate Database
POA	Plane of the Array
PV	Photovoltaic
RED II	Renewable Energy Directive 2
RQ	Research Questions

SAPM	Sandia Array Performance Model
SCADA	Supervisory Control and Data Acquisition
SDES	Short-duration energy storage
SEMO	Single Electricity Market Operator
SSP	Shared Socioeconomic Pathways
SSRD	Shortwave Solar Radiation Downward
SWGDN	Surface Incoming Shortwave Flux
SWGDNCLR	Clear Sky Surface Incoming Shortwave Flux
SWGNT	Surface Net Downward Shortwave Flux
T$2010	Trillion Dollars (Indexed to 2010)
TJ	Terajoule
TW	Terawatt
TWh	Terawatt-hour
UNFCCC	United Nations Framework Convention on Climate Change
VRE	Variable Renewable Energy
W	Watt
WACC	Weighted Average Cost of Capital
WEO	World Energy Outlook
Wp	Watt Peak Rating
Yr	Year

List of Figures

List of Tables

Chapter 1 Introduction

1.1.Background

In 2015 195 parties signed the Paris Agreement at the 21st session of the Conference of the Parties (COP) to the United Nations Framework Convention on Climate Change (UNFCCC). The objective of the agreement is to limit the increase in global average temperature to well below 2°C and to strive to achieve a 1.5°C limit above pre-industrial levels [1]. To achieve the objectives of the Paris Agreement and reduce the impacts of climate change, drastic cuts in greenhouse gas emissions are required. It is on this basis that many countries and regional bodies have set targets for emissions reduction with the term "net zero", meaning that annual anthropogenic greenhouse gas emissions and sinks sum to zero, rising to prominence in climate policy. The Paris Agreement states the need to "achieve a balance between anthropogenic emissions by sources and removals by sinks of greenhouse gases in the second half of this century" [1]. The energy sector accounts for approximately three quarters of global greenhouse gas emissions [2] and, consequently, the sector is a key area for the emissions reductions required to achieve the Paris Agreement's objectives. Owing to its theoretical potential as a clean energy vector, hydrogen has often been referred to as a "Swiss Army knife" of energy system decarbonisation that could technically serve a wide range of different roles [3,4]. At the commencement of the research underpinning this thesis in 2020, interest and enthusiasm for hydrogen, particularly hydrogen produced via electrolysis from renewable electricity sources, was very high. In 2022, the invasion of Ukraine and subsequent geopolitical fallout led to exceptionally high energy commodity prices across the globe [5,6] and the spotlight was shone on the higher energetic losses associated with the use of hydrogen to fulfil energy services relative to other competing technologies [7]. The costly inefficiencies of hydrogen in many use cases have tarnished the idea of hydrogen as a helpful Swiss Army knife for deep energy system decarbonisation and industry sentiment has swung from enthusiastic about hydrogen's prospective role to somewhat pessimistic. This is observed through recent project cancellations a frequent reference to the industry as being in the "trough of disillusionment" [8,9] .

This cycle of surging and waning enthusiasm for hydrogen as an energy technology has been seen before. A major peak in interest in hydrogen as an energy technology occurred during the oil crisis in the 1970s, when the term “Hydrogen Economy” first rose to prominence [10,11]. As we now know, the heralded hydrogen economy did not materialise. The next significant peak in interest in hydrogen occurred in the early 2000s and focussed primarily on hydrogen fuel cell vehicles. Once again however, large scale deployment of hydrogen energy technologies failed to materialise owing to complex infrastructure challenges and advances in battery technology leading to battery electric vehicles out-competing hydrogen fuel cell vehicles [11–13]. Notwithstanding the recent enthusiasm for hydrogen appearing to dissipate with very little hydrogen technology deployed, current research still points to important roles for hydrogen in the hard-to-abate sectors of a fully decarbonised global economy [12,14,15]. Consequently, policymakers and the wider energy industry are faced with an uncertain landscape regarding hydrogen. Wolfram et al. [16] note that key questions remain unanswered: How much hydrogen should be produced, where should it be used, and what might it cost? In answering such questions, it is common to deploy computer models. These models can be of various different archetypes, including integrated assessment models (IAMs), energy system models and power system models among others. [17].

In this thesis, deep decarbonisation scenarios that align with the Paris Agreement are considered. Consequently, IAMs’ ability to implicitly link climate outcomes with the energy system is attractive. However, IAMs face well-documented limitations such as low spatial and temporal resolutions [14,17,18] which are particularly pertinent to hydrogen considering hydrogen technologies’ potential roles as an energy vector or storage medium. These limitations suggest the need for supplementary modelling approaches that can provide higher spatial and temporal resolution analysis of hydrogen system integration. Indeed, Gambhir et al. [18] note that *“IAMs remain critically important in mitigation pathways analysis, because they can encompass a large number of technologies and policies in a consistent framework, but that they should increasingly be supplemented with other models and analytical approaches.”*

The motivation behind this thesis is to contribute to the mitigation of the uncertainty around the future role of hydrogen in deep decarbonisation scenarios aligned with the Paris Agreement and to identify practices or assumptions that may unduly influence the role of hydrogen in model outputs. In doing so, the impacts of weather data inputs for renewable power generation, model spatio-temporal resolution, and the sectoral scope of models are examined. The primary challenge identified is that of the Energy System Modelling Trilemma – balancing the tradeoffs between computational tractability, spatio-temporal resolution and endogeneity or model scope in energy system models. This thesis addresses modelling gaps as identified across the literature by developing a high-resolution global electricity-hydrogen system modelling framework that can supplement IAM analysis by extending the work of [19,20] to include the hydrogen sector. The resulting framework is leveraged to quantify the benefits of proactive integrated electricity-hydrogen planning versus reactive or isolated system approaches, providing evidence-based insights to bridge the disconnect between hydrogen's cyclical hype patterns and its realistic potential contribution to achieving Paris Agreement objectives.

1.2. Thesis Aim

The primary overarching research question of this thesis is simply: how can the present uncertainty around hydrogen's future role in a decarbonised energy system be mitigated? However, this question is general in nature and of sufficient scope that it would command many more complete theses in order to wholly address it. The aim of this work is to contribute in some part to addressing it. In order to do so, four more precise research questions are examined under two parallel strands. This is depicted in figure 1.1 below. The first strand focuses on modelling improvements that can help to quantitatively mitigate the prevalent uncertainty around hydrogen. Central to Strand 1 of this thesis is the concept of the Energy System Modelling Trilemma. In order to maintain consistency of each chapter's content in line with the journal publications on which they are based, the Energy System Modelling Trilemma is not formally introduced until Chapter 4 but the concepts that constitute it are prevalent throughout this thesis. In Strand 2, the methods developed in Strand 1 are applied in exploring the potential consequences of persisting uncertainty and failing to advance the state of the art.

In this thesis, the following research questions (RQs) are explored:

Strand 1

RQ-1: Does the low efficiency common of hydrogen energy pathways provide error propagation mechanisms for bias errors on meteorological reanalysis datasets like MERRA-2 and ERA-5?

RQ-2: How can high-resolution electricity-hydrogen system models supplement IAM analysis for better understanding optimal hydrogen integration pathways?

Strand 2

RQ-3: What is the cost of global delay or hesitation in reactively planning for clean electrolytic hydrogen as opposed to proactively planning for an integrated coupled electricity and hydrogen system?

RQ-4: What is the cost of asserting strict isolation of the electrolytic hydrogen system from the power sector in a scenario where the coupling of the two sectors is prohibited? What does this mean for hydrogen system modelling?

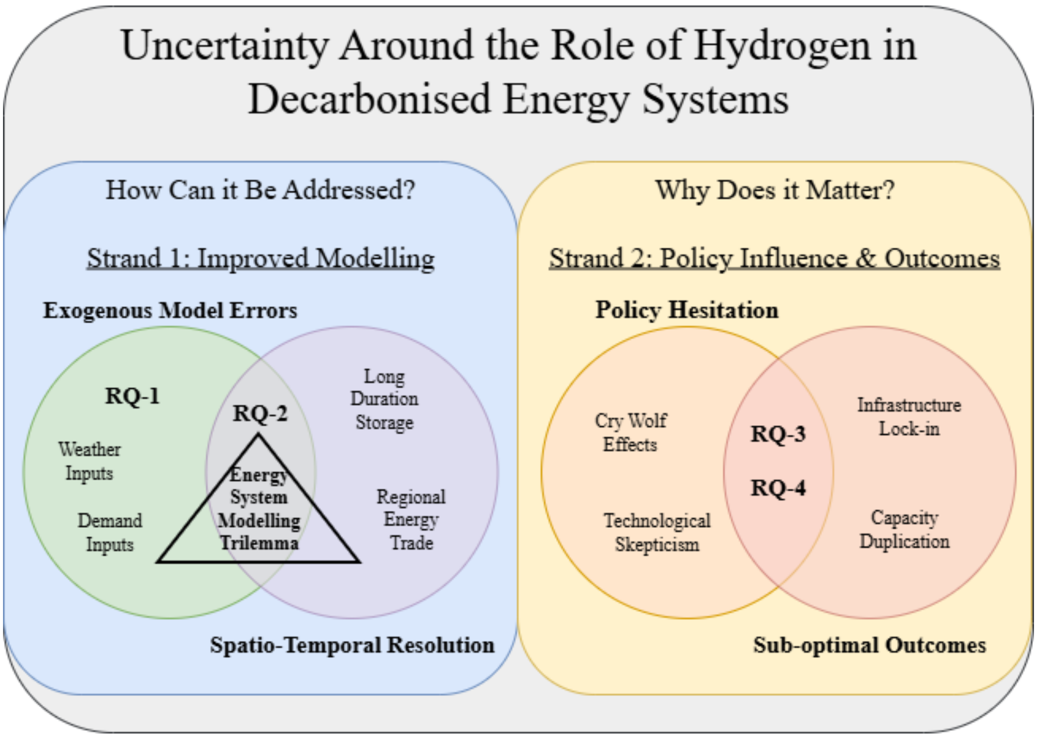

FIGURE 1.1 RESEARCH QUESTIONS BEHIND THIS THESIS

The chapters in this thesis go some way to answering each both through literature review and novel original research though they are not exhaustive. Table 1.1 maps each research question the chapters of this thesis in which they are primarily addressed.

Research Question	Chapter of Thesis
RQ-1	Chapter 2, Chapter 5
RQ-2	Chapter 3, Chapter 5
RQ-3	Chapter 4, Chapter 5
RQ-4	Chapter 4, Chapter 5

TABLE 1.1 CHAPTER-RESEARCH QUESTION MAP

At the outset, these research questions may appear remarkably specific and heterogeneous considering the broad overarching aim: to seek to mitigate the present uncertainty around hydrogen's role in a future decarbonised energy system. However, in this thesis it is considered that tackling the broad uncertainty regarding hydrogen's future role requires the examination of both how models represent hydrogen and how those representations can influence policy-relevant conclusions. To this end, the subsequent chapters frame hydrogen's role through the lens of an Energy System Modelling Trilemma - highlighting how choices around model inputs, resolution, scope and computational tractability influence model outputs and demonstrate how these modelling choices can shape path-dependent infrastructure and policy outcomes.

1.3. Positioning of this Thesis

Regarding the modelling of the role of hydrogen in future decarbonised energy systems, the state of the art is extensively explored throughout Chapters 2, 3 and 4 of this thesis. However, it is pertinent to clearly outline the wider positioning of this thesis and the overarching research gap it seeks to address with respect to the state of the art. As is discussed throughout this work, integrated assessment models (IAMs) exhibit desirable characteristics when it comes to assessing individual technology roles in future energy scenarios. The ability of IAMs to link socio-economic and climate outcomes to the composition of the energy system means that they are widely used to investigate prospective roles of individual technologies. For example, across [21–24] IAMs are deployed to study a range of technologies from carbon capture and storage to nuclear power and biomass. IAMs have also been used to study hydrogen in the energy system [14,17,25]. However, the ambitious scope typical of IAMs is not without trade-offs [17,18,26] and some of these trade-offs pose particular problems to the representation of hydrogen. Typically, IAMs have coarse spatial and/or temporal resolutions to maintain computational tractability, which is problematic for hydrogen, a technology whose prospective roles are often framed in terms of moving energy across space and time. In such cases, hydrogen's roles in storage, flexibility and long-distance trade may not be well captured within IAMs.

It is of course possible to model hydrogen at higher spatial and temporal resolutions with models that are smaller or narrower in scope. Under the taxonomy of hydrogen models proposed in [17], this corresponds to the "Power System Model" archetype. Yet these models also pose trade-offs when modelling the prospective roles of hydrogen. Their narrower scope can yield limited cross-sector consistency outside of the power sector, and final consumptions of electricity and hydrogen are typically exerted exogenously. Naturally, an exogenous assertion of hydrogen demand defeats the utility of such a model when the underlying research question seeks to determine the extent of future hydrogen demand. In contrast, IAMs can endogenously project hydrogen demand as a candidate technology to meet relevant energy service demands such as high-temperature industrial heat.

To mitigate the uncertainty surrounding the future role of hydrogen, a natural course of action is to perform further modelling studies. However, considering the state of the art, one overarching thesis-level research gap emerges as a barrier to this. Of the many tools and model archetypes currently available, there is no single integrated treatment that simultaneously handles (i) endogenous projection of individual technologies' roles to meet energy service demands, (ii) high temporal-resolution with full representation of energy storage, and (iii) high spatial-resolution representation of energy commodity flows and demand. Moreover, as explored in Chapter 2, the modelling of low-efficiency energy technologies such as hydrogen is further complicated by bias error propagation mechanisms and sensitivity to exogenous data quality. Taken together, these issues constitute what is termed in this thesis the "Energy System Modelling Trilemma": the challenge of balancing model scope, spatio-temporal resolution and computational tractability when studying hydrogen's future roles. In short, best-practice, comprehensive approaches to modelling hydrogen in deep decarbonisation scenarios are non-trivial.

To address this gap, the challenges faced when setting out to model the role of hydrogen in decarbonised energy systems are explored across all Chapters in this thesis. Chapter 2 demonstrates how data uncertainty can propagate through low-efficiency storage technologies, Chapter 3 develops a soft-linked global electricity–hydrogen framework that partially resolves the trilemma, and Chapter 4 applies this framework to quantify the cost impacts of different policy and investment pathways. However, even with improved modelling methodologies, uncertainty around hydrogen's future role cannot be eliminated entirely; at best it can be reduced and better characterised. Considering this, the interactions between uncertainty and action are also explored through the lens of the path-dependency of infrastructure choices and hesitant policy. Early choices about pipelines, generation and storage can lock in later configurations and costs. As noted in [17], "Some studies have examined the consequences of having limited foresight, but not for hydrogen systems". In this thesis, the cost impacts of limited foresight are modelled in a context that directly relates to present concerns relating to hydrogen.

In [12,15] it is highlighted that recent research points towards important roles for clean hydrogen, at least in hydrogen's current use-cases, in deep decarbonisation scenarios, yet an implementation gap is observed, with limited deployment of associated infrastructure [15]. In this thesis, the manner in which this uncertain deployment pathway could lead to sub-optimal infrastructure lock-in in the future is explored. Furthermore, the cost implications of restrictive policy regarding sector coupling between hydrogen and the power sector are investigated. In [12] the authors note that, in the short term, using renewable electricity to displace fossil fuel power generation is more effective than using it to produce green hydrogen in terms of emissions abatement. This important finding is reflective of the concerns surrounding upstream emissions impacts of electrolysis in the power sector that motivated the strict operating rules for grid-connected electrolysers under the European Union's Renewable Electricity Directive II (RED II) [27–30]. However, there have been criticisms of this ruleset as being overly restrictive and costly for grid-connected electrolyser installations [27,28]. In this thesis, the uncertainty in the hydrogen sector and the path-dependency of infrastructure investment are therefore also examined through the lens of restricted sector coupling, to determine the potential cost impacts.

In seeking to understand the uncertainty facing the future role of hydrogen, the overall positioning of this thesis therefore explores the two strands introduced in Section 1.2: (1) modelling methods that address the Energy System Modelling Trilemma, and (2) the potential consequences of uncertainty for long-lived infrastructure and policy, including path-dependency and lock-in.

1.4. Contribution of this Thesis

This thesis makes a number of contributions to the field of energy systems modelling concerning the future role of hydrogen in a decarbonized global economy. One central narrative of this thesis is to move the hydrogen energy debate from a historical pattern of "hype and disillusionment" to a model-driven, quantitative assessment of hydrogen’s potential role. However, in order to enable this, there are gaps in existing research and fundamental limitations in existing modelling methodologies that need addressing. This thesis contributes to the bridging of these gaps by developing new and supplementary methodologies, providing actionable recommendations, and quantifying the economic consequences of different policy pathways.

Chapter 2: **Systematic Bias in Reanalysis-Derived Solar Power Profiles & the Potential for Error Propagation in Long Duration Energy Storage Studies**

Chapter 2 investigates bias errors on irradiance variables in two meteorological reanalysis datasets, ERA-5 and MERRA-2, which are commonly used to develop solar power timeseries inputs for energy system modelling studies. Chapter 2 presents a foundational contribution by establishing a specific and previously unexamined mechanism for error propagation through the low round-trip efficiency of hydrogen-based long-duration energy storage that can lead to distorted energy system model outputs. The study's conclusion provides an actionable recommendation for the energy modelling community. Modellers should migrate from MERRA-2 to ERA-5 to improve the integrity of their results, especially in studies involving low-efficiency storage technologies. Moreover, an updated ERA-5 based global solar power timeseries dataset at the PLEXOS World spatial resolution is provided and has already been used in other work [31].

Chapter 3: **A Framework for High Resolution Coupled Global Electricity & Hydrogen Models Based on Integrated Assessment Model Scenarios**

Chapter 3 addresses the "Energy Modelling Trilemma" (which is later introduced in Chapter 4) regarding the coarse spatial and temporal resolution of IAMs and the potential impact on their representation of hydrogen. This chapter extends the 256 region PLEXOS World model of [19] and the soft-linking methodology of [20] to include the hydrogen sector, including the integration of a linearised shipping model to represent global hydrogen derivative trade. The approach is validated through a detailed benchmarking exercise with an integrated assessment model scenario, and the utility of the framework is explored through the lens of hydrogen infrastructure optimisation and future hydrogen commodity trade. The primary contribution of Chapter 3 is in providing an engine that can leverage the macro-level narrative of IAM scenarios while enabling detailed, high-resolution analysis of global hydrogen and electricity systems.

Chapter 4: **The Boy Who Cried Hydrogen: Examining the Cost Impact of Proactive Vs Reactive Policy for Electrolytic Hydrogen.**

In Chapter 4, the Energy Systems Modelling Trilemma that is fundamental to this thesis is formally introduced. In the same manner that the “Energy Trilemma” of sustainability, security and affordability has become a principal concept across the energy sector, it is hoped that the Energy Systems Modelling Trilemma will become an enduring contribution to the field of energy system modelling.

Chapter 4 explores how hydrogen's historical boom-bust cycles may lead to policy hesitation resulting in suboptimal system integration strategies. The contributions therein lie in the transformation of qualitative policy-related risks into quantifiable economic penalties. By comparing a "proactively planned" scenario with a "reactively planned" one this thesis provides contextual figures on the cost of delay if a significant role for hydrogen arises in the future. An additional policy-relevant contribution is made in Chapter 4 wherein the economic cost of a policy-enforced sectoral isolation is estimated. This estimation is made in the context of the debate around the European Union's strict emissions and additionality requirements for electrolytic hydrogen under the Renewable Energy Directive (RED II) and has the potential to inform further debate. From a modelling perspective, this exercise also highlights the potential impacts of modelling the hydrogen sector without modelling interactions with the electricity sector.

Chapter 5: Conclusions & Future Work

The final chapter presents the conclusions arising from this thesis, briefly outlines ongoing work and also makes recommendations for future work that could build on this thesis to further address research and modelling gaps regarding the modelling of hydrogen in energy systems.

1.5. Role of Collaborators

Chapter 2: This chapter is based on a peer-reviewed journal article published in Applied Energy of which I am the lead author. I performed the literature review, undertook the modelling work and wrote the initial draft. Dr. Paul Deane reviewed drafts of the manuscript and provided supervisory guidance. The paper was also revised based on the suggestions of anonymous reviewers on behalf of the Journal.

Chapter 3: This chapter is based on a peer-reviewed journal article published in the International Journal of Hydrogen Energy of which I am the lead author. Dr Maarten Brinkerink built the underlying PLEXOS world model and integrated assessment model soft-link framework which I extended and refactored to include the hydrogen sector. I wrote the initial full draft of the manuscript. Both Dr. Paul Deane and Dr. Maarten Brinkerink reviewed the drafts of the manuscript and Dr. Deane provided overall supervisory guidance. The paper was also revised based on the suggestions of anonymous reviewers on behalf of the Journal.

Chapter 4: This chapter is based on a peer-reviewed journal article published in the International Journal of Hydrogen Energy. I am the lead author of the publication. I performed the underlying modelling work and wrote the chapter in its entirety. Dr. Paul Deane contributed to the study design, concept development, reviewed drafts of the manuscript and provided overall guidance.

1.6. Thesis Outputs

1.6.1. Journal Papers

Mathews D, Ó Gallachóir B, Deane P (2023). Systematic bias in reanalysis-derived solar power profiles & the potential for error propagation in long duration energy storage studies. Applied Energy 336: 120819. doi: 10.1016/j.apenergy.2023.120819

Mathews D, Brinkerink M, Deane P (2025). A framework for high resolution coupled global electricity & hydrogen models based on integrated assessment model scenarios. International Journal of Hydrogen Energy 97: doi: 10.1016/j.ijhydene.2024.11.077

Mathews D, Deane P (2025). The Boy Who Cried Hydrogen: Examining the Cost Impact of Proactive Vs Reactive Policy for Electrolytic Hydrogen. International Journal of Hydrogen Energy 191: doi: 10.1016/j.ijhydene.2025.152350

1.6.2. Peer Review

In parallel to carrying out the research underpinning this thesis I have carried out reviews for:

A submission titled "Integrated Planning of Net-Zero Power Systems for All" to Nature Energy.

A submission titled "Comparing the Role of Long Duration Energy Storage Technologies for Zero-Carbon Electricity Systems" to Sustainable Energy Technologies and Assessments.

1.6.3. Seminar & Workshop Presentations

Mathews D (2023). Modelling Global Trade of Hydrogen and its Derivatives in the Universal Class. Conference presentation as part of Energy Exemplar's Xcelerate Singapore. March 29th, 2023.

Mathews D (2024). Solving For H: Politely Asking a High Resolution Global Coupled Electricity & Hydrogen Model to Solve. Conference presentation as part of Energy Exemplar's Xcelerate Melbourne. March 7th, 2024.

Mathews D (2024). Global Coupled Electricity & Hydrogen Modelling Framework. Webinar presentation as part of the CIGRE C1.50 Working Group. May 17th, 2024.

Mathews D (2024). Energy Commodity Shipping: Modelling Proposals for Consideration by C1.50 WG. Webinar presentation as part of the CIGRE C1.50 Working Group. August 27th, 2024.

1.6.4. Professional Activities

CIGRE C1.50 is a Working Group within CIGRE's Study Committee C1 (Power System Development and Economics) focused on the Global Sustainable Energy System Coupling of Electricity and Hydrogen. In CIGRE C1.50, I am one of two lead modellers and a general participant.

1.6.5. Data Availability

Under the principles of FAIR (findable, accessible, interoperable and reproducible), the simulated PV outputs of this work, the corresponding SCADA data, the PLEXOS model and the required inputs to the work of Chapter 2 are published in a data repository at:

Mathews, Duncan (2022), "Systematic Bias in Reanalysis-Derived Solar Power Profiles & the Potential for Error Propagation in Long Duration Energy Storage Studies Data Repository", Mendeley Data, V1, doi: 10.17632/jf27d9wy3z.1

The PLEXOS model and all required inputs for recreation of results in Chapter 3 are published on github at: https://github.com/DuncanDotPY/MESSAGEix-GLOBIOM-EN-NPi2020-500-Soft-Link

The PLEXOS models and all required inputs for recreation of results in Chapter 4 are published in a data repository at:

Mathews, Duncan; Deane, Paul (2025), “The Boy Who Cried Hydrogen: Examining the Cost Impact of Proactive Vs Reactive Policy for Electrolytic Hydrogen.”, Mendeley Data, V2, doi: 10.17632/pj7sxvmzy2.2

Chapter 2 Systematic Bias in Reanalysis-Derived Solar Power Profiles & the Potential for Error Propagation in Long Duration Energy Storage Studies

Mathews D, Ó Gallachóir B, Deane P (2023). Systematic bias in reanalysis-derived solar power profiles & the potential for error propagation in long duration energy storage studies. Applied Energy 336: 120819. doi: 10.1016/j.apenergy.2023.120819

2.1. Abstract

This study consolidates the literature relating to the systematic bias of model-derived irradiance data and further characterises the same for ERA-5 and MERRA-2, two reanalysis datasets that are frequently used to model renewable power in energy system modelling studies. The bias errors yielded when modelling Solar PV generation for solar parks in Australia and Northern Ireland are compared under the optics of typically clear versus typically cloudy respective climates. Evidence is presented that MERRA-2 exhibits a significant global overestimation bias, contrary to some literature that suggests local variation and underestimation in some locations. Based on the trends identified, it is proposed that overestimation bias proliferates in more cloudy climates for both reanalysis datasets. The implications of such bias for studies involving long-duration energy storage with low round-trip efficiency are investigated and an unfortunate mechanism for error propagation is highlighted. A simplified power system consisting of wind, solar, and energy storage is modelled to demonstrate this effect with solar power profiles derived from metered generation, ERA-5, and MERRA-2. It shown that greater systematic bias of MERRA-2, in combination with the opportunity for error propagation through low-round trip efficiency, has the potential to significantly distort the charging & discharging pattern, overall utilization, and total energy requirement of long duration energy storage infrastructure. ERA-5, despite also exhibiting systematic bias, was better able to reproduce the simulated results of the metered generation scenario. Finally, it is recommended that energy modellers using MERRA-2 data to simulate solar PV outputs should now migrate to ERA-5 if reanalysis data is to be used.

2.2. Introduction

Reanalysis datasets, such as MERRA-2 [32] and ERA-5 [33], are increasingly used to model meteorologically driven renewable power sources in energy system modelling studies. Pfenninger & Staffell [34,35] provide the backbone to the renewables.ninja tool which employs the MERRA-2 dataset (amongst others) and allows the user to simulate wind and solar power timeseries data across the globe. The Open Power System Data platform [36] provides an interface for downloading selected MERRA-2 data in addition to country-level MERRA-2 derived solar PV & Wind capacity factor timeseries from the renewables.ninja tool along with other useful energy-system related data. With regards to the modelling of solar energy resources specifically, satellite data is also widely used. The National Solar Radiation Database (NSRDB) [37] is generally considered the “gold standard” of freely available resources for modelling Solar PV across its domain and has been reasonably well validated [37–39]. The NSRDB irradiance variables are derived principally from satellite data but also incorporates MERRA-2 reanalysis aerosol data. Pfenninger & Staffell [34] also explore the use of the satellite-derived SARAH dataset [40,41] for modelling solar PV timeseries data. However, both SARAH and the NSRDB are limited in their geographic domains, as is typical of any one satellite derived irradiance dataset. In this instance, the global domain common of reanalysis datasets offers a particular advantage. For example, Brinkerink et al. [42] use the renewables.ninja framework to model worldwide wind and solar power profiles with MERRA-2 data for input into a detailed global electricity model. Ruggles & Caldeira [43] also leverage MERRA-2 data to simulate both wind and solar PV power profiles for electricity systems in France and different regions across the U.S.

A second attractive feature of reanalysis datasets is the multitude of meteorological variables they offer. This allows for co-examination of different renewable power drivers and their relationships. Bett & Thornton [44] examined the climatological relationships between wind and solar power supply in Britain using the ERA-interim reanalysis dataset [45,46]. Based on their analysis, the authors find an optimal ratio of wind and solar nameplate capacity that minimises seasonal balancing requirements with respect to an arbitrary static load. Strikingly, this is found to consist of a mix consisting of approximately 70% solar and 30% wind capacity.

Similarly, Jurasz et al. [47] used the ERA-5 reanalysis to examine the complementarity of wind and solar energy in Poland and present an analysis of periods of "drought" in renewable power production. As in Bett & Thornton [44] the authors find a general complementarity between the two power sources but note spatial variability in the strength of this trend.

As exhibited by the sample of works discussed above, reanalysis datasets can be seen to be enabling of important work that examines topics which are vital to the energy transition and the agile integration of variable renewable power sources into power grids globally. However, reanalysis datasets are not without their limitations. The occurrence of significant biases in solar radiation data derived from numerical weather and earth system models is well documented across the literature. Xie et al. [48] remark "a dramatic and unexpected bias is found in the routine computation of DNI" (Direct Normal Irradiance). Mathieson et al. [49] found significant positive bias in the forecast global horizontal irradiance (GHI) from both the Global Forecasting System (GFS) and the North American Mesoscale Forecast System (NAM) over the continental United States. Sianturi et al. [50] compared both the ERA-5 and MERRA-2 reanalysis datasets to radiation observations made on the ground over Indonesia. The authors find a systematic overestimation of surface incoming shortwave radiation by ERA-5 and a systematic underestimation by MERRA-2. However, we note that in conducting their analysis the authors have compared the Shortwave Solar Radiation Downward (SSRD) variable of ERA-5 and the Surface Net Downward Shortwave Flux (SWGNT) from the MERRA-2 dataset to the ground observations. It is suggested that the Surface Incoming Shortwave Flux (SWGDN) from the MERRA-2 dataset would be a more appropriate comparison. In this case it is hypothesised that the MERRA-2 data would also yield a significantly positive bias contrary to the authors' analysis. Khatibi et al. [51] make a similar observation with regards to the use of the SWGNT variable in [50], however they explain that SWGNT is "not global irradiance, but the sum of direct and diffuse irradiance". For clarity, it should be noted that global irradiance is itself the sum of direct and diffuse incoming irradiance. The SWGNT variable is, more specifically, the sum of all incoming sources of shortwave radiation less the sum of the outgoing shortwave radiation. Hence, it is the net downward shortwave radiation (such that radiation incoming towards the surface assumes the positive sign convention)[52,53]. The same apparent conflation between the net downward shortwave radiation flux and the surface incoming shortwave radiation flux of the MERRA-2 dataset is made in Urraca et al. [54] wherein an analysis of the performance of several reanalysis datasets and the SARAH satellite dataset is presented through comparison to ground observations of global irradiance. This is concerning given that the authors found the MERRA-2 dataset exhibits a strong positive bias. If this strong positive bias has indeed been derived of MERRA-2's net downward solar radiation variable, it is likely that the actual bias when analysing the surface incoming radiation is significantly worse. For context, one might expect the SWGDN variable to be about 33% greater than the SWGNT variable on average when considering a surface albedo of approximately 0.25. Encouragingly however, the authors also found that the ERA-5 dataset significantly reduced the quality gap between reanalysis data and satellite data with ERA-5 exhibiting a similar bias to the satellite data over less cloudy inland regions. This is an interesting observation and is similarly reflected in the findings of [50] who noted a strong variation in the overall bias on a basis of the observation-estimated clearness index whereby the reanalysis datasets had a lesser tendency to overestimate global surface irradiance when the actual conditions were clear. Clarke et al. [55]also compared ERA-5 and MERRA-2 data to weather observations. The authors found a tendency for overestimation bias on incident shortwave radiation across both datasets which was more significant in the case of MERRA-2. In agreement with [50], the authors also highlight a bias trend that varies with cloudiness.

Polo et al. [56] give a useful summary of the need to correct model-derived irradiances for systematic bias considering both satellite and reanalysis datasets. Indeed, Pfenninger & Staffell [34] highlight the same need for bias correction of model-derived irradiance under the context of modelling solar PV outputs. Notably, the authors find multiplicative scaling factors to correct the average capacity factor biases observed when modelling PV outputs using the MERRA-2 and SARAH datasets. Li et al. [57] similarly find multiplicative corrective factors for MERRA-2 when modelling solar PV in China, however these are applied to MERRA-2 GHI data based on observed bias at meteorological stations and geospatially interpolated to account for geographic variation. It is also necessary to consider the extent to which a static correction factor truly improves the overall model if the model biases are dynamic in nature and vary strongly with the cloudiness or clearness at any one time. For example, if a significant monthly trend in cloud cover is typical at any one location or area, the overall profile of monthly modelled generation could be distorted, which may have implications for energy system studies involving solar power generation.

Recently, the role of storage and hydrogen has attracted attention in future-looking studies of renewable power systems, in which these reanalysis datasets are commonly used. Hydrogen and its derivatives have been proposed as one possible solution for long-duration energy storage. Conceptually speaking, hydrogen storage could allow for a 100% renewable power-grid through the conversion of renewable electricity to hydrogen (or a derivative) during periods of high renewable generation, and reconversion to electricity during periods of 'drought' in renewable production. Similar power system pathways, with the addition of other technologies such as pumped-hydro storage, are explored in the likes of Jacobsen et al. [58], Steinke et al. [59], Colbertaldo et al. [60] and Maruf [61] for example. In discussing hydrogen or other potential long duration storage technologies, it is important to consider the concept of round-trip efficiency. In the conversion of electricity into hydrogen and the subsequent generation of electricity using the stored hydrogen, the conversion processes incur significant losses due to the limited efficiencies of the fundamental processes involved. These losses lead to a low 'round-trip efficiency', the percentage of the input power consumed in filling the storage that is recoverable later when the storage discharges. For long-duration hydrogen storage, the round-trip efficiency depends on the precise technologies involved, but a value of 30% could be considered typical [62,63]. Consequently, where an overestimation bias on a renewable power profile leads to a corresponding underestimation in the required delivery of stored power, the underestimation on the total energy requirement of the scenario will be even larger. More simply, if more electrical energy must be delivered by the long duration storage than originally estimated, it follows that additional energy must also be lost in the conversion processes. This is true for technologies of any round-trip efficiency (less than 100%) but is far more pronounced for those of low round-trip efficiencies where a greater proportion of input energy is lost in a storage cycle.

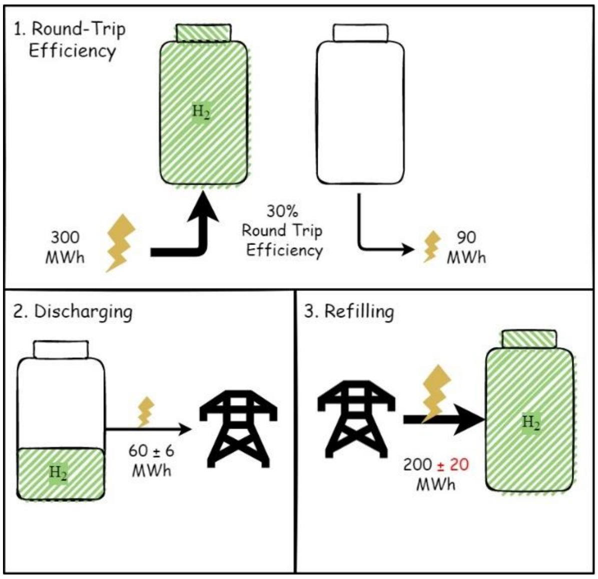

FIGURE 2.1 ERROR PROPAGATION THROUGH AN ENERGY STORAGE CYCLE

To illustrate this, consider figure 2.1. Part 1 is a simple diagrammatic representation of a hypothetical hydrogen-based long duration energy storage unit with a round-trip efficiency of 30% as per above. Consider the scenario where, due to a shortfall of available renewable power during a given period, it is modelled that 60 MWh of electrical energy must be discharged from the (initially full) storage unit in order to meet demand. Consider further that, due to error associated with the renewable power profiles, the error on the shortfall of available renewable power during the period in question is arbitrarily ± 6MWh. This is represented by part 2 of figure 2.1 where 60 ± 6 MWh is discharged from the storage unit to the grid. Subsequently, as per part 3, 200 ± 20 MWh of electrical energy would be required to fully refill the storage unit. In this case, the original error of 6 MWh has propagated to become an error of 20 MWh on the total energy requirement due to losses in the storage cycle. To this end, it is hypothesized that the bias that is documented to arise on reanalysis-derived renewable power profiles could undergo significant propagation in certain energy systems modelling scenarios.

Kies et al. [64] examined the implications that different model-derived renewable generation datasets might have for European power system modelling studies. It was found that differences in levelized cost of 10% could occur and the choice of dataset could therefore impact policy advice. In the context of energy system planning and optimisation models, this raises important questions. Indeed, the European Network of Transmission System Operators for Electricity (ENTSO-e) leverage reanalysis data for the Pan-European Climate Database (PECD) [65] which is used for loss of load expectation calculations in the European Resource Adequacy Assessment (ERAA) studies [66]. With the European Commission's Hydrogen Strategy [67] targeting 40 GW of electrolysers in Europe by 2030, future studies incorporating this growth in Power-to-X (P2X) technology could potentially experience amplified error propagation that could distort important metrics, such as loss of load expectation. Between the documented bias on reanalysis-derived solar irradiance and the rapid growth in European solar PV capacity, it is considered that there is particular potential for solar PV to exacerbate this.

In the current work, an approach like that of Pfenninger & Staffell [34] is taken in that the output of multiple PV installations is simulated using hourly reanalysis data and compared to actual generation data. In doing so, the expected typical bias when modelling PV output is quantified, rather than that of the reanalysis irradiance variables through comparison to ground-based measurements. Given the documentation of significant bias on model-derived irradiances across the literature, it is hypothesized that these are the primary driver of bias in the subsequent modelling of PV output using such data. Nonetheless, it is also likely that the intermediate modelling work in estimating PV output from the meteorological inputs introduces some bias. In any case, it is deemed useful to quantify the net resulting biases when good or best practice is followed in simulating PV output using reanalysis datasets, given the increasing number of studies that do so. In this paper, we further examine the extent to which the occurrence of bias is dynamic. Rather than examining the net annual or indeed multi-annual bias that arises, a closer look is taken at intra-annual variation in bias as well as the variation in bias with the modelled clearness index as per each reanalysis dataset. Each of these aspects are characterised across two different locations representing different climates. In rather loose meteorological terms, these two locations, Northern Ireland and Australia, represent a distinctly cloudy and a typically clear climate respectively.

We aim to place context around the potential implications of any biases found on prospective power system studies with large solar buildouts. Specifically, we examine the effects of biased solar profiles with respect to the topical issue of seasonal or long-duration energy storage, such as green hydrogen or its derivatives, where low round-trip efficiencies could amplify the influence of any intra-annual bias and distort patterns or trends in charging and discharging. It is further aimed to provide some indication as to whether any potential implications found are of equal concern in clearer climates or more relevant to cloudy climates where reanalysis datasets are seen to suffer in terms of accurately resolving the effects of cloud on surface irradiance. It must be noted, however, that rather than attempting to precisely quantify any potential impacts for a specific region or power system with a complete and representative power system model, the intention behind this work is to highlight one potential mechanism by which the differences in outcome found in the likes of Kies et al. [64] could propagate in further studies involving P2X based storage.

2.3. Data & Sources

2.3.1. Solar Park Static Data

For each solar park, capacity data along with the tilt angle of the panels were researched manually through planning applications and industry articles or documents as available. Blanket assumptions of due south and due north azimuth angles are applied to solar parks in the northern and southern hemispheres, respectively. Data was collected for three Australian solar parks; Whiterock, Nyngan and Royalla and three Northern Irish solar parks; Rasharkin, Maghaberry and Lisburn.

2.3.2. ERA-5

The ERA-5 reanalysis dataset was accessed from the Copernicus Climate Data Store via the CDS API. It was downloaded in its native hourly 0.25° x 0.25° resolution in NetCDF format for the relevant locations using simple nearest point interpolation for the years 2019 and 2020. The following variables were downloaded and processed:

surface_solar_radiation_downwards – converted from J to average value in W/m^2 over each period to represent the global horizontal irradiance (GHI).

surface_solar_radiation_downward_clear_sky – converted from J to average value in W/m^2 over each period to represent the global horizontal irradiance (GHI) under a cloudless sky.

10m_u_component_of_wind & 10m_v_component_of_wind – the 10m above ground u and v vector components of wind. The magnitude of the wind vector is calculated to give the windspeed.

2m_temperature – the 2m above ground air temperature, converted from K to °C

2.3.3. MERRA-2

The MERRA-2 dataset was accessed via NASA's Goddard Earth Sciences Data and Information Services Centre. It was downloaded in its native hourly 0.5° x 0.625° resolution in NetCDF format for the relevant locations using simple nearest point interpolation for the years 2019 and 2020. The following variables were downloaded and processed:

SWGDN – the surface incoming shortwave flux (GHI)

SWGDNCLR, – the surface incoming shortwave flux assuming a clear sky (GHI)

U10M, V10M – the 10m above ground u and v vector components of wind. The magnitude of the wind vector is calculated to give the windspeed.

T2m – the 2m above ground air temperature, converted from K to °C

2.3.4. SCADA

Metered power output data for the Australian solar parks was obtained from the Australian Electricity Market Operator (AEMO) [68] for the full years of 2019 and 2020 in the form of supervisory control and data acquisition **(**SCADA) data and was not adjusted or processed further.

Metered SCADA data for the Northern Irish solar parks was obtained from the Single Electricity Market Operator (SEMO) [69] for the full years of 2019 and 2020 and was not further processed or adjusted.

2.4. Methodology

2.4.1. PV Model

The open-source PVLIB Python [70,71] forms the backbone of the Solar PV modelling work in this study. Using the PVLIB Python package, one can quickly apply some of the best-established irradiance decomposition & transposition models with various PV performance models. Conveniently PVLIB Python includes data from the Sandia module parameter database for application to the Sandia Array Performance Model (SAPM) [72]. The SAPM is widely validated and has been shown to correspond well to actual PV power output measurements [73–75]. As neither the MERRA-2 dataset nor the ERA-5 explicitly provide both the DNI and DHI variables a decomposition model is used to calculate them. The same methodology is applied to both datasets for direct comparison; however, it should be noted that it is possible to calculate the DHI directly from the variables provided by the ERA-5 dataset. The DNI could then be subsequently calculated. Based on the conclusions of Lave et al. [76], the DIRINT decomposition model [77] is chosen for this work, as it was found to be the least biased of the decomposition models examined at all locations studied. This provides an estimation of the DNI and allows for the subsequent calculation of the DHI via equation (2.1), where φ is the solar zenith angle:

$$DHI = GHI - (DNI \times \cos(\varphi)) \tag{2.1}$$

Having decomposed the GHI into its modelled direct and diffuse components, a transposition model can be applied to estimate the irradiances incident on the plane of the array (POA). [76] found, when coupled with a decomposition model, mean bias differences were typically smaller with the Hay/Davies model [78] than with other transposition models. On this basis, the Hay/Davies transposition model is applied. Finally, between the modelled POA irradiances along with wind and temperature variables from the reanalysis datasets, we have all meteorological input variables required to model solar PV generation as per the Sandia Array Performance Model (SAPM) [72]. The SAPM is a well-validated empirical model [72–75] which is conveniently integrated in PVLIB Python. In this work, the relevant parameters of the latest module in the Sandia Module database included with PVLIB python, a

2014 monocrystalline/amorphous silicon hybrid module, are taken as the SAPM module parameters. The temperature parameters for a glass/polymer open rack module as per King et al. [72] are used in the SAPM cell temperature model. Next, rather than assuming a string or central inverter design, we model only the DC power availability of the chosen module and normalize the resulting timeseries by the nominal Wp capacity of the module. This normalized timeseries is then applied to the solar park in question by scaling it by the MWp capacity of the said solar park. To account for clipping, any potential DC generation greater than the solar park's MWac capacity (inverter capacity) is set equal to the AC capacity. Here it is important to highlight that, while clipping has been accounted for, DC/AC conversion losses are not accounted for and assumed to be zero. Consequently, we can already expect to see a 2-4% positive bias in our model on this account. Finally, it should be highlighted that this approach does not consider the possible shading of module rows by other modules in a solar park. Row shading in solar parks is usually most prominent very briefly in the morning and evening when the sun is low in the sky. During these times, solar power output tends to be low. Furthermore, efforts are typically made to minimise the effects of shading when designing solar parks. As a result, the omission of a shading model is not expected to significantly distort the resulting modelled solar profiles.

2.4.2. Power System & LDES Model

To examine the possible implications of biased reanalysis-derived PV generation profiles on power system pathways involving long-duration storage and high solar build-out, a power system dispatch model is developed in the software PLEXOS. The model is highly simplified so as to neatly distil dynamics at the generation and storage interface. Consequently, it is important to preface that this model is not intended to represent a robust and comprehensive power-system pathway, but rather, a means to examine or demonstrate a potential mechanism of error propagation in certain pathways and models. For the purposes of demonstration, the simulation is based on the Northern Irish units as they exhibit greater bias errors. No simulation is performed based on the Australian sites as it is not intended to give the impression that it is attempted to quantify the degree of error propagation for a given reanalysis dataset in each location. Naturally, the degree of propagation will vary with different energy system models. Rather, it is simply sought to demonstrate a potentially problematic dynamic that may need to be given some degree of consideration when it comes to energy system modelling. The model is built in PLEXOS to consist of 2 generators, one wind generator and one solar generator. The solar profiles were created by taking the average load factor of the Lisburn and Maghaberry Northern Irish sites as according to either the metered generation, the ERA-5 based model, or the MERRA-2 based model depending on the scenario. Rasharkin solar park was excluded on the basis that it is known to be connected to a particularly congested grid node with a maximum export capacity well below its actual inverter capacity (this was accounted for in the original model). The wind and demand profiles are taken from Ireland's Commission for Regulation of Utilities' (CRU) PLEXOS model [79] which is publicly available. The simulation is run (arbitrarily) for the year 2024, in which the CRU project an average demand of approximately 5400 MW and a peak demand of approximately 8000 MW. The simulated and metered solar profiles are based off the data for 2020, another leap year, so as the timeseries can overlap. The wind and solar generators were sized to loosely reflect the finding of [44] that a portfolio of 70% solar and 30% wind capacity would minimise variability in renewable power generation. In addition to the renewable generators, a short-duration energy storage (SDES) battery unit and the H2 long-duration energy storage (LDES) unit are modelled using the PLEXOS battery object. The SDES is included given its greater round-trip efficiency for intra-day balancing of generation and demand reduces the total energy demand. As a result, it has been found that a hybrid combination of short and long duration storage can yield more cost-effective systems relative to reliance solely on less efficient long-duration storage [80,81]. The short duration energy storage is sized to yield 2 hours of storage at the nominal capacity which is set equal to peak demand. The long duration energy storage is sized for 200 hours of storage at the nominal capacity. The modelled system is an isolated electricity island in that no interconnection is modelled. The system is summarised in table 2.1 below.

Generator	Capacity (MW)	Storage Capacity (MWh)	Charge Efficiency (%)	Discharge Efficiency (%)
Wind	15000	-	-	-
Solar PV	30000	-	-	-
SDES (Battery)	8000	16000	90	90
LDES (H2)	7000	200000	70	50

TABLE 2.1. SIMULATION CAPACITIES & STORAGE EFFICIENCIES

The model is effectively an economic dispatch model with zero marginal cost generators with all units assumed available/committed. However, to ensure the battery and hydrogen-based storage units are utilized as intended, a per-MWh use of system charge is applied to the long-duration energy storage so as to implement a merit order among the storage technologies and ensure the short-duration storage is dispatched preferentially. No constraints are placed on the flexibility of either energy storage unit; however, the long-duration storage is constrained so as its state of charge at the end of the simulation is equal to its initial state of charge of 50%. The model is solved in a single step using the Gurobi solver. Three model scenarios are run; The 'MET', 'ERA' and 'MERRA' scenarios whereby the solar profiles are derived from metered generation, the ERA-5 based PV model, and the MERRA-2 based PV model respectively.

2.5. Results & Discussion

2.5.1. PV Model Performance

Figures 2.2 and 2.3 show density scatter plots of the modelled PV outputs from both MERRA-2 and ERA-5 sources against the measured SCADA data for the Australian and Northern-Irish sites respectively. A dense cluster of datapoints is observed around the red guideline along across all three Australian sites for both the MERRA-2 and ERA-5 based models indicating good agreement. However, White Rock exhibits a large number of outlier datapoints where the modelled outputs are significantly overestimating by higher load-factors for both datasets. Given the more symmetrical spread of errors at the Nyngan and Royalla sites, this possibly indicates more significant dispatch down or partial outage of the White Rock solar park. Here, dispatch down refers to the reduction in power output from the maximum available due to a network constraint or system level curtailment.

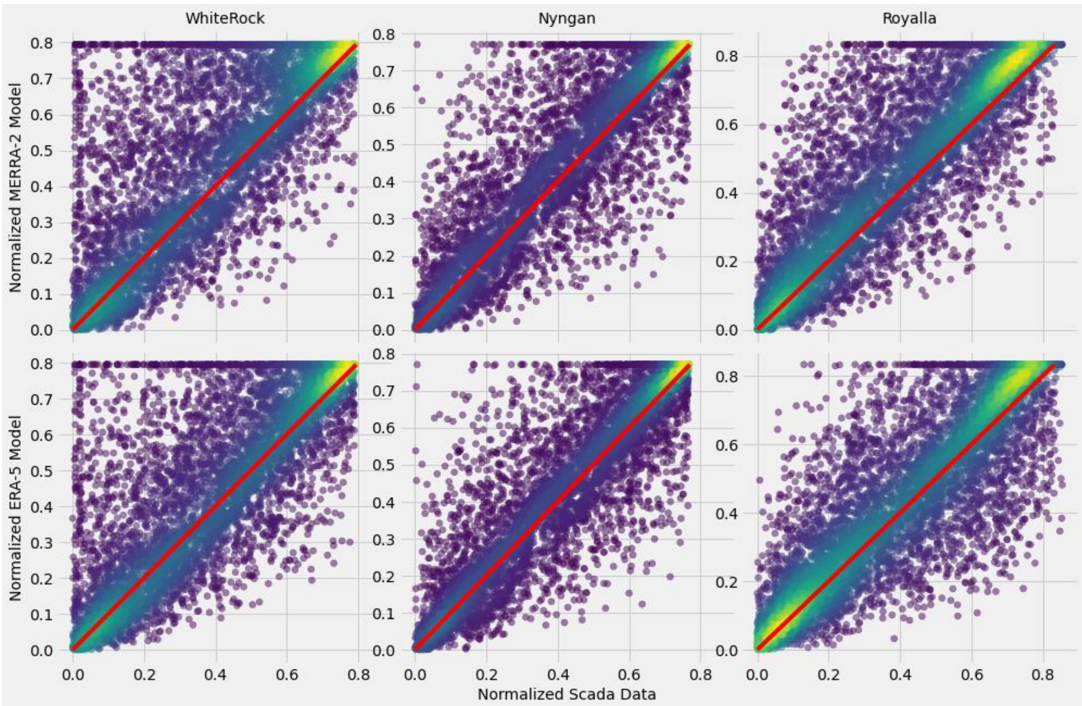

Figure 2.2. Australian Sites PV Model Correlation, 2019-2020

The Northern-Irish sites do not exhibit the same dense cluster of datapoints around the guidelines, but instead show a persistent, wide spread of errors as per figure 2.3.

Notably, the MERRA-2 derived model exhibits a slightly denser line of outliers at the top of the y-axis where the model is expecting clipping due to the DC power availability exceeding the inverter capacity, but the actual metered generation realised is lower. This indicates that the MERRA-2 based model may be overestimating high generation periods more frequently than ERA-5. This is in line with [55] wherein the authors' findings demonstrate a stronger overestimation bias on the shortwave irradiance for MERRA-2 than ERA-5 at meteorological measurement stations in Ireland. In any case, it is clear that both the MERRA-2 and ERA-5 based model suffer in performance in the cloudier Northern Irish climate relative to the clearer Australian climate.

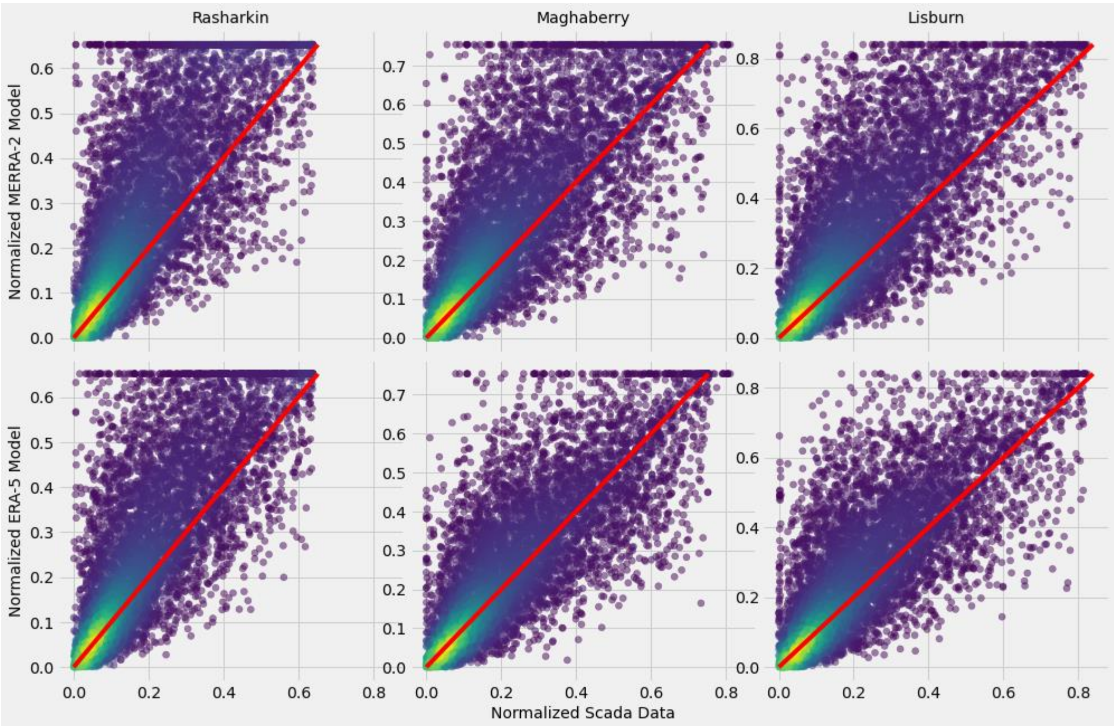

FIGURE 2.3. NORTHERN IRISH SITES PV MODEL CORRELATION, 2019-2020

Before further commenting on any overall bias, it is important to discuss data quality and highlight some assumptions. As the SCADA data measures the net metered output injected to the grid, thought must be given to the effects of dispatch down events due to constraints and curtailment. A precise discrepancy between the SCADA data inclusive of dispatch down and the potential generation in the absence of such dispatch is typically difficult to quantify for any individual power plant over a given data point. Indeed, attempting to adjust for such discrepancies without exact dispatch down data is likely to introduce bias error in any case. As such, we expect to see a degree of positive bias, where the model overestimates relative to corresponding SCADA data points when the plant has been dispatched down. This will also affect the correlations observed in figures 2.2 and 2.3.

In the case of the Australian Solar Parks, each of the sites are in New South Wales, the Australian state with the lowest percentage levels of curtailment of variable renewable power over 2019 & 2020 as per reporting by the Australian TSO [82]. According to AEMO's report, we would expect to see the bias introduced by curtailment amounting to less than 4%, though this is likely to vary from site to site. The system operator in Northern Ireland, SONI publishes similar reports [83,84] indicating dispatch down equivalent to 4.2% and 6.3% of the available solar energy in 2019 and 2020 respectively. Consequently, we expect dispatch down to have introduced a bias of 5%. This is, of course, expected to vary by site.

MBE %

Site	**WhiteRock**	**Nyngan**	**Royalla**	**Rasharkin**	**Maghaberry**	**Lisburn**
ERA-5	**13.1**	**1.6**	**7.6**	**33.1**	**11.8**	**22**
MERRA-2	**19.1**	**4.8**	**17.2**	**43.1**	**29**	**37.3**

Table 2.2 PV Model Mean Bias Errors

Table 1 lists the mean bias errors (MBEs) of both models as a percentage of the actual metered generation. When considering unmodelled inverter losses, module soiling and dispatch down events, the ERA-5 based simulations of the Australian sites do not appear to exhibit any large bias. In the case of the MERRA-2 data however, there is evidence of moderate overestimation bias. Nyngan solar park exhibits a weaker MBE than the other two sites for both reanalysis datasets. It is possible that this arises in part because the Nyngan park is made up of cadmium telluride (CdTe) modules, which perform better in high temperatures than crystalline silicon modules, which are the assumed module technology in our PV model. For the Northern-Irish sites the large positive bias errors suggest a general overestimation bias when modelling solar PV with both reanalysis datasets. This is in line with the underestimation of cloud events by numerical weather models that is well documented across the literature and evident in figures 2.4 and 2.5. Figures 2.4 and 2.5 plot the (DC) capacity-normalised mean bias error for both models at each site against percentiles of the clearness index 'k_t' according to the reanalysis data. The clearness index is calculated as per equation (2) by taking the ratio of the surface incoming radiation to the surface incoming radiation assuming a clear sky. A dynamic bias trend with a reasonably consistent general outline is revealed across all sites. Due to this difficulty experienced by the numerical models in resolving cloud events, it follows that the models' overestimation biases deteriorate further when the actual climate is typically cloudier. This is apparent through the comparison of the Australian and Irish sites. This trend is also potentially evident amongst the three Australian solar sites whereby Nyngan solar park seems to exhibit a weaker dynamic bias trend with the modelled clearness index than the other two sites. Nyngan is located inland in a drier area of New South Wales relative to the other two sites. In nearly every case examined, ERA-5 outperforms MERRA-2 under the current modelling framework with both the overall bias and dynamic bias trend reduced with ERA-5 relative to MERRA-2.

$$k_t = \frac{GHI}{GHI_{clr}} \tag{2}$$

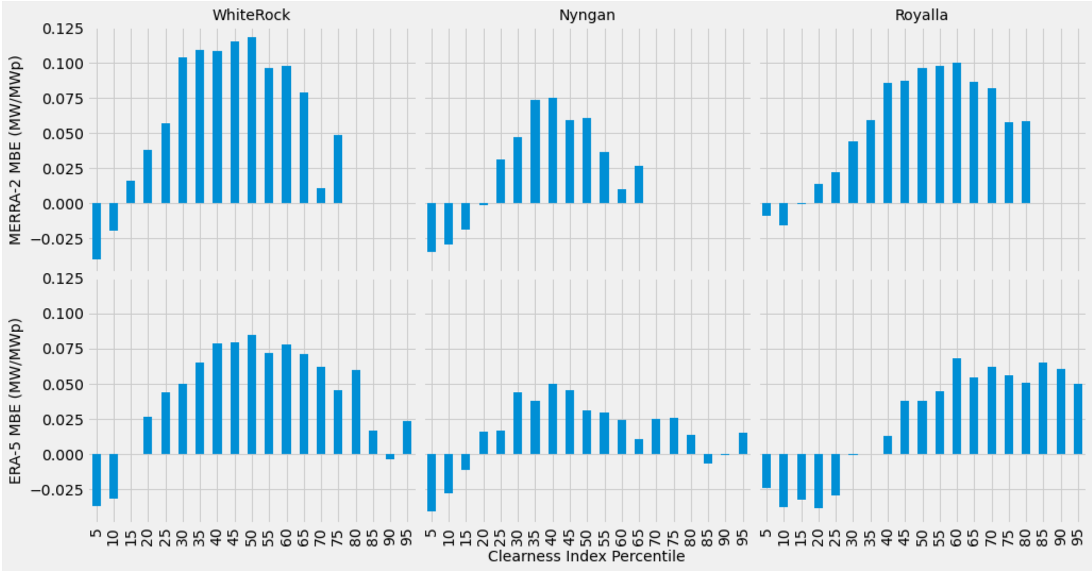

FIGURE 2.4. MODEL MEAN BIAS ERROR VS. CLEARNESS INDEX, AUSTRALIAN SITES.

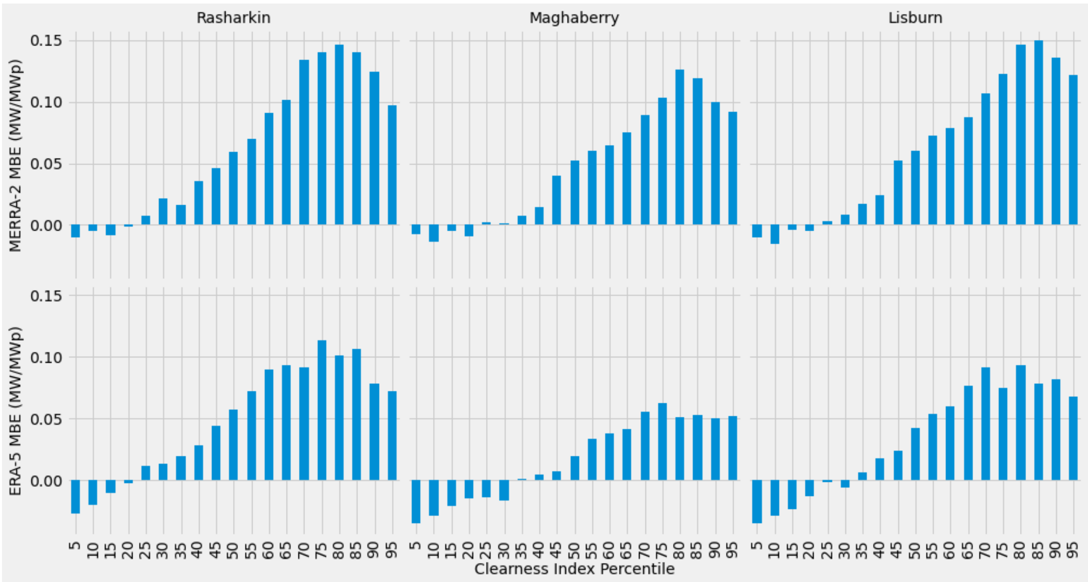

FIGURE 2.5. MODEL MEAN BIAS ERROR VS. CLEARNESS INDEX, NORTHERN IRISH SITES

Given the dynamic bias trends exhibited in figures 2.4 and 2.5, it follows that, where a strong seasonal trend exists in the clearness index (or cloud patterns), it is possible that a strong seasonal bias is introduced to the overall solar profile. This could introduce error when studying the seasonal complementarity of wind and solar power as in [44] or hybrid wind-solar power systems with long-duration storage. Take for example, the Northern Irish sites studied. Figure 2.6 demonstrates a significant monthly trend in the average clearness index according to the MERRA-2 data with a profile that generally suggests clearer less cloudy summers and cloudier winters. The ERA-5 data appears to disagree with that of MERRA-2 and suggests clearer less cloudy weather in the spring and a flatter cloudier trend from midsummer onwards. In line with the dynamic bias trend with clearness index and the apparent seasonality of the MERRA-2 clearness index, the MERRA-2 derived model exhibits a monthly trend in the overall bias error as seen in figure 2.7. Similarly, the ERA-5 derived model also exhibits greater bias in the months that the clearness index is thought to be higher as per the original ERA-5 data. Notably, it follows that, if one were to examine the role that Solar PV might play in balancing the lower wind power production on the Irish grid during the summer months, the MERRA-2 dataset could overstate the contribution of solar PV or indeed underestimate the need for seasonal storage in low-wind summer months in particular.

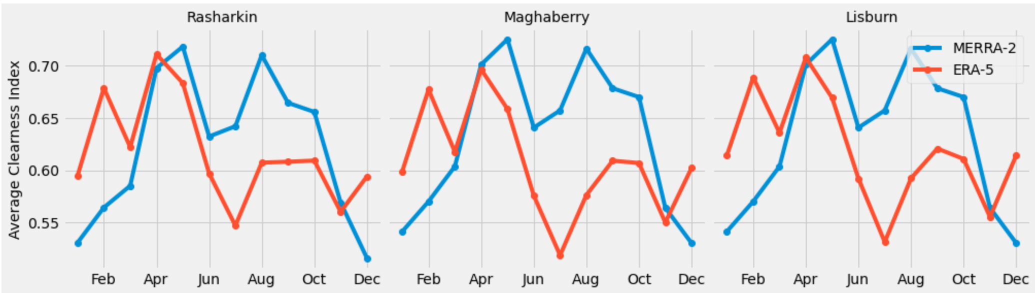

FIGURE 2.6. 2019-2020 MONTHLY AVERAGE CLEARNESS INDEX, NORTHERN IRISH SITES

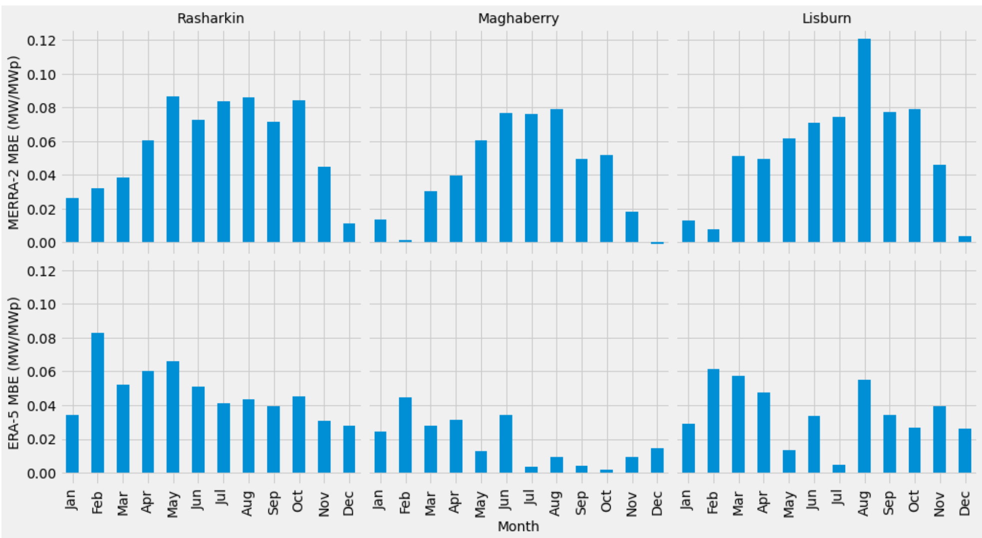

FIGURE 2.7. 2019-2020 MONTHLY AVERAGE MODEL MBE, NORTHERN IRISH SITES

Locational biases are a common feature of reanalysis datasets and it would therefore be pertinent to point out the limited sample size of solar farms in the current work before drawing inference. However, when considering both the literature and the recurring trend of bias and clearness index, the overall picture is indicative of consistent systematic overestimation bias. To better contextualise this on a global level, the MERRA-2 derived renewables.ninja solar profiles for the large bank of solar farms in the PLEXOS World model of [42] are compared to a simulation of the same, over the same full year (2015) using the current work's PV model with ERA-5 as input data. The resulting capacity factors are displayed in figure 2.8. The red line marks where the x and y axes are equal in value for easier visualization. If the consistently better performance of ERA-5 under the current work's modelling framework is extrapolated onto figure 2.8, a marked global overestimation bias by MERRA-2 is suggested. The two models can be seen to be in better agreement for sites with higher capacity factors which supports the thesis of a generally smaller degree of bias in less cloudy regions with higher solar potential. In addition to the site-specific analyses presented, this trend raises a warning in terms of extrapolation of studies or validations from countries with high solar potential and lower cloud incidence to cloudier climates with lower solar potential.

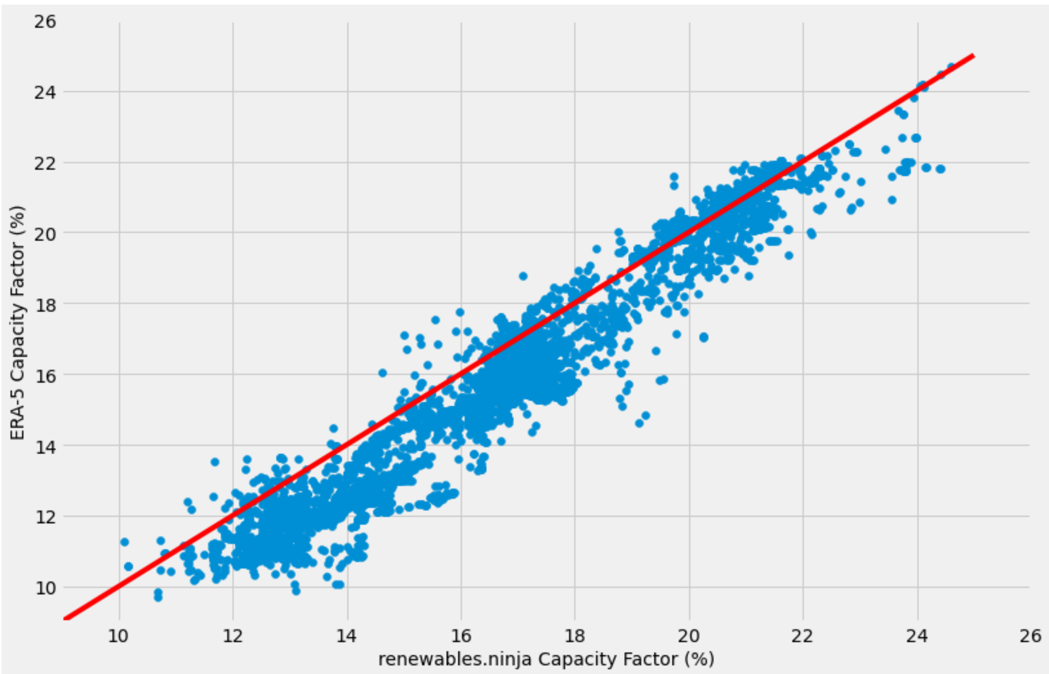

FIGURE 2.8. ERA-5 DERIVED CAPACITY FACTORS VS. PLEXOS WORLD PV CAPACITY FACTORS

2.5.2. LDES Modelling

Having run the simple PLEXOS model for each solar input data scenario the operational pattern of the LDES (Hydrogen storage) infrastructure and its total energy requirement can be examined with consideration of the influence of the biases exhibited in section 4.1. Figure 2.9 shows the ‘state-of-charge’ of the long duration storage for each simulation scenario, referred to here as the normalized hydrogen reserve. To some extent, agreement amongst the scenarios at the start and end of the simulation is forced due to the constraint on the initial and final state of charge. Outside of this, the metered generation based solar profile scenario and the ERA-5 based solar profile scenario are generally in close agreement with the exception of August & September. However, the MERRA-2 based solar profile scenario, whilst roughly agreeing on the timing of peaks and troughs in hydrogen reserves, differs quite significantly on their magnitudes and is distinctly distorted relative to the ‘MET’ scenario. This is interesting given that the MERRA scenario solar profile is more biased than the ERA scenario profile. Most notably, the MERRA scenario does not see the H2 reserve charged to the high peak in May/June that both the ERA and MET scenario agree closely on. It is hypothesized that this is likely due to the utilization charge associated with the LDES and greater estimated solar generation in the summer according to the MERRA-2 derived profile, as this would allow the simulation to simply cycle the short-duration battery energy storage more frequently for less cost than charging and discharging the LDES. As a result, the MERRA scenario appears to underestimate the need for seasonal storage during the low-wind summer months for the given solar power generation capacity. This follows logically from the dynamic bias-profile previously observed and the strong intra-annual trend in clearness index suggested by the MERRA-2 data.

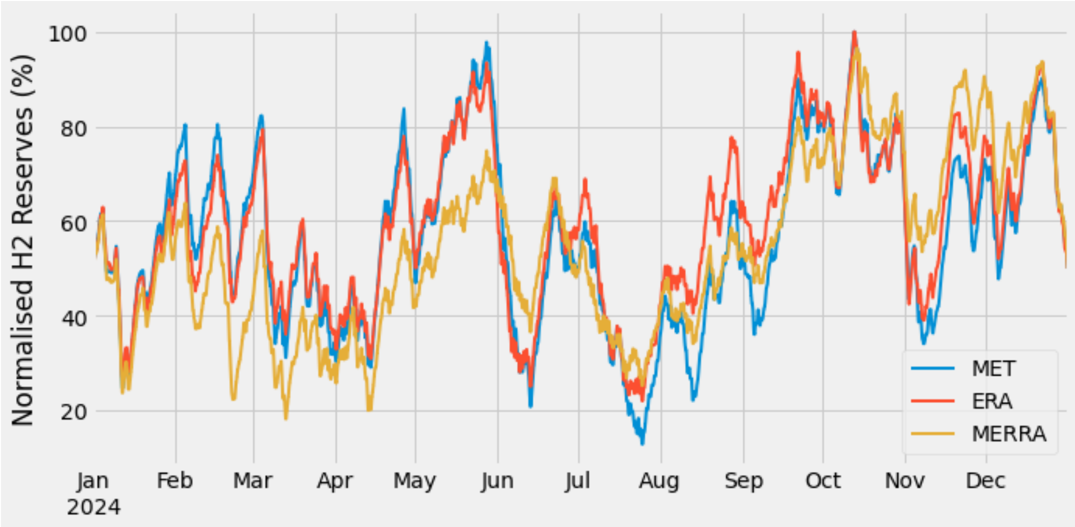

FIGURE 2.9. SIMULATED HYDROGEN STORAGE CHARGE STATE

Figure 2.10 plots the average monthly utilization, calculated as the absolute value of the net generation of the LDES, in each scenario. Again, the MET and ERA scenarios agree reasonably closely whereas the MERRA scenario significantly underestimates the utilization of the LDES unit. It would follow that, per the given capacity in this scenario, the levelized cost of storage (LCOS) of the P2X-based storage is distorted. In this case, the levelized cost of storage would be inflated in the MERRA scenario given a lower volume of stored electricity delivered to the system over which to spread the capital cost of the installation.

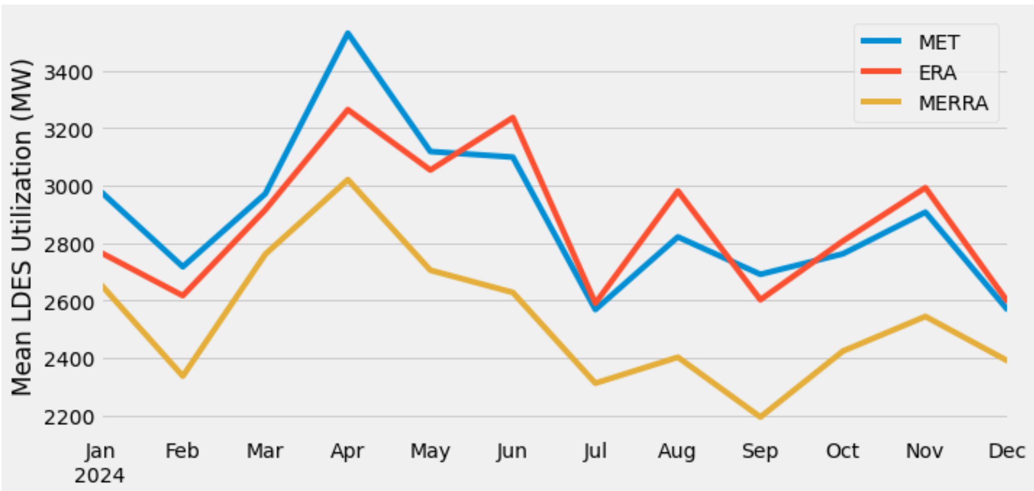

FIGURE 2.10 SIMULATED HYDROGEN STORAGE UTILIZATION

Figure 2.11 shows the cumulative difference in the de-rated margin and the cumulative difference in the electrolyser load between the MERRA and the MET scenarios. In this case, the de-rated margin is defined as the sum of the renewable generation less the underlying system demand (or simply the net generation once the charging and discharging of storage is excluded). Clearly, the moderate bias error on the generation profile which yields the difference in net generation between scenarios proliferates into a much more significant error on the total electrical load requirement of the electrolyser. This is demonstrated through the total cumulative error just shy of a gigajoule on the de-rated margin culminating in close to 2.5 GJ in cumulative error on the electrolyser load over the simulated period. In other words, an error on the available energy supply has yielded an error on the total energy requirement of the simulation that is magnified by a factor of approximately 2.5. This demonstrates the mechanism by which low-round trip efficiencies can lead to the propagation of initial bias error on power profiles resulting in larger errors on the total energy requirement of a simulation as originally hypothesized. Evidently, this could skew resource adequacy assessments of certain power system pathways to a concerning extent, particularly over long simulation periods.

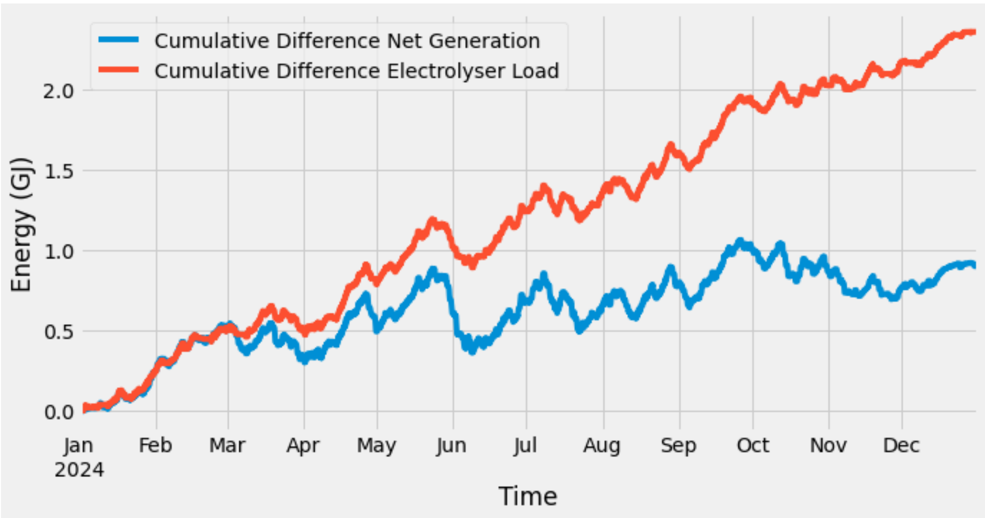

FIGURE 2.11 BIAS ERROR PROPAGATION

Chapter 3 A Framework for High Resolution Coupled Global Electricity & Hydrogen Models Based on Integrated Assessment Model Scenarios

Mathews D, Brinkerink M, Deane P (2025). A framework for high resolution coupled global electricity & hydrogen models based on integrated assessment model scenarios. International Journal of Hydrogen Energy 97: doi: 10.1016/j.ijhydene.2024.11.077

3.1. Abstract

Technology-rich Integrated Assessment Models (IAMs) offer the possibility to endogenously resolve hydrogen demand as a function of competition between technologies to meet energy service demands while considering wider interactions with climate and the economy. Such models are typically configured with relatively low spatial and temporal resolution thereby limiting their utility in studying future global hydrogen trade scenarios. This work presents a framework for the soft-linking of IAM scenarios to a higher spatial and temporal resolution global model. This framework provides an "engine" with which to generate future-looking coupled hydrogen & electricity models with the co-optimisation of production capacity, storage, and transmission infrastructure that allow the user to vary key technoeconomic input parameters. The modelling framework is applied to an IAM scenario and validated against the parent IAM. The utility of the model when examining electricity & hydrogen commodity trade in future scenarios is then demonstrated.

3.2. Introduction

3.2.1. Role of Integrated Assessment Models in Global Energy Systems Modelling

Integrated Assessment Models (IAMs) facilitate the study of interactions between larger macro drivers across energy, economy and the environment. Most notably, integrated assessment models are the backbone of energy-climate-economic modelling informing the Intergovernmental Panel on Climate Change's (IPCC) Assessment Reports. IAMS feature significantly in the contributions of working group III to the 6th assessment report (AR6) [85–87]. When referring to IAMs for the purpose of this study it is with reference to process-based IAMs which "*Represent explicitly the drivers and processes of change in global energy and land-use systems linked to the broader economy, often with a high degree of technological resolution in the energy supply*" as defined in Wilson et al. [26]. Commonly, within the energy system component of such IAMs, energy service demands are projected or optimized based on interactions with the economic component of the model. Candidate technologies are allowed to "compete" to fulfill energy service demands on a cost optimization basis with an overarching objective to maximize global welfare. In the MESSAGEix model, seven specific energy service demands are provided exogenously but can be adjusted endogenously in response to macro-driving trends via the MESSAGEix-MACRO link (MACRO being the macroeconomic component of the wider MESSAGEix-GLOBIOM IAM) [88,89]. The energy system as a whole is then optimized to ensure that each service demand is met by a least-cost portfolio of technologies. This optimization of the energy system with due consideration for socio and macro-economic drivers means that process-based IAMs can be useful tools for the examination of the potential roles of individual technologies in future energy system scenarios.

3.2.2. IAMs & Modelling the Future Role of Hydrogen

In recent years hydrogen and its derivatives have been a hot topic of debate regarding both the magnitude and scope of their roles as energy carriers in decarbonization scenarios. Indeed, Wolfram et al. [16] note that "*key questions including how much hydrogen should be produced, where it should be used, and what it may cost remain unanswered*". IAMs have the potential to offer insight into the role of hydrogen in future energy system scenarios.

In a study examining the roles that hydrogen could play in the global energy system and the resulting impact on costs, Wolfram et al. [16] implement improved hydrogen representation in the GCAM integrated assessment model and simulate 25 future scenarios. Across the range of scenarios simulated, the authors find that hydrogen only reaches moderate levels of demand (3%-9% of final energy consumption) but can reduce the overall cost of total system decarbonization by 2050 by 15%-22%. These significant cost reductions for such a small share of global final energy demand underscore the importance of modelling the role of hydrogen so that appropriate policy measures can be put in place to unlock system efficiencies.

In a more specific study of low emission pathways for global steel production considering Carbon Capture & Storage (CCS) and hydrogen technologies, Benavides et al. [25] leverage the MIT EPPA integrated assessment model finding that steelmaking with CCS is more competitive than hydrogen-based steelmaking unless hydrogen production costs reduce. Similarly, in the scenario with the highest hydrogen demand, Wolfram et al. [16] found that hydrogen only achieved a 10% market share with regards to the sector-specific energy demand for steelmaking.

Hanley et al. [90] presents a review of the role of hydrogen across low-carbon scenarios according to different Energy System Optimization Models (ESOMs) including the ETSAP-TIAM integrated assessment model. The authors note large uncertainty surrounding hydrogen between different scenarios and identify specific drivers of hydrogen deployment such as low CCS deployment and high renewable electricity penetration. These findings are consistent with Kouchaki-Penchah et al. [91], an ESOM based study of energy transition scenarios for Quebec, which also finds that hydrogen competes with CCS deployment. In this case the authors find that, across scenarios with the same emissions reduction targets, scenarios with higher deployment of hydrogen can experience increased marginal abatement costs but reduced risks associated with heavy reliance on direct air capture.

3.2.3. Limitations of IAMs with Respect to Hydrogen Studies

Whilst it has been established that useful and consistent insights regarding the future of hydrogen can be drawn from integrated assessment model studies, IAMs are not without their limitations. Gambhir et al. [18] reviews criticism of IAMs across the literature with particular focus on Bioenergy with Carbon Capture and Storage (BECCS) deployment across IAM scenarios. In this case, Gambhir et al. note some significant criticism of IAMs in general and criticism specific to the representation of BECCS in the models. Among the general criticisms are:

i. Dated or inappropriate input assumptions into IAMs

ii. Lack of technology and energy system detail at higher geographic and temporal scales

iii. Lack of transparency around model inputs and outputs

Integrated assessment models' representation of global energy systems and their interplay with land use, socioeconomic and macroeconomic factors is often made computationally viable through reduced spatial and temporal resolutions. Considering the potential of hydrogen and hydrogen derivatives to move energy in both space and time as a low-carbon energy carrier, limitations regarding model geographic and temporal resolution highlighted in Gambhir et al. may prove particularly pertinent to hydrogen-centric studies. Taking the MESSAGEix-GLOBIOM model for example, the IAM is generally configured to run in timesteps of 5 or 10 years with energy system flexibility requirements being resolved on a parametric basis [88,89] based on the work of [92]. Natively the MESSAGEix-GLOBIOM framework divides the world into 11 regions though it may also be run in other spatial configurations.

Considering the temporal and spatial variability of renewable power generation, the flexibility parameterization of the MESSAGEix-GLOBIOM model may fail to yield a generation portfolio that would ensure sufficient flexibility to match power demand in an equivalent higher temporal resolution. Indeed, Brinkerink et al. [20]soft-links a global power system model to a MESSAGEix-GLOBIOM scenario and observes significant unserved energy when implementing the IAM scenario generation capacity portfolio at a higher spatial and temporal resolution. Moreover, the limited spatial resolution may see restrained hydrogen production cost differentials rather than more extreme cost differentials at higher spatial resolution, potentially overlooking aspects of hydrogen trade.

On account of the BECCS-specific and more general criticism of the IAMs, Gambhir et al. [18] consider three possible solutions. They are, i) "*scrap"* the use of IAMs all together, ii) transform the IAMs to rectify the highlighted shortfalls or iii) supplement the IAMs with other model and analytical approaches. The authors conclude that scrapping the use of the IAMs is not realistic considering their significant utility as structured frameworks within which the performance of different fuels or technologies can be examined and the absence of alternative tools for modelling pathways to decarbonized economies. With regards to the transformation of IAMs to incorporate additional dynamics criticized as being absent, the authors note that this transformation is already underway to some degree. However, a full transformation to address each criticism would likely place excessive demand on the integrated assessment models and the finite resources available to the IAM modelers. This ongoing transformation of IAMs is evident in improvement of the representation of Hydrogen in the GCAM model in [16]. The authors conclude that the supplementation of IAMs with other models and supporting analytical approaches is of significant merit with the combined approach leading to a "*bringing together of potentially diverse analytical communities from across the physical, engineering and social sciences, so as to achieve a genuinely cross-disciplinary perspective on BECCS and other key low-carbon technology options*." In the current work, it is aimed to provide one such other approach to supplement IAMs, not for BECCS, but for the examination of the future role of Hydrogen.

3.2.4. Non-IAM Studies on Future Hydrogen Trade

The limited spatial resolutions mean that IAMs may not be best placed to examine the extent to which hydrogen and its derivatives may be globally traded commoditized energy carriers in future energy system scenarios. Non IAM-based approaches have been applied in recent studies exploring hydrogen trade futures, such as [93,94] and the large 3-part study by IRENA [95–97].

Brauer et al. [93] presents a multi-criteria analysis of countries with which the European Union could partner to develop hydrogen import opportunities to meet EU policy targets. The authors find that prospective supply of ammonia to the EU is likely to evolve with sufficiently diverse import options but gaseous hydrogen supply warrants prompt strategic partnership with prospective exporters to build and scale the necessary infrastructure and facilitate cost reductions. This conclusion arguably points towards a pressing need for more detailed optimization studies to inform strategic investment in support of the policy targets.

Franzmann et al. [94] derives cost-potential curves of green liquid hydrogen for international export for a sample of 28 countries. The renewable resource potential of each country is assessed before its prospective liquid hydrogen export infrastructure is optimized on an individual basis to minimize the cost of liquid hydrogen 'on ship' at the given country's ports. The authors find that countries with abundant solar resources in Africa and the Middle East yield the cheapest green hydrogen at port. Based on a projected political landscape in 2050, the authors also find that democratic nations on average see an export cost premium of approximately 7% at port compared to autocratic nations, raising geopolitical considerations for the future of green hydrogen trade.

As part of the IRENA study, [97] presents an analysis of global green hydrogen production and cost potential for the year 2050 under an optimistic scenario and a pessimistic scenario. The resource potential and production modelling include multi-criteria land eligibility assessment considering factors such as water availability, population density and protected areas. Rather than modelling the complete coupled power system alongside the global hydrogen model, dedicated renewable power generation connected to islanded electrolysers are optimized to minimize the levelized cost of hydrogen (LCOH). In contrast to [94], the IRENA study is not focused on the cost of hydrogen exports at port and consequently, the regional merit order of hydrogen costs includes more regions with expansive inland renewable energy resources at the lower cost end of the merit order stack. For example, in [97] inland reaches of both China and Australia are projected to exhibit very low LCOHs in 2050 and therefore feature among the cheapest countries in terms of LCOH. Franzmann et al. also highlight differences in key technological parameters such as technology CAPEX, WACC, and electrolyser efficiency that further influence differences in results. Regardless, countries with abundant solar resources dominate the cheaper end of the hydrogen production and export stack in both studies.

In a technology review of hydrogen carriers, [96] analyses and assesses different hydrogen transport technologies including gaseous hydrogen pipelines, shipping as liquid hydrogen, ammonia, or Liquid Organic Hydrogen Carriers (LOHCs). There are many significant conclusions in [96] that warrant a detailed examination beyond summarizing here in brief. For instance, an analysis of least-cost hydrogen transmission and transportation as a function of transport distance and annual transport volumes is provided. It was found that liquid hydrogen requires the highest capital investment of all carriers and consequently its deployment is sensitive to the cost of capital. Under IRENA's base assumptions, liquid hydrogen is not competitive in the pessimistic scenario, while LOHC is uncompetitive in both the pessimistic and optimistic scenarios. An important implication of these conclusions is that ammonia may be the most economical carrier for shipped hydrogen under IRENA's scenario assumptions.

Finally, [95] builds on the work of [97] and [96] to present a general trade outlook under the same optimistic and pessimistic 2050 cost scenarios. An optimization model built using the commercial software PLEXOS cost optimizes hydrogen production and trade across the globe with an hourly temporal resolution. Spatially, the world is divided into 34 individual regions. Importantly, the authors note that "trade volumes and patterns are dependent on the geographical resolution used in the model. As regions are disaggregated into individual countries, more extreme hydrogen production cost values are possible, potentially leading to new trading countries". In [95], dedicated renewable power and off-grid electrolyser systems are co-optimized, however hydrogen demand for the power sector is explicitly netted off from the total hydrogen demand in IRENA's World Energy Transitions Outlook 2022: 1.5°C Pathway scenario [98] rather than resolved implicitly by a coupled model. In line with this, the wider power sector is not modelled. Rather, it is assumed that electricity interconnection between regions is maximal, and that nodal hydrogen demand must be serviced with dedicated hydrogen transport infrastructure only. This assumption may yield bias in favor of inter-regional hydrogen trade over and above inter-regional electricity trade powering electrolysers for local hydrogen production. Notably, [95] finds that of the total investment required for hydrogen production and trade from 2020 to 2050, the investment costs associated with the additional power generation required to service green hydrogen demands is greater than all other required investment costs combined (including electrolyser, conversion plants, pipeline, battery, ships and hydrogen storage investment costs). In another key conclusion that should be highlighted, it is noted that under a uniform WACC across all regions, global trade volumes are reduced by 15% compared to modelling regionally unique WACCS as the uniform WACC reduces trade incentive. This conclusion holds pertinence to other global studies including the current work.

3.2.5. The Contribution of This Research

The non-IAM-based studies examined above yield important insights into the potential future of international hydrogen and hydrogen derivative trade. However, the scope of these studies does not comprehensively cover future hydrogen trade in a global sector-coupled electricity & hydrogen system. As the effort required for model building and generally conducting large-scale global studies is significant, considerable barriers exist to the assessment of global hydrogen trade scenarios as a function of key parameters. For instance, while [95–97] present both an optimistic and a pessimistic scenario with some additional sensitivities specifically explored, it would be useful to examine further sensitivities under a multitude of hydrogen demand scenarios. Additionally, the global hydrogen trade landscape may be influenced heavily by drivers associated with sector-coupling between hydrogen and the power sector which [93–95] do not explicitly model in favor of modelling dedicated electricity sector resources for hydrogen production only.

To this end, the endogenous projections of hydrogen demand based on technological competition within the IAMs remains a desirable modelling feature, albeit one that is not likely to be tractable at very high spatial and temporal resolutions.

The current work presents a new model framework wherein production, storage and transmission of both hydrogen and electricity are co-optimized globally at a high spatial and temporal resolution whilst leveraging electricity & hydrogen demand derived from integrated assessment model scenarios. To handle the uncertainty surrounding the future role and demand of hydrogen, the model framework facilitates the soft-linking of a wide range of future scenarios via the Integrated Assessment Model Consortium's AR6 Database [99] with a capacity allocation and economic dispatch model. Consequently, the sector-coupled model framework presented in this paper is capable of simulating hydrogen commodity trade flows at high spatial and temporal resolutions across many differing future scenarios wherein coincident hydrogen and electricity demands have typically been resolved implicitly as a result of competition between technologies to fulfill projected energy service demands. Overall, it is intended that the combination of the methodologies outlined in this paper along with integrated assessment modelling can enable detailed insight into inter-regional hydrogen & electricity trade & optimal regional technology portfolios across a wide range of future scenarios.

3.3. Methodology

3.3.1. Integrated Assessment Model Soft-link

The foundational framework for this study is based on the multi-model soft-linking methodology of Brinkerink et al. [20] and the underlying 256 region spatial domain of the PLEXOS-World model [19]. In essence, the soft-linking methodology of [20] revolves around the following steps:

1. Mapping the lower resolution IAM spatial domain to the 256 region PLEXOS-World spatial domain.
2. Spatially downscaling the annual regional electricity demand from the IAM domain to the 256-region PLEXOS-World spatial resolution.
3. Temporally downscaling the resulting annual regional electricity demands to hourly resolution.
4. Asserting IAM region capacity retirement and expansion constraints for each generation technology type for the set of constituent PLEXOS-World regions relative to the 2015 PLEXOS-World Model capacity baselines.

The motivation behind [20] is to provide a multi-model framework to assess the technical feasibility of climate change mitigation scenarios from the power system perspective, and as a result, the degree of coupling between the PLEXOS-World based power system model and the chosen IAM scenario is relatively high. In the current work, the intention is to enable the examination of global future coupled hydrogen-electricity system dynamics rather than to strictly assess and maintain a high degree of fidelity to the chosen IAM scenario. Moreover, the aim of this work is to provide an "engine" to generate future-looking coupled hydrogen & electricity models with the co-optimisation of production capacity, storage, and transmission infrastructure that allows the user to vary key input parameters and costs. As a result, the degree of linkage between the sector coupled PLEXOS model and the IAM is more relaxed in the current framework. In particular, storage and electrolysis capacities are not soft-linked to the IAM scenario and are instead resolved by the PLEXOS model's capacity expansion model on a basis of technology cost parameters which can be varied by the user of the current framework. Meanwhile, the soft-link with the IIASA AR6 Scenario Database [99] allows for the selection of a range of explainable decarbonisation scenarios with varied hydrogen and electricity demand & different outlooks regarding technologies like CCS.

Figure 3.1 outlays the general flow of data and the various processes involved in the soft-link modelling framework. For electricity and hydrogen demand timeseries inputs, the total final consumption of the IAM regions in 2050 are both temporally and spatially downscaled using the methodology applied in [20]. An important assumption to highlight is that hydrogen demand is spatially downscaled on the same basis as electricity demand considering the lack of mature hydrogen demand data from which to develop a comparable empirical basis. The net result being that PLEXOS-World regions that are projected to consume a higher proportion of the corresponding IAM region's electricity demand, are also projected to consume a higher proportion of the IAM region's hydrogen demand.

Before applying this methodology to hydrogen, the total final consumption of hydrogen is de-rated by the electrolytic fraction of hydrogen production for each IAM region. Non-electrolytic hydrogen is not included in this study to reduce the complexity of the resulting model. In effect, the non-electrolytic hydrogen is simply netted off the hydrogen demand in each region. Furthermore, given the uncertainty about the precise end uses, a flat, continuous demand profile is asserted for hydrogen demand at each node for the example scenario presented in this work.

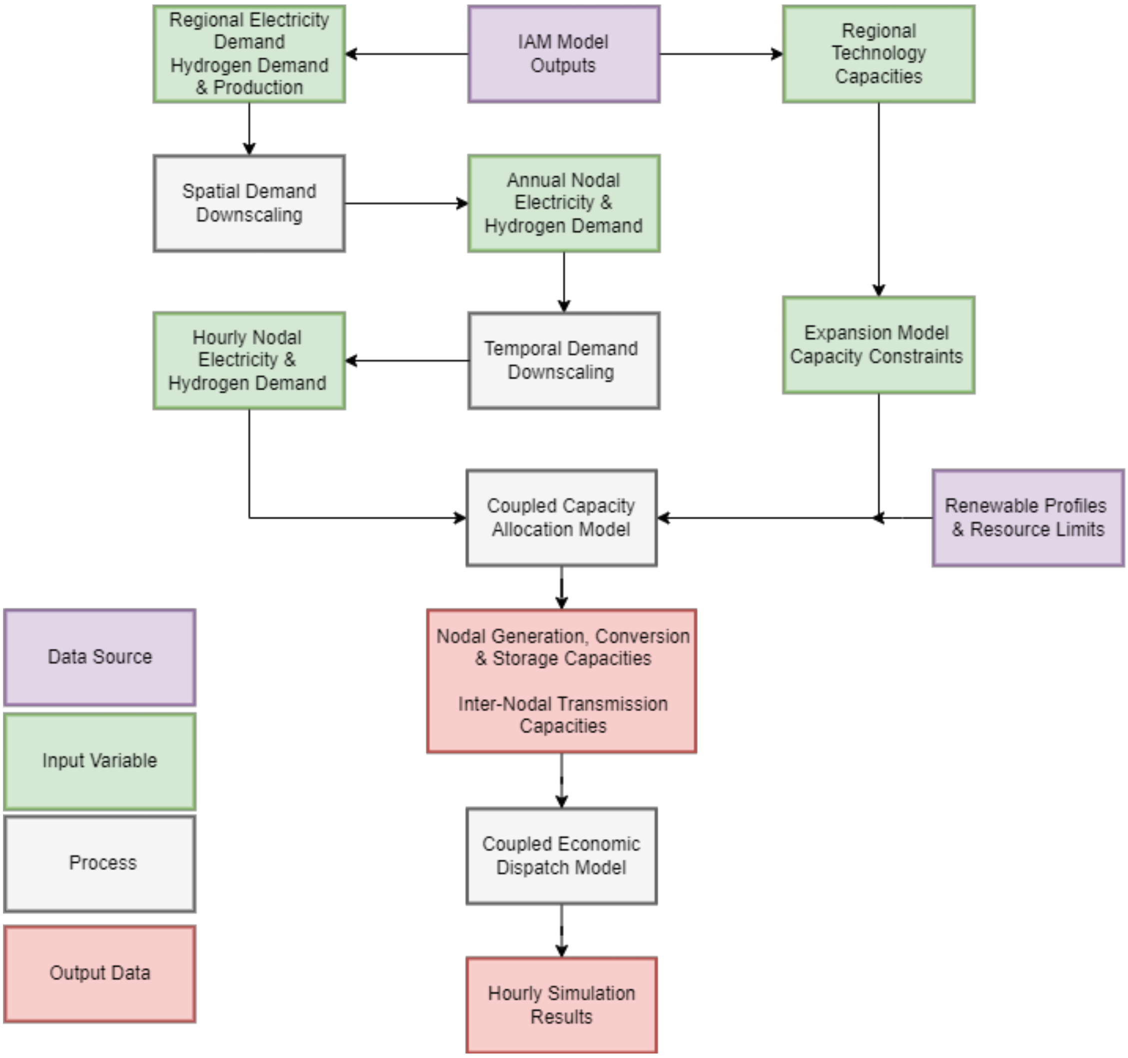

FIGURE 3.1 SOFT-LINK MODELLING FRAMEWORK

The soft-linking methodology for power generation capacity is similar to [20] although, the capacity expansion model in this study does not model power plant retirement relative to the PLEXOS-World 2015 baseline system as in [20], but rather optimises capacity allocation on a green-field basis for 2050.

The capacity soft-link is applied via equality constraints in the capacity allocation & expansion model phase such that the sum of the capacity for each generation type across the nodes that make up a corresponding IAM model region is equal to the capacity from the IAM scenario. However, in [20] it was found that the treatment of intraregional transmission and the lower spatial resolution of the MESSAGEix-GLOBIOM IAM causes underestimation of the curtailment of variable renewable energy (VRE) resources. Significant unserved energy was also observed in the soft-linked power system model (between 2.5% and 5% of global electricity demand). On the back of this finding, an exception is made for the regional capacity equality constraints for wind and solar technologies such that the capacity expansion & allocation model can build a minimum of 100% and up to a maximum of 150% of the regional IAM capacity for each of the VRE technologies. This will allow the model to choose to compensate for the additional expected curtailment and unserved energy through the allocation of additional capacity with an associated build cost incurred.

In this study, the PLEXOS model is soft-linked to the outputs of the MESSAGEix-GLOBIOM scenario as published at the "R5" spatial aggregation (see figure 3.2 below) in which the world is divided into 5 regions. This allows a greater degree of freedom for the higher resolution model to optimise resources across a large spatial domain at the capacity allocation phase with a more relaxed capacity soft-link. Generator fuel prices and the carbon price are applied uniformly at the global level based on the IAM scenario data.

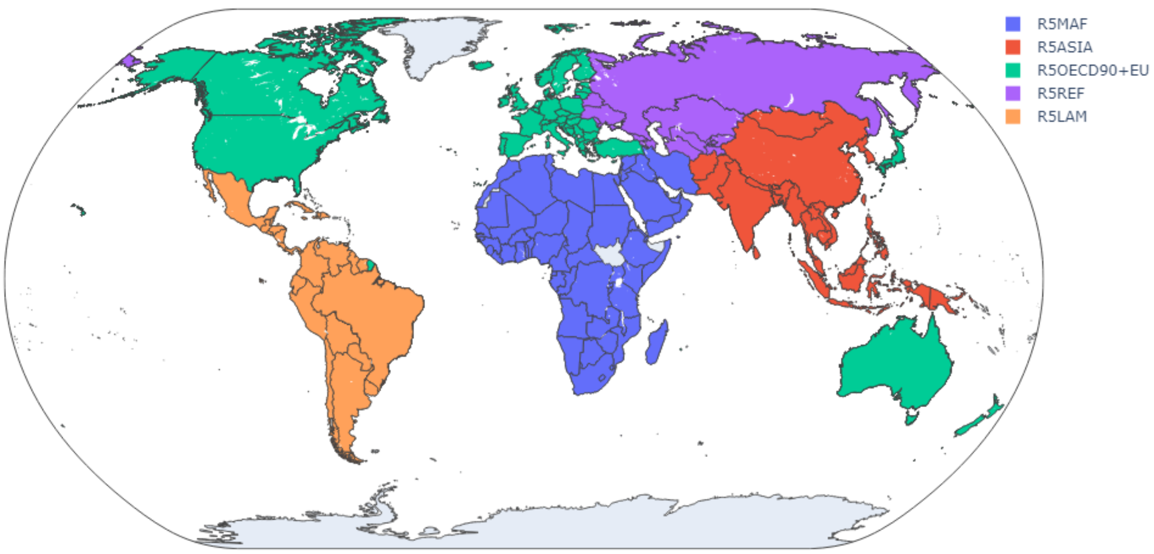

FIGURE 3.2 5 REGION "R5" SPATIAL MAPPING AT A COUNTRY LEVEL. LARGE COUNTRIES ARE FURTHER SUB-DIVIDED IN THE PLEXOS-WORLD SPATIAL MAPPING, SUCH AS THE USA, AUSTRALIA, CANADA, CHINA, INDIA, RUSSIA, AND BRAZIL.

3.3.2. The MESSAGEix-GLOBIOM ENGAGE SSP2 NPi2020 500 Scenario

For benchmarking and validation against the same scenario of [20], the soft-linking framework presented in this paper is applied to the ENGAGE SSP2 NPI2020 500 scenario simulated by the MESSAGEix-GLOBIOM integrated assessment model [89,100]. Of the Shared Socioeconomic Pathways (SSPs), SSP2 scenarios represent "middle of the road" scenarios wherein social, economic, and technological trends are comparable to those observed historically with uneven economic development and progress towards sustainable development goals. An exploration of the SSP2 narrative is examined based on key quantifiable markers in [101]. The NPI2020 500 scenario is consistent with warming limited to 1.5°C at the end of the century without exhibiting temperature overshoot. The [13]scenario ranks in the top 25% in the IIASA AR6 Scenario Explorer database on a hydrogen production basis. Of the total hydrogen produced in the scenario, approximately 78% is produced from electricity. The prevalence of hydrogen production (and electrolytic hydrogen production in particular) in the chosen scenario renders it an appropriate scenario for demonstration of the coupled hydrogen and electricity model framework. Figures 3.3 & 3.4 illustrate the context of the scenario with respect to the extent of hydrogen production and electricity-hydrogen system coupling (electrolytic fraction of hydrogen production) relative to other scenarios in the AR6 Scenario database.

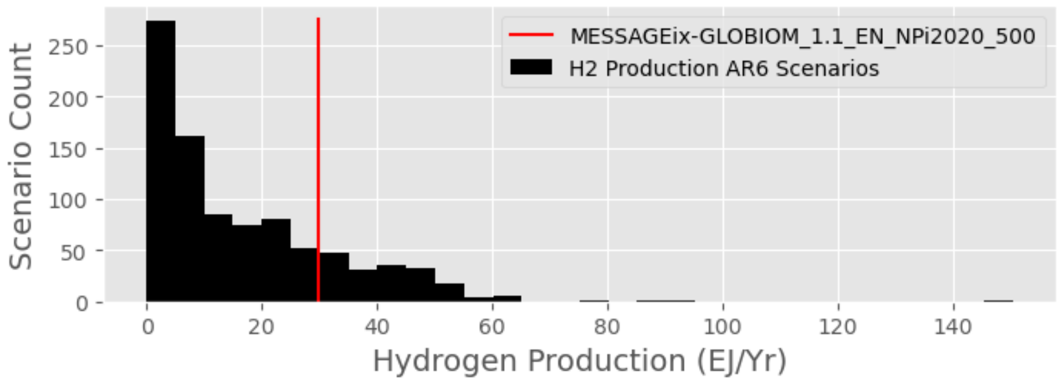

FIGURE 3.3 EXTENT OF HYDROGEN PRODUCTION FOR SCENARIOS ACROSS THE AR6 SCENARIO DATABASE [99].

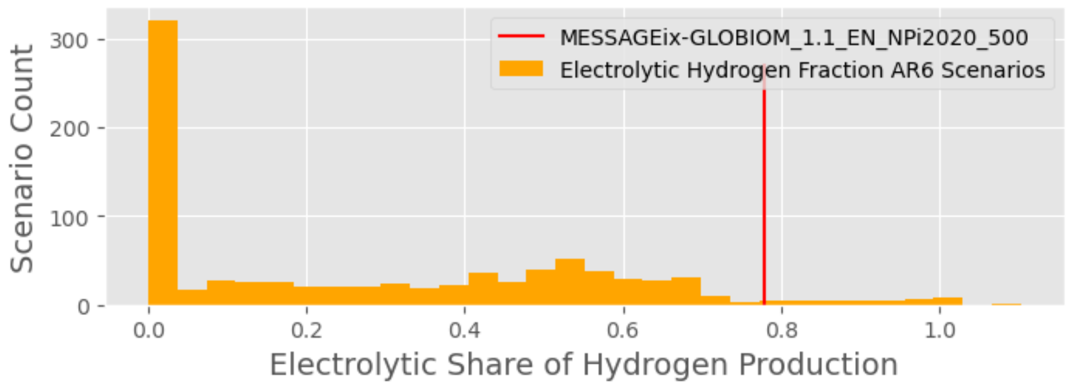

FIGURE 3.4 SHARE OF ELECTROLYTIC HYDROGEN FOR SCENARIOS ACROSS THE AR6 SCENARIO DATABASE [99].

3.3.3. Hydrogen Sector Representation

Figure 3.5 outlines the physical representation of the hydrogen (green) & ammonia (purple) systems and potential conversion pathways. In this study, the technology options are simplified to enable higher temporal and spatial resolution without incurring excessive computational penalties through more detailed representation. Considering the additional computational burden that explicitly modelling additional 'shippable' hydrogen derivatives might yield, ammonia is the only chosen carrier for shipping to be modelled based on the conclusions around the competitiveness of the different shippable carriers considered in [96]. Total final consumption of ammonia is not specifically published in the AR6 database for the SSP2 NPI2020 500 scenario, indeed the final consumption of hydrogen for ammonia production is published for only 3 of the 3241 scenarios in the AR6 scenario database at the time of writing. Given the lack of explicit scenario-aligned ammonia demand data, specific ammonia demand is not modelled. By default, it is assumed that ammonia must be cracked back into hydrogen to serve the hydrogen end use demand. However, considering that some of the final consumption of hydrogen will be for use as a feedstock for ammonia production, the ability to reconfigure the model to allow ammonia to service hydrogen demand directly without reconversion losses is provided for in the model framework. This is highlighted by the red dashed arrow in Figure 3.5.

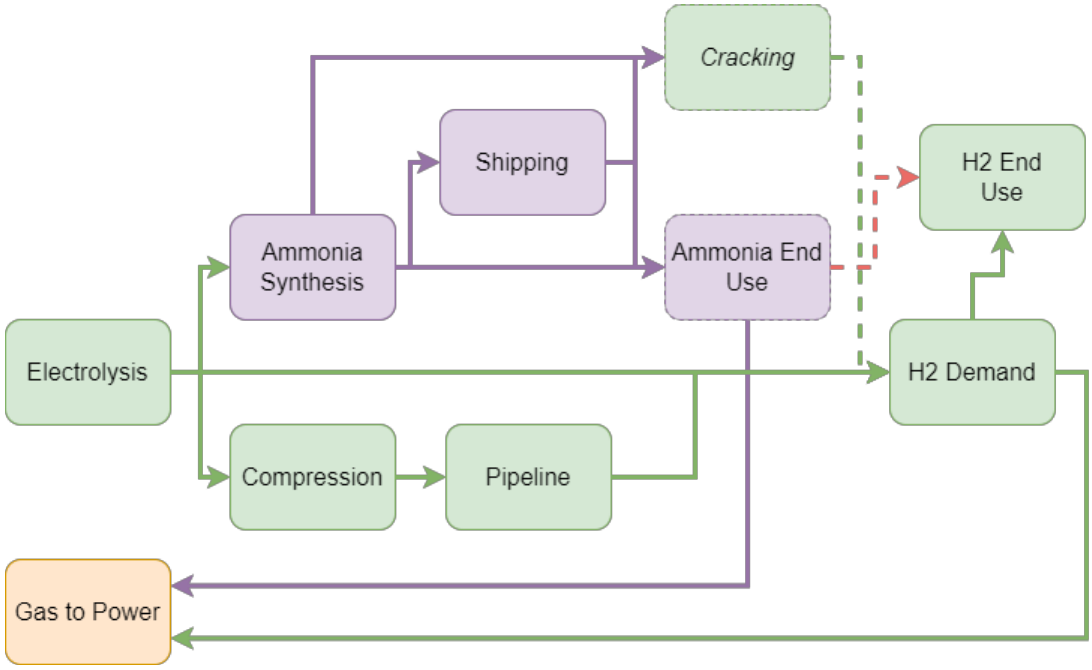

FIGURE 3.5 HYDROGEN & AMMONIA REPRESENTATION

In the MESSAGEix-GLOBIOM parameterization of power system flexibility requirements, long-duration storage via power-to-gas-to-power (P2G2P) does not appear to be explicitly represented. According to the MESSAGEix-GLOBIOM documentation [89], the IAM does allow for the blending of natural gas and hydrogen. Meanwhile, it is not explicitly stated as to what extent the blending of hydrogen and natural gas is permitted for power generation in gas turbines and no hydrogen specific power generation candidates are listed. In any case, considering the coefficient-based parameterization of system flexibility needs derived from [92] with short duration electricity storage assigned the maximum flexibility contribution, it is unlikely that hydrogen-based long duration storage could compete with battery storage on cost in the IAM.

Considering the lack of explicit representation of hydrogen long duration storage in the MESSAGEix-GLOBIOM IAM, the final consumption of hydrogen as soft-linked from the IAM is assumed to exclude hydrogen demand in the power sector in the current model which is allowed to resolve hydrogen (or hydrogen derivative) consumption in the power sector endogenously. Both hydrogen and ammonia-fired combined cycle gas turbines are modelled in the current work as a means for providing long-duration power system storage.

3.3.4. Transmission and Shipping

The electricity interconnector cost modelling and potential interconnection routes are the same as in [20]. Essentially, all adjacent land-based connections, all existing sub-sea routes and further sub-sea routes of significant potential as identified through the analysis in [102] are permitted. Initially, potential hydrogen pipeline routes are allowed to be built along the same pathways as the electricity interconnectors. Hydrogen pipeline costs for the modelling framework are consistent with the electricity interconnector cost modelling of [20] with cost inputs adapted from [96]. Pipe and compression losses are represented using an assumed loss of 2% per 1000 km based on [96,103].

As pointed out in [104], in the absence of some simplifying interventions reducing the number of possible shipping routes, globally co-optimising shipping within a model with many regions greatly inflates computational complexity of the model. In the example model run presented in this work, the candidate shipping routes of [104] are therefore leveraged rather than allowing all possible shipping routes.

Key physical properties to be modelled for shipped energy include the time taken to ship discrete volumes of energy from the origin node to the destination node. As the capacity allocation & expansion model phase is linearized to reduce the model's computational effort, the discretization of shipment loads is relaxed, and the shipping routes are modelled as continuously flowing connections. To represent the shipping time delay, the maximum energetic flow rate of the shipping routes is de-rated by the time taken for a shipment to travel its sea route. The net result is that the upper limit on the flow rate across a shipping route is still effectively limited by the capacity of the ships, the number of ships operating the route and the time taken for a shipment to be delivered across the route. For ammonia shipping, the traversal time is calculated using an assumed ship speed of 30 km/h and with distances calculated using the SeaRoute py python library [105] in line with the methodology employed by [104].

In this model, any given ammonia ship is effectively bound to operate only one potential trade-route. Rather than strictly operating the same route back and forth with an empty ballast (return) journey, carriers may choose to divert to another destination mid route or operate another route and bunker as convenient on the return journey to the origin node. Considering this, the maximum continuous flow rates of the route are not directionally constrained to maintain a more representative degree of flexibility in the operation of shipping routes. Ammonia carrier cargo capacity of 375000 MWh (LHV) is assumed based on the range of values for ammonia carrier cargo capacity discussed in [96] and carrier fuel consumption is applied as an efficiency loss of cargo along the route using a figure of 1% of cargo per 5000 km also based on [96].

By way of illustration, consider a potential shipping route between New South Wales, Australia and Singapore. SeaRoute yields a route with a total distance of 7626 km. The equivalent per-ship continuous flow capacity as implemented in the model can be calculated according to equation 3.1. With the assumed speed of 30 km/h and cargo capacity of 375000 MWh, the per-ship de-rated continuous capacity along the shipping route is 1,475MW. This assumption assumes that a ship does not necessarily run an empty ballast journey (in which case the capacity should be derated by twice the route distance in equation 3.1). Instead, it is proposed that future work should examine an appropriate de-rating multiplier of the route distance that should assume a value between 1 and 2. Finally, the route is assigned a globally uniform build cost per ship, and fixed operation and maintenance costs depending on the desired modelling inputs. In this case, a default placeholder per-ship build cost is assigned (initially negating the cost of additional port infrastructure), based on [96] and a placeholder fixed-operation & maintenance cost is applied.

$$Capacity_{cont.}(MW) = \frac{Ship\ Speed\ \left(\frac{km}{h}\right) \times Cargo\ (MWh)}{Route\ Distance\ (km)} \tag{3.1}$$

3.3.5. Energy Resource Potentials

Upper limits representing the maximum resource potentials for wind, solar and hydro resources at the PLEXOS-World spatial resolution are applied as in [20]. Respectively, these limits, as summarized in Table 1, are derived from [106] for solar potential, [107] for both onshore & offshore wind potential, and [108] for hydro potential. These sources are consistent with those used in the MESSAGEix-GLOBIOM IAM.

Resource	Study	Includes GIS-Based Physical Exclusions	Includes Economic Exclusions
Solar	[106]	Yes	Yes
Wind|Onshore	[107]	Yes	Yes
Wind|Offshore	[107]	Yes	Yes
Hydro	[108]	Yes	Yes
Geothermal	None	No	No

TABLE 3.1 REGIONAL NON-FOSSIL POWER GENERATION RESOURCE CONSTRAINTS

The hourly variability of wind and solar technologies is input into the model with two different sets of capacity factor timeseries. For wind, the capacity factors are the same as those in [20] developed from the Renewables Ninja platform [109,110]. For hourly power profiles, [20] leveraged capacity factor timeseries simulations derived from the Renewables Ninja platform using the MERRA-2 reanalysis dataset [32] for solar PV capacity factors. In [110] the authors note the need to correct the systematic bias of solar capacity factor simulations from the renewables.ninja platform while [111] suggests significantly lower overestimation bias exhibited by capacity factors simulated using the ERA-5 [33] rather than MERRA-2 reanalysis dataset. For this study, the solar power profiles from [19,20] have been updated based on the methodology and findings of [111] using the ERA-5 reanalysis dataset with the same locations and PLEXOS-World regional aggregation methodology. In the case of hydro, the same monthly capacity factor timeseries data developed from the work of [108,112] as in [19] are applied. For all three technologies (wind, solar & hydro) the capacity factor timeseries are based off the weather year of 2015.

Resource	Methodology
Solar	[111], [19]
Wind|Onshore	[19,109]
Wind|Offshore	[19,109]
Hydro	[19,108]

TABLE 3.2 RENEWABLE RESOURCE CAPACITY FACTOR TIMESERIES

3.3.6. Notes on Computational Aspects

For capacity expansion problems with high levels of variable renewables, the challenge of balancing computational effort versus the sufficient capture of the underlying variability is well treated across the literature [113–116].

The global coupled hydrogen & electricity model presented in this study is computationally intensive. At the target number of representative sample days of 2 representative days per month (i.e. a total of 24 sample days per year) and a reduced two-hourly resolution for the capacity expansion phase, the overall model run time was 6 hours and 2 minutes running on an Intel(R) Core(TM) i9-10900 CPU processor with 32 GB of RAM. The capacity allocation & expansion model phase took 3 hours and 12 minutes to run and consists of 27,552,931 non-zeros, 7,289,128 variables, of which 6,247,720 are continuous and the remaining 1,041,408 are binary integer variables. Meanwhile, the economic dispatch phase took 2 hours and 50 minutes to run with each daily step (at hourly resolution) consisting of 1,349,070 non-zeros, 512,007 variables, of which 437,847 are continuous and the remaining 74,160 are binary integer variable.

It would be possible to achieve lower model computation times with more rigorous capacity expansion sample settings (for example, with an hourly resolution rather than 2-hourly) by solving the capacity expansion of the R5 regions separately, stitching the solutions, and subsequently optimising cross-regional interconnection. However, other work has examined the impacts of spatial extent, and the representative sample size used for capacity expansion problem reduction found that solving across larger spatial extents yielded greater cost savings than solving for greater representative day sample sizes [116]. Brinkerink et al. [31] provide a framework for decision making surrounding model spatial extent and resolution and notes that more geographically extensive models may be of merit where constrained trade of commodities is an important factor, as is the case when examining future hydrogen trade scenarios in the current model framework.

3.4. Results & Discussion

3.4.1. Benchmarking & Validation

Examination of the the ENGAGE SSP2 NPI2020 500 scenario PLEXOS model run indicates that the modelling framework is functioning as intended. Both hydrogen and electricity nodal demands are seen to be met with electricity generation arising from diverse nodal technology portfolios. Figure 3.6 a) shows the power generation capacity portfolios built throughout the nodes that constitute the R5LAM (Latin America) region. In figure 3.6 b), these capacities are summed cumulatively from left to right and plotted next to the original soft-linked IAM capacities (R5LAM IAM) on the right-hand side demonstrating that the capacity soft-link is consistent with the IAM scenario regional capacity.

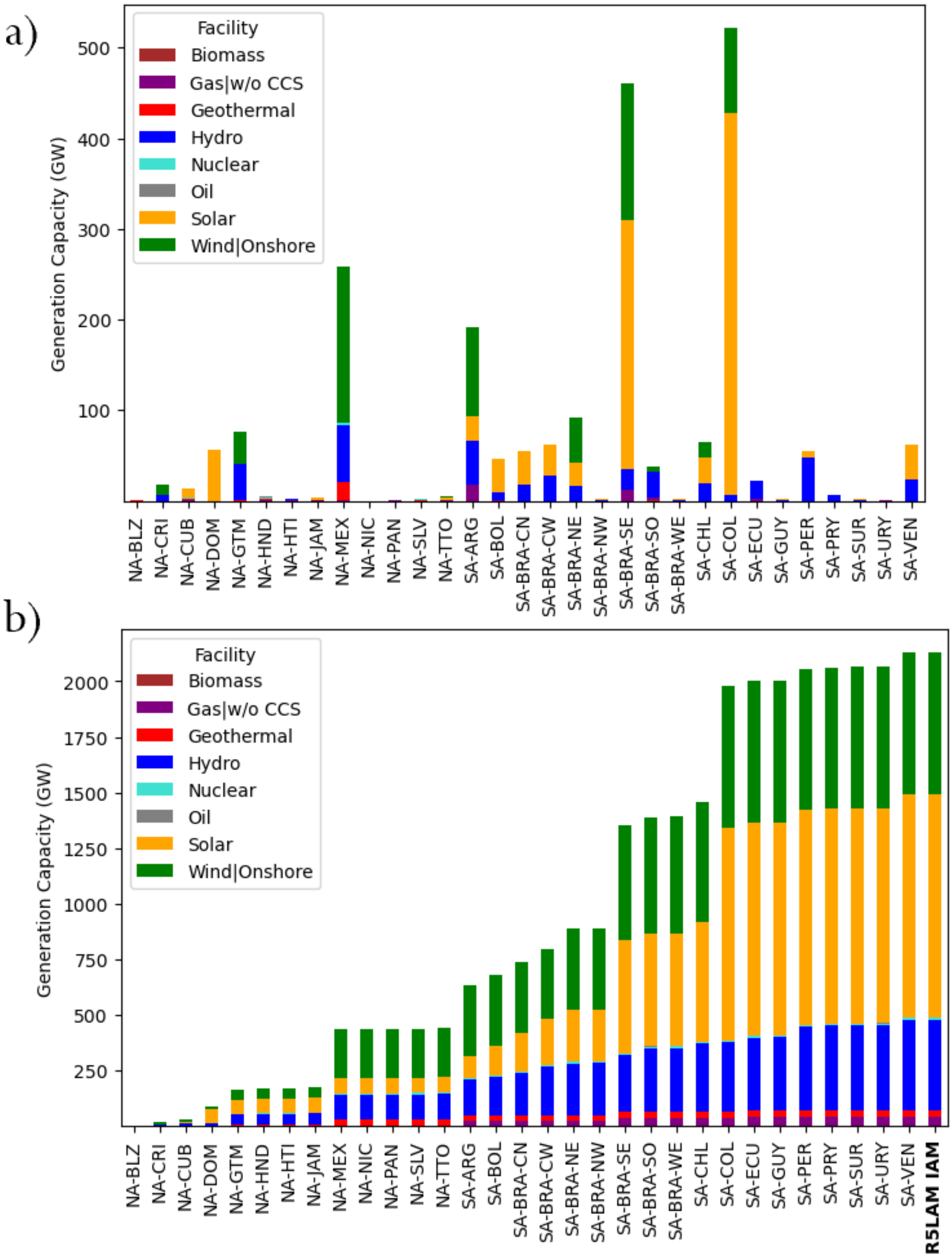

Figure 3.6 a) Nodal and b) Cumulative Power Generation Capacities Built at Nodes in the R5LAM region.

Figure 3.7 compares total global power generation by each generic power plant type in the soft-link model and the original IAM scenario. The soft-link model sees significantly less biomass power generation relative to the IAM output. In the AR6 scenario database, biomass with CCS power generation capacity in 2050 in the MESSAGEix-GLOBIOM NPI2020 500 scenario is reported as 0. However, in contradiction, power generation from Biomass with CCS in 2050 is reported to be 2.52 EJ. This reporting issue that sees biomass with CCS power generation capacity reported as 0 in the database despite non-zero generation is similarly observed for gas generation with CCS. Comparison of the Gas with CCS generation reported in the database at 5.85 EJ and the total Gas with CCS generation capacity reported in the database at 4.41 GW, implying a non-physical capacity factor above 4000%. This matter was queried with IIASA, the host institution of the AR6 Database. The apparent reporting conflict was known and arose due to the structure of the underlying MESSAGE model only allowing for the reporting of greenfield capacity additions of the CCS power generation technologies whilst substantial retrofit CCS capacity is seen in the EN NPi2020 500 scenario. This issue has been rectified for more recent MESSAGE model configurations.

Gas power generation without CCS is much higher in the soft-link model compared to the IAM scenario. This is due to the need to compensate for the missing biomass with CCS and gas with CCS generation, however, the implications of the static CO2 price in the soft-link model versus a binding emissions constraint in the IAM should also be considered in soft-linking studies where it is intended to closely emulate or study the original IAM scenario.

For geothermal, hydro, and nuclear power, the agreement is good, however the current model exhibits slightly higher generation for each technology. This is best explained by the lack of explicit maintenance outage rate modelling in the current work leading to elevated capacity factors for dispatchable technologies. A shortfall in wind and solar power generation is observed in figure 3.7, which will be discussed in following analysis.

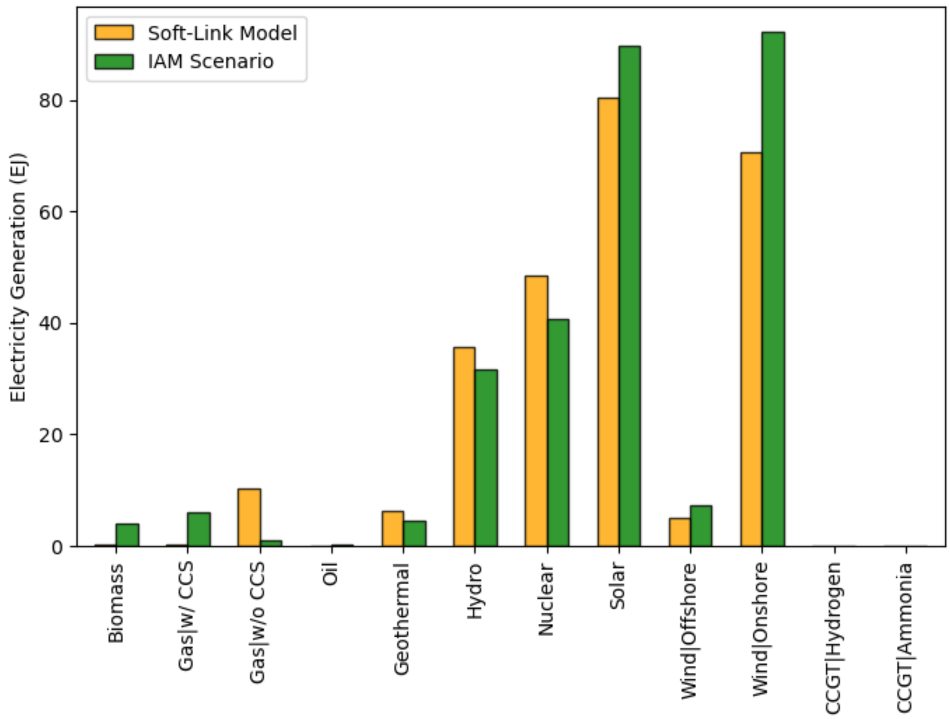

FIGURE 3.7 GLOBAL ELECTRICITY GENERATION BY FACILITY TYPE (2050)

When examining the global buildout of capacity for each power generation technology type, the soft-link model did not choose to build additional wind and solar capacity relative to the integrated assessment model as can be seen for the R5LAM region in figure 3.6 b). This contradicts our hypothesis that the model would need to build more capacity compared to the IAM scenario to compensate for the additional curtailment and incidence of unserved energy as observed by [20].

While some unserved energy is seen in the current soft-link model, it is less than that observed in [20] with 0.049% of global electricity demand and 1.04% of global hydrogen demand unmet compared to between 2.5% and 5% of global electricity demand unmet in [20]. Globally, curtailment of Solar PV relative to the total availability falls within the lower end of the range of 4 to 11% observed across the scenarios in [20] at 4.99% curtailment in the current model. For onshore and offshore wind, the capacity weighted average curtailment falls outside of the observed range of 4% to 8% in [20] at only 3.18% globally.

Considering limited unserved energy, relatively low curtailment levels and approximately equal wind and solar capacities, the question remains, where has the "missing" wind and solar electricity generation observed in figure 3.7 gone in the soft-link model? Some of the discrepancies between the IAM scenario wind & solar generation and those of the soft-link model are attributable to differences in the asserted resource availability. [111] suggested overestimation of the solar PV capacity factors in [20], which in turn were noted to be conservative compared to those in the MESSAGEix-GLOBIOM model scenario. However, in total, approximately 20 EJ less electricity generation is seen across all technologies compared to the IAM scenario, which must be accounted for.

In the MESSAGEix-GLOBIOM model scenario, a global portfolio of nearly 6 TW (24 TWh) of battery storage is seen in 2050 and is associated with 18.46 EJ of round-trip losses as seen in figure 3.8 a), which charts energy flows in the IAM scenario. In comparison, the soft-link model builds 3.2 TW (12.8TWh) of battery storage globally and is associated with 3.16 EJ in round-trip losses as seen in figure 3.8 b). The significant difference in storage losses between the models is explained by the lower capacity and utilization seen in the soft-link model, with 47% capacity weighted average utilization in the soft-link model versus an implied utilization of approximately 88% in the IAM scenario (calculated assuming the 80% round-trip efficiency noted in [20]). Considering that battery capacity deployment in the IAM is driven by a parameterized reliability constraint, rather than the resolution of short-term variability of supply and demand, the differences in the extent of battery deployment are not surprising. Here, battery storage losses have been shown to account for over three quarters of the difference in overall electricity generation between the models, a balance of approximately 4.7 EJ, or 1.7% of the total electricity generation in the original IAM scenario, remains to be accounted for.

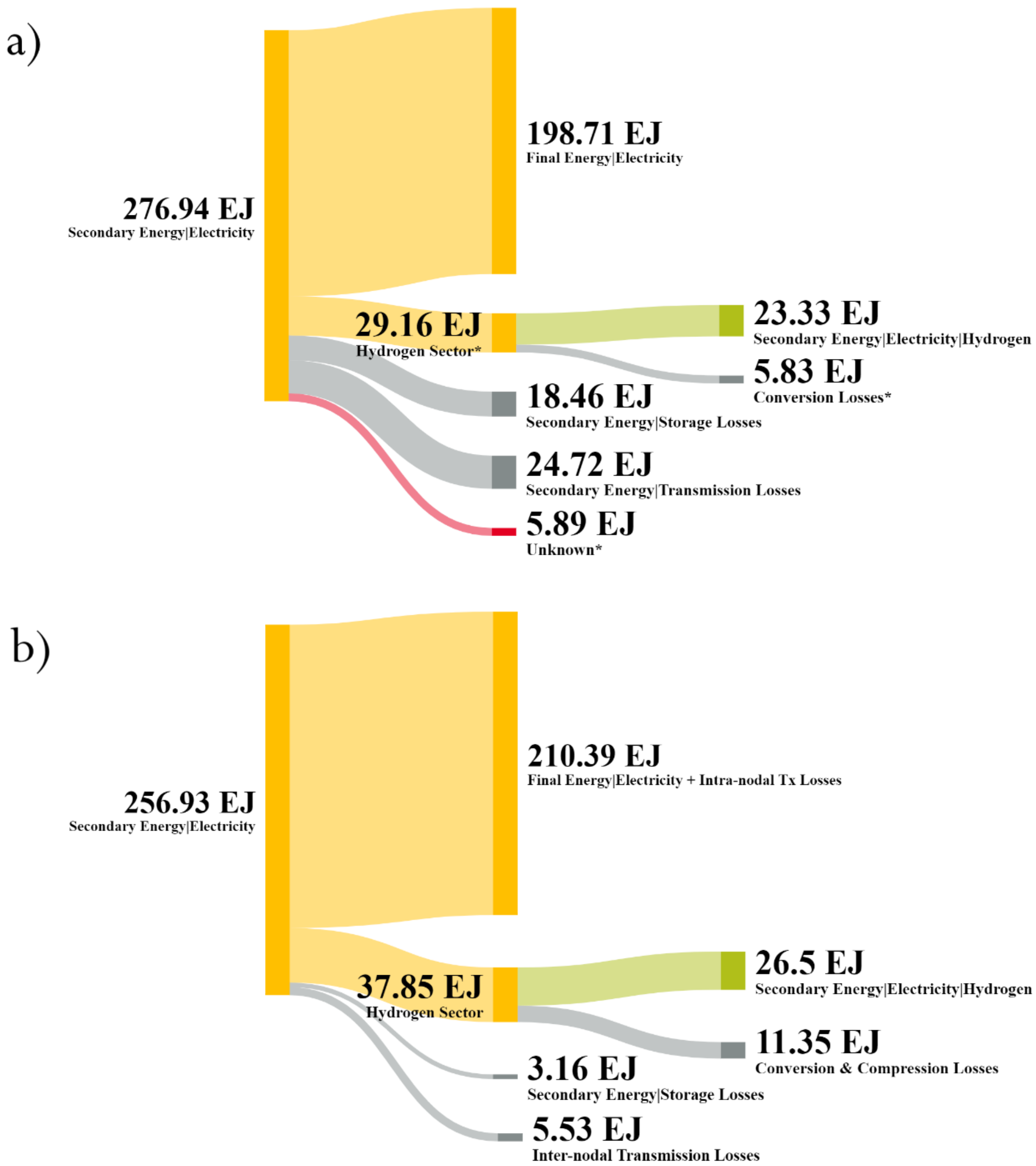

FIGURE 3.8 A) IAM SCENARIO AND B) SOFT-LINK MODEL ENERGY FLOWS IN 2050. *VARIABLE IS INFERRED.

Variables marked with * in figure 3.8 a) are calculated assuming electrolysis conversion efficiency of 80% in line with that assumed in the original IAM scenario according to [20]. Notably, these calculated values leave 5.89 EJ unaccounted for indicating unreported electricity consumption or a more conservative hydrogen production efficiency than the assumed 80%. In the current model we are accounting for hydrogen production once it has been compressed with an electricity to compressed hydrogen conversion efficiency of 70% whereas the pressure at which hydrogen production is counted in the IAM scenario is not explicitly stated.

Due to the configuration of the spatial domain in the soft-link model, intra-nodal (domestic) transmission and distribution losses are represented separately to inter-nodal transmission losses as in [20]. Effectively, intra-nodal losses are added to the final demand as reflected by the additional 11.68 EJ attributed to the Final Energy|Electricity (+ Intra-nodal Tx Losses) in figure 3.8 b). This, 11.68 EJ domestic losses combined with the 5.53 EJ internodal losses amounts to 7.51 EJ less transmission loss compared to the 24.72 EJ losses in the IAM.

Considering that neither the precise electricity to hydrogen conversion efficiency and the pressure at which hydrogen energy is being counted are not explicitly published for any given scenario in the AR6 scenario database, the 'unknown' electricity consumption estimated in figure 3.8 a), and the lower electricity transmission losses in the soft-link model, we can consider the remaining electricity generation discrepancy of only 1.7% of generation in the original IAM scenario to be accounted for therein.

At this point, differences in global production of electricity and electrolytic hydrogen between models have been accounted for and the high-level production, conversion and consumption dynamics of the model can be seen to function as intended. However, the differences observed underscore the pivotal importance of conversion efficiency assumptions as inputs in sector-coupled models, particularly when soft-linking power generation capacities to the original IAM scenario levels. If the soft-link model sees marginally more efficient pathways from primary energy to final consumption as in the current work, soft-linking the capacities to the original IAM may force an excess of power capacity. This can contribute to the deficit in wind and solar generation observed in figure 3.7 if the model is less energy constrained and can afford to allocate wind and solar capacity to regions of lower resource potential if it avoids incremental transmission or storage investment.

Of the benchmarked results explored in this comparison exercise, one further aspect warrants explanation. That is, considering that the model is not energy constrained, why does the unserved energy observed arise in the first place? Furthermore, why is the level of unserved energy lower in the current model than that of [20] despite additional energy demand incorporated through the hydrogen sector? In this case the occurrence of unserved energy in the current work is attributable to the chronological sampling in the capacity allocation phase of the soft-link model failing to capture extremes in the hourly renewable power profiles outside of the sampled representative days. This also raises the implication that at least some of the unserved energy and curtailment observed in [20] also derives from the sampling configuration in the capacity allocation and distribution.

Logically, expansion models driven by representative samples have the potential to encounter challenges in the case of global models with deep wind & solar power penetration such as the MESSAGEix-GLOBIOM SSP2 EN2020 500 scenario.

In PLEXOS, sampling of the representative periods is carried out such that similar periods are eliminated from the sample set, leaving a reduced set that is representative of the variation in the original timeseries. From this reduced set, a number of samples are then drawn per the user-defined settings, and the average magnitude of the samples are scaled to match the parent set [117]. This means that in this case this study, the availability factors of the renewable resources across the two representative days sampled per month are scaled to equal the average availability across their original parent month. In a model with global extent, this statistical elimination process has the potential to be "noisy" given that a day or week that is statistically similar at one node may be statistically dissimilar at another. For instance, weekly solar capacity factors at some nodes along the equator may see many statistically similar weeks, while nodes further from the equator will see greater weekly variation. As a result, sampling a few representative sample weeks per year will have more difficulty in capturing the annual nature of renewable resources than sampling a couple of days per month. By asserting that a number of representative days must be sampled each month rather than a number of weeks per year, the capacity expansion phase of the model is able to build capacity portfolios that better account for seasonal resource balancing. However, [20] highlights that sampling daily profiles for wind power can lead to an unrealistic diurnal shape that may favor storage buildout over and above transmission investments. Consequently, while global unserved energy levels are lower in the current model, the potential influence of the resulting sample patterns on technology preference should be considered carefully. In fact, while representative sampling is generally well treated across the literature [118–120], further work examining optimal sampling strategies for global or spatially extensive models may be of merit.

3.4.2. Model Framework Utility: Future Global Energy Trade

The primary focus of the discussion has been the benchmarking and validation of the model framework; however, it would be remiss not to demonstrate the utility of the framework with respect to the stated aim of enabling detailed insight into inter-regional hydrogen & electricity trade. To this end, some high-level analysis of the results from the soft-link model is presented here to demonstrate proof of concept of the model function.

Figure 3.9 illustrates energy trade occurring between nodes via electricity interconnectors, hydrogen pipelines and ammonia shipping routes with total annual energy exchange proportional to the thickness of the route lines. The high-level dynamics are as expected with internodal electricity trade leading that of gaseous hydrogen which in turn leads that of shipped ammonia based on total annual energy exchange. Figure 3.10 shows the annual nodal electricity generation net of the annual nodal electricity demand at each node in the soft-link model with surplus net generation marked in yellow, and net deficits (where local demand exceeds local production) marked in brown. Similarly, figure 3.11 shows a) nodal net hydrogen production with surpluses marked in green, and deficits in red and b) nodal net ammonia production with surpluses marked in turquoise, and deficits in purple. Several interesting observations relating to energy trade aligned with the NPI2020 500 scenario emerge from figures 3.9, 3.10 and 3.11.

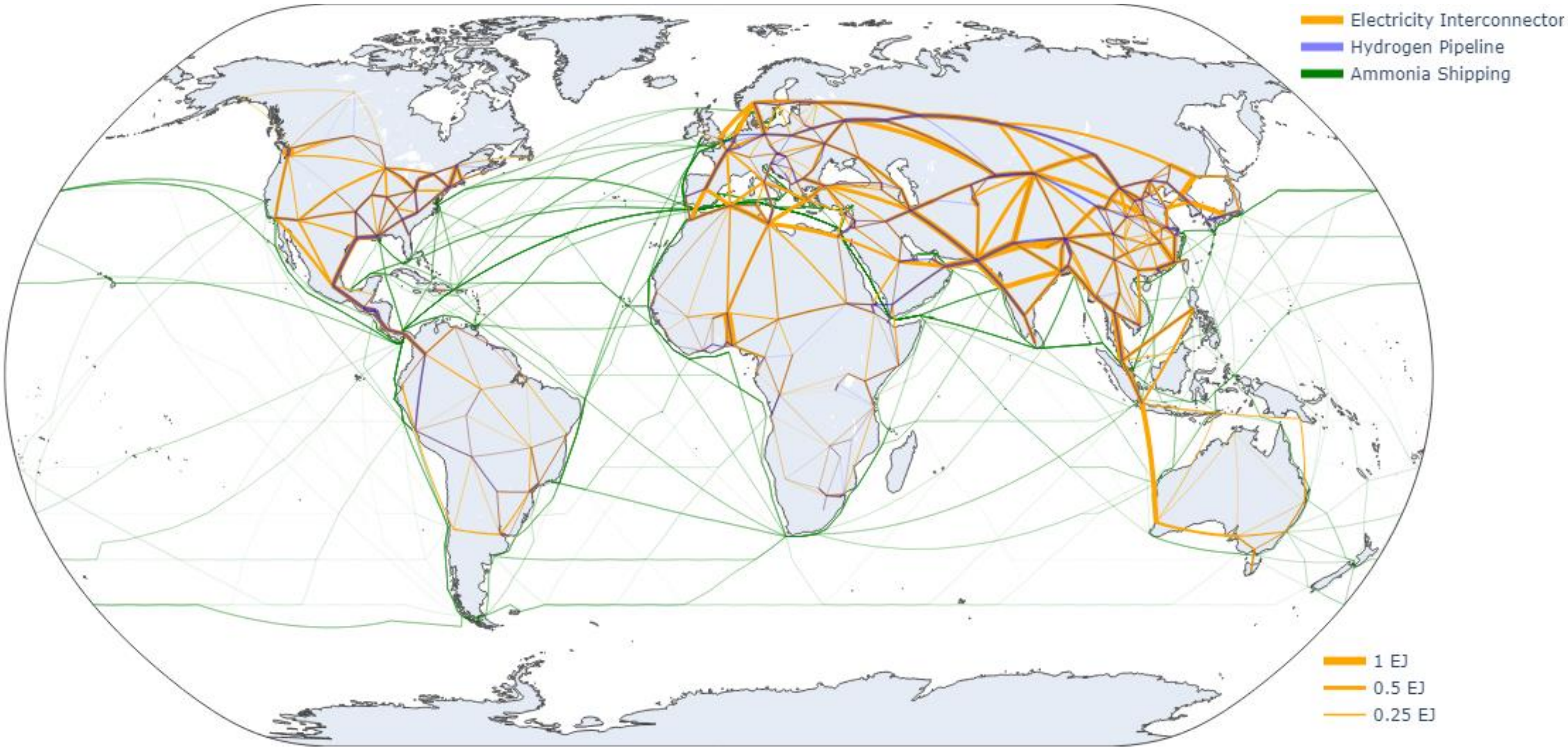

FIGURE 3.9 TOTAL ANNUAL ENERGY EXCHANGE (2050)

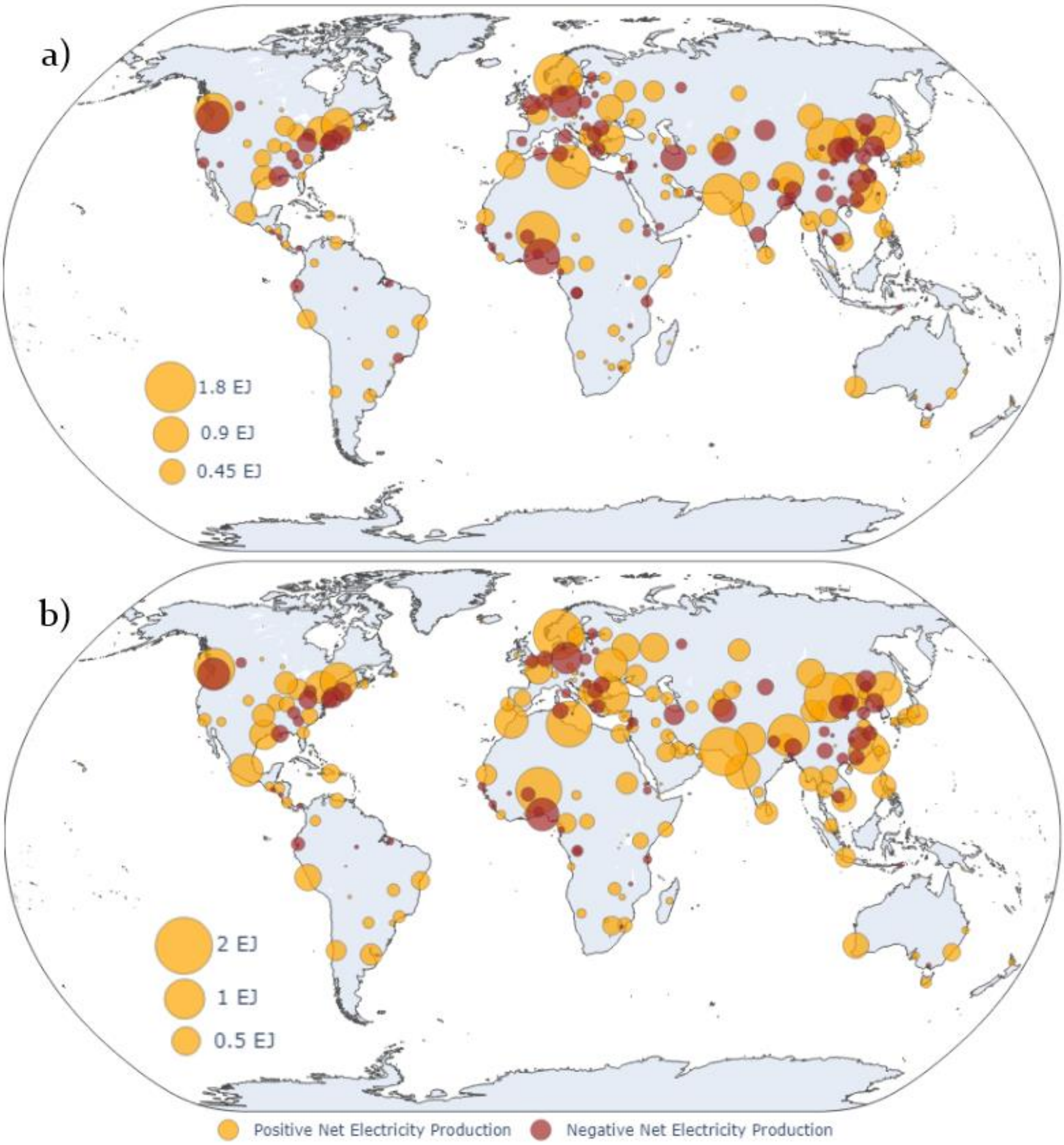

FIGURE 3.10 NET NODAL ELECTRICITY GENERATION A) INCLUDING AND B) EXCLUDING ELECTRICITY DEMAND FOR ELECTROLYSIS (2050)

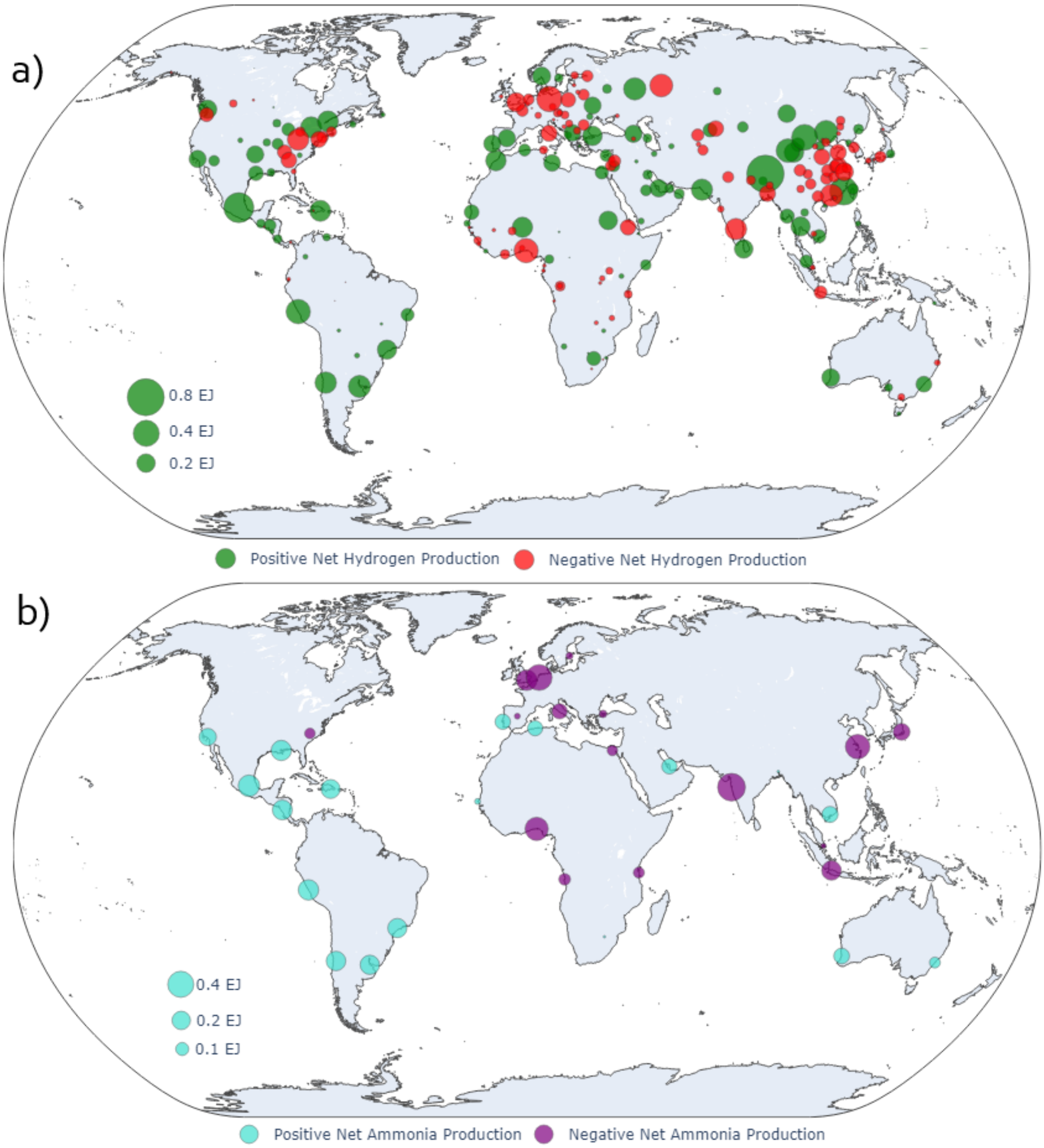

FIGURE 3.11 NET NODAL A) HYDROGEN AND B) AMMONIA PRODUCTION (2050)

From figures 3.10 and 3.11 it is apparent that net-deficits of electricity and hydrogen production in regions of very high projected demand such as in Central Europe, Eastern China and to a lesser extent, Central Asia are being fulfilled through net surpluses in surrounding regions such as Western Russia, Mongolia, and Pakistan respectively. This drives extensive interconnection and East-West energy exchange across the Eurasian Continent.

The concentration of energy demand in Central Europe, observed through deficits of both Electricity and Hydrogen in figures 3.10 and 3.11, also drives significant electricity interconnection between North Africa and Southern Europe. In figure 3.9, a "spine" of hydrogen flows emerges from the Iberian Peninsula, through France and into the Netherlands, Belgium, Germany and Poland. Interestingly, considerable electricity is exported from Morrocco to Spain and Portugal, both of which are seen to exhibit deficits in net electricity production in figure 3.10 a). However, figure 3.10 b) shows the two countries producing significant surpluses of electricity when electrolysis is excluded. Moreover, figure 3.11 a) shows significant surpluses of hydrogen production in the two countries. In other words, electricity is being imported by Spain and Portugal to produce hydrogen for export northwards along the hydrogen "spine". Considering that some hydrogen is also directly exported from Morrocco and into Portugal as seen in figures 3.9 and 3.11, this raises the interesting question as to when it is more valuable to export hydrogen from Region A to Region B directly, or to export electricity from Region A to Region B and use it to produce hydrogen locally at Region B. In a coupled electricity and hydrogen system, the answer to such a question is non-trivial, with the optimal capacity of an individual technology at a system node being a function of both the benefit of the capacity to the electricity and hydrogen system needs individually, and the value provided by cross-sectoral interaction.

A similar "spine" of hydrogen pipeline flows emerges from South America, through Central America and up the Eastern Seaboard of the USA with net surpluses for both electricity and hydrogen seen across South and Central America in figures 3.10 and 3.11. Some of this surplus hydrogen production is ultimately exported as ammonia. Figure 3.11 b) shows net nodal ammonia production with South and Central America leading global ammonia exports. This underscores the notable trans-Atlantic ammonia trade in figure 3.9 with the Netherlands, the UK, and Nigeria seen as ammonia importers in figure 3.11 b). In the Indian Ocean and Asia-Pacific, India, China, Indonesia and Japan are the largest ammonia importers with Australia, Vietnam and Qatar leading ammonia exports. These exports are further supplemented with trans-Pacific ammonia shipping from South and Central America as seen in figure 3.9.

Naturally, the analysis presented here is not exhaustive and it would be possible to more closely examine trade dynamics in specific regions or, of course, to analyse other potential variables of interest such as optimal regional power generation capacities and the distribution of electrolysis capacity. In any case, it has been demonstrated that the modelling framework can enable substantial insight into electricity and hydrogen energy trade in future scenarios associated with a given set of techno-economic input assumptions. In doing so, the ubiquity of electricity interconnection and the development of snaking hydrogen “spines” is noted in the modelled scenario.

Chapter 4 The Boy Who Cried Hydrogen: Examining the Cost Impact of Proactive Vs Reactive Policy for Electrolytic Hydrogen.

Mathews D, Deane P (2025). The Boy Who Cried Hydrogen: Examining the Cost Impact of Proactive Vs Reactive Policy for Electrolytic Hydrogen. International Journal of Hydrogen Energy 191: 152350 doi: 10.1016/j.ijhydene.2025.152350

4.1.1. Abstract

Hydrogen as an energy carrier has experienced repeated hype cycles with periodically surging enthusiasm subsequently followed by low levels of deployment and waning enthusiasm. Despite these anticlimactic false dawn events, research points towards important roles for hydrogen in a future decarbonized global economy. The repeated nature of these cycles opens the hydrogen sector to "the boy who cried wolf" effect which may see policymakers hesitate to subsidize and plan for the hydrogen sector considering multiple "false alarms". This work contextualizes potential cost penalties if a significant future demand for hydrogen arises in a policy environment defined by hesitation. Overall, we find that reactively rather than proactively integrating the electrolytic hydrogen sector with the power sector could be 8-15% more expensive costing between 27 and 31 billion USD annually in 2050. We further find an isolated rather than integrated electrolytic hydrogen system could be 33-41% more expensive, costing between 82 and 106 billion USD annually in 2050.

4.2. Introduction

4.2.1. Context & Hype

From the late 20th century hydrogen as an energy vector has experienced cycles of interest and investment which have subsequently dissipated before the heralded "hydrogen economy" could materialize [11,12,121]. The pronounced and repetitive nature of this phenomenon is such that the hydrogen 'hype' has become a regular topic in studies examining technology hype cycle models [13,122–124]. In recent years, it appears that the peak of one such hydrogen hype cycle may again be giving way to headwinds with high numbers of hydrogen project cancellations reported [15]. Moreover, references to the "trough of disillusionment" are seen frequently across industry and social media [8,9,125]. The "trough of disillusionment" is a term associated with the Gartner Hype Cycle Model [124] in which the trough is followed by the "slope of enlightenment" and "plateau of productivity" as the technology matures and fulfills a realistic (rather than exaggerated) role.

Naturally, technological development and deployment pathways do not strictly adhere to any one model however useful they may be in examining technological progression or hype. Rather than strictly following the Gartner Cycle, hydrogen energy technologies have experienced several 'peaks of inflated expectation' and subsequent 'troughs of disillusionment.' However, these cycles have not yet resulted in the significant deployment levels that would indicate a true 'plateau of productivity' phase [10,11,13,15]. Notwithstanding the challenges the low carbon hydrogen sector is presently facing, recent literature points towards important roles for hydrogen in a decarbonized future global economy [12,14,15,17,121] and, consequently, an important role for subsidy [12,15].

This places policymakers in the unenviable position of determining appropriate subsidy levels and mechanisms to meet long-term decarbonization targets while navigating confounding cycles of exaggeration and disillusion in the clean hydrogen sector. Here, we suggest that the potentially important role of hydrogen in conjunction with its pronounced hype cycles open the door to a possible "boy who cried wolf" or "false alarm" effect. The erosion of trust due to repeated unfulfilled statements is a well-studied social phenomenon. This effect is often studied in relation to societal responses to severe weather warnings, for example, where hesitation to act on a potential false alarm has been observed to lead to sub-optimal responses [126,127].

In relation to hydrogen, this poses a risk that the repeated false starts of the hydrogen sector erode policymakers' trust in the underlying technologies leading to hesitancy and delays in infrastructure investment as policymakers become wary of committing resources to initiatives that may not materialize as promised. This is compounded by concerns around the impact of electrolysis loads on power sector emissions in the short term while the power sector is still in the process of decarbonisation. Such concerns have formed the rationale behind the European Union's strict requirements around emissions and renewable power generation additionality for electrolytic hydrogen under the Renewable Energy Directive (RED II) [29,30]. In [128] however, it is shown that allowing unrestricted use of grid electricity for hydrogen production, without applying constraints on the electricity's fuel mix, can lead to significantly lower production costs. Importantly, this does not necessarily result in higher emissions compared to the current use of unabated fossil hydrogen. Both [128] and[27] highlight increased costs of electrolytic hydrogen production under RED II. The authors of [27] find that with a sufficiently high carbon price, emissions benefits of electrolytic hydrogen can be maintained without the temporal congruency rule in RED II.

This work does not critique future competitiveness of hydrogen technologies or their short-term impact on emissions and instead we seek to understand the costs implications of uncertainty in policy planning for electrolytic hydrogen. Here we focus on electrolytic hydrogen specifically given the potential for close integration with the power sector. This coupling could lead to significant benefit through mechanisms like capacity sharing and flexibility provision, or indeed it could lead to increased stress on the power sector as RED II aims to avoid. Should a significant future role for hydrogen fail to materialize, policy hesitation on the matter would not be expected to pose significant consequences. However, if a significant future role for hydrogen does arise, hesitant or restrictive policy could lead to sub-optimal outcomes. This paper therefore puts some context on two particular research questions that arise as a result of these concerns. Specifically, what is the cost of global delay or hesitation in reactively planning for clean electrolytic hydrogen as opposed to proactively planning for an integrated coupled electricity and hydrogen system? Secondly, what is the cost of asserting isolation of the electrolytic hydrogen system from the power sector in a scenario where the coupling of the two sectors is discouraged by restrictive policy? Current literature points to cost penalties for restricted coupling of electricity and hydrogen at the hydrogen project level [122,123]. In this work, we will examine the global system-level impact of restricted coupling to capture knock-on effects in the power sector. In examining these questions under two scenarios in which significant demand for hydrogen emerge, this study aims to serve as a prompt upon which future work can build more exhaustively.

4.2.2. Hydrogen System Modelling & Co-Optimisation

A range of modelling approaches have been developed to analyse the role of hydrogen in energy systems, each varying in scope, complexity, and application. The full taxonomy of hydrogen system models across the literature and the benefits and trade-offs of each model archetype have been examined in [17]. These include integrated assessment models (IAMs), energy system models (ESMs), and power system models among other model archetypes. Regarding IAMs, the authors of [17] highlight their broad scope and ability to represent interactions between the energy system, the economy, and earth systems. However, such models exhibit low spatial and temporal resolutions considering the need to balance model complexity and tractability. ESMs and power system models both exhibit lower respective sectoral scopes than IAMs thereby affording greater flexibility for higher spatial and temporal resolution. However, these respective reductions in complexity require further exogenous inputs or assumptions at the boundaries with the other sectors outside of the models' scope. In model formulation terms, this reduction in scope or complexity (from IAM to power system model for example) amounts to a reduction in endogenous variables.

In [129], the framework for high resolution global coupled electricity and hydrogen models that will underpin the modelling in the current work was introduced. The issues of computational intensity, spatio-temporal resolution and sectoral scope or endogeneity are also prevalent in [129] wherein a power system model is soft-linked to an IAM to preserve the endogenously resolved hydrogen demand of the IAM within a higher resolution model. As these issues are a recurring theme across the energy system modelling discipline [14,17,31,129–131] I propose the definition of the "Energy Modelling Trilemma" (see figure 4.1) of computational tractability, spatio-temporal resolution and endogeneity (or scope) much like the "Energy Trilemma" of security, affordability and sustainability.

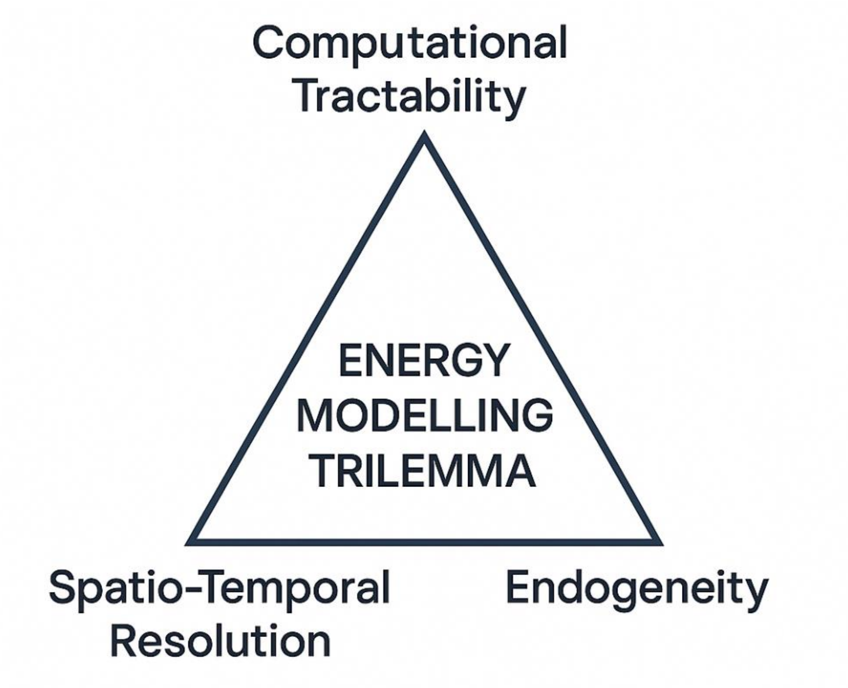

FIGURE 4.1: THE ENERGY SYSTEM MODELLING TRILEMMA

In physical terms, a reduction in endogeneity as model scope is reduced often manifests as a reduction in the degree to which the relevant sectors are co-optimised. It is established across industry and academic literature that co-optimisation has significant potential to deliver cost-savings, whether that encompass the co-optimisation of the planning and or operation of integrated sectors or intersectoral co-optimisation of energy and reserves in the power system for example [132–134]. Conversely, negating to co-optimise and integrate can lead to cost penalties. In this study, a system in which hydrogen is reactively planned is considered a system in which the electricity system is exogenous to the hydrogen sector model as it has already been planned and built around electricity demand only. In other words, the hydrogen demands are only known after the electricity system has been built. The proactive hydrogen system is that which is endogenously co-optimised alongside the electricity system with perfect foresight. In examining the relative cost penalty, it will contribute to the research gap identified in [17] in which it was noted that "Some studies have examined the consequences of having limited foresight, but not for hydrogen systems".

The same concepts extend to an isolated hydrogen system. From a modelling perspective, the electricity system is exogenous to the isolated hydrogen system, which does not interact with the power sector other than through competition for renewable power generation potential. Hydrogen is frequently modelled as an isolated system across the literature often to reduce the complexity of the model. For example, the large three-part study by the International Renewable Energy Agency[95–97] models a future global hydrogen system that is isolated and not co-optimised alongside an existing power sector while [94] optimises isolated country level hydrogen systems for least cost green hydrogen exports. In the current work, in examining the costs of a forcibly isolated electrolytic hydrogen system, we will also provide a sense of the potential system cost error impact of negating to explicitly model a coupled electricity sector when not specifically modelling off-grid hydrogen systems.

4.3. Methodology

4.3.1. Existing Modelling Framework

The base model in this study is derived from the high spatial and temporal resolution global electricity & hydrogen framework presented in [129]. The modelling framework presented in [129] is centered around PLEXOS, a commercial modelling tool typically used to model power systems. The framework builds on the soft-linking methodology of [20] in which a power system model is soft-linked to an IAM scenario so as to downscale and assess the scenario at higher spatio-temporal resolution. In [129], this framework is extended to include the hydrogen sector and validated against an IAM scenario.

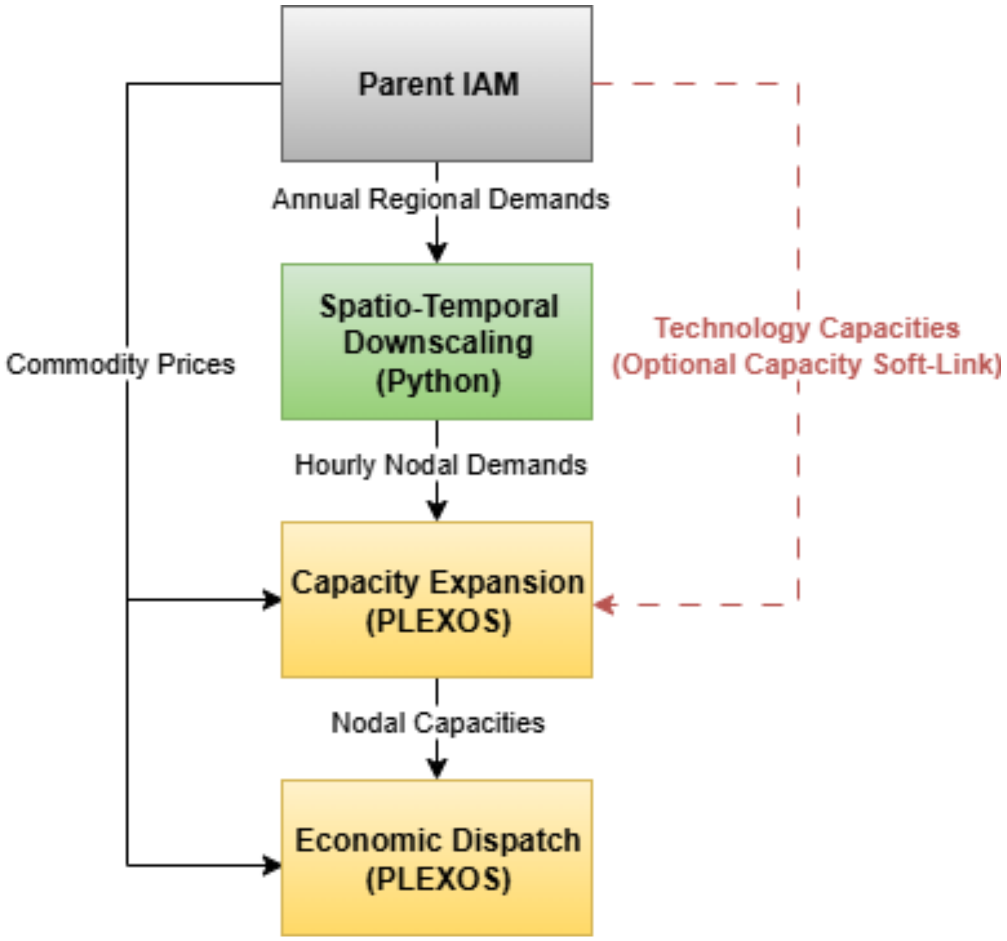

FIGURE 4.2: EXISTING MODEL FRAMEWORK

Figure 4.2 presents a summary flow chart of the existing modelling framework. The annual regional electricity and hydrogen demands from the parent IAM scenario are spatially and temporally downscaled as outlined in [20] and [129] and passed exogenously to the core 256 region PLEXOS model. The core model is implemented in two phases, a capacity expansion phase and an operational economic dispatch phase. In both [20] and [129], the IAM regional power generation technology capacities are fixed in the capacity expansion phase via an equality constraint. Effectively, in [20] and [129], the capacity expansion model is simply determining the geographic distribution of the technology capacity and not the overall level. In the current work, the model is configured to perform a capacity expansion for each candidate technology without constraining them to equal those from the parent IAM scenario. However, the hydrogen and electricity demand inputs are still derived from IAM scenarios in this study. This is to ground the energy commodity demands at a level that has been resolved endogenously in an energy system model with technological competition. As in [129], the capacity expansion models are run on a greenfield basis for a single target year - 2050. This simplification versus a multi-annual horizon is to maintain computational tractability at high temporal and spatial resolution. The temporal resolution of each model phase is flexibly configurable. In this study, we maintain an hourly resolution for the economic dispatch model phase and the two-hourly resolution for the capacity expansion model phase as in [129] but with a reduced sample of one representative day per month for computational efficiency. The objective function of both model phases is to minimize the total system costs subject to typical energy balance and capacity constraints. Full details on the mathematical formulation of the PLEXOS model are provided in the appendix of [129] and the data inputs needed to recreate these results in PLEXOS are provided in the data repository at DOI: 10.17632/pj7sxvmzy2.1 [135].

4.3.2. Study Conceptual Design

The high-level design of the study is illustrated in figure 4.3 below with the core model run in three different configurations to simulate i) the proactively planned scenario, ii) the reactively planned scenario, and iii) the isolated systems scenario. Across the configurations, all demand and cost inputs remain the same, only the sequence of optimization is varied. Note, when referring to cost in the study design, we are referring to total annualized system costs.

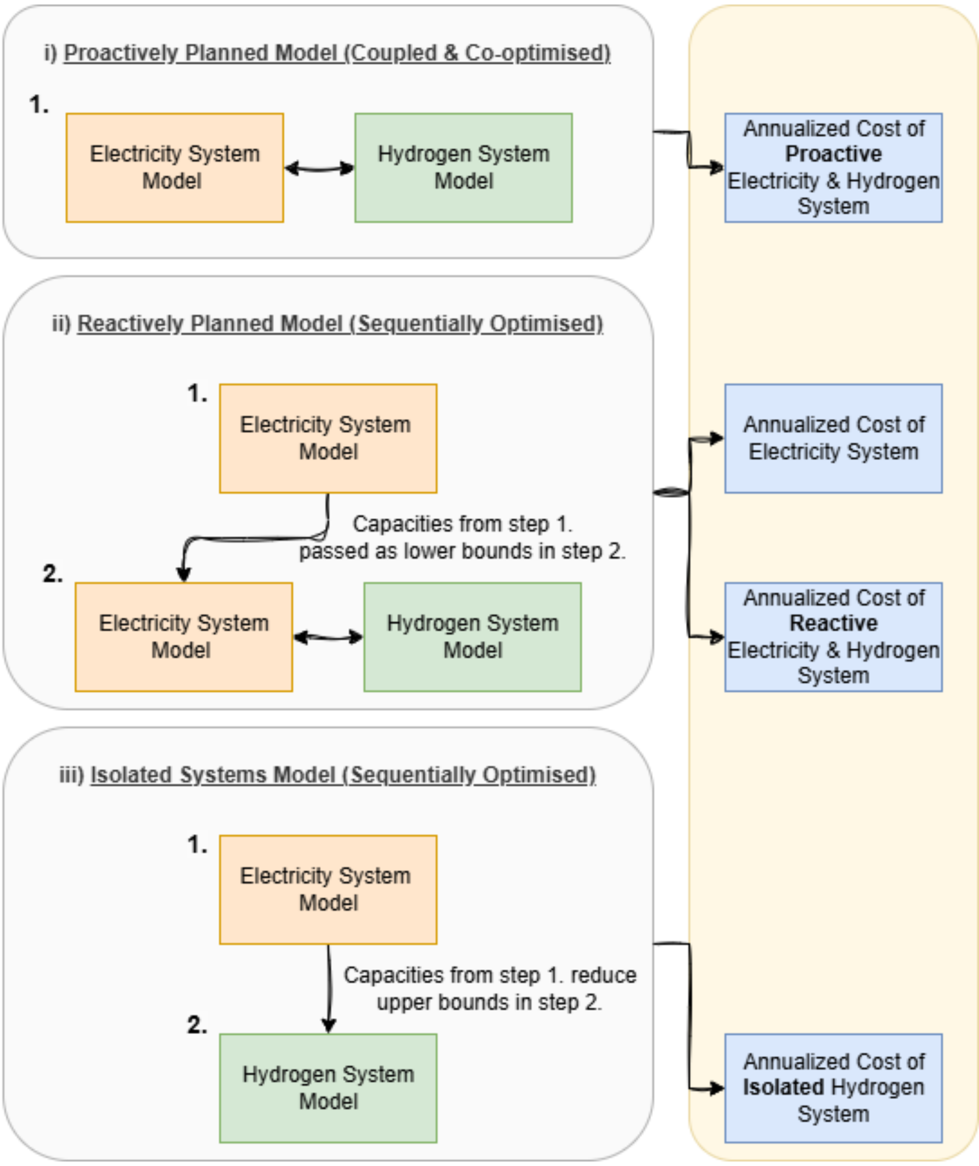

FIGURE 4.3: HIGH LEVEL DESIGN

In configuration i), the proactively planned scenario, the model is configured to serve both the hydrogen and electricity system final demands via a co-optimised system with no limitations on sector coupling. From this configuration the costs of the proactively planned coupled system can be determined.

In configuration ii), the reactively planned scenario, the model is configured sequentially in two steps. In the first step, the electricity sector is optimized first with hydrogen demand switched off such that the model need only serve the final demand for electricity. Then, the resulting electricity-only solution is passed to the second step in a coupled electricity and hydrogen configuration. In this second step, minimum capacity constraints are asserted so that the electricity only capacities built in step one are fixed. In effect, the electricity system is optimized to meet electricity sector demand only and the hydrogen system is then optimized around it after the fact (with full sector-coupling permitted). From this configuration, the costs of the electricity system only can be calculated (from step one), as can the cost of the reactively planned coupled system.

In configuration iii), the isolated systems scenario is also run as a sequential two-step configuration. The first step is identical to that of configuration ii) in that the electricity sector is optimized in isolation. Then, in step two, the hydrogen system is also run in isolation with final demand for electricity switched off. In step two, we do not allow the capacity expansion model to build fossil or biomass candidates to serve the isolated hydrogen demand. This is to avoid the blurring of our demarcation between electrolytic hydrogen production and hydrogen produced from steam methane reforming or gasification of biomass which is outside the scope of this study. To ensure that the technical resource potentials for each resource-constrained technologies are not violated between the two steps, the upper bound on the maximum capacity constraints in the capacity expansion formulation are revised downwards by the amount 'absorbed' by the power sector in step 1. From this configuration, the costs of the isolated hydrogen system can be analyzed.

It should be highlighted that this approach assumes rather binary definitions of proactive versus reactive planning and coupled versus isolated systems. In reality, various degrees of proactivity and system coupling are possible between these boundary scenarios. The aim of the current work is simply to shed context on the relative costs at these boundaries.

4.3.3. IAM Scenario Demands

To provide context on the sensitivity of the relative costs to the overall electricity & hydrogen demand levels, the analysis is performed for two IAM scenarios. Namely, these are the SSP1_SPA1_26I_RE scenario derived from the IMAGE 3.2 integrated assessment model and the CEMICS_SSP1-1p5C-minCDR scenario derived from the REMIND-MAgPIE 2.1-4.2 integrated assessment model [136]. Figure 4.4 below demonstrates the relative position of these two scenarios in respect of electricity and electrolytic hydrogen final consumption in 2050 compared to the other IAM scenarios in the AR6 Scenario Explorer and Database [99]. As in [129], the final consumption is de-rated by the fraction of hydrogen production that is from electrolysis. The resulting annual global demands are presented in Table 1. The SSP1_SPA1_26I_RE can be characterized by mid-high electricity consumption and a high penetration of electrolytic hydrogen in 2050 while the CEMICS_SSP1-1p5C-minCDR presents very high final consumption of electricity and lower (but still relatively high) demand for electrolytic hydrogen.

IAM Model	**IAM Scenario**	**Electricity Demand, 2050**	**Hydrogen Demand, 2050**	**Electrolytic Fraction, 2050**	**De-Rated Hydrogen Demand, 2050**
IMAGE 3.2	SSP1_SPA1_26I_RE	182.28 EJ/yr	26.95 EJ/yr	0.34	9.05 EJ/yr
REMIND-MAgPIE 2.1-4.2	CEMICS_SSP1-1p5C-minCDR	223.37 EJ/yr	6.05 EJ/yr	0.86	5.20 EJ/yr

TABLE 4.1: IAM SCENARIO DEMANDS

Both scenarios can be characterized as exhibiting significant outturning electrolytic hydrogen demand which forms the primary rationale behind their selection. Note that, when comparing the representativeness of hydrogen demand across all AR6 scenarios, it is necessary to consider differences between integrated assessment models and their treatment of hydrogen as explored in [129] and [14]. We do not examine a scenario in which electrolytic hydrogen plays a relatively small role as the overall costs of the sector would then be entirely dwarfed by the power sector and the consequences of reactive planning or forced de-coupling would be expected to be small in absolute terms.

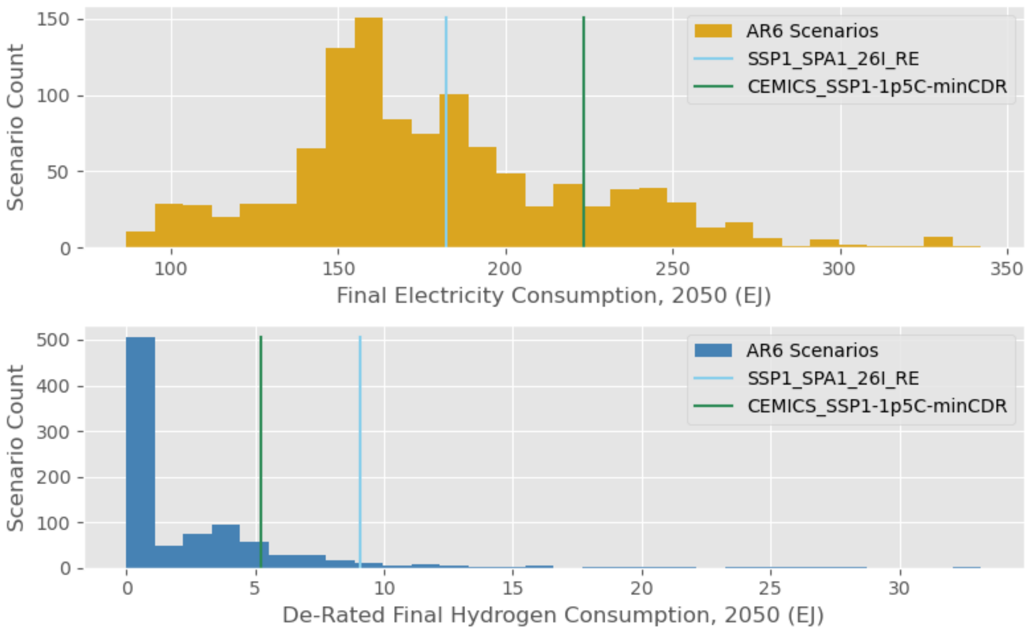

FIGURE 4.4: AR6 SCENARIO ELECTRICITY & ELECTROLYTIC HYDROGEN CONSUMPTION

4.3.4. Key Inputs & Assumptions

In general, the methodologies and modelling assumptions applied to the model framework in the current work are the same as those in [129] including but not limited to wind and solar load factor inputs, the temporal and spatial downscaling of the regional annual demands for electricity and hydrogen, and the technical resource potential of energy-limited technologies at each node.

In [129], it was not necessary to input realistic build costs and operational costs for many technologies given that most were constrained by the capacity soft-link with the parent IAM scenario. Given that this study is chiefly concerned with system costs and employs the framework of [129] with the capacity soft-link disabled, appropriate technology costs must be input to the modelling framework. For power generation technologies, total installation costs and operational costs are derived from the International Agency's (IEA) World Energy Outlook 2023 (WEO 2023) [137], while those for Power-to-X technologies, such as electrolysers or ammonia synthesis plants are derived from the IEA's Global Hydrogen Review 2023 [7]. In all cases, where cost figures are presented regionally, the median regional value is taken to assume a uniform global value. This is to simplify the analysis and filter out geographic trends that are not driven by technical resource potential. All costs are referred to 2010 US dollars in keeping with the convention of the AR6 Scenario Database to facilitate comparison to the parent IAM scenario. The resulting technology cost figures and assumed economic lifetimes are published in the supplementary information accompanying this paper.

For energy commodity prices we assume those of the parent CEMICS_SSP1-1p5C-minCDR scenario as published in the AR6 Scenario Database [99]. This includes prices for biomass for power generation for which we also set a maximum consumption constraint equal to the consumption in the CEMICS_SSP1-1p5C-minCDR scenario to preserve the price-demand equilibrium of the biomass supply from the IAM scenario. As with the commodity costs, a carbon price (of a significant 765 $/t) in line with the CEMICS_SSP1-1p5C-minCDR IAM scenario is asserted. In addition, a constraint is added such that the system must exhibit net-zero emissions.

In [129] it was noted that the role of geothermal power generation in the soft-linked IAM parent scenario was limited and therefore the need for geospatial technical potential constraints for geothermal power was negligible. However, preliminary model runs with the IEA WEO 2023 cost inputs and arbitrarily high maximum resource constraints for geothermal units exhibited extremely high build-out of geothermal power capacity. As a result, technical potential constraints for geothermal power generation were asserted in the PLEXOS model based on the work of [138]. The authors of [138] leverage GIS to estimate the global technical potential of enhanced geothermal systems (EGS) at a 1°×1° spatial resolution. Aggregated EGS power generation capacity potentials are provided by country in levelized cost of energy (LCOE) increments of 5 €/MWh for 2050. We assert the total MW potential for each country summed across all LCOE increments except the last > 100 €/MWh column as capacity upper bounds in the current model. This column is excluded as the capacity potential significantly balloons to incorporate the most technically challenging and expensive sites at which point our technology cost assumptions are likely to deviate significantly. For the countries in the current 256 region model that are broken down further into sub-national regions, the technical potentials are asserted on the national collection of sub-regional nodes.

Finally, while the model framework presented in [129] is an energy only model that does not include any operational constraints around reserve or inertia in the power sector, we consider that this is an aspect in which sector coupling may exhibit some efficiencies. To this end, we upscale the demand profiles of both electricity and hydrogen by 20% for the capacity expansion model phase in all configurations so that the system is optimised to be resilient to 120% of the demand of energy commodity. In effect, this is stipulating that a 20% dynamic energy reserve be available in the power sector for example, although such a margin is not enforced at the unit commitment and economic dispatch model phase. This 20% figure is consistent with recommended reserve margins by the International Energy Agency (IEA) and current practice by the North American Electric Reliability Corporation (NERC) [139,140].

4.3.5. Calculation & framing of relative costs

For clarity, most of the following analysis will be framed with respect to the additional cost of the hydrogen system in addition to the optimal electricity only system rather than the total combined electricity and hydrogen system cost. Notwithstanding the relatively high electrolytic hydrogen penetrations of the chosen scenarios, final demand for electricity significantly surpasses that of hydrogen in both scenarios. As a result, if the cost savings of proactivity vs reactivity regarding the integration of the hydrogen sector were presented as a percentage of the total coupled system cost, the magnitudes may appear misleadingly insignificant owing to the smaller role of hydrogen envisaged by the IAMs. From an optimization perspective, for a high-resolution global model, it is possible that there are multiple optimal solutions and comparing individual technology capacities at each regional node from one scenario to another may not yield particularly useful insights. However, the globally aggregated costs can be more directly compared. Figure 4.5 below extends figure 4.3 to clarify the derivation of key cost metrics in this study and how they are calculated from the model framework.

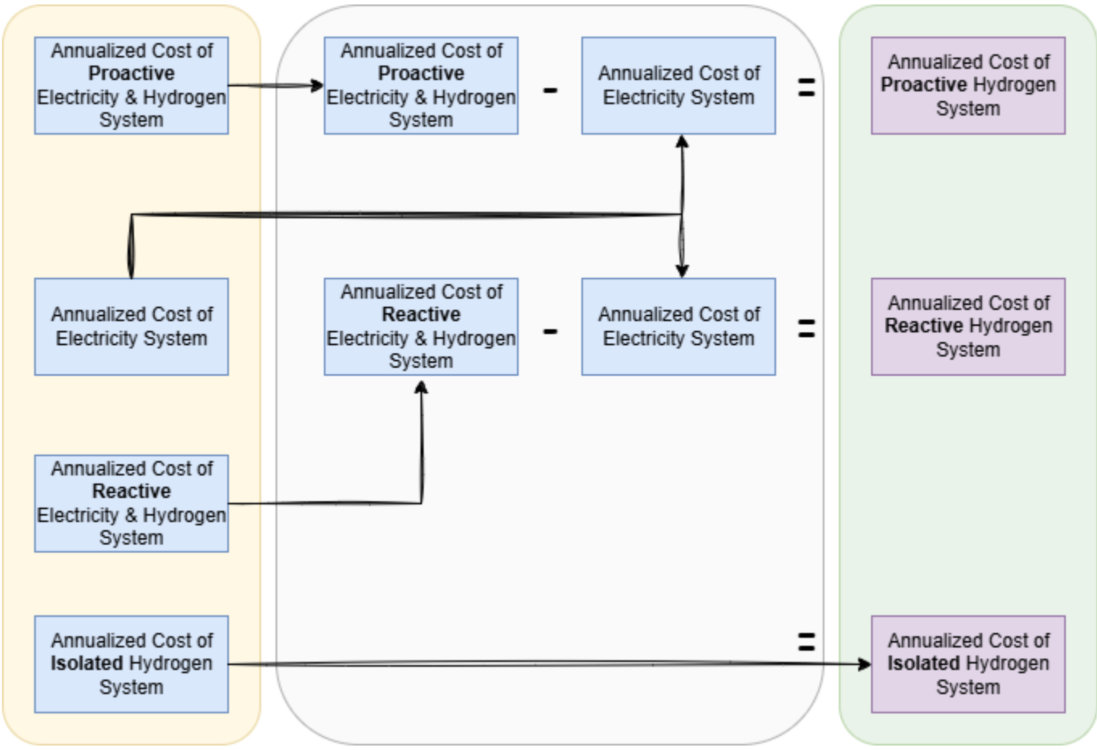

FIGURE 4.5 SUPERPOSITION OF GLOBAL SYSTEM COSTS

Step one of model configuration ii) (see figure 4.3) provides the cost of the electricity system only. We can then subtract the associated global total system cost of this system from that of the proactive coupled system costs from configuration i) and the reactive coupled system costs from step two in configuration ii). This yields our proactive and reactive hydrogen system costs or, more precisely, the additional system costs due to the hydrogen final demand. The isolated hydrogen system cost can be inferred more directly from step 2 of model configuration iii) in which the electricity final demand is not seen by the isolated hydrogen system model. At this point, the hydrogen system costs associated with each of the proactive, reactive and isolated scenarios have been calculated as shown in purple in figure 4.5.

Where capital expenditure (CAPEX) costs are annualized for ready comparison or summation with annual operation costs (OPEX), the following formula is applied as in equation (4.1) below:

$$Annualized\ CAPEX_f = CAPEX_f \times \frac{r}{1-(1+r)^{-n_f}} \qquad (4.1)$$

Where the subscript "f" is the index denoting a specific facility such as a generator, storage facility or transmission line, r is the assumed interest rate of 10% applied uniformly to all projects and n_f is the specific economic lifetime of the facility type in years. Here it is important to highlight that the actual cost of capital is not uniform globally. In this study, for the same reasons that we are not accounting for geopolitical factors such as trade restrictions between rival states, we are assuming a uniform global WACC. This is to maintain model dynamics and system costs driven by technical resource potentials and technology costs and not driven by perceived risk margins or regional politics that may change considerably between now and 2050. Notwithstanding this, the resulting impacts of a uniform cost of capital are explored in [141,142] and should be considered when interpreting this study. A global rate of 10% has been chosen as the base case to align with ESMAP's cost of capital assumptions for a nascent hydrogen sector [143] and to reflect the high cost of capital for the power sector in developing countries [141,144]. However, sensitivity of our results to the discount rate is examined in the following section.

4.4.Results & Discussion

Scenario	Discount Rate	Reactive Elec & H2 (T$2010/yr)	Proactive Elec & H2 (T$2010/yr)	Elec Only (T$2010/yr)	Isolated H2 (T$2010/yr)
SSP1_SPA1_26I_RE	5%	6.7	6.69	6.51	0.24
	10%	8.44	8.41	8.21	0.29
	15%	10.27	10.26	10	0.35
CEMICS_SSP1-1p5C-minCDR	5%	5.58	5.57	5.3	0.34
	10%	7.07	7.04	6.72	0.42
	15%	8.62	8.59	8.2	0.53

TABLE 4.2: TOTAL ANNUALIZED SYSTEM COSTS BY CONFIGURATION

Table 4.2 presents the total annualized total system costs for each modelling configuration for both scenarios in 2010 US Dollars. The base case data corresponding to a weighted average cost of capital of 10% is highlighted in yellow for ease of reference and results for the 5% and 15% WACC sensitivities are also presented. Applying the calculation framework as shown in figure 4.5 yields the total annualized hydrogen system costs in the proactive, reactive and isolated hydrogen system planning scenarios as presented in billions of US Dollars in Table 4.3. As expected, the costs of each hydrogen system configuration increase steeply with the assumed WACC.

Scenario	Discount Rate	Reactive H2 (B$2010/yr)	Proactive H2 (B$2010/yr)	Isolated H2 (B$2010/yr)
SSP1_SPA1_26I_RE	5%	187.82	179.4	239.88
	10%	231.95	204.43	287.27
	15%	276.65	261.83	347.63
CEMICS_SSP1-1p5C-minCDR	5%	278.7	264.68	346.12
	10%	349.51	318.95	424.72
	15%	426.17	393.06	531.16

TABLE 4.3 TOTAL ANNUALIZED H2 SYSTEM COSTS

In examining the impacts of reactive planning and system isolation, the reactive and isolated planning penalties are calculated by subtracting the cost of the proactively integrated hydrogen system cost from the reactive and isolated hydrogen system costs respectively from Table 4.3. These figures are presented below in Table 4.4 both in absolute terms (in billions of US Dollars) and in relative terms as a percentage of the proactively integrated hydrogen system cost. A general trend of increasing absolute reactive planning and isolation penalties with increasing cost of capital is observed, with the exception of the 15% WACC in the SSP1_SPA1_26I_RE demand scenario. No trend is apparent for the relative percentage penalties which vary between 5% to 13% of the proactively planned hydrogen system costs for reactive planning and 31% to 41% of the proactive hydrogen system costs for isolation.

Scenario	Discount Rate	Reactive Penalty (B$2010/yr)	Isolated Penalty (B$2010/yr)	Reactive Penalty (% of Proactive)	Isolated Penalty (% of Proactive)
CEMICS_SSP1-1p5C-minCDR	5%	8.42	60.48	5%	34%
	10%	27.52	82.84	13%	41%
	15%	14.82	85.8	6%	33%
SSP1_SPA1_26I_RE	5%	14.02	81.44	5%	31%
	10%	30.56	105.77	10%	33%
	15%	33.11	138.1	8%	35%

TABLE 4.4 CALCULATED ABSOLUTE & RELATIVE REACTIVE PLANNING & ISOLATION PENALTIES

Figure 4.6 below presents the base case (10% WACC) relative cost penalty of the reactive planning and isolated hydrogen system configurations as a percentage of the annualized hydrogen system cost in the proactive planning configuration. From Figure 4.6 we can see that the cost penalty of reactive planning is between 9 and 14 % of the annualized proactive hydrogen system costs for both of the IAM demand scenarios. However, the cost penalty of a reactive and isolated hydrogen system vs the proactive system is significant, between 33 and 41% across both scenarios. This is an important finding given that, as noted in [129] and the introduction of the current work, many higher temporal and spatial resolution global hydrogen-focused studies model the future hydrogen system independently of the power system. For example, the large three-part study by the International Renewable Energy Agency (IRENA) [95–97] models an independent electrolytic hydrogen sector. Here, the implication is that such studies may yield a potential future system that is structurally different and more expensive than a sector-coupled system. Furthermore, there is potential for the same cost-impact dynamic to extend to other sectors or sub-sectors when they too are assumed away in a model. For example, in the manner that non-electrolytic hydrogen is not explicitly represented in the current work or in that of [129]. Moreover, the harsh cost penalty for isolating the hydrogen sector from the electricity sector suggests that policy and regulation regarding power generation capacity additionality and grid integration of electrolytic hydrogen production should be approached with care so as to not overly disincentivize efficient coupling dynamics.

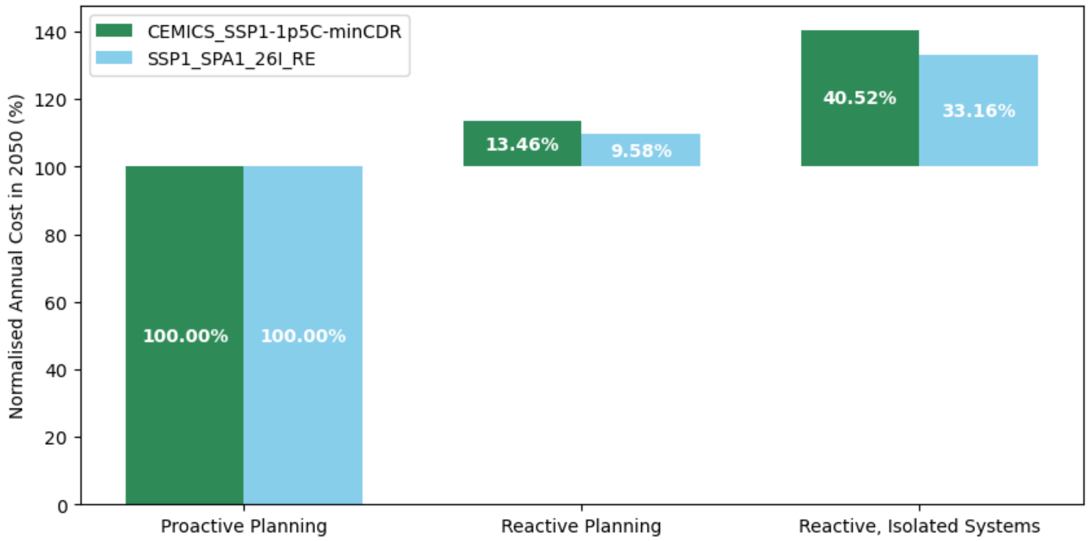

FIGURE 4.6: RELATIVE TOTAL SYSTEM COST PENALTIES

Notably, the base case relative cost penalties are higher in the CEMICS_SSP1-1p5C-minCDR demand scenario in both the reactive and isolated model configurations despite the scenario exhibiting less electrolytic hydrogen demand than the SSP1_SPA1_26I_RE scenario. This is due to the larger overall combined electricity and hydrogen demand in the SSP1_SPA1_26I_RE scenario leading to tighter competition for the cheapest power generation resources. The methodology of the current work is limited in that the reactive policy scenario only allows the hydrogen sector to be optimized after the entire electricity sector has been optimized, it is also assumed that it is socially acceptable to build out the maximum technical potential of a given technology at a given system node. Public acceptance and community opposition to large-scale energy projects are well treated across the literature [145–147]. For example, [147] examines public acceptance of renewable energy and grid expansion in Germany, finding that landscape modification is the most important factor influencing local acceptance. Large scale modification of the landscape at one node owing to significant resource potential at the node is unlikely to be wholly exploitable due to limitations around social acceptance. Regarding this study, this raises the implication that the technology specific nodal capacity constraints understate the degree to which the system is constrained and that the relative cost penalties of reactive planning may be even greater. To this end, the results of the current work should be considered with the understanding that the binary representation of reactive planning likely overstates the relative cost penalty of reactive planning, while the omission of social acceptance limitations on technology capacity limits would be expected to have the converse effect.

Figure 4.7 breaks down the annualized hydrogen system costs (for the base case WACC) in all configurations by technology for both demand scenarios. While differing in magnitudes, the pattern of investment across each hydrogen system configuration is similar for both demand scenarios. Hydrogen system costs can be seen to be dominated by investment in solar PV, onshore wind and electrolyser facilities across the board. Immediately of note is the spike in battery storage costs in both demand scenarios for the isolated hydrogen system configuration. The additional cost attributable to solar PV and onshore wind in the isolated hydrogen system is also notable. In the reactive planning hydrogen configuration, while the differences are apparent, the drivers of cost differences with the proactively planned hydrogen system appear more nuanced.

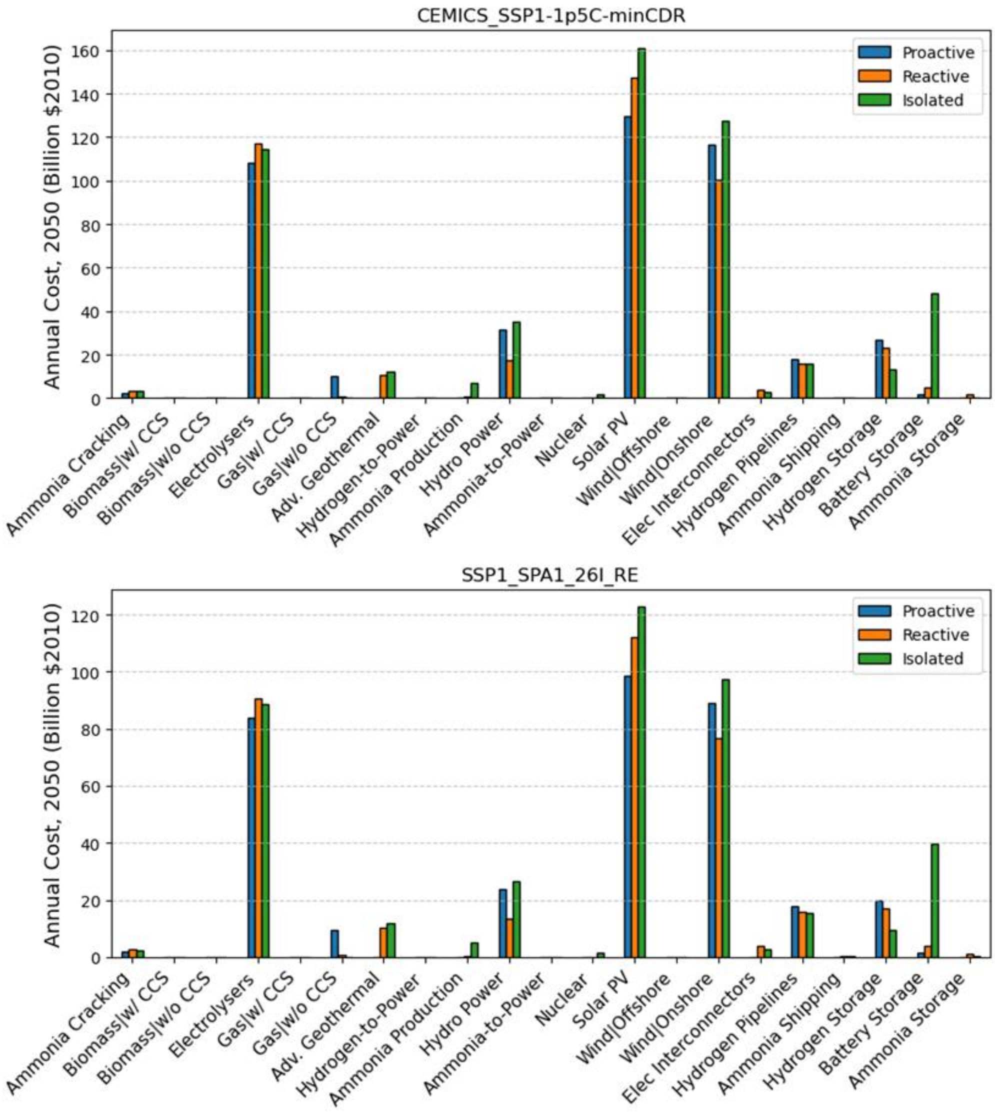

FIGURE 4.7: ANNUAL HYDROGEN SYSTEM COSTS BY TECHNOLOGY (BASE CASE WACC)

Figure 4.8 plots the additional total annualized cost of reactive rather than proactive hydrogen integration broken down by individual technologies so that the differences observed in Figure 4.7 are clearer and more accentuated. The pattern is nearly identical across the two IAM demand scenarios with differing magnitudes. In both scenarios, the reactive planning configuration results in less expenditure on hydrogen pipelines, hydrogen storage, gas-fired power generation without carbon capture and storage, hydro power and onshore wind generation. On the other hand, the reactive configuration results in significantly more expenditure on solar PV, advanced geothermal power, electrolysis and electricity interconnection. The need for additional expenditure on electrolysis, battery storage and electricity interconnection in the reactive planning configuration suggests that sub-optimal locational infrastructure lock-in is a key driver of the reactive planning penalty.

Figure 4.8 also shows that both IAM demand scenarios incur higher costs related to ammonia technologies under reactive planning, including ammonia-to-power generation, ammonia synthesis and cracking plants, storage, and shipping. This further underlines the impact of spatial lock-in with the model deploying costly and inefficient ammonia transport while spending less on hydrogen pipeline infrastructure.

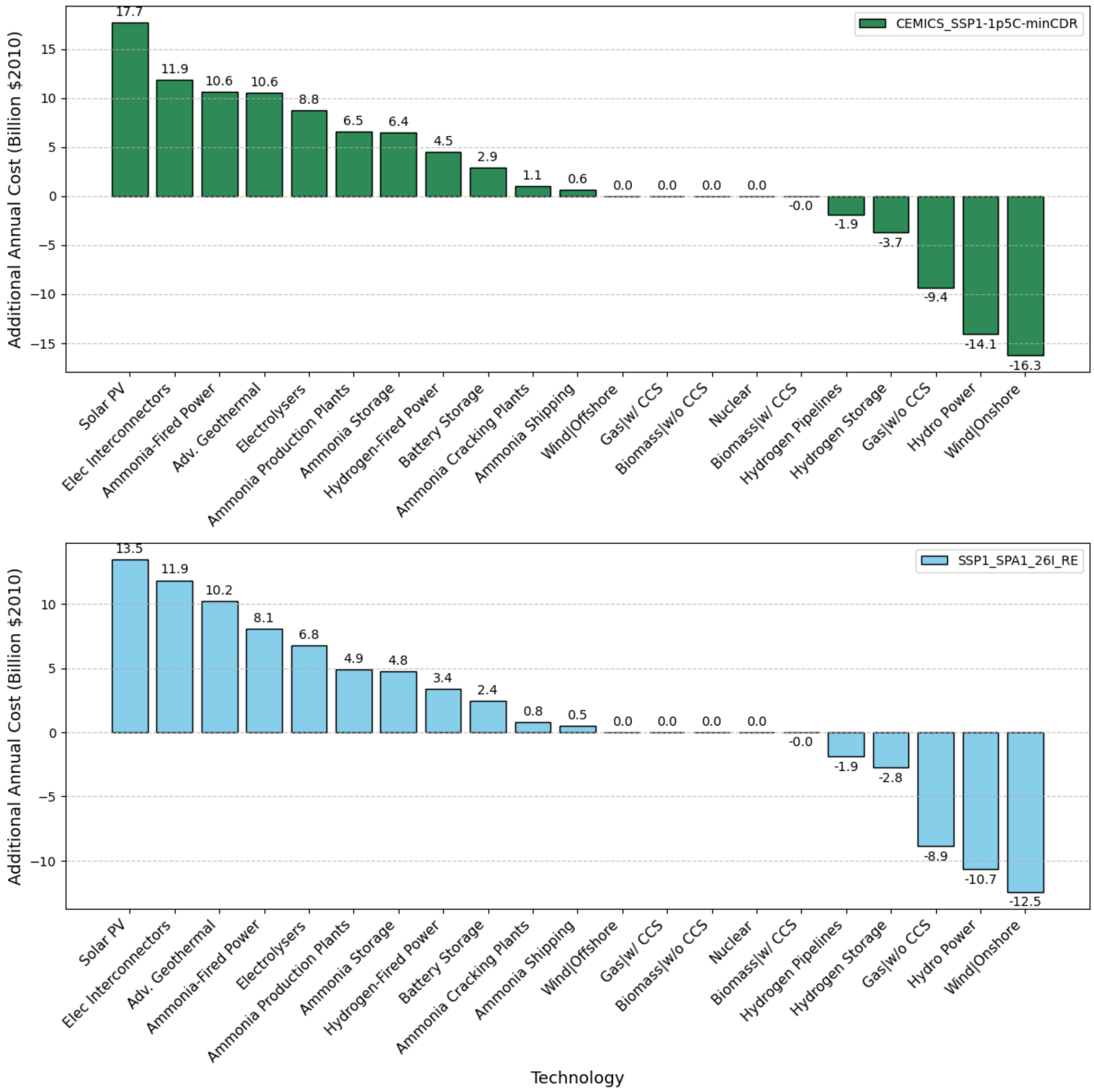

FIGURE 4.8: ADDITIONAL COSTS OF REACTIVE VS PROACTIVE H2 INTEGRATION

Figure 4.9 plots the additional total annualized cost of the isolated hydrogen system rather than the proactive sector-coupled hydrogen system configuration broken down by individual technologies. As in Figure 8 the pattern is consistent across both IAM demand scenarios with differing overall magnitudes. The largest cost difference in both demand scenarios is driven by battery storage as is also clearly seen in Figure 7. Additional costs are also associated with the need for additional power generation capacity compared to the coupled system including both variable renewable sources and clean firm power from advanced geothermal and nuclear power generation technologies. Overall, the effects of isolation are quite direct. In the absence of capacity sharing benefits through sector coupling, significant additional battery storage and power generation capacity is required in the hydrogen sector to facilitate high electrolysis load factors and avoid excessive curtailment of variable renewable power. This finding of significant additional costs when the electrolytic hydrogen sector is restricted to additional power generation capacity (that is inherently temporally congruent in this study) is consistent with the findings of [28] and [27].

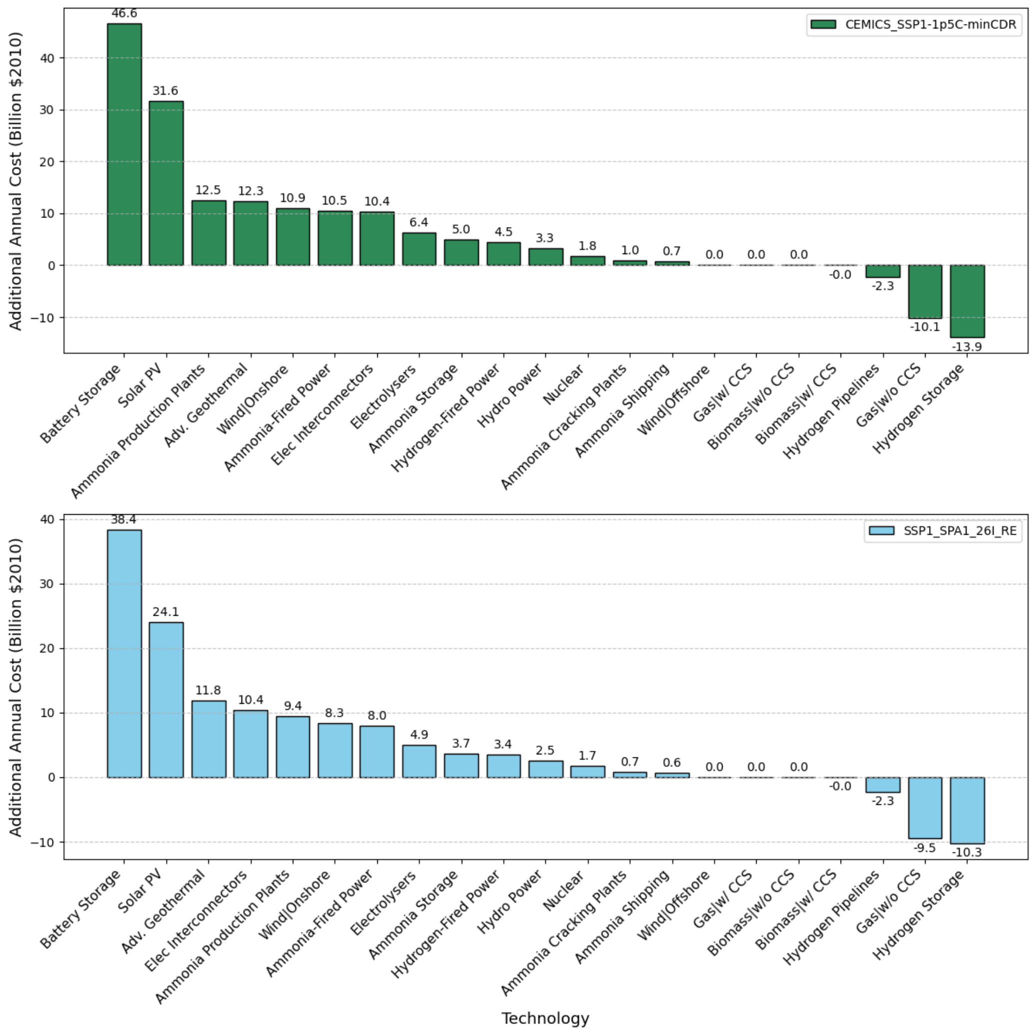

FIGURE 4.9: ADDITIONAL COSTS OF ISOLATED VS COUPLED PROACTIVE H2 INTEGRATION

Naturally, there are limitations to the work that warrant highlighting. Our results are sensitive to the cost assumptions that are input into the modelling framework. This is especially pertinent given that these costs are formulated at fixed values projected to 2050 rather than as a function of today's costs, a learning rate and level of deployment. Moreover, the greenfield approach overlooks the fact that some assets already in existence may still be in service in 2050 and doesn't account for the manner in which the inclusion of additional years across a longer time horizon can impact the optimal solution in the target year of study. It should also be noted that, at the intranodal level the model exhibits a copperplate assumption and therefore some of the capacity sharing efficiencies unlocked through sector coupling could actually warrant further cost due to the need for additional transmission capacity. This copperplate assumption could therefore overstate the cost savings associated with capacity sharing efficiencies. Lastly, we are assuming that the global electricity and hydrogen system would be planned with perfect foresight of demand in each modelling configuration, but in the reactive planning scenario the starting electricity system is fixed. This is an imperfect binary simulation of reactive planning but does provide insight into the dynamics of infrastructure lock-in. Notwithstanding these limitations, the current approach does provide some needed context around the cost penalties of reactive planning and forced isolation of the electrolytic hydrogen system from the power sector.

Chapter 5 Conclusions & Future Work

5.1. Overview & Synthesis

The central aim of this thesis has been to address the question of how the present uncertainty around hydrogen's future role in a decarbonised energy system can be mitigated. Hydrogen has moved through repeated cycles of enthusiasm and disillusionment, leaving policymakers and investors uncertain about how seriously to take its long-term potential. To move this debate from qualitative speculation to quantitative assessment, the thesis has focused on how hydrogen is represented in models and how those models are used to inform infrastructure and policy choices. In doing so, a recurring challenge emerges: models that capture the breadth of interactions between energy, economy and climate typically do so at coarse spatial and temporal resolution, while models that resolve operational detail often treat hydrogen demand as an exogenous input. This challenge is formalised in this work as the Energy System Modelling Trilemma, namely the difficulty of simultaneously achieving wide model scope, high spatio-temporal resolution and computational tractability.

Across the three core papers, this thesis demonstrates how data quality, model architecture and policy design choices interact to shape hydrogen's apparent role in future energy systems. Chapter 2 shows that bias in reanalysis-derived solar power profiles can be magnified by low-efficiency hydrogen storage, with implications for long-duration storage studies that rely on MERRA-2 and similar datasets. Chapter 3 develops and validates a global electricity-hydrogen soft-link framework that combines IAM scenario narratives with high-resolution modelling of generation, storage and cross-border energy trade. Overall, the modelling strategy developed here follows the trajectory advocated by Gambhir et al. [18], retaining IAMs as the backbone for mitigation pathways while supplementing them with specialised, high-resolution sectoral models to scrutinise critical technologies such as hydrogen in much greater detail. Chapter 4 applies this framework to examine how proactive versus reactive integration of electrolytic hydrogen, and coupled versus isolated system configurations, change total system costs under different policy assumptions.

In combination, the methods and results developed in this thesis speak to both strands set out in the introduction: they show how hydrogen can be modelled more rigorously across data, resolution and sector-coupling choices, and they quantify why the remaining uncertainty still matters by translating hesitant or restricted integration of hydrogen into concrete system and policy cost penalties.

The Energy System Modelling Trilemma frames the methodological strand by highlighting how choices about scope and resolution interact with computational limits. At the same time, basing the analysis on IAM scenarios retains endogenous projection of hydrogen demand and, through the Chapter 3 framework, allows hydrogen's roles in storage and transport to be resolved within a high-resolution, sector-coupled model rather than being fixed in advance or poorly captured at low spatio-temporal resolution. The scenario analysis in Chapter 4 speaks to the second strand, demonstrating how uncertainty about hydrogen's eventual role can translate into specific, path-dependent infrastructure build-outs and additional system costs. These cost penalties, in turn, strengthen the case for further improving modelling practice, so that uncertainty is more transparent and less likely to lead to expensive or irreversible mis-steps in system design and policy. Moreover, the significant cost penalty of isolated hydrogen systems quantified in this work provides a critical contrast to the hydrogen sector modelling approaches frequently seen in other major studies, such as those by IRENA [95–97].

5.2. Conclusions on Meteorological Reanalysis Bias Error Propagation Through H2-Based LDES (RQ-1)

In Chapter 2, I have consolidated the existing literature with respect to biased model-derived irradiance data and further examined ERA-5 and MERRA-2, two reanalysis datasets that are frequently applied to model renewable power profiles in energy modelling studies. While some studies suggest local variance in the direction of bias on these irradiance datasets, this thesis presents evidence that suggests the MERRA-2 reanalysis dataset exhibits a generally global overestimation bias. It is further suggested that in cloudier local climates with poorer solar resources, the overestimation bias by MERRA-2 is larger. The ERA-5 dataset, whilst exhibiting a better performance relative to MERRA-2 when modelling Solar PV output, also presents a deterioration in cloudy climates that leads to overestimation bias.

In many instances, such as in clearer climates, the bias errors yielded in modelling solar PV with reanalysis data could be relatively small if fully accounting for losses in the PV model chain. However, this work has demonstrated that studies involving storage technologies with low round-trip efficiency, such as long-duration Hydrogen based storage, could see large propagation in these initial input errors.

In this case, the underlying source of error cannot be mitigated through additional endogenous variables or broader model scope, nevertheless, the parallels with the Energy System Modelling Trilemma are apparent in that a distinct sensitivity of hydrogen to exogenous sources of error in energy and power system models is uncovered. Additionally, the ERA-5 dataset managed to commendably reproduce simulated outputs close to those yielded when profiles leveraging actual metered generation data were input, but the MERRA-2 based model led to significantly distorted charging and discharging patterns and underestimated the utilization of the long-duration storage asset. Herein lies an interesting parallel with the Energy System Modelling Trilemma, in that ERA-5 is a later generation meteorological reanalysis dataset with a higher spatial resolution than MERRA-2 and created with greater computational resource afforded to it. More broadly, the results of Chapter 2 show that input data quality is a first-order concern in studies that include low-efficiency energy pathways such as hydrogen-based long-duration storage, rather than a secondary detail. In such settings, modest biases in resource data do not simply add noise, but can propagate through the storage cycle to distort utilisation patterns and apparent system needs.

Based on this work, I recommend energy system-modellers employing MERRA-2 to simulate solar PV output should now migrate to ERA-5 to avoid significant errors in estimating total energy requirement, levelized cost of storage, or capacity requirements for low-round trip efficiency energy storage technologies.

5.3. Conclusions on the Supplementation of IAMs with a High Spatio-Temporal Resolution Electricity & Hydrogen Soft-Linking Framework (RQ-2)

Chapter 3 provides a framework for the generation of high spatial and temporal resolution global coupled electricity and hydrogen models based on IAM scenarios. Through the proposed approach, multi-scenario analysis of future hydrogen and hydrogen-derivative commodity trade is tractable whilst navigating the computational energy modelling trilemma of spatial, temporal and technological detail. By leveraging the proposed framework in conjunction with technology-rich IAMs, energy commodity demands that are driven by technological competition and boundary interactions with economy and environment can be examined at higher spatial and temporal resolution. Where the parent IAM's lower spatio-temporal resolution may fail to capture hydrogen's potential roles as an energy storage medium or as an energy trade vector, the supplementary high-resolution model endogenously resolves these potential demands while remaining consistent with the overall end-use demand for hydrogen in other roles. One such high-resolution soft-link model derived from the proposed framework has been examined with reference to the parent integrated assessment model scenario and an earlier power-system-only soft-link model. Through this benchmarking exercise, the high-level electricity and hydrogen production, trade and consumption dynamics of the soft-link model derived from the current framework have been validated.

Additionally, inconsistencies were encountered in data examined from the AR6 scenario database and, consequently, the application of the modelling framework to individual scenarios should be undertaken cautiously with appropriate reference to IAM model documentation and expert insights where feasible. While the harmonization of model output reporting is presumably challenging considering the wide range of integrated assessment models involved, measures have been identified that would significantly benefit the utility of the AR6 Scenario Database to energy modelers outside of the integrated assessment modelling community and would go some way to addressing the criticism surrounding the transparency of integrated assessment modelling observed in the literature. These are:

1. The rectification of inconsistencies where possible, and the "flagging" of inconsistencies at the point of publication where rectification is not possible.

2. The addition of footnotes to data entries, for example, to identify where different models or groups may have reported variables differently when necessitated by the model structure.
3. The reporting of assumed key process conversion efficiencies such as those for electrolysis and ammonia synthesis, and,
4. The reporting of additional variables such as individual chemical production and demand.

Addressing these recommendations would benefit modellers seeking to supplement Integrated Assessment Models with higher resolution models in order to navigate the corners of the Energy System Modelling Trilemma. Items 3 and 4 in particular would assist supplemental modelling focused on hydrogen as significant projected demands for specific chemicals like ammonia or other hydrogen derivates are likely to influence the hydrogen infrastructure landscape.

More generally, the work in Chapter 3 underlines the value of coordinated multi-model efforts in which IAMs and high-resolution power-system models are linked in a transparent way rather than run in isolation. In the spirit of the AR6 scenario database and IAMC activities, tighter coupling between these communities, with open data and clear documentation, can provide more coherent and policy-relevant insight into hydrogen's role than any single model class can deliver on its own.

5.4. Conclusions on the Proactive Coupled Integration of Hydrogen Versus Reactive Isolated Integration (RQ-3 & RQ-4)

In Chapter 4, the focus is primarily on the second strand of this thesis' examination of uncertainty around the future role of hydrogen in the energy system: why does it matter? With that said, it is in this chapter that the concept of the Energy System Modelling Trilemma is formally defined, and the tools of the previous chapters are deployed in Chapter 4's investigations. In examining why the mitigation of the uncertainty surrounding hydrogen's future role is important, the potential for hydrogen's repeated "false alarms" to lead to "cry wolf" effects and subsequent policy hesitation has been highlighted. On the back of this consideration, two "hesitant" policy scenarios were modelled wherein a significant future demand for hydrogen arises in the future. In the first scenario the cost penalty of reactively rather than proactively planning for the global integration of electrolytic hydrogen into the power sector given a significant demand for hydrogen in the future has been estimated. This cost penalty is estimated to be of the order of an additional 8-15% of the optimally integrated proactively planned hydrogen system cost depending on the overall combined global electricity and hydrogen demand. This corresponds to between 27 and 31 billion 2010 US dollars of additional costs annually in 2050. In general, this cost penalty can be expected to be greater when the cost of capital is higher and lesser when the cost of capital is lower. Whilst not catastrophic, the potential penalties due to sub-optimal infrastructure lock-in are not insignificant. The second scenario considers a case wherein sector coupling is disincentivized. In this case the cost penalty of isolating a future electrolytic hydrogen sector from the electricity sector is estimated to be of the order of an additional 33-41% of the cost of an optimally integrated and proactively planned hydrogen system. This corresponds to between 82 and 106 billion 2010 US dollars of additional costs annually in 2050. Under a lower cost of capital this range still comes in between 60 to 80 billion 2010 US dollars of additional costs annually in 2050. Consequently, policymakers should beware of policy that discourages optimal coupling of a future electrolytic hydrogen sector or face significant additional system costs in the event of significant future hydrogen demand arising. For example, concerns around the restrictiveness of RED II's requirements for grid-connected electrolysis should be evaluated seriously so as to minimize any isolating effects that aren't absolutely necessary to meet other objectives. The quantified cost penalties make explicit that policy choices and path-dependent infrastructure choices taken under uncertainty about hydrogen's role can lock systems into more expensive configurations, even when the underlying technology set is the same.

These findings underscore the importance of "systems thinking" and forward scenario planning. While this thesis focuses particularly on electrolytic hydrogen and the power sector, it is likely that similar sub-optimal cost penalty dynamics extend into other coupled sectors in the energy system. Moreover, the considerable impact on costs of "assuming away" interactions at the boundary of the model's scope further emphasizes the significance of "Endogeneity" or "Scope" corner of the Energy Systems Modelling trilemma.

5.5. Limitations

While this thesis addresses several important gaps in the modelling of hydrogen in future energy systems, a number of limitations should be acknowledged.

5.5.1. Limitations in Chapter 2

The empirical analysis of reanalysis bias in Chapter 2 is based on a finite set of utility-scale PV sites in Australia and Northern Ireland over 2019–2020. The identified bias patterns and their dependence on clearness index are therefore directly validated only for a limited set of climates and technologies; wind and other variable renewable resources are not examined explicitly. The error-propagation mechanism is demonstrated in a deliberately stylised single-system PLEXOS model with one hydrogen-based long-duration storage configuration and a specific mix of wind, solar and storage technologies, rather than across multiple, fully realistic power systems. However, it is worth noting that this simplicity benefits the clarity of the bias error propagation demonstration. The global indication of MERRA-2 overestimation is inferred via comparison with ERA-5-driven PV simulations for the PLEXOS World sites, rather than from site-by-site ground truth worldwide. Consequently, the mechanism by which bias propagates through low-efficiency storage pathways is likely to be general, but the precise magnitude and seasonal pattern of the effect may differ in other systems, climates and technology mixes.

5.5.2. Limitations in Chapter 3

The global electricity-hydrogen soft-linking framework in Chapter 3 is demonstrated and benchmarked with respect to one primary integrated assessment model scenario from the AR6 database. This means that the soft-linking framework is not fully tested for bugs or complications across the full suite of integrated assessment models and scenarios in the AR6 database and, considering the data quality and standardisation issues encountered, means manual intervention is likely to be required in further scenarios.

Techno-economic parameters for generation, storage, pipelines and shipping are treated as static for the model year, so endogenous learning and path-dependent cost reductions are not represented. Spatial and temporal detail, while high by IAM standards, is still limited to 256 regions and a combination of full-year dispatch with representative-day sampling in the capacity allocation phase, and network elements such as shipping are linearised to maintain tractability. The explicit sectoral scope is restricted to co-optimisation of electricity and electrolytic hydrogen and therefore the modelling framework does not capture non-electrolytic hydrogen production and trade. Hydrogen derivatives are simplified to a single shipped carrier (ammonia) and a constrained set of shipping and pipeline routes, which narrows the range of possible infrastructure configurations and may omit some niche carriers or routing patterns that could be relevant under different assumptions

5.5.3. Limitations in Chapter 4

The path-dependency and policy analyses in Chapter 4 use a greenfield capacity expansion formulation for 2050 scenarios, rather than simulating a full transition from the present system with explicit asset vintages, retirements and sunk costs. This isolates the structural effects of proactive versus reactive and coupled versus isolated configurations on long-run system costs, but does not capture the full complexity of moving from today's asset base, including stranded assets or short-term institutional, regulatory and political constraints. The model assumes static foresight and globally coherent optimisation within each scenario, rather than representing multiple heterogeneous decision-makers with differing objectives, evolving information and time horizons. Techno-economic parameters are again static within each scenario, so learning, induced innovation, and feedbacks between deployment decisions and future costs are not modelled explicitly. The policy configurations examined, such as delayed planning for hydrogen integration and enforced sectoral isolation, are stylised representations of broader debates, and real-world policy processes are likely to be more incremental and contested than the discrete cases considered here. The cost penalties reported should therefore be interpreted as indicative of the direction and potential scale of path-dependent effects under these stylised conditions, rather than as precise forecasts of realised costs under any specific policy package.

5.5.4. Cross-Cutting Limitations on Uncertainty

Across Chapters 2–4, uncertainty is handled through scenario analysis and contrasting configurations rather than through fully stochastic modelling. Weather, technology cost and policy uncertainties are explored via discrete cases and sensitivity choices, not via probabilistic ensembles or explicit decision-under-uncertainty formalisms. The focus on selected 2050 snapshots and a limited set of IAM scenarios means that dynamic adjustment pathways, institutional evolution and behavioural responses are not represented in detail. These omissions are deliberate, in order to keep the models tractable and to focus on structural mechanisms, but they underline the need for future work that extends the empirical basis of the Chapter 2 analysis, broadens the range of IAM scenarios and techno-economic assumptions explored in Chapters 3 and 4, and couples high-resolution, sector-coupled models with richer representations of learning, transition dynamics and decision-making under uncertainty.

5.6. Future Work

Building on the limitations outlined in Section 5.5, there are two main avenues of future work that would further address the research gaps identified in this thesis. These are i) continually improving the representation of hydrogen and its derivatives in modelling studies and ii) pushing the limits of the energy modelling trilemma that was presented in chapter 4 to yield increasingly precise insights into hydrogen's optimal future role.

5.6.1. Improved Representation of Hydrogen & Its Derivatives in Modelling Studies

This avenue for future work considers weaknesses of this thesis that could be improved upon. In Chapter 3 it was briefly highlighted that it was not always if the published figures for final consumption of hydrogen in different integrated assessment model scenarios were inclusive of hydrogen consumption for chemical feedstocks or were for energy-only consumption. In the EN_NPI2020_500 scenario benchmarked in Chapter 3 it was assumed that chemical feedstock demand was included in the hydrogen total final consumption figure given that no specific chemical feedstock demand was published for the scenario in the AR6 Scenario Database. This meant that no explicit ammonia demand was asserted in the resulting higher resolution model and was assumed to be implicit in the hydrogen demand levels asserted. This may mean that ammonia infrastructure, such as storage and shipping, may be underrepresented in the model results given that the pathways available to ammonia to meet the final hydrogen demand are through an additional ammonia cracking step. The disaggregation of the "hydrogen" demand into demand for hydrogen explicitly and demand for ammonia would allow for a more accurate resulting model. This is particularly pertinent considering that fertiliser production is a key application for which clean hydrogen derived ammonia is essential in a future decarbonised global economy [12]. Moreover, in Chapter 4 it was demonstrated how separate planning (or modelling) of the electricity sector to the electrolytic hydrogen sector yielded more expensive systems than an integrated system. It likely that this finding extends more generally and has implications, for example, for the work in this thesis that negates to model hydrogen from non-electrolytic sources. Therefore, future work should extend this framework to non-electrolytic sources of hydrogen rather than treat it separately.

To an extent, this work is ongoing as part of the CIGRE C1.50 working group in which I am participating as a modeller. In addition to the explicit representation of ammonia demand, further work is underway that aims improve the overall representation of the hydrogen sector. This includes examining further linearized representations of shipping considering that the current formulation forces the model to dedicate ships to a given route and doesn't allow them to seasonally serve alternative shipping routes. An alternative formulation, such as that given below in equation (5.1) is under consideration. Where the $Shipping\ Flow_n$ is the linearized continuous flow of energy being transferred across shipping route "n" and the other variables are consistent with equation (3.1) as defined in Chapter 3. This alternative formulation is effectively the same as the implementation in Chapter 3 except that ship capacity is now shared across all trade routes rather than locked individually. As this may amount to an overcorrection and assign excessive flexibility to global shipping, the multiple of 2 is reintroduced meaning that it is assumed that the ships are making an empty ballast journey. Critical examination of this formulation is presently on-going.

$$\sum \frac{Shipping\ Flow_n(MW) \times 2 \times Route\ Distance_n(km)}{Ship\ Speed\ (km/h)\ \times Cargo\ (MWh)} \leq No.\ Ships\ Commissioned\ Globally \quad (5.1)$$

Additionally, the CIGRE C1.50 model will incorporate non-electrolytic hydrogen, such as that produced from natural gas with CCS. In summary, the C1.50 model will incorporate improvements identified with respect to this work. However, the C1.50 model exhibits a significantly lower spatial resolution than the framework within this thesis, and therefore the expansion of this work to incorporate similar improvements in the scope and representation of the hydrogen sector would still be of merit.

5.6.2. Pushing the Limits of the Energy Modelling Trilemma

In Chapter 4 the concept of the energy modelling trilemma was introduced. Like the well-established concept of the energy trilemma: affordability, sustainability and security, the energy modelling trilemma outlines the challenges of maintaining detailed models of broad scope at sufficient spatio-temporal resolution whilst maintaining computational tractability. However, as optimisation solvers continue to improve and access to high performance cloud computing capacity becomes more attainable, the boundaries of the energy modelling trilemma will relax, and modellers will be able to be become increasingly ambitious with the extent and resolutions of their studies. As this arises, there will be significant scope to closely examine realistic roles for hydrogen endogenously as a function of technological competition to meet energy service demands (across all prospective applications of hydrogen) at increasing spatial and temporal resolution. This would lend greater confidence to the optimal role of hydrogen in future energy scenarios and contribute to the resolution of the underlying research gaps and modelling challenges identified in [12,14,17] and eventually negate the need for supplementary modelling frameworks.

Bibliography

[1] United Nations Framework Convention on Climate Change (UNFCCC). Paris Agreement 2015.

[2] Greenhouse Gas Emissions from Energy Data Explorer – Data Tools - IEA n.d. https://www.iea.org/data-and-statistics/data-tools/greenhouse-gas-emissions-from-energy-data-explorer (accessed August 9, 2025).

[3] Dillman KJ, Heinonen J. A 'just' hydrogen economy: A normative energy justice assessment of the hydrogen economy. Renewable and Sustainable Energy Reviews 2022;167:112648. https://doi.org/10.1016/J.RSER.2022.112648.

[4] Vezzoni R. How "clean" is the hydrogen economy? Tracing the connections between hydrogen and fossil fuels. Environ Innov Soc Transit 2024;50:100817. https://doi.org/10.1016/J.EIST.2024.100817.

[5] Urbano EM, Kampouropoulos K, Romeral L. Energy Crisis in Europe: The European Union's Objectives and Countries' Policy Trends—New Transition Paths? Energies 2023, Vol 16, Page 5957 2023;16:5957. https://doi.org/10.3390/EN16165957.

[6] Ruhnau O, Stiewe C, Muessel J, Hirth L. Natural gas savings in Germany during the 2022 energy crisis. Nature Energy 2023 8:6 2023;8:621–8. https://doi.org/10.1038/s41560-023-01260-5.

[7] - International Energy Agency I. Global Hydrogen Review 2023. 2023.

[8] Tengler M. Is the hydrogen industry falling into a trough of disillusionment? 2024. https://www.linkedin.com/posts/mtengler_is-the-hydrogen-industry-falling-into-a-trough-activity-7260633612734099456-jtu2/ (accessed May 18, 2025).

[9] Rosenow J. Hydrogen is currently on the peak of a hype cycle. 2023. https://www.linkedin.com/posts/janrosenow_hydrogen-is-currently-on-the-peak-of-a-hype-activity-7044699519870980096-nld5/?originalSubdomain=bo (accessed May 18, 2025).

[10] Dignum M. The power of large technological visions : the promise of hydrogen energy (1970-2010) 2013. https://doi.org/10.6100/IR759497.

[11] Kyung D, Yu C-H, Lin Y-P, Yap J, Mclellan B. A Historical Analysis of Hydrogen Economy Research, Development, and Expectations, 1972 to 2020. Environments 2023, Vol 10, Page 11 2023;10:11. https://doi.org/10.3390/ENVIRONMENTS10010011.

[12] Johnson N, Liebreich M, Kammen DM, Ekins P, McKenna R, Staffell I. Realistic roles for hydrogen in the future energy transition. Nature Reviews Clean Technology 2025 2025:1–21. https://doi.org/10.1038/s44359-025-00050-4.

[13] Bakker S, Budde B. Technological hype and disappointment: Lessons from the hydrogen and fuel cell case. Technol Anal Strateg Manag 2012;24:549–63. https://doi.org/10.1080/09537325.2012.693662;WEBSITE:WEBSITE:TFOPB;PAGEGROUP:STRING:PUBLICATION.

[14] Ghaboulian Zare S, Amirmoeini K, Bahn O, Baker RC, Mousseau N, Neshat N, et al. The role of hydrogen in integrated assessment models: A review of recent developments. Renewable and Sustainable Energy Reviews 2025;215:115544. https://doi.org/10.1016/J.RSER.2025.115544.

[15] Odenweller A, Ueckerdt F. The green hydrogen ambition and implementation gap. Nature Energy 2025 10:1 2025;10:110–23. https://doi.org/10.1038/s41560-024-01684-7.

[16] Wolfram P, Kyle P, Fuhrman J, O’Rourke P, McJeon H. The hydrogen economy can reduce costs of climate change mitigation by up to 22%. One Earth 2024;7:885–95. https://doi.org/10.1016/j.oneear.2024.04.012.

[17] Blanco H, Leaver J, Dodds PE, Dickinson R, García-Gusano D, Iribarren D, et al. A taxonomy of models for investigating hydrogen energy systems. Renewable and Sustainable Energy Reviews 2022;167:112698. https://doi.org/10.1016/J.RSER.2022.112698.

[18] Gambhir A, Butnar I, Li PH, Smith P, Strachan N. A Review of Criticisms of Integrated Assessment Models and Proposed Approaches to Address These,

through the Lens of BECCS. Energies 2019, Vol 12, Page 1747 2019;12:1747. https://doi.org/10.3390/EN12091747.

[19] Brinkerink M, Gallachóir B, Deane P. Building and Calibrating a Country-Level Detailed Global Electricity Model Based on Public Data. Energy Strategy Reviews 2021;33:100592. https://doi.org/10.1016/J.ESR.2020.100592.

[20] Brinkerink M, Zakeri B, Huppmann D, Glynn J, Ó Gallachóir B, Deane P. Assessing global climate change mitigation scenarios from a power system perspective using a novel multi-model framework. Environmental Modelling & Software 2022;150:105336. https://doi.org/10.1016/J.ENVSOFT.2022.105336.

[21] Rogner M, Riahi K. Future nuclear perspectives based on MESSAGE integrated assessment modeling. Energy Strategy Reviews 2013;1:223–32. https://doi.org/10.1016/J.ESR.2013.02.006.

[22] Yu S, Yarlagadda B, Siegel JE, Zhou S, Kim S. The role of nuclear in China's energy future: Insights from integrated assessment. Energy Policy 2020;139:111344. https://doi.org/10.1016/J.ENPOL.2020.111344.

[23] Mori S, Miyaji K, Kamegai K. CCS, Nuclear Power and Biomass An Assessment of Option Triangle under Global Warming Mitigation Policy by an Integrated Assessment Model MARIA-23. Energy Procedia 2013;37:7474–83. https://doi.org/10.1016/J.EGYPRO.2013.06.691.

[24] Hiremath M, Viebahn P, Samadi S. An Integrated Comparative Assessment of Coal-Based Carbon Capture and Storage (CCS) Vis-à-Vis Renewable Energies in India's Low Carbon Electricity Transition Scenarios. Energies 2021, Vol 14, Page 262 2021;14:262. https://doi.org/10.3390/EN14020262.

[25] Benavides K, Gurgel A, Morris J, Mignone B, Chapman B, Kheshgi H, et al. Mitigating emissions in the global steel industry: Representing CCS and hydrogen technologies in integrated assessment modeling. International Journal of Greenhouse Gas Control 2024;131:103963. https://doi.org/10.1016/J.IJGGC.2023.103963.

[26] Wilson C, Guivarch C, Kriegler E, van Ruijven B, van Vuuren DP, Krey V, et al. Evaluating process-based integrated assessment models of climate change mitigation. Climatic Change 2021 166:1 2021;166:1–22. https://doi.org/10.1007/S10584-021-03099-9.

[27] Ruhnau O, Schiele J. Flexible green hydrogen: The effect of relaxing simultaneity requirements on project design, economics, and power sector emissions. Energy Policy 2023;182:113763. https://doi.org/10.1016/J.ENPOL.2023.113763.

[28] Brandt J, Iversen T, Eckert C, Peterssen F, Bensmann B, Bensmann A, et al. Cost and competitiveness of green hydrogen and the effects of the European Union regulatory framework. Nat Energy 2024;9:703–13. https://doi.org/10.1038/S41560-024-01511-Z;SUBJMETA.

[29] Delegated regulation - 2023/1184 - EN - EUR-Lex n.d. https://eur-lex.europa.eu/legal-content/EN/TXT/?uri=uriserv%3AOJ.L_.2023.157.01.0011.01.ENG&toc=OJ%3AL%3A2023%3A157%3ATOC (accessed June 12, 2025).

[30] Delegated regulation - 2023/1185 - EN - EUR-Lex n.d. https://eur-lex.europa.eu/legal-content/EN/TXT/?uri=uriserv%3AOJ.L_.2023.157.01.0020.01.ENG&toc=OJ%3AL%3A2023%3A157%3ATOC (accessed June 12, 2025).

[31] Brinkerink M, Mayfield E, Deane P. The role of spatial resolution in global electricity systems modelling. Energy Strategy Reviews 2024;53:101370. https://doi.org/10.1016/J.ESR.2024.101370.

[32] Gelaro R, McCarty W, Suárez MJ, Todling R, Molod A, Takacs L, et al. The modern-era retrospective analysis for research and applications, version 2 (MERRA-2). J Clim 2017;30:5419–54. https://doi.org/10.1175/JCLI-D-16-0758.1.

[33] Hersbach H, Bell B, Berrisford P, Hirahara S, Horányi A, Muñoz-Sabater J, et al. The ERA5 global reanalysis. Quarterly Journal of the Royal Meteorological Society 2020;146:1999–2049. https://doi.org/10.1002/qj.3803.

[34] Pfenninger S, Staffell I. Long-term patterns of European PV output using 30 years of validated hourly reanalysis and satellite data. Energy 2016;114:1251–65. https://doi.org/10.1016/j.energy.2016.08.060.

[35] Staffell I, Pfenninger S. Using bias-corrected reanalysis to simulate current and future wind power output. Energy 2016;114:1224–39. https://doi.org/10.1016/j.energy.2016.08.068.

[36] Wiese F, Schlecht I, Bunke WD, Gerbaulet C, Hirth L, Jahn M, et al. Open Power System Data – Frictionless data for electricity system modelling. Appl Energy 2019;236:401–9. https://doi.org/10.1016/J.APENERGY.2018.11.097.

[37] Sengupta M, Xie Y, Lopez A, Habte A, Maclaurin G, Shelby J. The National Solar Radiation Data Base (NSRDB). Renewable and Sustainable Energy Reviews 2018;89:51–60. https://doi.org/10.1016/j.rser.2018.03.003.

[38] Yang D. Validation of the 5-min irradiance from the National Solar Radiation Database (NSRDB). Journal of Renewable and Sustainable Energy 2021;13:016101. https://doi.org/10.1063/5.0030992.

[39] Yang D. A correct validation of the National Solar Radiation Data Base (NSRDB). Renewable and Sustainable Energy Reviews 2018;97:152–5. https://doi.org/10.1016/j.rser.2018.08.023.

[40] Müller R, Pfeifroth U, Träger-Chatterjee C, Cremer R, Trentmann J, Hollmann R. Surface Solar Radiation Data Set - Heliosat (SARAH) - Edition 1. Satellite Application Facility on Climate Monitoring 2015.

[41] Müller R, Pfeifroth U, Träger-Chatterjee C, Trentmann J, Cremer R. Digging the METEOSAT treasure-3 decades of solar surface radiation. Remote Sens (Basel) 2015;7:8067–101. https://doi.org/10.3390/rs70608067.

[42] Brinkerink M, Gallachóir B, Deane P. Building and Calibrating a Country-Level Detailed Global Electricity Model Based on Public Data. Energy Strategy Reviews 2021;33:100592. https://doi.org/10.1016/j.esr.2020.100592.

[43] Ruggles TH, Caldeira K. Wind and solar generation may reduce the inter-annual variability of peak residual load in certain electricity systems. Appl Energy 2022;305:117773. https://doi.org/10.1016/J.APENERGY.2021.117773.

[44] Bett PE, Thornton HE. The climatological relationships between wind and solar energy supply in Britain. Renew Energy 2016;87:96–110. https://doi.org/10.1016/j.renene.2015.10.006.

[45] Berrisford P, Dee D, Poli P, Brugge R, Fielding K, Fuentes M, et al. The ERA-Interim archive Version 2.0. 2011.

[46] Dee DP, Uppala SM, Simmons AJ, Berrisford P, Poli P, Kobayashi S, et al. The ERA-Interim reanalysis: Configuration and performance of the data assimilation system. Quarterly Journal of the Royal Meteorological Society 2011;137:553–97. https://doi.org/10.1002/qj.828.

[47] Jurasz J, Mikulik J, Abek PBD˛, Guezgouz M, Ka´zmierczak BK. Complementarity and "Resource Droughts" of Solar and Wind Energy in Poland: An ERA5-Based Analysis 2021. https://doi.org/10.3390/en14041118.

[48] Xie Y, Sengupta M, Liu Y, Long H, Min Q, Liu W, et al. A Physics-Based DNI Model Assessing All-Sky Circumsolar Radiation. IScience 2020;23:100893. https://doi.org/10.1016/j.isci.2020.100893.

[49] Mathiesen P, Kleissl J. Evaluation of numerical weather prediction for intra-day solar forecasting in the continental United States. Solar Energy 2011;85:967–77. https://doi.org/10.1016/j.solener.2011.02.013.

[50] Sianturi Y, Marjuki, Sartika K. Evaluation of ERA5 and MERRA2 reanalyses to estimate solar irradiance using ground observations over Indonesia region. AIP Conf Proc 2020;2223:20001. https://doi.org/10.1063/5.0000854.

[51] Khatibi A, Krauter S. Validation and Performance of Satellite Meteorological Dataset MERRA-2 for Solar and Wind Applications. Energies 2021, Vol 14, Page 882 2021;14:882. https://doi.org/10.3390/EN14040882.

[52] Penna B, Herdies D, Costa S. Estimates of direct radiative forcing due to aerosols from the MERRA-2 reanalysis over the Amazon region. Atmospheric Chemistry and Physics Discussions 2018:1–17. https://doi.org/10.5194/ACP-2018-355.

[53] Liu H, Liu X, Dong B. Influence of Central Siberian Snow-Albedo Feedback on the Spring East Asian Dust Cycle and Connection With the Preceding

Winter Arctic Oscillation. Journal of Geophysical Research: Atmospheres 2018;123:13,368-13,385. https://doi.org/10.1029/2018JD029385.

[54] Urraca R, Huld T, Gracia-Amillo A, Martinez-de-Pison FJ, Kaspar F, Sanz-Garcia A. Evaluation of global horizontal irradiance estimates from ERA5 and COSMO-REA6 reanalyses using ground and satellite-based data. Solar Energy 2018;164:339–54. https://doi.org/10.1016/J.SOLENER.2018.02.059.

[55] Clarke ED, Griffin S, McDermott F, Correia JM, Sweeney C. Which Reanalysis Dataset Should We Use for Renewable Energy Analysis in Ireland? Atmosphere 2021, Vol 12, Page 624 2021;12:624. https://doi.org/10.3390/ATMOS12050624.

[56] Polo J, Wilbert S, Ruiz-Arias JA, Meyer R, Gueymard C, Súri M, et al. Preliminary survey on site-adaptation techniques for satellite-derived and reanalysis solar radiation datasets. Solar Energy 2016;132:25–37. https://doi.org/10.1016/j.solener.2016.03.001.

[57] Li M, Virguez E, Shan R, Tian J, Gao S, Patiño-Echeverri D. High-resolution data shows China's wind and solar energy resources are enough to support a 2050 decarbonized electricity system. Appl Energy 2022;306:117996. https://doi.org/10.1016/j.apenergy.2021.117996.

[58] Jacobson MZ, Delucchi MA, Bauer ZAF, Goodman SC, Chapman WE, Cameron MA, et al. 100% Clean and Renewable Wind, Water, and Sunlight All-Sector Energy Roadmaps for 139 Countries of the World. Joule 2017;1:108–21. https://doi.org/10.1016/J.JOULE.2017.07.005.

[59] Steinke F, Wolfrum P, Hoffmann C. Grid vs. storage in a 100% renewable Europe. Renew Energy 2013;50:826–32. https://doi.org/10.1016/J.RENENE.2012.07.044.

[60] Colbertaldo P, Agustin SB, Campanari S, Brouwer J. Impact of hydrogen energy storage on California electric power system: Towards 100% renewable electricity. Int J Hydrogen Energy 2019;44:9558–76. https://doi.org/10.1016/J.IJHYDENE.2018.11.062.

[61] Maruf MNI. Open model-based analysis of a 100% renewable and sector-coupled energy system–The case of Germany in 2050. Appl Energy 2021;288:116618. https://doi.org/10.1016/J.APENERGY.2021.116618.

[62] Escamilla A, Sánchez D, García-Rodríguez L. Assessment of power-to-power renewable energy storage based on the smart integration of hydrogen and micro gas turbine technologies. Int J Hydrogen Energy 2022;47:17505–25. https://doi.org/10.1016/J.IJHYDENE.2022.03.238.

[63] Kelly NA. Hydrogen production by water electrolysis. Advances in Hydrogen Production, Storage and Distribution 2014:159–85. https://doi.org/10.1533/9780857097736.2.159.

[64] Kies A, Schyska BU, Bilousova M, el Sayed O, Jurasz J, Stoecker H. Critical review of renewable generation datasets and their implications for European power system models. Renewable and Sustainable Energy Reviews 2021;152:111614. https://doi.org/10.1016/J.RSER.2021.111614.

[65] ENTSO-E. ENTSO-E PECD (European Climate Database) 2020. https://doi.org/10.5281/ZENODO.3702418.

[66] ENTSO-E. European Network of Transmission System Operators for Electricity European Resource Adequacy Assessment 2021.

[67] A Hydrogen Strategy for a Climate-Neutral Europe. 2020.

[68] AEMO. AEMO | Nemweb data n.d. https://www.aemo.com.au/energy-systems/electricity/national-electricity-market-nem/data-nem/market-data-nemweb (accessed February 7, 2022).

[69] SEMO. SEMO Market Data n.d. https://www.sem-o.com/market-data/ (accessed February 7, 2022).

[70] Holmgren WF, Andrews RW, Lorenzo AT, Stein JS. PVLIB Python 2015. 2015 IEEE 42nd Photovoltaic Specialist Conference, PVSC 2015, Institute of Electrical and Electronics Engineers Inc.; 2015. https://doi.org/10.1109/PVSC.2015.7356005.

[71] F. Holmgren W, W. Hansen C, A. Mikofski M. pvlib python: a python package for modeling solar energy systems. J Open Source Softw 2018;3:884. https://doi.org/10.21105/joss.00884.

[72] King DL, Boyson WE, Kratochvil JA. Photovoltaic array performance model. Sandia Report No 2004-3535 2004;8:1–19. https://doi.org/10.2172/919131.

[73] Stein Joshua, Hansen CW, King BH, Sutterlueti J, Ransome S. OUTDOOR PV PERFORMANCE EVALUATION OF THREE DIFFERENT MODELS: SINGLE-DIODE SAPM AND LOSS FACTOR MODEL. 2013.

[74] Hansen CW, Riley DM, Jaramillo M. Calibration of the Sandia array performance model using indoor measurements. Conference Record of the IEEE Photovoltaic Specialists Conference, 2012, p. 3067–72. https://doi.org/10.1109/PVSC.2012.6318229.

[75] Peng J, Lu L, Yang H, Ma T. Validation of the Sandia model with indoor and outdoor measurements for semi-transparent amorphous silicon PV modules. Renew Energy 2015;80:316–23. https://doi.org/10.1016/j.renene.2015.02.017.

[76] Lave M, Hayes W, Pohl A, Hansen CW. Evaluation of global horizontal irradiance to plane-of-array irradiance models at locations across the United States. IEEE J Photovolt 2015;5:597–606. https://doi.org/10.1109/JPHOTOV.2015.2392938.

[77] Ineichen P, Perez RR, Seal RD, Maxwell EL, Zalenka A. Dynamic global-to-direct irradiance conversion models. ASHRAE Trans 1992;98:354–69.

[78] Hay JE, Davies JA. Calculation of the Solar Radiation Incident on an Inclined Surface. Proceedings of the 1st Canadian Solar Radiation Data Workshop 1980.

[79] CRU, UREGNI. SEM-20-003 SEM PLEXOS Forecast Model (2020-2025) 2020. https://www.semcommittee.com/publications/sem-20-003-sem-plexos-forecast-model-2020-2025 (accessed December 15, 2021).

[80] Puranen P, Kosonen A, Ahola J. Technical feasibility evaluation of a solar PV based off-grid domestic energy system with battery and hydrogen energy storage in northern climates. Solar Energy 2021;213:246–59. https://doi.org/10.1016/J.SOLENER.2020.10.089.

[81] Jansen G, Dehouche Z, Corrigan H. Cost-effective sizing of a hybrid Regenerative Hydrogen Fuel Cell energy storage system for remote & off-grid

telecom towers. Int J Hydrogen Energy 2021;46:18153–66. https://doi.org/10.1016/J.IJHYDENE.2021.02.205.

[82] AEMO. Quarterly Energy Dynamics Q2 2021 Market Insights and WA Market Operations 2021.

[83] EIRGRID, SONI. Annual Renewable Energy Constraint and Curtailment Report 2019. 2020.

[84] EIRGRID, SONI. Annual Renewable Energy Constraint and Curtailment Report 2020 2021.

[85] Technical Summary. Climate Change 2022 - Mitigation of Climate Change 2023:51–148. https://doi.org/10.1017/9781009157926.002.

[86] Mitigation Pathways Compatible with Long-term Goals. Climate Change 2022 - Mitigation of Climate Change 2023:295–408. https://doi.org/10.1017/9781009157926.005.

[87] Annex III: Scenarios and Modelling Methods. Climate Change 2022 - Mitigation of Climate Change 2023:1841–908. https://doi.org/10.1017/9781009157926.022.

[88] Krey V, Havlik P, Fricko O, Zilliacus J, Gidden M, Strubegger M, et al. Message-globiom 1.0 documentation. International Institute for Applied Systems Analysis: Laxenburg, Austria 2016.

[89] Krey V, Havlik P, Kishimoto PN, Fricko O, Zilliacus J, Gidden M, et al. MESSAGEix-GLOBIOM Documentation – 2020 release. Laxenburg, Austria: 2020. https://doi.org/10.22022/iacc/03-2021.17115.

[90] Hanley ES, Deane JP, Gallachóir BPÓ. The role of hydrogen in low carbon energy futures–A review of existing perspectives. Renewable and Sustainable Energy Reviews 2018;82:3027–45. https://doi.org/10.1016/J.RSER.2017.10.034.

[91] Kouchaki-Penchah H, Bahn O, Bashiri H, Bedard S, Bernier E, Elliot T, et al. The role of hydrogen in a net-zero emission economy under alternative policy scenarios. Int J Hydrogen Energy 2023. https://doi.org/10.1016/J.IJHYDENE.2023.07.196.

[92] Sullivan P, Krey V, Riahi K. Impacts of considering electric sector variability and reliability in the MESSAGE model. Energy Strategy Reviews 2013;1:157–63. https://doi.org/10.1016/J.ESR.2013.01.001.

[93] Brauer J, Truby J, Villavicencio M. Establishing low-carbon hydrogen trade relations - where to go and who to partner with? International Conference on the European Energy Market, EEM 2022;2022-September. https://doi.org/10.1109/EEM54602.2022.9921065.

[94] Franzmann D, Heinrichs H, Lippkau F, Addanki T, Winkler C, Buchenberg P, et al. Green hydrogen cost-potentials for global trade. Int J Hydrogen Energy 2023;48:33062–76. https://doi.org/10.1016/J.IJHYDENE.2023.05.012.

[95] IRENA. Global Hydrogen Trade to Meet the 1.5°C Climate Goal: Part I - Trade Outlook for 2050 and Way Forward. Global Hydrogen Trade to Meet the 15°C Climate Goal: Trade Outlook for 2050 and Way Forward 2022:114.

[96] IRENA. Global hydrogen trade to meet the 1.5 °C climate goal: Part II – Technology review of hydrogen carriers. Global Hydrogen Trade to Meet the 15°C Climate Goal: Technology Review of Hydrogen Carriers 2022.

[97] IRENA. Global Hydrogen Trade to Meet the 1.5°C Climate Goal: Green Hydrogen Cost and Potential. Global Hydrogen Trade to Meet the 15°C Climate Goal: Green Hydrogen Cost and Potential 2022:1–114.

[98] IRENA. World Energy Transitions Outlook 2022: 1.5°C Pathway. Abu Dhabi: 2022.

[99] Byers E, Krey V, Kriegler E, Riahi K, Schaeffer R, Kikstra J, et al. AR6 Scenarios Database 2022. https://doi.org/10.5281/zenodo.7197970.

[100] Huppmann D, Gidden M, Fricko O, Kolp P, Orthofer C, Pimmer M, et al. The MESSAGEix Integrated Assessment Model and the ix modeling platform (ixmp): An open framework for integrated and cross-cutting analysis of energy, climate, the environment, and sustainable development. Environmental Modelling & Software 2019;112:143–56. https://doi.org/10.1016/j.envsoft.2018.11.012.

[101] Fricko O, Havlik P, Rogelj J, Klimont Z, Gusti M, Johnson N, et al. The marker quantification of the Shared Socioeconomic Pathway 2: A middle-of-

the-road scenario for the 21st century. Global Environmental Change 2017;42:251–67. https://doi.org/10.1016/J.GLOENVCHA.2016.06.004.

[102] Brinkerink M, Gallachóir B, Deane P. A comprehensive review on the benefits and challenges of global power grids and intercontinental interconnectors. Renewable and Sustainable Energy Reviews 2019;107:274–87. https://doi.org/10.1016/J.RSER.2019.03.003.

[103] Guidehouse. European Hydrogen Backbone: How a Dedicated Hydrogen Infrastructure Can Be Created. 2020.

[104] Linsel O, Bertsch V. A flexible approach to GIS based modelling of a global hydrogen transport system. Int J Hydrogen Energy 2024;52:334–49. https://doi.org/10.1016/J.IJHYDENE.2023.08.199.

[105] searoute · PyPI n.d. https://pypi.org/project/searoute/ (accessed February 12, 2024).

[106] Pietzcker RC, Stetter D, Manger S, Luderer G. Using the sun to decarbonize the power sector: The economic potential of photovoltaics and concentrating solar power. Appl Energy 2014;135:704–20. https://doi.org/10.1016/J.APENERGY.2014.08.011.

[107] Eurek K, Sullivan P, Gleason M, Hettinger D, Heimiller D, Lopez A. An improved global wind resource estimate for integrated assessment models. Energy Econ 2017;64:552–67. https://doi.org/10.1016/J.ENECO.2016.11.015.

[108] Gernaat DEHJ, Bogaart PW, Vuuren DPV, Biemans H, Niessink R. High-resolution assessment of global technical and economic hydropower potential. Nature Energy 2017 2:10 2017;2:821–8. https://doi.org/10.1038/s41560-017-0006-y.

[109] Staffell I, Pfenninger S. Using bias-corrected reanalysis to simulate current and future wind power output. Energy 2016;114:1224–39. https://doi.org/10.1016/J.ENERGY.2016.08.068.

[110] Pfenninger S, Staffell I. Long-term patterns of European PV output using 30 years of validated hourly reanalysis and satellite data. Energy 2016;114:1251–65. https://doi.org/10.1016/J.ENERGY.2016.08.060.

[111] Mathews D, Ó Gallachóir B, Deane P. Systematic bias in reanalysis-derived solar power profiles & the potential for error propagation in long duration energy storage studies. Appl Energy 2023;336:120819. https://doi.org/10.1016/J.APENERGY.2023.120819.

[112] Lehner B, Liermann CR, Revenga C, Vörömsmarty C, Fekete B, Crouzet P, et al. High-resolution mapping of the world's reservoirs and dams for sustainable river-flow management. Front Ecol Environ 2011;9:494–502. https://doi.org/10.1890/100125.

[113] Poncelet K, Hoschle H, Delarue E, Virag A, Drhaeseleer W. Selecting representative days for capturing the implications of integrating intermittent renewables in generation expansion planning problems. IEEE Transactions on Power Systems 2017;32:1936–48. https://doi.org/10.1109/TPWRS.2016.2596803.

[114] Reichenberg L, Hedenus F. The error induced by using representative periods in capacity expansion models: system cost, total capacity mix and regional capacity mix. Energy Systems 2022:1–18. https://doi.org/10.1007/S12667-022-00533-4/TABLES/2.

[115] Pineda S, Morales JM. Chronological time-period clustering for optimal capacity expansion planning with storage. IEEE Transactions on Power Systems 2018;33:7162–70. https://doi.org/10.1109/TPWRS.2018.2842093.

[116] Frew BA, Jacobson MZ. Temporal and spatial tradeoffs in power system modeling with assumptions about storage: An application of the POWER model. Energy 2016;117:198–213. https://doi.org/10.1016/J.ENERGY.2016.10.074.

[117] PLEXOS Desktop n.d. https://portal.energyexemplar.com/unified-help/plexos-desktop/index.htm#t=Main.Welcome.html (accessed July 16, 2024).

[118] Li C, Conejo AJ, Siirola JD, Grossmann IE. On representative day selection for capacity expansion planning of power systems under extreme operating conditions. International Journal of Electrical Power & Energy Systems 2022;137:107697. https://doi.org/10.1016/J.IJEPES.2021.107697.

[119] Jiménez F, Webster M. Optimal Selection of Sample Weeks for Approximating the Net Load in Generation Planning Problems 2013.

[120] Collins S, Deane JP, Poncelet K, Panos E, Pietzcker RC, Delarue E, et al. Integrating short term variations of the power system into integrated energy system models: A methodological review. Renewable and Sustainable Energy Reviews 2017;76:839–56. https://doi.org/10.1016/J.RSER.2017.03.090.

[121] Frowijn LSF, Baneke DM, Kramer GJ. Imagining a hydrogen economy: From grand technological utopia to enabler of the energy transition in three waves since the 1970s. Energy Res Soc Sci 2025;126:104084. https://doi.org/10.1016/J.ERSS.2025.104084.

[122] Dedehayir O, Steinert M. The hype cycle model: A review and future directions. Technol Forecast Soc Change 2016;108:28–41. https://doi.org/10.1016/J.TECHFORE.2016.04.005.

[123] de Cuveland K, Choi E, Shin M. Social dynamics of hyperbole–social media sentiment analysis for hype detection in emerging technologies: a conceptual approach. Technol Anal Strateg Manag 2025. https://doi.org/10.1080/09537325.2025.2502599;WGROUP:STRING:PUBLICATION.

[124] Dedehayir O, Steinert M. The hype cycle model: A review and future directions. Technol Forecast Soc Change 2016;108:28–41. https://doi.org/10.1016/J.TECHFORE.2016.04.005.

[125] Hampel C. Will the green hydrogen dream take shape? – pv magazine International 2025. https://www.pv-magazine.com/2025/04/05/will-the-green-hydrogen-dream-take-shape/ (accessed May 18, 2025).

[126] LeClerc J, Joslyn S. The cry wolf effect and weather-related decision making. Risk Analysis 2015;35:385–95. https://doi.org/10.1111/RISA.12336;SUBPAGE:STRING:FULL.

[127] Sawada Y, Kanai R, Kotani H. Impact of cry wolf effects on social preparedness and the efficiency of flood early warning systems. Hydrol Earth Syst Sci 2022;26:4265–78. https://doi.org/10.5194/HESS-26-4265-2022,.

[128] Brandt J, Iversen T, Eckert C, Peterssen F, Bensmann B, Bensmann A, et al. Cost and competitiveness of green hydrogen and the effects of the European Union regulatory framework. Nat Energy 2024;9:703–13. https://doi.org/10.1038/S41560-024-01511-Z;SUBJMETA=159,2790,4014,4077,4086,639,909;KWRD=ECONOMICS,ENERGY+MODELLING,HYDROGEN+ENERGY.

[129] Mathews D, Brinkerink M, Deane P. A framework for high resolution coupled global electricity & hydrogen models based on integrated assessment model scenarios. Int J Hydrogen Energy 2025;97:516–31. https://doi.org/10.1016/J.IJHYDENE.2024.11.077.

[130] Pfenninger S, Hawkes A, Keirstead J. Energy systems modeling for twenty-first century energy challenges. Renewable and Sustainable Energy Reviews 2014;33:74–86. https://doi.org/10.1016/J.RSER.2014.02.003.

[131] Kotzur L, Nolting L, Hoffmann M, Groß T, Smolenko A, Priesmann J, et al. A modeler's guide to handle complexity in energy systems optimization. Advances in Applied Energy 2021;4:100063. https://doi.org/10.1016/J.ADAPEN.2021.100063.

[132] Papavasiliou A, Avila D. Welfare Benefits of Co-Optimising Energy and Reserves. 2024.

[133] Nazari-heris M, Jabari F, Mohammadi-ivatloo B, Asadi S, Habibnezhad M. An updated review on multi-carrier energy systems with electricity, gas, and water energy sources. J Clean Prod 2020;275:123136. https://doi.org/10.1016/J.JCLEPRO.2020.123136.

[134] Dranka GG, Ferreira P, Vaz AIF. A review of co-optimization approaches for operational and planning problems in the energy sector. Appl Energy 2021;304:117703. https://doi.org/10.1016/J.APENERGY.2021.117703.

[135] Mathews D, Deane P. The Boy Who Cried Hydrogen: Examining the Cost Impact of Proactive Vs Reactive Policy for Electrolytic Hydrogen. 2025.

[136] Luderer G, Bauer N, Baumstark L, Bertram C, Leimbach M, Pietzcker R, et al. REMIND - REgional Model of INvestments and Development - Version 2.1.3 2020.

[137] - International Energy Agency I. World Energy Outlook 2023. 2023.

[138] Aghahosseini A, Breyer C. From hot rock to useful energy: A global estimate of enhanced geothermal systems potential. Appl Energy 2020;279:115769. https://doi.org/10.1016/J.APENERGY.2020.115769.

[139] Lee J, Cho Y. Determinants of reserve margin volatility: A new approach toward managing energy supply and demand. Energy 2022;252:124054. https://doi.org/10.1016/J.ENERGY.2022.124054.

[140] NERC. 2024 Long-Term Reliability Assessment Report 2024.

[141] Egli F, Steffen B, Schmidt TS. Bias in energy system models with uniform cost of capital assumption. Nat Commun 2019;10:1–3. https://doi.org/10.1038/S41467-019-12468-Z;SUBJMETA.

[142] Bogdanov D, Child M, Breyer C. Reply to 'Bias in energy system models with uniform cost of capital assumption.' Nat Commun 2019;10:4587. https://doi.org/10.1038/S41467-019-12469-Y.

[143] Scaling Hydrogen Financing for Development. Scaling Hydrogen Financing for Development 2024. https://doi.org/10.1787/0287B22E-EN.

[144] Ameli N, Dessens O, Winning M, Cronin J, Chenet H, Drummond P, et al. Higher cost of finance exacerbates a climate investment trap in developing economies. Nat Commun 2021;12:1–12. https://doi.org/10.1038/S41467-021-24305-3;TECHMETA.

[145] Bertsch V, Hyland M, Mahony M. What drives people's opinions of electricity infrastructure? Empirical evidence from Ireland. Energy Policy 2017;106:472–97. https://doi.org/10.1016/J.ENPOL.2017.04.008.

[146] Hyland M, Bertsch V. The Role of Community Involvement Mechanisms in Reducing Resistance to Energy Infrastructure Development. Ecological Economics 2018;146:447–74. https://doi.org/10.1016/J.ECOLECON.2017.11.016.

[147] Bertsch V, Hall M, Weinhardt C, Fichtner W. Public acceptance and preferences related to renewable energy and grid expansion policy: Empirical insights for Germany. Energy 2016;114:465–77. https://doi.org/10.1016/J.ENERGY.2016.08.022.

Appendix A
Capacity Expansion & Allocation Model Formulation

Indices

f	Facility
p	Flow Path
s	Flow Storage
d	Sample Day
t	Time Period
c	Commodity
n	Node

Variables

N_d	Number of Days a Sample Day is mapped to Represent
$Units_{f,p,s}$	Number of Units Built of a Facility, Flow Path or Flow Storage in the Capacity Expansion Phase
$P_{out,f}$	Power Equivalent Commodity Production Output from a Facility (MW)
$P_{in,f}$	Power Equivalent Commodity Consumption Input to a Facility (MW)
$P_{max,ft}$	Maximum Generic Output Rating of a Facility (MW)
η_f	Facility Conversion Efficiency
CF_{ft}	Maximum Load Factor of Renewable Resource (%)
$Flow_p$	Power Equivalent Flow Along a Flow Path Object (MW)
η_p	Flow Path Transmission Efficiency
$\eta_{inj,s}$	Flow Storage Injection Efficiency
$\eta_{with,s}$	Flow Path Withdrawal Efficiency
$InvOp_{st}$	Flow Storage Opening Inventory at timestep t
$Inv_{max,s}$	Flow Storage Max Inventory per Unit Built

Capacity Allocation & Expansion Model Objective Function

$$\sum_{(f)} \sum_{(d)} [N_d \times \sum_{(t)} \text{Production Cost}_{fdt}] + \sum_{(f)} \text{Build Cost}_f + \sum_{(f)} \text{FOM Costs}_f$$

$+ \sum_{(p)}$ Build Cost $_p$ $+ \sum_{(f)}$ FOM Costs $_p$ $+ \sum_{(s)}$ Build Cost $_s$ $+ \sum_{(S)}$ FOM Costs $_s$

Where Production Cost $_{fdt}$ = VOM $_{fdt}$ + Emission Costs $_{fdt}$ + Fuel Costs $_{fdt}$

Economic Dispatch Model Objective Function

In sequential steps of 1 day:

$$\sum_{(f)} \left[\sum_{(t)} \text{Production Cost}_{ft} \right]$$

Where Production Cost $_{ft}$ = VOM $_{ft}$ + Emission Costs $_{ft}$ + Fuel Costs $_{ft}$

Subject to:

Minimum and Maximum Facility Production Constraints

$P_{out,ft} \leq P_{max,f} \times Units_f$

$P_{out,ft} \geq 0$

Where:

$P_{out,ft} = \eta_f \times P_{in,ft}$

Hourly Capacity Factor Constraints for Wind & Solar:

$P_{max,ft} = 100 \times CF_{ft}$

Note: For hydro power generation, this capacity factor constraint is upheld on a monthly, rather than hourly, basis.

Flow Path Minimum and Maximum Flow Constraints

$Flow_p \leq Flow_{max,p} \times Units_p$

$Flow_p \geq -1 \times Flow_{max,p} \times Units_p$

Energy Storage Balance

$$[\eta_{inj,s} \times P_{inj,st}] - [\frac{1}{\eta_{with,s}} \times P_{with,st}] + Inv_{Open,st} - Inv_{Open,s(t+1)} = 0$$

Where:

<u>Flow Storage Minimum and Maximum Inventory</u>

$Inv_{Open,st} \leq Inv_{max,s} \times Units_s$

$Inv_{Open,st} \geq 0$

<u>Flow Storage Minimum and Maximum Injection & Withdrawal Constraints</u>

$P_{inj,st} \leq P_{inj,max,s} \times Units_s$

$P_{inj,st} \geq 0$

$P_{with,st} <= P_{with,max,s} \times Units_s$

$P_{with,st} \geq 0$

<u>Nodal Energy Balance</u>

$$\sum_{(f)} P_{out,ft} + \sum_{(s)} P_{with,st} + \sum_{(p)} Flow_{pt} - \sum_{(s)} P_{inj,st} - Demand_{nt} = 0$$

Appendix B

As outlined in the core text of this work, the economic parameters for each technology type, as presented in Table B.1 below, are de-regionalized by assuming the median value across all regions as per the International Energy Agency's (IEA's) World Energy Outlook (WEO) 2023 [137]. For storage technologies, the costs are defined per kWh of storage capacity as per Table B.2.

Facility	Build Cost ($2010/kW)	Fixed Operation & Maintenance Cost ($2010/kW)	Economic Life (Years)	References
Wind|Onshore	1095.15	28.31	25	IEA WEO 2023
Wind|Offshore	1549.60	48.43	25	IEA WEO 2023
Solar	335.25	8.94	25	IEA WEO 2023
Hydro	1564.50	37.25	50	IEA WEO 2023
Geothermal	1676.25	33.53	50	IEA WEO 2023
Biomass|w/ CCS	3352.50	119.20	50	IEA WEO 2023
Biomass|w/o CCS	1564.50	55.88	50	IEA WEO 2023
Gas|w/ CCS	1564.50	48.43	50	IEA WEO 2023
Gas|w/o CCS	596.00	18.63	50	IEA WEO 2023
Nuclear	2980.00	119.20	50	IEA WEO 2023
Electrolysis	462.96	17.76	15	IEA WEO 2023
Ammonia Synthesis	804.03	24.12	50	IEA Hydrogen Review 2023
Ammonia Cracker	505.20	15.16	50	IEA Hydrogen Review 2023
Hydrogen/Ammonia CCGT	819.50	22.35	50	IEA WEO 2023

TABLE B.0.1 FACILITY TECHNOECONOMIC PARAMETERS

Storage	Build Cost ($2010/kWh)	Fixed Operation & Maintenance Cost ($2010/kWh)	Economic Life (Years)	References
Battery Storage	100.575	1.51	10	IEA WEO 2023
Hydrogen Storage	7.45	0.22	25	IEA Hydrogen Review 2023
Ammonia Storage	37.25	1.12	25	IEA Hydrogen Review 2023

TABLE B.0.2 STORAGE TECHNOECONOMIC PARAMETERS

Electricity interconnector techno-economics are identical to those developed in [20] with a full derivation provided therein. However, for comprehensiveness, the resulting techno-economics are provided in Table B.3. Note that these specifications are based on a maximum interregional capacity of 50 GW per line. As a linearized model, the model can build a fraction of the capacity at an equal fraction of the resulting costs. In this work, Electricity Interconnectors are assumed to have an economic lifetime of 50 years.

From	To	KM distance	HVAC/HVDC/Subsea	Build Cost ($2010 in $000)	Annual FO&M (3.5% of CAPEX) ($2010 in $000)	Losses
AF-COD	AF-COG	9	HVAC	4200435	147015	0%
EU-AUT	EU-SVK	56	HVAC	5702900	199600	0%
EU-KOS	EU-MKD	77	HVAC	6374215	223100	1%
AS-LBN	AS-SYR	84	HVAC	6597990	230930	1%
SA-BRA-J1	SA-BRA-SO	94	HVAC	6917660	242120	1%
AS-CHN-GD	AS-CHN-MA	107	HVAC	7333240	256665	1%
AS-ISR	AS-JOR	111	HVAC	7461110	261140	1%
AS-CHN-BE	AS-CHN-TJ	113	HVAC	7525045	263375	1%
EU-HRV	EU-SVN	118	HVAC	7684880	268970	1%
AF-MOZ	AF-SWZ	122	HVAC	7812750	273445	1%
AF-GIN	AF-SLE	128	HVAC	8004555	280160	1%
AS-CHN-GD	AS-CHN-HK	128	HVAC	8004555	280160	1%

NA-USA-NY	NA-USA-RE	128	HVAC	8004555	280160	1%
EU-ALB	EU-MNE	132	HVAC	8132425	284635	1%
AS-CHN-AN	AS-CHN-JS	143	HVAC	8484065	296940	1%
AF-BEN	AF-TGO	145	HVAC	8548000	299180	1%
EU-ALB	EU-MKD	154	HVAC	8835705	309250	1%
EU-KOS	EU-MNE	157	HVAC	8931610	312605	1%
AS-CHN-SH	AS-CHN-ZH	162	HVAC	9091445	318200	1%
EU-HUN	EU-SVK	164	HVAC	9155380	320440	1%
AF-GMB	AF-SEN	165	HVAC	9187345	321555	1%
AF-GAB	AF-GNQ	169	HVAC	9315215	326035	1%
EU-BLR	EU-LTU	170	HVAC	9347185	327150	1%
AS-CHN-HB	AS-CHN-SX	171	HVAC	9379150	328270	1%
EU-BGR	EU-MKD	172	HVAC	9411120	329390	1%
EU-BIH	EU-MNE	172	HVAC	9411120	329390	1%
EU-ARM	EU-GEO	173	HVAC	9443085	330510	1%
EU-BEL	EU-NLD	173	HVAC	9443085	330510	1%
NA-GTM	NA-SLV	175	HVAC	9507020	332745	1%
AF-BDI	AF-RWA	176	HVAC	9538990	333865	1%
AF-BEN	AF-NGA	176	HVAC	9538990	333865	1%
AS-JOR	AS-SYR	176	HVAC	9538990	333865	1%
EU-ALB	EU-KOS	186	HVAC	9858660	345055	1%
EU-BEL	EU-LUX	187	HVAC	9890630	346170	1%
AS-CHN-GA	AS-CHN-QI	192	HVAC	10050465	351765	1%
NA-CAN-BC	NA-USA-NW	193	HVAC	10082435	352885	1%
AS-KOR	AS-PRK	195	HVAC	10146370	355125	1%
AS-KAZ	AS-KGZ	196	HVAC	10178335	356240	1%
EU-BIH	EU-SRB	198	HVAC	10242270	358480	1%
SA-ARG	SA-URY	205	HVAC	10466045	366310	1%
AS-ISR	AS-LBN	211	HVAC	10657845	373025	1%
AF-ERI	AF-ETH	212	HVAC	10689815	374145	1%
AS-KHM	AS-VNM	212	HVAC	10689815	374145	1%
AS-ISR	AS-SYR	213	HVAC	10721780	375260	1%
EU-AUT	EU-HUN	217	HVAC	10849650	379740	2%

NA-HND	NA-SLV	219	HVAC	10913585	381975	2%
AS-AFG	AS-TJK	223	HVAC	11041455	386450	2%
AS-CHN-HJ	AS-CHN-JI	234	HVAC	11393095	398760	2%
AS-CHN-JS	AS-CHN-ZH	240	HVAC	11584900	405470	2%
NA-HND	NA-NIC	240	HVAC	11584900	405470	2%
AF-NGA	AF-TGO	242	HVAC	11648835	407710	2%
EU-KOS	EU-SRB	246	HVAC	11776705	412185	2%
EU-AUT	EU-CZE	251	HVAC	11936545	417780	2%
AS-BGD	AS-IND-EA	253	HVAC	12000475	420015	2%
NA-DOM	NA-HTI	257	HVAC	12128345	424490	2%
EU-BEL	EU-FRA	261	HVAC	12256215	428970	2%
AS-CHN-HU	AS-CHN-JX	262	HVAC	12288185	430085	2%
EU-LTU	EU-LVA	263	HVAC	12320150	431205	2%
AS-CHN-HB	AS-CHN-TJ	265	HVAC	12384085	433445	2%
AS-CHN-BE	AS-CHN-HB	266	HVAC	12416055	434560	2%
AS-JPN-CE	AS-JPN-SH	267	HVAC	12448020	435680	2%
NA-USA-RM	NA-USA-RW	267	HVAC	12448020	435680	2%
AS-CHN-JS	AS-CHN-SH	268	HVAC	12479990	436800	2%
AF-BWA	AF-ZAF	272	HVAC	12607860	441275	2%
AS-CHN-CH	AS-CHN-SC	272	HVAC	12607860	441275	2%
AS-CHN-JI	AS-CHN-LI	276	HVAC	12735725	445750	2%
EU-AUT	EU-SVN	277	HVAC	12767695	446870	2%
EU-EST	EU-LVA	279	HVAC	12831630	449105	2%
AS-BTN	AS-CHN-TI	281	HVAC	12895565	451345	2%
EU-CZE	EU-DEU	281	HVAC	12895565	451345	2%
EU-MNE	EU-SRB	281	HVAC	12895565	451345	2%
EU-BIH	EU-HRV	287	HVAC	13087370	458060	2%
EU-FRA	EU-LUX	288	HVAC	13119335	459175	2%
AS-CHN-HN	AS-CHN-JX	289	HVAC	13151305	460295	2%
EU-CZE	EU-SVK	289	HVAC	13151305	460295	2%
SA-BRA-J1	SA-BRA-SE	290	HVAC	13183270	461415	2%

AS-CHN-HN	AS-CHN-HU	293	HVAC	13279175	464770	2%
AF-CMR	AF-GNQ	295	HVAC	13343110	467010	2%
EU-BGR	EU-ROU	297	HVAC	13407040	469245	2%
NA-USA-NE	NA-USA-NY	298	HVAC	13439010	470365	2%
EU-FIN	AS-RUS-NW	300	HVAC	13502945	472605	2%
EU-HRV	EU-HUN	302	HVAC	13566880	474840	2%
AS-BGD	AS-IND-NE	304	HVAC	13630815	477080	2%
AF-CIV	AF-GHA	307	HVAC	13726715	480435	2%
AS-TJK	AS-UZB	309	HVAC	13790650	482675	2%
EU-EST	AS-RUS-NW	317	HVAC	14046390	491625	2%
EU-HUN	EU-SRB	317	HVAC	14046390	491625	2%
AS-CHN-AN	AS-CHN-HU	319	HVAC	14110325	493860	2%
AF-GHA	AF-TGO	321	HVAC	14174260	496100	2%
EU-MKD	EU-SRB	323	HVAC	14238195	498335	2%
AS-CHN-AN	AS-CHN-ZH	328	HVAC	14398030	503930	2%
EU-BGR	EU-SRB	330	HVAC	14461965	506170	2%
AS-CHN-CH	AS-CHN-GU	332	HVAC	14525900	508405	2%
NA-CAN-ON	NA-USA-RM	333	HVAC	14557870	509525	2%
AF-GIN	AF-GNB	334	HVAC	14589835	510645	2%
AF-SWZ	AF-ZAF	337	HVAC	14685740	514000	2%
AS-CHN-BE	AS-CHN-EM	337	HVAC	14685740	514000	2%
NA-CRI	NA-NIC	343	HVAC	14877540	520715	2%
NA-USA-SC	NA-USA-SE	344	HVAC	14909510	521835	2%
SA-BRA-SE	SA-BRA-SO	344	HVAC	14909510	521835	2%
AS-CHN-GA	AS-CHN-NI	347	HVAC	15005410	525190	2%
SA-GUY	SA-SUR	349	HVAC	15069345	527425	2%
AF-LSO	AF-ZAF	354	HVAC	15229185	533020	2%
EU-DEU	EU-DNK	355	HVAC	15261150	534140	2%
EU-MDA	EU-ROU	357	HVAC	15325085	536380	2%
AF-LBR	AF-SLE	360	HVAC	15420990	539735	2%

AS-CHN-HE	AS-CHN-SX	361	HVAC	15452955	540855	2%
NA-GTM	NA-HND	361	HVAC	15452955	540855	2%
AS-CHN-LI	AS-PRK	366	HVAC	15612790	546450	3%
EU-HRV	EU-SRB	366	HVAC	15612790	546450	3%
NA-USA-SE	NA-USA-SV	366	HVAC	15612790	546450	3%
SA-BRA-J3	SA-BRA-NW	371	HVDC	15662760	548195	3%
AS-CHN-HB	AS-CHN-HE	374	HVDC	15690745	549175	3%
AS-CHN-EM	AS-CHN-LI	375	HVDC	15700070	549500	3%
AF-GNB	AF-SEN	376	HVDC	15709400	549830	3%
AF-RWA	AF-UGA	377	HVDC	15718730	550155	3%
AS-CHN-AN	AS-CHN-JX	377	HVDC	15718730	550155	3%
NA-USA-SN	NA-USA-SW	377	HVDC	15718730	550155	3%
AS-CHN-EM	AS-CHN-TJ	379	HVDC	15737385	550810	3%
AS-ARE	AS-OMN	381	HVDC	15756040	551460	3%
EU-HUN	EU-SVN	383	HVDC	15774695	552115	3%
AS-CHN-SX	AS-CHN-WM	388	HVDC	15821335	553745	3%
AS-CHN-NI	AS-CHN-WM	389	HVDC	15830665	554075	3%
AS-CHN-TI	AS-IND-NE	393	HVDC	15867975	555380	3%
EU-FIN	EU-SWE	393	HVDC	15867975	555380	3%
EU-LTU	EU-POL	393	HVDC	15867975	555380	3%
AF-ZMB	AF-ZWE	397	HVDC	15905290	556685	3%
EU-MDA	EU-UKR	400	HVDC	15933275	557665	3%
AS-JPN-CE	AS-JPN-TO	403	HVDC	15961255	558645	3%
EU-BLR	EU-LVA	403	HVDC	15961255	558645	3%
AF-BEN	AF-GHA	403	HVDC	15961255	558645	3%
AF-EGY	AS-ISR	404	HVDC	15970585	558970	3%
NA-BLZ	NA-GTM	406	HVDC	15989240	559625	3%
NA-CAN-QC	NA-USA-NE	406	HVDC	15989240	559625	3%
AF-MRT	AF-SEN	407	HVDC	15998570	559950	3%
NA-USA-SC	NA-USA-SW	410	HVDC	16026555	560930	3%

AF-BFA	AF-NER	415	HVDC	16073195	562560	3%
EU-NOR	EU-SWE	418	HVDC	16101175	563540	3%
AS-BHR	AS-SAU	422	HVDC	16138490	564845	3%
EU-BLR	EU-UKR	435	HVDC	16259755	569090	3%
AS-CHN-SD	AS-CHN-TJ	436	HVDC	16269080	569420	3%
AS-CHN-GU	AS-CHN-YU	438	HVDC	16287740	570070	3%
AS-CHN-HE	AS-CHN-SI	440	HVDC	16306395	570725	3%
AF-MOZ	AF-ZAF	443	HVDC	16334380	571705	3%
AS-CHN-GU	AS-CHN-GX	448	HVDC	16381020	573335	3%
EU-ROU	EU-SRB	448	HVDC	16381020	573335	3%
AF-CMR	AF-GAB	450	HVDC	16399675	573990	3%
AS-CHN-JX	AS-CHN-ZH	450	HVDC	16399675	573990	3%
EU-AZE	EU-GEO	450	HVDC	16399675	573990	3%
AF-DJI	AF-ETH	452	HVDC	16418330	574640	3%
EU-ARM	EU-AZE	454	HVDC	16436985	575295	3%
EU-HRV	EU-MNE	455	HVDC	16446315	575620	3%
NA-USA-FR	NA-USA-SE	461	HVDC	16502280	577580	3%
EU-GBR	EU-IRL	463	HVDC	16520940	578235	3%
AS-CHN-GD	AS-CHN-HA	464	HVDC	16530265	578560	3%
AS-CHN-AN	AS-CHN-HE	466	HVDC	16548925	579210	3%
AS-CHN-HE	AS-CHN-HU	468	HVDC	16567580	579865	3%
AS-KGZ	AS-UZB	470	HVDC	16586235	580520	3%
AS-CHN-JS	AS-CHN-SD	471	HVDC	16595565	580845	3%
NA-USA-ME	NA-USA-MW	473	HVDC	16614220	581500	3%
AS-QAT	AS-SAU	474	HVDC	16623545	581825	3%
EU-BLR	EU-POL	475	HVDC	16632875	582150	3%
AF-GIN	AF-LBR	478	HVDC	16660860	583130	3%
AS-JPN-CE	AS-JPN-KY	482	HVDC	16698170	584435	3%
NA-USA-SN	NA-USA-SS	483	HVDC	16707500	584765	3%
EU-GRC	EU-MKD	488	HVDC	16754140	586395	3%
EU-CHE	EU-FRA	490	HVDC	16772795	587050	3%
EU-ITA	EU-SVN	490	HVDC	16772795	587050	3%

EU-LVA	AS-RUS-NW	491	HVDC	16782125	587375	3%
AS-CHN-HB	AS-CHN-WM	494	HVDC	16810105	588355	3%
EU-ALB	EU-GRC	500	HVDC	16866075	590315	3%
AF-KEN	AF-UGA	503	HVDC	16894060	591290	3%
EU-BGR	AS-TUR	503	HVDC	16894060	591290	3%
NA-CAN-ON	NA-CAN-QC	503	HVDC	16894060	591290	3%
AS-CHN-GA	AS-CHN-SI	504	HVDC	16903385	591620	3%
EU-ESP	EU-PRT	504	HVDC	16903385	591620	3%
AS-CHN-FU	AS-CHN-GD	505	HVDC	16912715	591945	3%
AS-AFG	AS-UZB	507	HVDC	16931370	592600	3%
AS-CHN-HJ	AS-RUS-FE	509	HVDC	16950030	593250	3%
NA-CRI	NA-PAN	511	HVDC	16968685	593905	3%
AF-LBY	AF-TUN	514	HVDC	16996670	594885	3%
AS-CHN-GD	AS-CHN-GX	514	HVDC	16996670	594885	3%
EU-CZE	EU-POL	515	HVDC	17005995	595210	3%
EU-DEU	EU-POL	516	HVDC	17015325	595535	3%
AS-CHN-SI	AS-CHN-SX	517	HVDC	17024650	595865	3%
AS-CHN-FU	AS-CHN-JX	519	HVDC	17043310	596515	3%
AS-LAO	AS-THA	519	HVDC	17043310	596515	3%
AS-CHN-NI	AS-CHN-SI	522	HVDC	17071290	597495	3%
AS-CHN-GU	AS-CHN-SC	523	HVDC	17080620	597820	3%
EU-AUT	EU-DEU	524	HVDC	17089950	598150	3%
EU-BGR	EU-GRC	524	HVDC	17089950	598150	3%
NA-CAN-AB	NA-CAN-SK	525	HVDC	17099275	598475	3%
NA-USA-ER	NA-USA-SA	527	HVDC	17117930	599130	3%
EU-POL	EU-SVK	533	HVDC	17173900	601085	3%
NA-CAN-QC	NA-USA-NY	535	HVDC	17192555	601740	3%
AS-KHM	AS-THA	536	HVDC	17201885	602065	3%
AS-IND-EA	AS-IND-NE	537	HVDC	17211210	602390	3%
NA-USA-ME	NA-USA-RW	538	HVDC	17220540	602720	3%

AS-KWT	AS-SAU	539	HVDC	17229870	603045	3%
NA-USA-RW	NA-USA-SC	539	HVDC	17229870	603045	3%
AS-CHN-JI	AS-PRK	540	HVDC	17239195	603370	3%
EU-AZE	AS-IRN	543	HVDC	17267180	604350	3%
AS-CHN-EM	AS-CHN-JI	548	HVDC	17313820	605985	3%
NA-USA-SC	NA-USA-SV	548	HVDC	17313820	605985	3%
AS-CHN-AN	AS-CHN-SD	549	HVDC	17323150	606310	3%
AF-AGO	AF-COD	551	HVDC	17341805	606965	3%
AF-AGO	AF-COG	557	HVDC	17397775	608920	3%
AS-IRQ	AS-KWT	557	HVDC	17397775	608920	3%
AS-CHN-HE	AS-CHN-JS	562	HVDC	17444415	610555	3%
NA-CAN-ON	NA-USA-NY	562	HVDC	17444415	610555	3%
AS-CHN-GD	AS-CHN-HN	563	HVDC	17453740	610880	3%
AS-CHN-HB	AS-CHN-SD	563	HVDC	17453740	610880	3%
NA-USA-RW	NA-USA-SV	564	HVDC	17463070	611205	3%
AS-CHN-CH	AS-CHN-SI	567	HVDC	17491055	612185	3%
AS-BTN	AS-IND-EA	569	HVDC	17509710	612840	3%
EU-GRC	AS-TUR	570	HVDC	17519035	613165	3%
EU-DEU	EU-NLD	575	HVDC	17565675	614800	3%
AS-MMR	AS-THA	579	HVDC	17602990	616105	3%
NA-USA-AZ	NA-USA-CA	586	HVDC	17668285	618390	3%
EU-AUT	EU-CHE	591	HVDC	17714925	620020	3%
AS-CHN-GA	AS-CHN-SC	599	HVDC	17789550	622635	3%
EU-DEU	EU-LUX	602	HVDC	17817535	623615	3%
AS-CHN-TI	AS-NPL	603	HVDC	17826860	623940	3%
AS-CHN-EM	AS-CHN-HB	604	HVDC	17836190	624265	3%
AS-CHN-SC	AS-CHN-SI	604	HVDC	17836190	624265	3%
AF-MWI	AF-ZMB	613	HVDC	17920140	627205	3%

AF-DJI	AF-ERI	617	HVDC	17957455	628510	4%
NA-CAN-MB	NA-USA-MW	620	HVDC	17985440	629490	4%
AS-CHN-HE	AS-CHN-SD	622	HVDC	18004095	630145	4%
AS-CHN-GX	AS-CHN-YU	625	HVDC	18032080	631125	4%
AF-BFA	AF-GHA	632	HVDC	18097375	633410	4%
AS-RUS-CE	AS-RUS-NW	634	HVDC	18116030	634060	4%
AF-DZA	AF-TUN	635	HVDC	18125360	634390	4%
AS-CHN-SC	AS-CHN-YU	637	HVDC	18144015	635040	4%
AS-CHN-CH	AS-CHN-HN	639	HVDC	18162670	635695	4%
EU-HUN	EU-ROU	640	HVDC	18172000	636020	4%
NA-USA-RW	NA-USA-SW	642	HVDC	18190655	636675	4%
AS-CHN-GU	AS-CHN-HN	643	HVDC	18199985	637000	4%
AS-CHN-HU	AS-CHN-SI	650	HVDC	18265280	639285	4%
EU-BEL	EU-DEU	652	HVDC	18283935	639940	4%
OC-AUS-SA	OC-AUS-VI	654	HVDC	18302590	640590	4%
AS-IND-EA	AS-NPL	655	HVDC	18311920	640915	4%
EU-LTU	AS-RUS-NW	657	HVDC	18330575	641570	4%
NA-CAN-AR	NA-USA-NE	657	HVDC	18330575	641570	4%
NA-USA-MW	NA-USA-SN	658	HVDC	18339905	641895	4%
NA-USA-ER	NA-USA-SS	662	HVDC	18377215	643205	4%
NA-USA-SA	NA-USA-SE	662	HVDC	18377215	643205	4%
AS-KAZ	AS-UZB	665	HVDC	18405200	644180	4%
AS-CHN-GD	AS-CHN-JX	666	HVDC	18414525	644510	4%
AS-IRN	AS-TKM	669	HVDC	18442510	645490	4%
EU-CHE	EU-DEU	669	HVDC	18442510	645490	4%
NA-USA-RE	NA-USA-RW	669	HVDC	18442510	645490	4%

AF-KEN	AF-TZA	671	HVDC	18461165	646140	4%
NA-CAN-AB	NA-CAN-BC	674	HVDC	18489150	647120	4%
EU-BLR	AS-RUS-CE	675	HVDC	18498480	647445	4%
AS-CHN-FU	AS-CHN-ZH	677	HVDC	18517135	648100	4%
EU-CHE	EU-ITA	684	HVDC	18582430	650385	4%
AS-KGZ	AS-TJK	685	HVDC	18591760	650710	4%
AF-ERI	AF-SDN	686	HVDC	18601090	651040	4%
AS-PRK	AS-RUS-FE	689	HVDC	18629070	652015	4%
EU-ITA	EU-MLT	689	HVDC	18629070	652015	4%
AS-LAO	AS-MMR	690	HVDC	18638400	652345	4%
EU-POL	EU-UKR	691	HVDC	18647730	652670	4%
EU-BLR	AS-RUS-NW	692	HVDC	18657055	652995	4%
AF-BEN	AF-BFA	693	HVDC	18666385	653325	4%
AS-IRN	AS-IRQ	694	HVDC	18675710	653650	4%
AS-CHN-QI	AS-CHN-SC	695	HVDC	18685040	653975	4%
AS-CHN-EM	AS-CHN-SD	697	HVDC	18703695	654630	4%
AF-BEN	AF-NER	704	HVDC	18768990	656915	4%
AF-BFA	AF-MLI	704	HVDC	18768990	656915	4%
OC-AUS-SW	OC-AUS-VI	708	HVDC	18806305	658220	4%
AF-GIN	AF-SEN	709	HVDC	18815630	658545	4%
AF-GIN	AF-MLI	710	HVDC	18824960	658875	4%
NA-CAN-AB	NA-USA-NW	710	HVDC	18824960	658875	4%
NA-CAN-MB	NA-CAN-SK	711	HVDC	18834290	659200	4%
AS-CHN-SI	AS-CHN-WM	714	HVDC	18862270	660180	4%
AS-RUS-MV	AS-RUS-UR	717	HVDC	18890255	661160	4%
AS-CHN-SD	AS-CHN-SX	719	HVDC	18908915	661810	4%
AS-RUS-CE	AS-RUS-MV	720	HVDC	18918240	662140	4%
AS-CHN-EM	AS-CHN-HJ	727	HVDC	18983535	664425	4%
NA-USA-RE	NA-USA-SV	732	HVDC	19030175	666055	4%

AS-CHN-GA	AS-CHN-WM	733	HVDC	19039505	666385	4%
EU-GEO	AS-RUS-SO	733	HVDC	19039505	666385	4%
AS-CHN-AN	AS-CHN-HB	735	HVDC	19058160	667035	4%
NA-USA-SA	NA-USA-SC	739	HVDC	19095475	668340	4%
OC-AUS-QL	OC-AUS-SW	740	HVDC	19104800	668670	4%
EU-ROU	EU-UKR	745	HVDC	19151440	670300	4%
AS-CHN-CH	AS-CHN-HU	747	HVDC	19170095	670955	4%
NA-USA-MW	NA-USA-SW	747	HVDC	19170095	670955	4%
AS-IRQ	AS-SYR	751	HVDC	19207410	672260	4%
AF-BFA	AF-TGO	756	HVDC	19254050	673890	4%
AF-CIV	AF-LBR	756	HVDC	19254050	673890	4%
AS-KHM	AS-LAO	756	HVDC	19254050	673890	4%
AS-RUS-CE	EU-UKR	757	HVDC	19263375	674220	4%
AS-CHN-GX	AS-CHN-HN	759	HVDC	19282035	674870	4%
AS-RUS-SO	EU-UKR	760	HVDC	19291360	675200	4%
SA-BRA-NW	SA-BRA-WE	762	HVDC	19310020	675850	4%
EU-AUT	EU-ITA	764	HVDC	19328675	676505	4%
SA-COL	NA-PAN	773	HVDC	19412625	679440	4%
AS-CHN-EM	AS-CHN-WM	781	HVDC	19487250	682055	4%
AF-ETH	AF-SDN	782	HVDC	19496580	682380	4%
AF-CAF	AF-CMR	783	HVDC	19505905	682705	4%
EU-ARM	AS-IRN	786	HVDC	19533890	683685	4%
EU-FIN	EU-NOR	787	HVDC	19543220	684015	4%
NA-CAN-AR	NA-CAN-QC	789	HVDC	19561875	684665	4%
AS-CHN-YU	AS-LAO	790	HVDC	19571200	684990	4%
AF-NER	AF-NGA	799	HVDC	19655155	687930	4%
AS-IND-NO	AS-NPL	799	HVDC	19655155	687930	4%
NA-USA-RA	NA-USA-SS	805	HVDC	19711125	689890	4%
AS-IRQ	AS-JOR	807	HVDC	19729780	690540	4%

SA-BRA-CN	SA-BRA-J2	826	HVDC	19907010	696745	4%
AF-COG	AF-GAB	828	HVDC	19925665	697400	4%
AF-BFA	AF-CIV	831	HVDC	19953650	698380	4%
AS-JPN-HO	AS-JPN-TO	833	HVDC	19972305	699030	4%
SA-BRA-SO	SA-PRY	836	HVDC	20000290	700010	4%
AS-CHN-WM	AS-MNG	840	HVDC	20037605	701315	4%
AS-IND-SO	AS-IND-WE	840	HVDC	20037605	701315	4%
AS-ARE	AS-SAU	860	HVDC	20224165	707845	4%
AS-CHN-XI	AS-KAZ	860	HVDC	20224165	707845	4%
AS-CHN-JS	AS-CHN-SX	861	HVDC	20233490	708170	4%
AS-CHN-HB	AS-CHN-LI	871	HVDC	20326770	711435	4%
SA-BRA-CW	SA-BRA-J2	872	HVDC	20336100	711765	4%
SA-BRA-CW	SA-BRA-SE	872	HVDC	20336100	711765	4%
EU-DEU	EU-FRA	878	HVDC	20392070	713720	4%
AS-IND-WE	AS-PAK	888	HVDC	20485350	716985	4%
NA-USA-RA	NA-USA-SN	889	HVDC	20494675	717315	4%
AF-ESH	AF-MAR	895	HVDC	20550645	719275	4%
EU-HUN	EU-UKR	896	HVDC	20559975	719600	4%
AS-CHN-HN	AS-CHN-SC	904	HVDC	20634595	722210	5%
AS-LAO	AS-VNM	910	HVDC	20690565	724170	5%
AF-MOZ	AF-ZWE	918	HVDC	20765190	726780	5%
AF-CIV	AF-MLI	924	HVDC	20821155	728740	5%
AF-BWA	AF-ZWE	927	HVDC	20849140	729720	5%
AF-BWA	AF-NAM	928	HVDC	20858470	730045	5%
NA-USA-SA	NA-USA-SS	929	HVDC	20867800	730375	5%
SA-BRA-J2	SA-BRA-NE	932	HVDC	20895780	731350	5%
NA-USA-AZ	NA-USA-RA	941	HVDC	20979735	734290	5%
AF-CAF	AF-TCD	944	HVDC	21007720	735270	5%
AF-CMR	AF-NGA	944	HVDC	21007720	735270	5%
AS-CHN-JS	AS-CHN-SI	952	HVDC	21082340	737880	5%

NA-USA-SA	NA-USA-SW	953	HVDC	21091670	738210	5%
AS-RUS-CE	AS-RUS-SO	958	HVDC	21138310	739840	5%
AS-BGD	AS-MMR	972	HVDC	21268905	744410	5%
AF-ZAF	AF-ZWE	979	HVDC	21334200	746695	5%
AS-IRQ	AS-SAU	994	HVDC	21474120	751595	5%
AF-CMR	AF-COG	996	HVDC	21492775	752245	5%
AF-CMR	AF-TCD	996	HVDC	21492775	752245	5%
SA-COL	SA-ECU	998	HVDC	21511430	752900	5%
AF-MWI	AF-TZA	999	HVDC	21520760	753225	5%
EU-SVK	EU-UKR	1000	HVDC	21530085	753555	5%
SA-BOL	SA-BRA-WE	1004	HVDC	21567400	754860	5%
AS-TKM	AS-UZB	1006	HVDC	21586055	755510	5%
NA-USA-MW	NA-USA-RW	1008	HVDC	21604710	756165	5%
SA-BOL	SA-PRY	1018	HVDC	21697990	759430	5%
AF-DZA	AF-LBY	1019	HVDC	21707320	759755	5%
AF-KEN	AF-SOM	1021	HVDC	21725975	760410	5%
AF-CAF	AF-COG	1026	HVDC	21772615	762040	5%
SA-COL	SA-VEN	1027	HVDC	21781945	762370	5%
AS-AFG	AS-TKM	1030	HVDC	21809930	763350	5%
AF-DZA	AF-MAR	1031	HVDC	21819255	763675	5%
AF-CAF	AF-COD	1032	HVDC	21828585	764000	5%
SA-ARG	SA-PRY	1037	HVDC	21875225	765635	5%
SA-GUY	SA-VEN	1046	HVDC	21959175	768570	5%
AF-MLI	AF-MRT	1047	HVDC	21968505	768900	5%
AF-ESH	AF-MRT	1047	HVDC	21968505	768900	5%
AF-MLI	AF-SEN	1049	HVDC	21987160	769550	5%
EU-ESP	EU-FRA	1054	HVDC	22033800	771185	5%
AS-CHN-XI	AS-KGZ	1055	HVDC	22043130	771510	5%
AF-BWA	AF-ZMB	1056	HVDC	22052455	771835	5%
NA-GTM	NA-MEX	1060	HVDC	22089770	773140	5%
AS-SYR	AS-TUR	1063	HVDC	22117755	774120	5%
SA-BRA-CW	SA-BRA-NE	1063	HVDC	22117755	774120	5%
AS-SAU	AS-YEM	1067	HVDC	22155065	775425	5%
AS-CHN-CH	AS-CHN-SX	1075	HVDC	22229690	778040	5%
AS-CHN-HN	AS-CHN-SX	1077	HVDC	22248345	778690	5%

SA-BRA-CW	SA-BRA-SO	1081	HVDC	22285655	780000	5%
AF-TZA	AF-UGA	1085	HVDC	22322970	781305	5%
EU-NOR	AS-RUS-NW	1086	HVDC	22332295	781630	5%
AF-DJI	AF-SOM	1087	HVDC	22341625	781955	5%
NA-USA-SA	NA-USA-SN	1092	HVDC	22388265	783590	5%
SA-BRA-CN	SA-SUR	1099	HVDC	22453560	785875	5%
AF-MLI	AF-NER	1100	HVDC	22462890	786200	5%
AS-IND-NO	AS-PAK	1100	HVDC	22462890	786200	5%
AS-CHN-GD	AS-CHN-YU	1101	HVDC	22472220	786530	5%
EU-FRA	EU-ITA	1107	HVDC	22528185	788485	5%
NA-CAN-ON	NA-USA-MW	1109	HVDC	22546840	789140	5%
EU-AZE	AS-RUS-SO	1113	HVDC	22584155	790445	5%
NA-USA-MW	NA-USA-RA	1114	HVDC	22593480	790770	5%
SA-BRA-NW	SA-GUY	1120	HVDC	22649450	792730	5%
SA-BRA-CN	SA-BRA-J3	1126	HVDC	22705420	794690	5%
SA-BRA-NW	SA-SUR	1129	HVDC	22733400	795670	5%
AS-IND-NE	AS-MMR	1130	HVDC	22742730	795995	5%
AS-CHN-EM	AS-MNG	1132	HVDC	22761385	796650	5%
AS-CHN-YU	AS-MMR	1133	HVDC	22770715	796975	5%
SA-ARG	SA-CHL	1137	HVDC	22808025	798280	5%
SA-ECU	SA-PER	1138	HVDC	22817355	798605	5%
AF-RWA	AF-TZA	1154	HVDC	22966605	803830	5%
OC-AUS-SA	OC-AUS-SW	1159	HVDC	23013245	805465	5%
AF-BDI	AF-TZA	1161	HVDC	23031900	806115	5%
AF-CIV	AF-GIN	1161	HVDC	23031900	806115	5%
AS-IND-NO	AS-IND-WE	1162	HVDC	23041225	806445	5%
NA-BLZ	NA-MEX	1174	HVDC	23153165	810360	5%

AF-NAM	AF-ZAF	1178	HVDC	23190475	811665	5%
AS-MYS	AS-THA	1184	HVDC	23246445	813625	5%
AS-IDN	AS-MYS	1185	Subsea	26542010	928970	5%
AS-CHN-CH	AS-CHN-HB	1191	HVDC	23311740	815910	6%
AS-OMN	AS-SAU	1205	HVDC	23442330	820480	6%
NA-MEX	NA-USA-ER	1211	HVDC	23498300	822440	6%
NA-CAN-SK	NA-USA-NW	1227	HVDC	23647550	827665	6%
NA-CAN-NO	NA-CAN-SK	1231	HVDC	23684860	828970	6%
SA-BRA-NW	SA-GUF	1235	HVDC	23722175	830275	6%
SA-BRA-SO	SA-URY	1238	HVDC	23750155	831255	6%
AS-CHN-GD	AS-CHN-SC	1241	HVDC	23778140	832235	6%
AF-MOZ	AF-ZMB	1251	HVDC	23871420	835500	6%
AS-CHN-SC	AS-CHN-TI	1251	HVDC	23871420	835500	6%
AS-CHN-TI	AS-CHN-YU	1251	HVDC	23871420	835500	6%
AS-CHN-QI	AS-CHN-TI	1259	HVDC	23946045	838110	6%
NA-CAN-AB	NA-CAN-NO	1263	HVDC	23983355	839415	6%
NA-CAN-SK	NA-USA-MW	1267	HVDC	24020670	840725	6%
AS-CHN-NI	AS-CHN-SD	1270	HVDC	24048655	841705	6%
AS-CHN-XI	AS-RUS-SI	1291	HVDC	24244540	848560	6%
SA-BRA-CN	SA-BRA-NW	1293	HVDC	24263200	849210	6%
AS-IND-EA	AS-IND-NO	1306	HVDC	24384465	853455	6%
EU-ARM	AS-TUR	1310	HVDC	24421775	854760	6%
EU-GEO	AS-TUR	1316	HVDC	24477745	856720	6%
AS-CHN-GU	AS-CHN-JS	1317	HVDC	24487070	857045	6%
AS-JOR	AS-SAU	1335	HVDC	24654975	862925	6%
AF-MOZ	AF-MWI	1340	HVDC	24701615	864555	6%
SA-ARG	SA-BRA-SO	1343	HVDC	24729600	865535	6%

AS-CHN-GA	AS-MNG	1344	HVDC	24738925	865860	6%
AS-CHN-GX	AS-VNM	1346	HVDC	24757585	866515	6%
AS-CHN-TI	AS-IND-NO	1350	HVDC	24794895	867820	6%
NA-USA-AZ	NA-USA-SS	1351	HVDC	24804225	868150	6%
AS-AFG	AS-PAK	1354	HVDC	24832210	869125	6%
AS-KAZ	AS-RUS-SI	1372	HVDC	25000110	875005	6%
SA-BRA-J2	SA-BRA-J3	1380	HVDC	25074735	877615	6%
AS-RUS-SI	AS-RUS-UR	1401	HVDC	25270625	884470	6%
AF-NER	AF-TCD	1411	HVDC	25363905	887735	6%
SA-BRA-CN	SA-GUY	1413	HVDC	25382560	888390	6%
AF-NAM	AF-ZMB	1420	HVDC	25447855	890675	6%
AF-NGA	AF-TCD	1426	HVDC	25503825	892635	6%
AS-CHN-JX	AS-CHN-WM	1441	HVDC	25643745	897530	6%
AS-CHN-QI	AS-CHN-XI	1443	HVDC	25662400	898185	6%
AS-CHN-GA	AS-CHN-JS	1449	HVDC	25718370	900145	6%
SA-BRA-NE	SA-BRA-SE	1455	HVDC	25774340	902100	6%
SA-BRA-CW	SA-PRY	1463	HVDC	25848960	904715	6%
AS-BRN	AS-MYS	1480	HVDC	26007540	910265	7%
SA-BRA-WE	SA-PER	1484	HVDC	26044850	911570	7%
NA-CAN-MB	NA-CAN-ON	1511	HVDC	26296705	920385	7%
AS-CHN-TI	AS-MMR	1512	HVDC	26306035	920710	7%
AF-TZA	AF-ZMB	1533	HVDC	26501925	927565	7%
NA-USA-CA	NA-USA-NW	1537	HVDC	26539235	928875	7%
AS-IND-EA	AS-IND-SO	1553	HVDC	26688485	934095	7%
NA-CAN-BC	NA-CAN-NO	1559	HVDC	26744455	936055	7%
AS-CHN-XI	AS-MNG	1561	HVDC	26763110	936710	7%
AF-BDI	AF-COD	1562	HVDC	26772435	937035	7%

AS-CHN-NI	AS-CHN-ZH	1566	HVDC	26809750	938340	7%
AF-AGO	AF-NAM	1581	HVDC	26949670	943240	7%
SA-BRA-CN	SA-BRA-CW	1595	HVDC	27080260	947810	7%
OC-AUS-QL	OC-AUS-SA	1603	HVDC	27154885	950420	7%
AS-CHN-TI	AS-CHN-XI	1605	HVDC	27173540	951075	7%
NA-CAN-NL	NA-CAN-QC	1608	HVDC	27201525	952055	7%
AS-IRQ	AS-TUR	1609	HVDC	27210855	952380	7%
AF-EGY	AF-SDN	1613	HVDC	27248165	953685	7%
SA-BOL	SA-PER	1614	HVDC	27257495	954010	7%
AS-CHN-GA	AS-CHN-XI	1625	HVDC	27360100	957605	7%
NA-USA-AZ	NA-USA-ER	1633	HVDC	27434725	960215	7%
AF-ERI	AF-SOM	1635	HVDC	27453380	960870	7%
AS-CHN-YU	AS-VNM	1641	HVDC	27509350	962825	7%
SA-BOL	SA-BRA-CW	1644	HVDC	27537335	963805	7%
NA-USA-NW	NA-USA-RA	1647	HVDC	27565320	964785	7%
AS-IND-EA	AS-IND-WE	1653	HVDC	27621285	966745	7%
AF-COD	AF-RWA	1658	HVDC	27667925	968375	7%
AF-COG	AF-RWA	1660	HVDC	27686585	969030	7%
AS-AFG	AS-IRN	1664	HVDC	27723895	970335	7%
AF-ETH	AF-KEN	1670	HVDC	27779865	972295	7%
AS-KAZ	AS-TKM	1670	HVDC	27779865	972295	7%
AS-CHN-XI	AS-TJK	1673	HVDC	27807845	973275	7%
AS-AFG	AS-CHN-XI	1682	HVDC	27891800	976215	7%
SA-BRA-CN	SA-BRA-NE	1689	HVDC	27957095	978500	7%
SA-BRA-NW	SA-VEN	1695	HVDC	28013065	980455	7%
AF-EGY	AF-LBY	1740	HVDC	28432825	995150	7%
NA-CAN-MB	NA-CAN-NO	1746	HVDC	28488795	997110	7%
EU-AZE	AS-TUR	1754	HVDC	28563415	999720	7%
AS-OMN	AS-YEM	1764	HVDC	28656695	1002985	8%

AS-RUS-NW	AS-RUS-UR	1781	HVDC	28815275	1008535	8%
NA-USA-AZ	NA-USA-NW	1782	HVDC	28824600	1008860	8%
SA-BRA-NW	SA-COL	1783	HVDC	28833930	1009190	8%
AF-AGO	AF-ZMB	1791	HVDC	28908555	1011800	8%
NA-CAN-NO	NA-USA-AK	1808	HVDC	29067130	1017350	8%
AS-CHN-YU	AS-CHN-ZH	1814	HVDC	29123100	1019310	8%
AS-MNG	AS-RUS-SI	1826	HVDC	29235035	1023225	8%
AF-DZA	AF-ESH	1865	HVDC	29598830	1035960	8%
AF-COD	AF-ZMB	1879	HVDC	29729420	1040530	8%
SA-COL	SA-PER	1880	HVDC	29738750	1040855	8%
AS-KAZ	AS-RUS-UR	1892	HVDC	29850685	1044775	8%
SA-BOL	SA-CHL	1897	HVDC	29897325	1046405	8%
SA-BRA-CW	SA-BRA-WE	1903	HVDC	29953295	1048365	8%
AS-IRN	AS-PAK	1913	HVDC	30046575	1051630	8%
AS-CHN-XI	AS-IND-NO	1918	HVDC	30093215	1053265	8%
AF-SDN	AF-TCD	1926	HVDC	30167835	1055875	8%
SA-BRA-CW	SA-BRA-NW	1933	HVDC	30233135	1058160	8%
SA-ARG	SA-BOL	1934	HVDC	30242460	1058485	8%
AF-CAF	AF-SDN	1973	HVDC	30606255	1071220	8%
AF-COD	AF-UGA	1987	HVDC	30736845	1075790	8%
NA-MEX	NA-USA-AZ	2029	HVDC	31128625	1089500	8%
AS-IRN	AS-TUR	2038	HVDC	31212575	1092440	8%
AS-IDN	AS-TLS	2084	HVDC	31641665	1107460	9%
NA-CAN-BC	NA-USA-AK	2088	HVDC	31678975	1108765	9%
SA-BRA-NW	SA-PER	2125	HVDC	32024115	1120845	9%
OC-AUS-SA	OC-AUS-WA	2133	HVDC	32098740	1123455	9%
NA-USA-MW	NA-USA-NW	2239	HVDC	33087510	1158065	9%
AF-MOZ	AF-TZA	2251	HVDC	33199445	1161980	9%
AF-LBY	AF-TCD	2318	HVDC	33824425	1183855	9%

SA-BRA-J3	SA-BRA-SE	2326	HVDC	33899045	1186465	9%
AS-KAZ	AS-RUS-MV	2409	HVDC	34673275	1213565	10%
AF-LBY	AF-NER	2429	HVDC	34859835	1220095	10%
AS-CHN-TI	AS-PAK	2437	HVDC	34934455	1222705	10%
AS-CHN-HE	AS-CHN-XI	2447	HVDC	35027740	1225970	10%
SA-CHL	SA-PER	2467	HVDC	35214300	1232500	10%
NA-MEX	NA-USA-CA	2506	HVDC	35578090	1245235	10%
AS-CHN-WM	AS-RUS-SI	2537	HVDC	35867260	1255355	10%
AF-DZA	AF-NER	2587	HVDC	36333660	1271680	10%
OC-AUS-NT	OC-AUS-SA	2622	HVDC	36660140	1283105	11%
OC-AUS-NT	OC-AUS-WA	2658	HVDC	36995950	1294860	11%
AF-COD	AF-TZA	2665	HVDC	37061245	1297145	11%
AF-COG	AF-TZA	2669	HVDC	37098560	1298450	11%
AF-LBY	AF-SDN	2739	HVDC	37751520	1321305	11%
AF-DZA	AF-MRT	2788	HVDC	38208595	1337300	11%
AS-CHN-XI	AS-PAK	2813	HVDC	38441795	1345465	11%
OC-AUS-NT	OC-AUS-QL	2849	HVDC	38777605	1357215	11%
AF-DZA	AF-MLI	2899	HVDC	39244005	1373540	11%
AS-CHN-GX	AS-CHN-XI	3009	HVDC	40270085	1409455	12%
AS-KAZ	AS-RUS-CE	3099	HVDC	41109610	1438835	12%
AS-CHN-HJ	AS-RUS-SI	3204	HVDC	42089050	1473115	13%
AS-RUS-FE	AS-RUS-SI	3713	HVDC	46837015	1639295	14%
AS-IDN	OC-PNG	4459	HVDC	53795720	1882850	17%
EU-EST	EU-FIN	83	Subsea	13206465	462225	2%
EU-BEL	EU-GBR	319	Subsea	16062355	562180	2%
EU-FRA	EU-GBR	341	Subsea	16328580	571500	3%
EU-GBR	EU-NLD	358	Subsea	16534300	578700	3%
EU-CYP	AS-ISR	367	Subsea	16643210	582510	3%
EU-DNK	EU-NOR	483	Subsea	18046955	631645	3%
AF-EGY	AS-JOR	494	Subsea	18180065	636300	3%
EU-DNK	EU-SWE	525	Subsea	18555205	649430	3%
OC-AUS-TA	OC-AUS-VI	593	Subsea	19378085	678235	3%
EU-ITA	AF-TUN	600	Subsea	19462795	681200	3%
EU-CYP	AF-EGY	602	Subsea	19487000	682045	3%

EU-DNK	EU-NLD	621	Subsea	19716920	690090	4%
EU-LTU	EU-SWE	678	Subsea	20406690	714235	4%
AS-IND-SO	AS-LKA	716	Subsea	20866535	730330	4%
EU-FRA	EU-IRL	777	Subsea	21604710	756165	4%
EU-POL	EU-SWE	810	Subsea	22004050	770140	4%
EU-DEU	EU-SWE	813	Subsea	22040355	771410	4%
EU-ESP	AF-MAR	833	Subsea	22282380	779885	4%
EU-DEU	EU-NOR	838	Subsea	22342885	782000	4%
AS-IDN	AS-SGP	894	Subsea	23020555	805720	4%
EU-NLD	EU-NOR	915	Subsea	23274680	814615	5%
EU-CYP	EU-GRC	915	Subsea	23274680	814615	5%
EU-DNK	EU-GBR	955	Subsea	23758730	831555	5%
EU-GRC	EU-ITA	1052	Subsea	24932545	872640	5%
EU-GBR	EU-NOR	1154	Subsea	26166870	915840	5%
EU-GBR	EU-ISL	1891	Subsea	35085470	1227990	8%
AS-MYS	AS-PHL	2467	Subsea	42055775	1471950	10%
AS-IDN	AS-PHL	2788	Subsea	45940265	1607910	11%
AS-ARE	AS-IRN	1218	Subsea	26941350	942945	6%
OC-AUS-QL	OC-PNG	2092	Subsea	37517815	1313125	9%
OC-AUS-WA	AS-IDN	3016	Subsea	48699345	1704475	12%
OC-AUS-WA	AS-TLS	2789	Subsea	45952365	1608335	11%
NA-CAN-NL	NA-GRL	1505	Subsea	30414400	1064505	7%
AS-CHN-FU	AS-TWN	358	Subsea	16534300	578700	3%
AS-CHN-SD	AS-KOR	616	Subsea	19656415	687975	4%
AS-CHN-SD	AS-PRK	578	Subsea	19196570	671880	3%
EU-CYP	AS-LBN	243	Subsea	15142660	529995	2%
EU-CYP	AS-SYR	327	Subsea	16159160	565570	2%
EU-CYP	AS-TUR	762	Subsea	21423195	749810	4%
AF-DJI	AS-YEM	433	Subsea	17441890	610465	3%
AF-DZA	EU-ESP	711	Subsea	20806030	728210	4%
AF-DZA	EU-FRA	1347	Subsea	28502405	997585	6%
AF-DZA	EU-ITA	991	Subsea	24194375	846805	5%
AF-EGY	AS-SAU	1645	Subsea	32108570	1123800	7%
AF-ERI	AS-SAU	1319	Subsea	28163575	985725	6%
AF-ERI	AS-YEM	565	Subsea	19039255	666375	3%
EU-GRC	AF-LBY	1110	Subsea	25634420	897205	5%
NA-GRL	EU-ISL	1249	Subsea	27316485	956075	6%
AS-JPN-CE	AS-KOR	821	Subsea	22137165	774800	4%

AS-JPN-HO	AS-RUS-FE	765	Subsea	21459495	751080	4%
AS-JPN-KY	AS-KOR	539	Subsea	18724620	655360	3%
AF-LBY	EU-MLT	356	Subsea	16510100	577855	3%
AF-MAR	EU-PRT	586	Subsea	19293380	675270	3%
EU-MLT	AF-TUN	401	Subsea	17054655	596915	3%
AS-IND-WE	AS-OMN	1562	Subsea	31104170	1088645	7%
AS-IRN	AS-OMN	1508	Subsea	30450705	1065775	7%
AS-OMN	AS-PAK	863	Subsea	22645415	792590	4%
AS-SAU	AF-SDN	1793	Subsea	33899550	1186485	8%
AF-SOM	AS-YEM	1483	Subsea	30148175	1055185	7%

TABLE B.0.3 ELECTRICITY INTERCONNECTOR TECHNOECONOMIC PARAMETERS

The technoeconomic modelling of hydrogen pipelines is identical to that of [129] which is consistent with the methodology applied to electricity interconnectors. A maximum nominal rating of 50 GW on interregional hydrogen pipeline transmission is asserted. Costs per MW and KM are derived from [103] with losses asserted at 0.2% per 100 km based on [96] and [103]. The full list of potential pipelines and their resulting technoeconomic parameters are presented in Table B.4. Hydrogen pipelines are assumed to have an economic lifetime of 50 years.

From	To	KM distance	Terrestrial/Subsea	Build Cost ($2010 in $000)	Annual FO&M (2 % of CAPEX) ($2010 in $000)	Losses
AF-COD	AF-COG	9	Terrestrial	96390	3374	0%
EU-AUT	EU-SVK	56	Terrestrial	599760	20992	0%
EU-KOS	EU-MKD	77	Terrestrial	824670	28863	0%
AS-LBN	AS-SYR	84	Terrestrial	899640	31487	0%
SA-BRA-J1	SA-BRA-SO	94	Terrestrial	1006740	35236	0%
AS-CHN-GD	AS-CHN-MA	107	Terrestrial	1145970	40109	0%
AS-ISR	AS-JOR	111	Terrestrial	1188810	41608	0%
AS-CHN-BE	AS-CHN-TJ	113	Terrestrial	1210230	42358	0%
EU-HRV	EU-SVN	118	Terrestrial	1263780	44232	0%
AF-MOZ	AF-SWZ	122	Terrestrial	1306620	45732	0%
AF-GIN	AF-SLE	128	Terrestrial	1370880	47981	0%
AS-CHN-GD	AS-CHN-HK	128	Terrestrial	1370880	47981	0%

NA-USA-NY	NA-USA-RE	128	Terrestrial	1370880	47981	0%
EU-ALB	EU-MNE	132	Terrestrial	1413720	49480	0%
AS-CHN-AN	AS-CHN-JS	143	Terrestrial	1531530	53604	0%
AF-BEN	AF-TGO	145	Terrestrial	1552950	54353	0%
EU-ALB	EU-MKD	154	Terrestrial	1649340	57727	0%
EU-KOS	EU-MNE	157	Terrestrial	1681470	58851	0%
AS-CHN-SH	AS-CHN-ZH	162	Terrestrial	1735020	60726	0%
EU-HUN	EU-SVK	164	Terrestrial	1756440	61475	0%
AF-GMB	AF-SEN	165	Terrestrial	1767150	61850	0%
AF-GAB	AF-GNQ	169	Terrestrial	1809990	63350	0%
EU-BLR	EU-LTU	170	Terrestrial	1820700	63725	0%
AS-CHN-HB	AS-CHN-SX	171	Terrestrial	1831410	64099	0%
EU-BGR	EU-MKD	172	Terrestrial	1842120	64474	0%
EU-BIH	EU-MNE	172	Terrestrial	1842120	64474	0%
EU-ARM	EU-GEO	173	Terrestrial	1852830	64849	0%
EU-BEL	EU-NLD	173	Terrestrial	1852830	64849	0%
NA-GTM	NA-SLV	175	Terrestrial	1874250	65599	0%
AF-BDI	AF-RWA	176	Terrestrial	1884960	65974	0%
AF-BEN	AF-NGA	176	Terrestrial	1884960	65974	0%
AS-JOR	AS-SYR	176	Terrestrial	1884960	65974	0%
EU-ALB	EU-KOS	186	Terrestrial	1992060	69722	0%
EU-BEL	EU-LUX	187	Terrestrial	2002770	70097	0%
AS-CHN-GA	AS-CHN-QI	192	Terrestrial	2056320	71971	0%
NA-CAN-BC	NA-USA-NW	193	Terrestrial	2067030	72346	0%
AS-KOR	AS-PRK	195	Terrestrial	2088450	73096	0%
AS-KAZ	AS-KGZ	196	Terrestrial	2099160	73471	0%
EU-BIH	EU-SRB	198	Terrestrial	2120580	74220	0%
SA-ARG	SA-URY	205	Terrestrial	2195550	76844	0%
AS-ISR	AS-LBN	211	Terrestrial	2259810	79093	0%
AF-ERI	AF-ETH	212	Terrestrial	2270520	79468	0%
AS-KHM	AS-VNM	212	Terrestrial	2270520	79468	0%
AS-ISR	AS-SYR	213	Terrestrial	2281230	79843	0%
EU-AUT	EU-HUN	217	Terrestrial	2324070	81342	0%
NA-HND	NA-SLV	219	Terrestrial	2345490	82092	0%
AS-AFG	AS-TJK	223	Terrestrial	2388330	83592	0%
AS-CHN-HJ	AS-CHN-JI	234	Terrestrial	2506140	87715	1%
AS-CHN-JS	AS-CHN-ZH	240	Terrestrial	2570400	89964	1%
NA-HND	NA-NIC	240	Terrestrial	2570400	89964	1%
AF-NGA	AF-TGO	242	Terrestrial	2591820	90714	1%
EU-KOS	EU-SRB	246	Terrestrial	2634660	92213	1%

EU-AUT	EU-CZE	251	Terrestrial	2688210	94087	1%
AS-BGD	AS-IND-EA	253	Terrestrial	2709630	94837	1%
NA-DOM	NA-HTI	257	Terrestrial	2752470	96336	1%
EU-BEL	EU-FRA	261	Terrestrial	2795310	97836	1%
AS-CHN-HU	AS-CHN-JX	262	Terrestrial	2806020	98211	1%
EU-LTU	EU-LVA	263	Terrestrial	2816730	98586	1%
AS-CHN-HB	AS-CHN-TJ	265	Terrestrial	2838150	99335	1%
AS-CHN-BE	AS-CHN-HB	266	Terrestrial	2848860	99710	1%
AS-JPN-CE	AS-JPN-SH	267	Terrestrial	2859570	100085	1%
NA-USA-RM	NA-USA-RW	267	Terrestrial	2859570	100085	1%
AS-CHN-JS	AS-CHN-SH	268	Terrestrial	2870280	100460	1%
AF-BWA	AF-ZAF	272	Terrestrial	2913120	101959	1%
AS-CHN-CH	AS-CHN-SC	272	Terrestrial	2913120	101959	1%
AS-CHN-JI	AS-CHN-LI	276	Terrestrial	2955960	103459	1%
EU-AUT	EU-SVN	277	Terrestrial	2966670	103833	1%
EU-EST	EU-LVA	279	Terrestrial	2988090	104583	1%
AS-BTN	AS-CHN-TI	281	Terrestrial	3009510	105333	1%
EU-CZE	EU-DEU	281	Terrestrial	3009510	105333	1%
EU-MNE	EU-SRB	281	Terrestrial	3009510	105333	1%
EU-BIH	EU-HRV	287	Terrestrial	3073770	107582	1%
EU-FRA	EU-LUX	288	Terrestrial	3084480	107957	1%
AS-CHN-HN	AS-CHN-JX	289	Terrestrial	3095190	108332	1%
EU-CZE	EU-SVK	289	Terrestrial	3095190	108332	1%
SA-BRA-J1	SA-BRA-SE	290	Terrestrial	3105900	108707	1%
AS-CHN-HN	AS-CHN-HU	293	Terrestrial	3138030	109831	1%
AF-CMR	AF-GNQ	295	Terrestrial	3159450	110581	1%
EU-BGR	EU-ROU	297	Terrestrial	3180870	111330	1%
NA-USA-NE	NA-USA-NY	298	Terrestrial	3191580	111705	1%
EU-FIN	AS-RUS-NW	300	Terrestrial	3213000	112455	1%
EU-HRV	EU-HUN	302	Terrestrial	3234420	113205	1%
AS-BGD	AS-IND-NE	304	Terrestrial	3255840	113954	1%
AF-CIV	AF-GHA	307	Terrestrial	3287970	115079	1%
AS-TJK	AS-UZB	309	Terrestrial	3309390	115829	1%
EU-EST	AS-RUS-NW	317	Terrestrial	3395070	118827	1%
EU-HUN	EU-SRB	317	Terrestrial	3395070	118827	1%

AS-CHN-AN	AS-CHN-HU	319	Terrestrial	3416490	119577	1%
AF-GHA	AF-TGO	321	Terrestrial	3437910	120327	1%
EU-MKD	EU-SRB	323	Terrestrial	3459330	121077	1%
AS-CHN-AN	AS-CHN-ZH	328	Terrestrial	3512880	122951	1%
EU-BGR	EU-SRB	330	Terrestrial	3534300	123701	1%
AS-CHN-CH	AS-CHN-GU	332	Terrestrial	3555720	124450	1%
NA-CAN-ON	NA-USA-RM	333	Terrestrial	3566430	124825	1%
AF-GIN	AF-GNB	334	Terrestrial	3577140	125200	1%
AF-SWZ	AF-ZAF	337	Terrestrial	3609270	126324	1%
AS-CHN-BE	AS-CHN-EM	337	Terrestrial	3609270	126324	1%
NA-CRI	NA-NIC	343	Terrestrial	3673530	128574	1%
NA-USA-SC	NA-USA-SE	344	Terrestrial	3684240	128948	1%
SA-BRA-SE	SA-BRA-SO	344	Terrestrial	3684240	128948	1%
AS-CHN-GA	AS-CHN-NI	347	Terrestrial	3716370	130073	1%
SA-GUY	SA-SUR	349	Terrestrial	3737790	130823	1%
AF-LSO	AF-ZAF	354	Terrestrial	3791340	132697	1%
EU-DEU	EU-DNK	355	Terrestrial	3802050	133072	1%
EU-MDA	EU-ROU	357	Terrestrial	3823470	133821	1%
AF-LBR	AF-SLE	360	Terrestrial	3855600	134946	1%
AS-CHN-HE	AS-CHN-SX	361	Terrestrial	3866310	135321	1%
NA-GTM	NA-HND	361	Terrestrial	3866310	135321	1%
AS-CHN-LI	AS-PRK	366	Terrestrial	3919860	137195	1%
EU-HRV	EU-SRB	366	Terrestrial	3919860	137195	1%
NA-USA-SE	NA-USA-SV	366	Terrestrial	3919860	137195	1%
SA-BRA-J3	SA-BRA-NW	371	Terrestrial	3973410	139069	1%
AS-CHN-HB	AS-CHN-HE	374	Terrestrial	4005540	140194	1%
AS-CHN-EM	AS-CHN-LI	375	Terrestrial	4016250	140569	1%
AF-GNB	AF-SEN	376	Terrestrial	4026960	140944	1%
AF-RWA	AF-UGA	377	Terrestrial	4037670	141318	1%
AS-CHN-AN	AS-CHN-JX	377	Terrestrial	4037670	141318	1%
NA-USA-SN	NA-USA-SW	377	Terrestrial	4037670	141318	1%
AS-CHN-EM	AS-CHN-TJ	379	Terrestrial	4059090	142068	1%
AS-ARE	AS-OMN	381	Terrestrial	4080510	142818	1%
EU-HUN	EU-SVN	383	Terrestrial	4101930	143568	1%
AS-CHN-SX	AS-CHN-WM	388	Terrestrial	4155480	145442	1%

AS-CHN-NI	AS-CHN-WM	389	Terrestrial	4166190	145817	1%
AS-CHN-TI	AS-IND-NE	393	Terrestrial	4209030	147316	1%
EU-FIN	EU-SWE	393	Terrestrial	4209030	147316	1%
EU-LTU	EU-POL	393	Terrestrial	4209030	147316	1%
AF-ZMB	AF-ZWE	397	Terrestrial	4251870	148815	1%
EU-MDA	EU-UKR	400	Terrestrial	4284000	149940	1%
AS-JPN-CE	AS-JPN-TO	403	Terrestrial	4316130	151065	1%
EU-BLR	EU-LVA	403	Terrestrial	4316130	151065	1%
AF-BEN	AF-GHA	403	Terrestrial	4316130	151065	1%
AF-EGY	AS-ISR	404	Terrestrial	4326840	151439	1%
NA-BLZ	NA-GTM	406	Terrestrial	4348260	152189	1%
NA-CAN-QC	NA-USA-NE	406	Terrestrial	4348260	152189	1%
AF-MRT	AF-SEN	407	Terrestrial	4358970	152564	1%
NA-USA-SC	NA-USA-SW	410	Terrestrial	4391100	153689	1%
AF-BFA	AF-NER	415	Terrestrial	4444650	155563	1%
EU-NOR	EU-SWE	418	Terrestrial	4476780	156687	1%
AS-BHR	AS-SAU	422	Terrestrial	4519620	158187	1%
EU-BLR	EU-UKR	435	Terrestrial	4658850	163060	1%
AS-CHN-SD	AS-CHN-TJ	436	Terrestrial	4669560	163435	1%
AS-CHN-GU	AS-CHN-YU	438	Terrestrial	4690980	164184	1%
AS-CHN-HE	AS-CHN-SI	440	Terrestrial	4712400	164934	1%
AF-MOZ	AF-ZAF	443	Terrestrial	4744530	166059	1%
AS-CHN-GU	AS-CHN-GX	448	Terrestrial	4798080	167933	1%
EU-ROU	EU-SRB	448	Terrestrial	4798080	167933	1%
AF-CMR	AF-GAB	450	Terrestrial	4819500	168683	1%
AS-CHN-JX	AS-CHN-ZH	450	Terrestrial	4819500	168683	1%
EU-AZE	EU-GEO	450	Terrestrial	4819500	168683	1%
AF-DJI	AF-ETH	452	Terrestrial	4840920	169432	1%
EU-ARM	EU-AZE	454	Terrestrial	4862340	170182	1%
EU-HRV	EU-MNE	455	Terrestrial	4873050	170557	1%
NA-USA-FR	NA-USA-SE	461	Terrestrial	4937310	172806	1%
EU-GBR	EU-IRL	463	Terrestrial	4958730	173556	1%
AS-CHN-GD	AS-CHN-HA	464	Terrestrial	4969440	173930	1%
AS-CHN-AN	AS-CHN-HE	466	Terrestrial	4990860	174680	1%
AS-CHN-HE	AS-CHN-HU	468	Terrestrial	5012280	175430	1%
AS-KGZ	AS-UZB	470	Terrestrial	5033700	176180	1%
AS-CHN-JS	AS-CHN-SD	471	Terrestrial	5044410	176554	1%

NA-USA-ME	NA-USA-MW	473	Terrestrial	5065830	177304	1%
AS-QAT	AS-SAU	474	Terrestrial	5076540	177679	1%
EU-BLR	EU-POL	475	Terrestrial	5087250	178054	1%
AF-GIN	AF-LBR	478	Terrestrial	5119380	179178	1%
AS-JPN-CE	AS-JPN-KY	482	Terrestrial	5162220	180678	1%
NA-USA-SN	NA-USA-SS	483	Terrestrial	5172930	181053	1%
EU-GRC	EU-MKD	488	Terrestrial	5226480	182927	1%
EU-CHE	EU-FRA	490	Terrestrial	5247900	183677	1%
EU-ITA	EU-SVN	490	Terrestrial	5247900	183677	1%
EU-LVA	AS-RUS-NW	491	Terrestrial	5258610	184051	1%
AS-CHN-HB	AS-CHN-WM	494	Terrestrial	5290740	185176	1%
EU-ALB	EU-GRC	500	Terrestrial	5355000	187425	1%
AF-KEN	AF-UGA	503	Terrestrial	5387130	188550	1%
EU-BGR	AS-TUR	503	Terrestrial	5387130	188550	1%
NA-CAN-ON	NA-CAN-QC	503	Terrestrial	5387130	188550	1%
AS-CHN-GA	AS-CHN-SI	504	Terrestrial	5397840	188924	1%
EU-ESP	EU-PRT	504	Terrestrial	5397840	188924	1%
AS-CHN-FU	AS-CHN-GD	505	Terrestrial	5408550	189299	1%
AS-AFG	AS-UZB	507	Terrestrial	5429970	190049	1%
AS-CHN-HJ	AS-RUS-FE	509	Terrestrial	5451390	190799	1%
NA-CRI	NA-PAN	511	Terrestrial	5472810	191548	1%
AF-LBY	AF-TUN	514	Terrestrial	5504940	192673	1%
AS-CHN-GD	AS-CHN-GX	514	Terrestrial	5504940	192673	1%
EU-CZE	EU-POL	515	Terrestrial	5515650	193048	1%
EU-DEU	EU-POL	516	Terrestrial	5526360	193423	1%
AS-CHN-SI	AS-CHN-SX	517	Terrestrial	5537070	193797	1%
AS-CHN-FU	AS-CHN-JX	519	Terrestrial	5558490	194547	1%
AS-LAO	AS-THA	519	Terrestrial	5558490	194547	1%
AS-CHN-NI	AS-CHN-SI	522	Terrestrial	5590620	195672	1%
AS-CHN-GU	AS-CHN-SC	523	Terrestrial	5601330	196047	1%
EU-AUT	EU-DEU	524	Terrestrial	5612040	196421	1%
EU-BGR	EU-GRC	524	Terrestrial	5612040	196421	1%
NA-CAN-AB	NA-CAN-SK	525	Terrestrial	5622750	196796	1%
NA-USA-ER	NA-USA-SA	527	Terrestrial	5644170	197546	1%
EU-POL	EU-SVK	533	Terrestrial	5708430	199795	1%
NA-CAN-QC	NA-USA-NY	535	Terrestrial	5729850	200545	1%

AS-KHM	AS-THA	536	Terrestrial	5740560	200920	1%
AS-IND-EA	AS-IND-NE	537	Terrestrial	5751270	201294	1%
NA-USA-ME	NA-USA-RW	538	Terrestrial	5761980	201669	1%
AS-KWT	AS-SAU	539	Terrestrial	5772690	202044	1%
NA-USA-RW	NA-USA-SC	539	Terrestrial	5772690	202044	1%
AS-CHN-JI	AS-PRK	540	Terrestrial	5783400	202419	1%
EU-AZE	AS-IRN	543	Terrestrial	5815530	203544	1%
AS-CHN-EM	AS-CHN-JI	548	Terrestrial	5869080	205418	1%
NA-USA-SC	NA-USA-SV	548	Terrestrial	5869080	205418	1%
AS-CHN-AN	AS-CHN-SD	549	Terrestrial	5879790	205793	1%
AF-AGO	AF-COD	551	Terrestrial	5901210	206542	1%
AF-AGO	AF-COG	557	Terrestrial	5965470	208791	1%
AS-IRQ	AS-KWT	557	Terrestrial	5965470	208791	1%
AS-CHN-HE	AS-CHN-JS	562	Terrestrial	6019020	210666	1%
NA-CAN-ON	NA-USA-NY	562	Terrestrial	6019020	210666	1%
AS-CHN-GD	AS-CHN-HN	563	Terrestrial	6029730	211041	1%
AS-CHN-HB	AS-CHN-SD	563	Terrestrial	6029730	211041	1%
NA-USA-RW	NA-USA-SV	564	Terrestrial	6040440	211415	1%
AS-CHN-CH	AS-CHN-SI	567	Terrestrial	6072570	212540	1%
AS-BTN	AS-IND-EA	569	Terrestrial	6093990	213290	1%
EU-GRC	AS-TUR	570	Terrestrial	6104700	213665	1%
EU-DEU	EU-NLD	575	Terrestrial	6158250	215539	1%
AS-MMR	AS-THA	579	Terrestrial	6201090	217038	1%
NA-USA-AZ	NA-USA-CA	586	Terrestrial	6276060	219662	1%
EU-AUT	EU-CHE	591	Terrestrial	6329610	221536	1%
AS-CHN-GA	AS-CHN-SC	599	Terrestrial	6415290	224535	1%
EU-DEU	EU-LUX	602	Terrestrial	6447420	225660	1%
AS-CHN-TI	AS-NPL	603	Terrestrial	6458130	226035	1%
AS-CHN-EM	AS-CHN-HB	604	Terrestrial	6468840	226409	1%
AS-CHN-SC	AS-CHN-SI	604	Terrestrial	6468840	226409	1%
AF-MWI	AF-ZMB	613	Terrestrial	6565230	229783	1%
AF-DJI	AF-ERI	617	Terrestrial	6608070	231282	1%
NA-CAN-MB	NA-USA-MW	620	Terrestrial	6640200	232407	1%
AS-CHN-HE	AS-CHN-SD	622	Terrestrial	6661620	233157	1%

AS-CHN-GX	AS-CHN-YU	625	Terrestrial	6693750	234281	1%
AF-BFA	AF-GHA	632	Terrestrial	6768720	236905	1%
AS-RUS-CE	AS-RUS-NW	634	Terrestrial	6790140	237655	1%
AF-DZA	AF-TUN	635	Terrestrial	6800850	238030	1%
AS-CHN-SC	AS-CHN-YU	637	Terrestrial	6822270	238779	1%
AS-CHN-CH	AS-CHN-HN	639	Terrestrial	6843690	239529	1%
EU-HUN	EU-ROU	640	Terrestrial	6854400	239904	1%
NA-USA-RW	NA-USA-SW	642	Terrestrial	6875820	240654	1%
AS-CHN-GU	AS-CHN-HN	643	Terrestrial	6886530	241029	1%
AS-CHN-HU	AS-CHN-SI	650	Terrestrial	6961500	243653	1%
EU-BEL	EU-DEU	652	Terrestrial	6982920	244402	1%
OC-AUS-SA	OC-AUS-VI	654	Terrestrial	7004340	245152	1%
AS-IND-EA	AS-NPL	655	Terrestrial	7015050	245527	1%
EU-LTU	AS-RUS-NW	657	Terrestrial	7036470	246276	1%
NA-CAN-AR	NA-USA-NE	657	Terrestrial	7036470	246276	1%
NA-USA-MW	NA-USA-SN	658	Terrestrial	7047180	246651	1%
NA-USA-ER	NA-USA-SS	662	Terrestrial	7090020	248151	1%
NA-USA-SA	NA-USA-SE	662	Terrestrial	7090020	248151	1%
AS-KAZ	AS-UZB	665	Terrestrial	7122150	249275	1%
AS-CHN-GD	AS-CHN-JX	666	Terrestrial	7132860	249650	1%
AS-IRN	AS-TKM	669	Terrestrial	7164990	250775	1%
EU-CHE	EU-DEU	669	Terrestrial	7164990	250775	1%
NA-USA-RE	NA-USA-RW	669	Terrestrial	7164990	250775	1%
AF-KEN	AF-TZA	671	Terrestrial	7186410	251524	1%
NA-CAN-AB	NA-CAN-BC	674	Terrestrial	7218540	252649	1%
EU-BLR	AS-RUS-CE	675	Terrestrial	7229250	253024	1%
AS-CHN-FU	AS-CHN-ZH	677	Terrestrial	7250670	253773	1%
EU-CHE	EU-ITA	684	Terrestrial	7325640	256397	1%
AS-KGZ	AS-TJK	685	Terrestrial	7336350	256772	1%
AF-ERI	AF-SDN	686	Terrestrial	7347060	257147	1%
AS-PRK	AS-RUS-FE	689	Terrestrial	7379190	258272	1%
EU-ITA	EU-MLT	689	Terrestrial	7379190	258272	1%
AS-LAO	AS-MMR	690	Terrestrial	7389900	258647	1%
EU-POL	EU-UKR	691	Terrestrial	7400610	259021	1%

EU-BLR	AS-RUS-NW	692	Terrestrial	7411320	259396	1%
AF-BEN	AF-BFA	693	Terrestrial	7422030	259771	1%
AS-IRN	AS-IRQ	694	Terrestrial	7432740	260146	1%
AS-CHN-QI	AS-CHN-SC	695	Terrestrial	7443450	260521	1%
AS-CHN-EM	AS-CHN-SD	697	Terrestrial	7464870	261270	1%
AF-BEN	AF-NER	704	Terrestrial	7539840	263894	1%
AF-BFA	AF-MLI	704	Terrestrial	7539840	263894	1%
OC-AUS-SW	OC-AUS-VI	708	Terrestrial	7582680	265394	1%
AF-GIN	AF-SEN	709	Terrestrial	7593390	265769	1%
AF-GIN	AF-MLI	710	Terrestrial	7604100	266144	1%
NA-CAN-AB	NA-USA-NW	710	Terrestrial	7604100	266144	1%
NA-CAN-MB	NA-CAN-SK	711	Terrestrial	7614810	266518	1%
AS-CHN-SI	AS-CHN-WM	714	Terrestrial	7646940	267643	1%
AS-RUS-MV	AS-RUS-UR	717	Terrestrial	7679070	268767	1%
AS-CHN-SD	AS-CHN-SX	719	Terrestrial	7700490	269517	1%
AS-RUS-CE	AS-RUS-MV	720	Terrestrial	7711200	269892	1%
AS-CHN-EM	AS-CHN-HJ	727	Terrestrial	7786170	272516	2%
NA-USA-RE	NA-USA-SV	732	Terrestrial	7839720	274390	2%
AS-CHN-GA	AS-CHN-WM	733	Terrestrial	7850430	274765	2%
EU-GEO	AS-RUS-SO	733	Terrestrial	7850430	274765	2%
AS-CHN-AN	AS-CHN-HB	735	Terrestrial	7871850	275515	2%
NA-USA-SA	NA-USA-SC	739	Terrestrial	7914690	277014	2%
OC-AUS-QL	OC-AUS-SW	740	Terrestrial	7925400	277389	2%
EU-ROU	EU-UKR	745	Terrestrial	7978950	279263	2%
AS-CHN-CH	AS-CHN-HU	747	Terrestrial	8000370	280013	2%
NA-USA-MW	NA-USA-SW	747	Terrestrial	8000370	280013	2%
AS-IRQ	AS-SYR	751	Terrestrial	8043210	281512	2%
AF-BFA	AF-TGO	756	Terrestrial	8096760	283387	2%
AF-CIV	AF-LBR	756	Terrestrial	8096760	283387	2%
AS-KHM	AS-LAO	756	Terrestrial	8096760	283387	2%
AS-RUS-CE	EU-UKR	757	Terrestrial	8107470	283761	2%
AS-CHN-GX	AS-CHN-HN	759	Terrestrial	8128890	284511	2%
AS-RUS-SO	EU-UKR	760	Terrestrial	8139600	284886	2%

SA-BRA-NW	SA-BRA-WE	762	Terrestrial	8161020	285636	2%
EU-AUT	EU-ITA	764	Terrestrial	8182440	286385	2%
SA-COL	NA-PAN	773	Terrestrial	8278830	289759	2%
AS-CHN-EM	AS-CHN-WM	781	Terrestrial	8364510	292758	2%
AF-ETH	AF-SDN	782	Terrestrial	8375220	293133	2%
AF-CAF	AF-CMR	783	Terrestrial	8385930	293508	2%
EU-ARM	AS-IRN	786	Terrestrial	8418060	294632	2%
EU-FIN	EU-NOR	787	Terrestrial	8428770	295007	2%
NA-CAN-AR	NA-CAN-QC	789	Terrestrial	8450190	295757	2%
AS-CHN-YU	AS-LAO	790	Terrestrial	8460900	296132	2%
AF-NER	AF-NGA	799	Terrestrial	8557290	299505	2%
AS-IND-NO	AS-NPL	799	Terrestrial	8557290	299505	2%
NA-USA-RA	NA-USA-SS	805	Terrestrial	8621550	301754	2%
AS-IRQ	AS-JOR	807	Terrestrial	8642970	302504	2%
SA-BRA-CN	SA-BRA-J2	826	Terrestrial	8846460	309626	2%
AF-COG	AF-GAB	828	Terrestrial	8867880	310376	2%
AF-BFA	AF-CIV	831	Terrestrial	8900010	311500	2%
AS-JPN-HO	AS-JPN-TO	833	Terrestrial	8921430	312250	2%
SA-BRA-SO	SA-PRY	836	Terrestrial	8953560	313375	2%
AS-CHN-WM	AS-MNG	840	Terrestrial	8996400	314874	2%
AS-IND-SO	AS-IND-WE	840	Terrestrial	8996400	314874	2%
AS-ARE	AS-SAU	860	Terrestrial	9210600	322371	2%
AS-CHN-XI	AS-KAZ	860	Terrestrial	9210600	322371	2%
AS-CHN-JS	AS-CHN-SX	861	Terrestrial	9221310	322746	2%
AS-CHN-HB	AS-CHN-LI	871	Terrestrial	9328410	326494	2%
SA-BRA-CW	SA-BRA-J2	872	Terrestrial	9339120	326869	2%
SA-BRA-CW	SA-BRA-SE	872	Terrestrial	9339120	326869	2%
EU-DEU	EU-FRA	878	Terrestrial	9403380	329118	2%
AS-IND-WE	AS-PAK	888	Terrestrial	9510480	332867	2%
NA-USA-RA	NA-USA-SN	889	Terrestrial	9521190	333242	2%
AF-ESH	AF-MAR	895	Terrestrial	9585450	335491	2%
EU-HUN	EU-UKR	896	Terrestrial	9596160	335866	2%
AS-CHN-HN	AS-CHN-SC	904	Terrestrial	9681840	338864	2%
AS-LAO	AS-VNM	910	Terrestrial	9746100	341114	2%
AF-MOZ	AF-ZWE	918	Terrestrial	9831780	344112	2%

AF-CIV	AF-MLI	924	Terrestrial	9896040	346361	2%
AF-BWA	AF-ZWE	927	Terrestrial	9928170	347486	2%
AF-BWA	AF-NAM	928	Terrestrial	9938880	347861	2%
NA-USA-SA	NA-USA-SS	929	Terrestrial	9949590	348236	2%
SA-BRA-J2	SA-BRA-NE	932	Terrestrial	9981720	349360	2%
NA-USA-AZ	NA-USA-RA	941	Terrestrial	10078110	352734	2%
AF-CAF	AF-TCD	944	Terrestrial	10110240	353858	2%
AF-CMR	AF-NGA	944	Terrestrial	10110240	353858	2%
AS-CHN-JS	AS-CHN-SI	952	Terrestrial	10195920	356857	2%
NA-USA-SA	NA-USA-SW	953	Terrestrial	10206630	357232	2%
AS-RUS-CE	AS-RUS-SO	958	Terrestrial	10260180	359106	2%
AS-BGD	AS-MMR	972	Terrestrial	10410120	364354	2%
AF-ZAF	AF-ZWE	979	Terrestrial	10485090	366978	2%
AS-IRQ	AS-SAU	994	Terrestrial	10645740	372601	2%
AF-CMR	AF-COG	996	Terrestrial	10667160	373351	2%
AF-CMR	AF-TCD	996	Terrestrial	10667160	373351	2%
SA-COL	SA-ECU	998	Terrestrial	10688580	374100	2%
AF-MWI	AF-TZA	999	Terrestrial	10699290	374475	2%
EU-SVK	EU-UKR	1000	Terrestrial	10710000	374850	2%
SA-BOL	SA-BRA-WE	1004	Terrestrial	10752840	376349	2%
AS-TKM	AS-UZB	1006	Terrestrial	10774260	377099	2%
NA-USA-MW	NA-USA-RW	1008	Terrestrial	10795680	377849	2%
SA-BOL	SA-PRY	1018	Terrestrial	10902780	381597	2%
AF-DZA	AF-LBY	1019	Terrestrial	10913490	381972	2%
AF-KEN	AF-SOM	1021	Terrestrial	10934910	382722	2%
AF-CAF	AF-COG	1026	Terrestrial	10988460	384596	2%
SA-COL	SA-VEN	1027	Terrestrial	10999170	384971	2%
AS-AFG	AS-TKM	1030	Terrestrial	11031300	386096	2%
AF-DZA	AF-MAR	1031	Terrestrial	11042010	386470	2%
AF-CAF	AF-COD	1032	Terrestrial	11052720	386845	2%
SA-ARG	SA-PRY	1037	Terrestrial	11106270	388719	2%
SA-GUY	SA-VEN	1046	Terrestrial	11202660	392093	2%
AF-MLI	AF-MRT	1047	Terrestrial	11213370	392468	2%
AF-ESH	AF-MRT	1047	Terrestrial	11213370	392468	2%
AF-MLI	AF-SEN	1049	Terrestrial	11234790	393218	2%
EU-ESP	EU-FRA	1054	Terrestrial	11288340	395092	2%
AS-CHN-XI	AS-KGZ	1055	Terrestrial	11299050	395467	2%
AF-BWA	AF-ZMB	1056	Terrestrial	11309760	395842	2%
NA-GTM	NA-MEX	1060	Terrestrial	11352600	397341	2%
AS-SYR	AS-TUR	1063	Terrestrial	11384730	398466	2%

SA-BRA-CW	SA-BRA-NE	1063	Terrestrial	11384730	398466	2%
AS-SAU	AS-YEM	1067	Terrestrial	11427570	399965	2%
AS-CHN-CH	AS-CHN-SX	1075	Terrestrial	11513250	402964	2%
AS-CHN-HN	AS-CHN-SX	1077	Terrestrial	11534670	403713	2%
SA-BRA-CW	SA-BRA-SO	1081	Terrestrial	11577510	405213	2%
AF-TZA	AF-UGA	1085	Terrestrial	11620350	406712	2%
EU-NOR	AS-RUS-NW	1086	Terrestrial	11631060	407087	2%
AF-DJI	AF-SOM	1087	Terrestrial	11641770	407462	2%
NA-USA-SA	NA-USA-SN	1092	Terrestrial	11695320	409336	2%
SA-BRA-CN	SA-SUR	1099	Terrestrial	11770290	411960	2%
AF-MLI	AF-NER	1100	Terrestrial	11781000	412335	2%
AS-IND-NO	AS-PAK	1100	Terrestrial	11781000	412335	2%
AS-CHN-GD	AS-CHN-YU	1101	Terrestrial	11791710	412710	2%
EU-FRA	EU-ITA	1107	Terrestrial	11855970	414959	2%
NA-CAN-ON	NA-USA-MW	1109	Terrestrial	11877390	415709	2%
EU-AZE	AS-RUS-SO	1113	Terrestrial	11920230	417208	2%
NA-USA-MW	NA-USA-RA	1114	Terrestrial	11930940	417583	2%
SA-BRA-NW	SA-GUY	1120	Terrestrial	11995200	419832	2%
SA-BRA-CN	SA-BRA-J3	1126	Terrestrial	12059460	422081	2%
SA-BRA-NW	SA-SUR	1129	Terrestrial	12091590	423206	2%
AS-IND-NE	AS-MMR	1130	Terrestrial	12102300	423581	2%
AS-CHN-EM	AS-MNG	1132	Terrestrial	12123720	424330	2%
AS-CHN-YU	AS-MMR	1133	Terrestrial	12134430	424705	2%
SA-ARG	SA-CHL	1137	Terrestrial	12177270	426204	2%
SA-ECU	SA-PER	1138	Terrestrial	12187980	426579	2%
AF-RWA	AF-TZA	1154	Terrestrial	12359340	432577	2%
OC-AUS-SA	OC-AUS-SW	1159	Terrestrial	12412890	434451	2%
AF-BDI	AF-TZA	1161	Terrestrial	12434310	435201	2%
AF-CIV	AF-GIN	1161	Terrestrial	12434310	435201	2%
AS-IND-NO	AS-IND-WE	1162	Terrestrial	12445020	435576	2%
NA-BLZ	NA-MEX	1174	Terrestrial	12573540	440074	2%
AF-NAM	AF-ZAF	1178	Terrestrial	12616380	441573	2%
AS-MYS	AS-THA	1184	Terrestrial	12680640	443822	2%
AS-IDN	AS-MYS	1185	Terrestrial	12691350	444197	2%

AS-CHN-CH	AS-CHN-HB	1191	Terrestrial	12755610	446446	2%
AS-OMN	AS-SAU	1205	Terrestrial	12905550	451694	2%
NA-MEX	NA-USA-ER	1211	Terrestrial	12969810	453943	2%
NA-CAN-SK	NA-USA-NW	1227	Terrestrial	13141170	459941	3%
NA-CAN-NO	NA-CAN-SK	1231	Terrestrial	13184010	461440	3%
SA-BRA-NW	SA-GUF	1235	Terrestrial	13226850	462940	3%
SA-BRA-SO	SA-URY	1238	Terrestrial	13258980	464064	3%
AS-CHN-GD	AS-CHN-SC	1241	Terrestrial	13291110	465189	3%
AF-MOZ	AF-ZMB	1251	Terrestrial	13398210	468937	3%
AS-CHN-SC	AS-CHN-TI	1251	Terrestrial	13398210	468937	3%
AS-CHN-TI	AS-CHN-YU	1251	Terrestrial	13398210	468937	3%
AS-CHN-QI	AS-CHN-TI	1259	Terrestrial	13483890	471936	3%
NA-CAN-AB	NA-CAN-NO	1263	Terrestrial	13526730	473436	3%
NA-CAN-SK	NA-USA-MW	1267	Terrestrial	13569570	474935	3%
AS-CHN-NI	AS-CHN-SD	1270	Terrestrial	13601700	476060	3%
AS-CHN-XI	AS-RUS-SI	1291	Terrestrial	13826610	483931	3%
SA-BRA-CN	SA-BRA-NW	1293	Terrestrial	13848030	484681	3%
AS-IND-EA	AS-IND-NO	1306	Terrestrial	13987260	489554	3%
EU-ARM	AS-TUR	1310	Terrestrial	14030100	491054	3%
EU-GEO	AS-TUR	1316	Terrestrial	14094360	493303	3%
AS-CHN-GU	AS-CHN-JS	1317	Terrestrial	14105070	493677	3%
AS-JOR	AS-SAU	1335	Terrestrial	14297850	500425	3%
AF-MOZ	AF-MWI	1340	Terrestrial	14351400	502299	3%
SA-ARG	SA-BRA-SO	1343	Terrestrial	14383530	503424	3%
AS-CHN-GA	AS-MNG	1344	Terrestrial	14394240	503798	3%
AS-CHN-GX	AS-VNM	1346	Terrestrial	14415660	504548	3%
AS-CHN-TI	AS-IND-NO	1350	Terrestrial	14458500	506048	3%
NA-USA-AZ	NA-USA-SS	1351	Terrestrial	14469210	506422	3%
AS-AFG	AS-PAK	1354	Terrestrial	14501340	507547	3%
AS-KAZ	AS-RUS-SI	1372	Terrestrial	14694120	514294	3%
SA-BRA-J2	SA-BRA-J3	1380	Terrestrial	14779800	517293	3%
AS-RUS-SI	AS-RUS-UR	1401	Terrestrial	15004710	525165	3%

AF-NER	AF-TCD	1411	Terrestrial	15111810	528913	3%
SA-BRA-CN	SA-GUY	1413	Terrestrial	15133230	529663	3%
AF-NAM	AF-ZMB	1420	Terrestrial	15208200	532287	3%
AF-NGA	AF-TCD	1426	Terrestrial	15272460	534536	3%
AS-CHN-JX	AS-CHN-WM	1441	Terrestrial	15433110	540159	3%
AS-CHN-QI	AS-CHN-XI	1443	Terrestrial	15454530	540909	3%
AS-CHN-GA	AS-CHN-JS	1449	Terrestrial	15518790	543158	3%
SA-BRA-NE	SA-BRA-SE	1455	Terrestrial	15583050	545407	3%
SA-BRA-CW	SA-PRY	1463	Terrestrial	15668730	548406	3%
AS-BRN	AS-MYS	1480	Terrestrial	15850800	554778	3%
SA-BRA-WE	SA-PER	1484	Terrestrial	15893640	556277	3%
NA-CAN-MB	NA-CAN-ON	1511	Terrestrial	16182810	566398	3%
AS-CHN-TI	AS-MMR	1512	Terrestrial	16193520	566773	3%
AF-TZA	AF-ZMB	1533	Terrestrial	16418430	574645	3%
NA-USA-CA	NA-USA-NW	1537	Terrestrial	16461270	576144	3%
AS-IND-EA	AS-IND-SO	1553	Terrestrial	16632630	582142	3%
NA-CAN-BC	NA-CAN-NO	1559	Terrestrial	16696890	584391	3%
AS-CHN-XI	AS-MNG	1561	Terrestrial	16718310	585141	3%
AF-BDI	AF-COD	1562	Terrestrial	16729020	585516	3%
AS-CHN-NI	AS-CHN-ZH	1566	Terrestrial	16771860	587015	3%
AF-AGO	AF-NAM	1581	Terrestrial	16932510	592638	3%
SA-BRA-CN	SA-BRA-CW	1595	Terrestrial	17082450	597886	3%
OC-AUS-QL	OC-AUS-SA	1603	Terrestrial	17168130	600885	3%
AS-CHN-TI	AS-CHN-XI	1605	Terrestrial	17189550	601634	3%
NA-CAN-NL	NA-CAN-QC	1608	Terrestrial	17221680	602759	3%
AS-IRQ	AS-TUR	1609	Terrestrial	17232390	603134	3%
AF-EGY	AF-SDN	1613	Terrestrial	17275230	604633	3%
SA-BOL	SA-PER	1614	Terrestrial	17285940	605008	3%
AS-CHN-GA	AS-CHN-XI	1625	Terrestrial	17403750	609131	3%
NA-USA-AZ	NA-USA-ER	1633	Terrestrial	17489430	612130	3%
AF-ERI	AF-SOM	1635	Terrestrial	17510850	612880	3%
AS-CHN-YU	AS-VNM	1641	Terrestrial	17575110	615129	3%
SA-BOL	SA-BRA-CW	1644	Terrestrial	17607240	616253	3%

NA-USA-NW	NA-USA-RA	1647	Terrestrial	17639370	617378	3%
AS-IND-EA	AS-IND-WE	1653	Terrestrial	17703630	619627	3%
AF-COD	AF-RWA	1658	Terrestrial	17757180	621501	3%
AF-COG	AF-RWA	1660	Terrestrial	17778600	622251	3%
AS-AFG	AS-IRN	1664	Terrestrial	17821440	623750	3%
AF-ETH	AF-KEN	1670	Terrestrial	17885700	626000	3%
AS-KAZ	AS-TKM	1670	Terrestrial	17885700	626000	3%
AS-CHN-XI	AS-TJK	1673	Terrestrial	17917830	627124	3%
AS-AFG	AS-CHN-XI	1682	Terrestrial	18014220	630498	3%
SA-BRA-CN	SA-BRA-NE	1689	Terrestrial	18089190	633122	3%
SA-BRA-NW	SA-VEN	1695	Terrestrial	18153450	635371	3%
AF-EGY	AF-LBY	1740	Terrestrial	18635400	652239	4%
NA-CAN-MB	NA-CAN-NO	1746	Terrestrial	18699660	654488	4%
EU-AZE	AS-TUR	1754	Terrestrial	18785340	657487	4%
AS-OMN	AS-YEM	1764	Terrestrial	18892440	661235	4%
AS-RUS-NW	AS-RUS-UR	1781	Terrestrial	19074510	667608	4%
NA-USA-AZ	NA-USA-NW	1782	Terrestrial	19085220	667983	4%
SA-BRA-NW	SA-COL	1783	Terrestrial	19095930	668358	4%
AF-AGO	AF-ZMB	1791	Terrestrial	19181610	671356	4%
NA-CAN-NO	NA-USA-AK	1808	Terrestrial	19363680	677729	4%
AS-CHN-YU	AS-CHN-ZH	1814	Terrestrial	19427940	679978	4%
AS-MNG	AS-RUS-SI	1826	Terrestrial	19556460	684476	4%
AF-DZA	AF-ESH	1865	Terrestrial	19974150	699095	4%
AF-COD	AF-ZMB	1879	Terrestrial	20124090	704343	4%
SA-COL	SA-PER	1880	Terrestrial	20134800	704718	4%
AS-KAZ	AS-RUS-UR	1892	Terrestrial	20263320	709216	4%
SA-BOL	SA-CHL	1897	Terrestrial	20316870	711090	4%
SA-BRA-CW	SA-BRA-WE	1903	Terrestrial	20381130	713340	4%
AS-IRN	AS-PAK	1913	Terrestrial	20488230	717088	4%
AS-CHN-XI	AS-IND-NO	1918	Terrestrial	20541780	718962	4%
AF-SDN	AF-TCD	1926	Terrestrial	20627460	721961	4%
SA-BRA-CW	SA-BRA-NW	1933	Terrestrial	20702430	724585	4%
SA-ARG	SA-BOL	1934	Terrestrial	20713140	724960	4%
AF-CAF	AF-SDN	1973	Terrestrial	21130830	739579	4%
AF-COD	AF-UGA	1987	Terrestrial	21280770	744827	4%

NA-MEX	NA-USA-AZ	2029	Terrestrial	21730590	760571	4%
AS-IRN	AS-TUR	2038	Terrestrial	21826980	763944	4%
AS-IDN	AS-TLS	2084	Terrestrial	22319640	781187	4%
NA-CAN-BC	NA-USA-AK	2088	Terrestrial	22362480	782687	4%
SA-BRA-NW	SA-PER	2125	Terrestrial	22758750	796556	4%
OC-AUS-SA	OC-AUS-WA	2133	Terrestrial	22844430	799555	4%
NA-USA-MW	NA-USA-NW	2239	Terrestrial	23979690	839289	5%
AF-MOZ	AF-TZA	2251	Terrestrial	24108210	843787	5%
AF-LBY	AF-TCD	2318	Terrestrial	24825780	868902	5%
SA-BRA-J3	SA-BRA-SE	2326	Terrestrial	24911460	871901	5%
AS-KAZ	AS-RUS-MV	2409	Terrestrial	25800390	903014	5%
AF-LBY	AF-NER	2429	Terrestrial	26014590	910511	5%
AS-CHN-TI	AS-PAK	2437	Terrestrial	26100270	913509	5%
AS-CHN-HE	AS-CHN-XI	2447	Terrestrial	26207370	917258	5%
SA-CHL	SA-PER	2467	Terrestrial	26421570	924755	5%
NA-MEX	NA-USA-CA	2506	Terrestrial	26839260	939374	5%
AS-CHN-WM	AS-RUS-SI	2537	Terrestrial	27171270	950994	5%
AF-DZA	AF-NER	2587	Terrestrial	27706770	969737	5%
OC-AUS-NT	OC-AUS-SA	2622	Terrestrial	28081620	982857	5%
OC-AUS-NT	OC-AUS-WA	2658	Terrestrial	28467180	996351	5%
AF-COD	AF-TZA	2665	Terrestrial	28542150	998975	5%
AF-COG	AF-TZA	2669	Terrestrial	28584990	1000475	5%
AF-LBY	AF-SDN	2739	Terrestrial	29334690	1026714	6%
AF-DZA	AF-MRT	2788	Terrestrial	29859480	1045082	6%
AS-CHN-XI	AS-PAK	2813	Terrestrial	30127230	1054453	6%
OC-AUS-NT	OC-AUS-QL	2849	Terrestrial	30512790	1067948	6%
AF-DZA	AF-MLI	2899	Terrestrial	31048290	1086690	6%
AS-CHN-GX	AS-CHN-XI	3009	Terrestrial	32226390	1127924	6%
AS-KAZ	AS-RUS-CE	3099	Terrestrial	33190290	1161660	6%
AS-CHN-HJ	AS-RUS-SI	3204	Terrestrial	34314840	1201019	6%
AS-RUS-FE	AS-RUS-SI	3713	Terrestrial	39766230	1391818	7%
AS-IDN	OC-PNG	4459	Terrestrial	47755890	1671456	9%
EU-EST	EU-FIN	83	Subsea	1777860	62225	0%
EU-BEL	EU-GBR	319	Subsea	6832980	239154	1%
EU-FRA	EU-GBR	341	Subsea	7304220	255648	1%

EU-GBR	EU-NLD	358	Subsea	7668360	268393	1%
EU-CYP	AS-ISR	367	Subsea	7861140	275140	1%
EU-DNK	EU-NOR	483	Subsea	10345860	362105	1%
AF-EGY	AS-JOR	494	Subsea	10581480	370352	1%
EU-DNK	EU-SWE	525	Subsea	11245500	393593	1%
OC-AUS-TA	OC-AUS-VI	593	Subsea	12702060	444572	1%
EU-ITA	AF-TUN	600	Subsea	12852000	449820	1%
EU-CYP	AF-EGY	602	Subsea	12894840	451319	1%
EU-DNK	EU-NLD	621	Subsea	13301820	465564	1%
EU-LTU	EU-SWE	678	Subsea	14522760	508297	1%
AS-IND-SO	AS-LKA	716	Subsea	15336720	536785	1%
EU-FRA	EU-IRL	777	Subsea	16643340	582517	2%
EU-POL	EU-SWE	810	Subsea	17350200	607257	2%
EU-DEU	EU-SWE	813	Subsea	17414460	609506	2%
EU-ESP	AF-MAR	833	Subsea	17842860	624500	2%
EU-DEU	EU-NOR	838	Subsea	17949960	628249	2%
AS-IDN	AS-SGP	894	Subsea	19149480	670232	2%
EU-NLD	EU-NOR	915	Subsea	19599300	685976	2%
EU-CYP	EU-GRC	915	Subsea	19599300	685976	2%
EU-DNK	EU-GBR	955	Subsea	20456100	715964	2%
EU-GRC	EU-ITA	1052	Subsea	22533840	788684	2%
EU-GBR	EU-NOR	1154	Subsea	24718680	865154	2%
EU-GBR	EU-ISL	1891	Subsea	40505220	1417683	4%
AS-MYS	AS-PHL	2467	Subsea	52843140	1849510	5%
AS-IDN	AS-PHL	2788	Subsea	59718960	2090164	6%
AS-ARE	AS-IRN	1218	Subsea	26089560	913135	2%
OC-AUS-QL	OC-PNG	2092	Subsea	44810640	1568372	4%
OC-AUS-WA	AS-IDN	3016	Subsea	64602720	2261095	6%
OC-AUS-WA	AS-TLS	2789	Subsea	59740380	2090913	6%
NA-CAN-NL	NA-GRL	1505	Subsea	32237100	1128299	3%
AS-CHN-FU	AS-TWN	358	Subsea	7668360	268393	1%
AS-CHN-SD	AS-KOR	616	Subsea	13194720	461815	1%
AS-CHN-SD	AS-PRK	578	Subsea	12380760	433327	1%
EU-CYP	AS-LBN	243	Subsea	5205060	182177	1%
EU-CYP	AS-SYR	327	Subsea	7004340	245152	1%
EU-CYP	AS-TUR	762	Subsea	16322040	571271	2%
AF-DJI	AS-YEM	433	Subsea	9274860	324620	1%
AF-DZA	EU-ESP	711	Subsea	15229620	533037	1%
AF-DZA	EU-FRA	1347	Subsea	28852740	1009846	3%
AF-DZA	EU-ITA	991	Subsea	21227220	742953	2%

AF-EGY	AS-SAU	1645	Subsea	35235900	1233257	3%
AF-ERI	AS-SAU	1319	Subsea	28252980	988854	3%
AF-ERI	AS-YEM	565	Subsea	12102300	423581	1%
EU-GRC	AF-LBY	1110	Subsea	23776200	832167	2%
NA-GRL	EU-ISL	1249	Subsea	26753580	936375	3%
AS-JPN-CE	AS-KOR	821	Subsea	17585820	615504	2%
AS-JPN-HO	AS-RUS-FE	765	Subsea	16386300	573521	2%
AS-JPN-KY	AS-KOR	539	Subsea	11545380	404088	1%
AF-LBY	EU-MLT	356	Subsea	7625520	266893	1%
AF-MAR	EU-PRT	586	Subsea	12552120	439324	1%
EU-MLT	AF-TUN	401	Subsea	8589420	300630	1%
AS-IND-WE	AS-OMN	1562	Subsea	33458040	1171031	3%
AS-IRN	AS-OMN	1508	Subsea	32301360	1130548	3%
AS-OMN	AS-PAK	863	Subsea	18485460	646991	2%
AS-SAU	AF-SDN	1793	Subsea	38406060	1344212	4%
AF-SOM	AS-YEM	1483	Subsea	31765860	1111805	3%

TABLE B.0.4 HYDROGEN PIPELINE TECHNOECONOMIC PARAMETERS

Ammonia shipping is also modelled simply in linearized form in line with the methodology outlined in [129], similar to [104]. The linearizing equation is given below (B.1). Ship capital expenditure is adapted from [7] while a crewing and annual maintenance cost is assumed at 2.5% of the capital expenditure as estimated in [96]. The economic lifetime of a hydrogen carrier is assumed to be 30 years. Carrier capacity and fuel consumption are assumed at 323750 MWh (the approximate energetic equivalent 60,000 tonnes of ammonia) and 1% of cargo per 5000 km respectively in line with [96]. The resulting ‘losses’ and de-rated continuous MW capacity per ship are provided in table B.5 below. The routes are selected based on the GIS-based study in [104].

$$Capacity_{cont.}(MW) = \frac{Ship\ Speed\ (km/h) \times Cargo\ (MWh)}{Route\ Distance\ (km)} \tag{B.1}$$

From	To	KM distance	Losses	Continuous Capacity (MW Per Ship)
EU-ITA	OC-NZL	19560	4%	575
EU-ITA	AS-IDN	15185	3%	741
EU-ITA	SA-BRA-SE	11028	2%	1020

EU-ITA	AS-VNM	14277	3%	788
EU-ITA	AF-AGO	10014	2%	1123
EU-ITA	AF-TZA	8762	2%	1284
EU-ITA	SA-PER	13796	3%	815
EU-ITA	OC-AUS-SW	17844	4%	630
EU-ITA	NA-TTO	9543	2%	1179
EU-ITA	EU-SWE	7401	1%	1520
EU-ITA	EU-NLD	5689	1%	1977
EU-ITA	AS-TUR	2510	1%	4483
EU-ITA	AS-CHN-SH	15901	3%	707
EU-ITA	SA-ARG	13456	3%	836
EU-ITA	AF-NGA	8831	2%	1274
EU-ITA	AF-EGY	2597	1%	4333
EU-ITA	AS-BGD	11197	2%	1005
EU-ITA	EU-ESP	2647	1%	4251
EU-ITA	AF-SEN	5889	1%	1910
EU-ITA	AS-JPN-TO	17310	3%	650
EU-ITA	OC-AUS-WA	13958	3%	806
EU-ITA	NA-USA-SV	9496	2%	1185
EU-ITA	AF-ZAF	12492	2%	901
EU-ITA	NA-USA-CA	17412	3%	646
EU-ITA	NA-USA-SA	11488	2%	979
EU-ITA	AS-QAT	8158	2%	1379
EU-ITA	EU-PRT	3618	1%	3110
EU-ITA	AS-SGP	11799	2%	953
EU-ITA	NA-MEX	11930	2%	943
EU-ITA	NA-NIC	12543	3%	897
EU-ITA	NA-DOM	9720	2%	1157
EU-ITA	SA-CHL	16618	3%	677
EU-ITA	AF-DZA	1980	0%	5681
EU-ITA	EU-GBR	5231	1%	2151
EU-ITA	AS-IND-WE	8073	2%	1394
EU-ITA	NA-USA-HA	19659	4%	572
OC-NZL	AS-IDN	6736	1%	1670
OC-NZL	SA-BRA-SE	13022	3%	864
OC-NZL	AS-VNM	10775	2%	1044
OC-NZL	AF-AGO	16298	3%	690
OC-NZL	AF-TZA	13639	3%	825
OC-NZL	SA-PER	11329	2%	993
OC-NZL	OC-AUS-SW	2261	0%	4976
OC-NZL	NA-TTO	14556	3%	773
OC-NZL	EU-SWE	22740	5%	495
OC-NZL	EU-NLD	21283	4%	529
OC-NZL	AS-TUR	17910	4%	628

OC-NZL	AS-CHN-SH	10163	2%	1107
OC-NZL	SA-ARG	10554	2%	1066
OC-NZL	AF-NGA	17653	4%	637
OC-NZL	AF-EGY	16964	3%	663
OC-NZL	AS-BGD	12137	2%	927
OC-NZL	EU-ESP	20245	4%	556
OC-NZL	AF-SEN	18149	4%	620
OC-NZL	AS-JPN-TO	9484	2%	1186
OC-NZL	OC-AUS-WA	6866	1%	1639
OC-NZL	NA-USA-SV	15824	3%	711
OC-NZL	AF-ZAF	12912	3%	871
OC-NZL	NA-USA-CA	11187	2%	1006
OC-NZL	NA-USA-SA	14891	3%	756
OC-NZL	AS-QAT	15220	3%	739
OC-NZL	EU-PRT	20166	4%	558
OC-NZL	AS-SGP	9388	2%	1198
OC-NZL	NA-MEX	14910	3%	755
OC-NZL	NA-NIC	11820	2%	952
OC-NZL	NA-DOM	13819	3%	814
OC-NZL	SA-CHL	10145	2%	1109
OC-NZL	AF-DZA	19546	4%	576
OC-NZL	EU-GBR	20728	4%	543
OC-NZL	AS-IND-WE	13240	3%	850
OC-NZL	NA-USA-HA	8000	2%	1406
AS-IDN	SA-BRA-SE	18443	4%	610
AS-IDN	AS-VNM	4039	1%	2785
AS-IDN	AF-AGO	15757	3%	714
AS-IDN	AF-TZA	10325	2%	1090
AS-IDN	SA-PER	17605	4%	639
AS-IDN	OC-AUS-SW	4974	1%	2262
AS-IDN	NA-TTO	19336	4%	582
AS-IDN	EU-SWE	20607	4%	546
AS-IDN	EU-NLD	18895	4%	595
AS-IDN	AS-TUR	13535	3%	831
AS-IDN	AS-CHN-SH	3741	1%	3008
AS-IDN	SA-ARG	17290	3%	651
AS-IDN	AF-NGA	17112	3%	657
AS-IDN	AF-EGY	12588	3%	894
AS-IDN	AS-BGD	6156	1%	1827
AS-IDN	EU-ESP	15870	3%	709
AS-IDN	AF-SEN	19094	4%	589
AS-IDN	AS-JPN-TO	4146	1%	2714
AS-IDN	OC-AUS-WA	3200	1%	3516
AS-IDN	NA-USA-SV	20605	4%	546

AS-IDN	AF-ZAF	12371	2%	909
AS-IDN	NA-USA-CA	11698	2%	962
AS-IDN	NA-USA-SA	19671	4%	572
AS-IDN	AS-QAT	10211	2%	1102
AS-IDN	EU-PRT	16823	3%	669
AS-IDN	AS-SGP	3408	1%	3301
AS-IDN	NA-MEX	19691	4%	571
AS-IDN	NA-NIC	15936	3%	706
AS-IDN	NA-DOM	18599	4%	605
AS-IDN	SA-CHL	16881	3%	666
AS-IDN	AF-DZA	15171	3%	742
AS-IDN	EU-GBR	18436	4%	610
AS-IDN	AS-IND-WE	8088	2%	1391
AS-IDN	NA-USA-HA	8693	2%	1294
SA-BRA-SE	AS-VNM	18665	4%	603
SA-BRA-SE	AF-AGO	6880	1%	1635
SA-BRA-SE	AF-TZA	10198	2%	1103
SA-BRA-SE	SA-PER	9312	2%	1208
SA-BRA-SE	OC-AUS-SW	14979	3%	751
SA-BRA-SE	NA-TTO	6044	1%	1861
SA-BRA-SE	EU-SWE	11498	2%	978
SA-BRA-SE	EU-NLD	9786	2%	1150
SA-BRA-SE	AS-TUR	11691	2%	962
SA-BRA-SE	AS-CHN-SH	20284	4%	555
SA-BRA-SE	SA-ARG	2583	1%	4355
SA-BRA-SE	AF-NGA	6442	1%	1746
SA-BRA-SE	AF-EGY	11646	2%	966
SA-BRA-SE	AS-BGD	16303	3%	690
SA-BRA-SE	EU-ESP	8639	2%	1302
SA-BRA-SE	AF-SEN	5417	1%	2077
SA-BRA-SE	AS-JPN-TO	21622	4%	520
SA-BRA-SE	OC-AUS-WA	15347	3%	733
SA-BRA-SE	NA-USA-SV	9033	2%	1245
SA-BRA-SE	AF-ZAF	6072	1%	1853
SA-BRA-SE	NA-USA-CA	14375	3%	783
SA-BRA-SE	NA-USA-SA	9621	2%	1169
SA-BRA-SE	AS-QAT	15295	3%	736
SA-BRA-SE	EU-PRT	7920	2%	1420
SA-BRA-SE	AS-SGP	16465	3%	683
SA-BRA-SE	NA-MEX	9852	2%	1142
SA-BRA-SE	NA-NIC	9506	2%	1183
SA-BRA-SE	NA-DOM	7137	1%	1576
SA-BRA-SE	SA-CHL	6435	1%	1748
SA-BRA-SE	AF-DZA	9063	2%	1241

SA-BRA-SE	EU-GBR	9326	2%	1206
SA-BRA-SE	AS-IND-WE	14708	3%	765
SA-BRA-SE	NA-USA-HA	16146	3%	697
AS-VNM	AF-AGO	15979	3%	704
AS-VNM	AF-TZA	10473	2%	1074
AS-VNM	SA-PER	19426	4%	579
AS-VNM	OC-AUS-SW	9014	2%	1248
AS-VNM	NA-TTO	20434	4%	551
AS-VNM	EU-SWE	19699	4%	571
AS-VNM	EU-NLD	17987	4%	625
AS-VNM	AS-TUR	12627	3%	891
AS-VNM	AS-CHN-SH	2320	0%	4849
AS-VNM	SA-ARG	19118	4%	588
AS-VNM	AF-NGA	17334	3%	649
AS-VNM	AF-EGY	11681	2%	963
AS-VNM	AS-BGD	5226	1%	2153
AS-VNM	EU-ESP	14962	3%	752
AS-VNM	AF-SEN	18186	4%	619
AS-VNM	AS-JPN-TO	3750	1%	3000
AS-VNM	OC-AUS-WA	5620	1%	2002
AS-VNM	NA-USA-SV	21702	4%	518
AS-VNM	AF-ZAF	12593	3%	893
AS-VNM	NA-USA-CA	12270	2%	917
AS-VNM	NA-USA-SA	20769	4%	542
AS-VNM	AS-QAT	9281	2%	1212
AS-VNM	EU-PRT	15916	3%	707
AS-VNM	AS-SGP	2478	0%	4540
AS-VNM	NA-MEX	20788	4%	541
AS-VNM	NA-NIC	16906	3%	665
AS-VNM	NA-DOM	19697	4%	571
AS-VNM	SA-CHL	20807	4%	541
AS-VNM	AF-DZA	14263	3%	789
AS-VNM	EU-GBR	17529	4%	642
AS-VNM	AS-IND-WE	7158	1%	1572
AS-VNM	NA-USA-HA	10275	2%	1095
AF-AGO	AF-TZA	7511	2%	1498
AF-AGO	SA-PER	13343	3%	843
AF-AGO	OC-AUS-SW	15261	3%	737
AF-AGO	NA-TTO	8628	2%	1304
AF-AGO	EU-SWE	10593	2%	1062
AF-AGO	EU-NLD	8881	2%	1267
AF-AGO	AS-TUR	10676	2%	1054
AF-AGO	AS-CHN-SH	17598	4%	639
AF-AGO	SA-ARG	8583	2%	1311

AF-AGO	AF-NGA	1652	0%	6810
AF-AGO	AF-EGY	10631	2%	1058
AF-AGO	AS-BGD	13616	3%	826
AF-AGO	EU-ESP	7625	2%	1476
AF-AGO	AF-SEN	4125	1%	2727
AF-AGO	AS-JPN-TO	18936	4%	594
AF-AGO	OC-AUS-WA	12689	3%	887
AF-AGO	NA-USA-SV	10684	2%	1053
AF-AGO	AF-ZAF	3386	1%	3323
AF-AGO	NA-USA-CA	16958	3%	663
AF-AGO	NA-USA-SA	11900	2%	945
AF-AGO	AS-QAT	12609	3%	892
AF-AGO	EU-PRT	6956	1%	1617
AF-AGO	AS-SGP	13779	3%	816
AF-AGO	NA-MEX	12334	2%	912
AF-AGO	NA-NIC	12089	2%	931
AF-AGO	NA-DOM	9591	2%	1173
AF-AGO	SA-CHL	11680	2%	963
AF-AGO	AF-DZA	8048	2%	1398
AF-AGO	EU-GBR	8421	2%	1336
AF-AGO	AS-IND-WE	12022	2%	936
AF-AGO	NA-USA-HA	19206	4%	586
AF-TZA	SA-PER	16508	3%	681
AF-TZA	OC-AUS-SW	12071	2%	932
AF-TZA	NA-TTO	14031	3%	802
AF-TZA	EU-SWE	14183	3%	793
AF-TZA	EU-NLD	12472	2%	902
AF-TZA	AS-TUR	7112	1%	1582
AF-TZA	AS-CHN-SH	12092	2%	930
AF-TZA	SA-ARG	11097	2%	1014
AF-TZA	AF-NGA	8867	2%	1269
AF-TZA	AF-EGY	6165	1%	1825
AF-TZA	AS-BGD	7398	1%	1521
AF-TZA	EU-ESP	9447	2%	1191
AF-TZA	AF-SEN	10900	2%	1032
AF-TZA	AS-JPN-TO	13430	3%	838
AF-TZA	OC-AUS-WA	8499	2%	1324
AF-TZA	NA-USA-SV	16278	3%	691
AF-TZA	AF-ZAF	4126	1%	2727
AF-TZA	NA-USA-CA	21627	4%	520
AF-TZA	NA-USA-SA	17608	4%	639
AF-TZA	AS-QAT	5494	1%	2048
AF-TZA	EU-PRT	10400	2%	1082
AF-TZA	AS-SGP	8001	2%	1406

AF-TZA	NA-MEX	17838	4%	631
AF-TZA	NA-NIC	17493	3%	643
AF-TZA	NA-DOM	15124	3%	744
AF-TZA	SA-CHL	13631	3%	825
AF-TZA	AF-DZA	8748	2%	1286
AF-TZA	EU-GBR	12013	2%	936
AF-TZA	AS-IND-WE	5167	1%	2177
AF-TZA	NA-USA-HA	19018	4%	592
SA-PER	OC-AUS-SW	13434	3%	837
SA-PER	NA-TTO	4813	1%	2337
SA-PER	EU-SWE	12998	3%	866
SA-PER	EU-NLD	11541	2%	975
SA-PER	AS-TUR	14458	3%	778
SA-PER	AS-CHN-SH	17525	4%	642
SA-PER	SA-ARG	6844	1%	1644
SA-PER	AF-NGA	12167	2%	925
SA-PER	AF-EGY	14413	3%	781
SA-PER	AS-BGD	22530	5%	499
SA-PER	EU-ESP	11407	2%	986
SA-PER	AF-SEN	9690	2%	1161
SA-PER	AS-JPN-TO	15676	3%	718
SA-PER	OC-AUS-WA	17702	4%	636
SA-PER	NA-USA-SV	6081	1%	1850
SA-PER	AF-ZAF	12382	2%	909
SA-PER	NA-USA-CA	7423	1%	1515
SA-PER	NA-USA-SA	5148	1%	2185
SA-PER	AS-QAT	19975	4%	563
SA-PER	EU-PRT	10424	2%	1079
SA-PER	AS-SGP	20277	4%	555
SA-PER	NA-MEX	5168	1%	2177
SA-PER	NA-NIC	3173	1%	3545
SA-PER	NA-DOM	4076	1%	2760
SA-PER	SA-CHL	2876	1%	3911
SA-PER	AF-DZA	11831	2%	951
SA-PER	EU-GBR	10986	2%	1024
SA-PER	AS-IND-WE	19889	4%	566
SA-PER	NA-USA-HA	9550	2%	1178
OC-AUS-SW	NA-TTO	16703	3%	674
OC-AUS-SW	EU-SWE	23266	5%	484
OC-AUS-SW	EU-NLD	21554	4%	522
OC-AUS-SW	AS-TUR	16194	3%	695
OC-AUS-SW	AS-CHN-SH	8474	2%	1328
OC-AUS-SW	SA-ARG	12511	3%	899
OC-AUS-SW	AF-NGA	16616	3%	677

OC-AUS-SW	AF-EGY	15247	3%	738
OC-AUS-SW	AS-BGD	10375	2%	1084
OC-AUS-SW	EU-ESP	18529	4%	607
OC-AUS-SW	AF-SEN	18649	4%	603
OC-AUS-SW	AS-JPN-TO	7984	2%	1409
OC-AUS-SW	OC-AUS-WA	5150	1%	2185
OC-AUS-SW	NA-USA-SV	17971	4%	626
OC-AUS-SW	AF-ZAF	11875	2%	947
OC-AUS-SW	NA-USA-CA	12166	2%	925
OC-AUS-SW	NA-USA-SA	17038	3%	660
OC-AUS-SW	AS-QAT	13504	3%	833
OC-AUS-SW	EU-PRT	19482	4%	577
OC-AUS-SW	AS-SGP	7627	2%	1475
OC-AUS-SW	NA-MEX	17057	3%	660
OC-AUS-SW	NA-NIC	13774	3%	817
OC-AUS-SW	NA-DOM	15966	3%	705
OC-AUS-SW	SA-CHL	12102	2%	930
OC-AUS-SW	AF-DZA	17830	4%	631
OC-AUS-SW	EU-GBR	21095	4%	533
OC-AUS-SW	AS-IND-WE	11524	2%	976
OC-AUS-SW	NA-USA-HA	8924	2%	1261
NA-TTO	EU-SWE	9296	2%	1210
NA-TTO	EU-NLD	7584	2%	1483
NA-TTO	AS-TUR	10206	2%	1102
NA-TTO	AS-CHN-SH	18533	4%	607
NA-TTO	SA-ARG	8472	2%	1328
NA-TTO	AF-NGA	7452	1%	1510
NA-TTO	AF-EGY	10161	2%	1107
NA-TTO	AS-BGD	18761	4%	600
NA-TTO	EU-ESP	7154	1%	1573
NA-TTO	AF-SEN	5020	1%	2241
NA-TTO	AS-JPN-TO	16684	3%	674
NA-TTO	OC-AUS-WA	19209	4%	586
NA-TTO	NA-USA-SV	3619	1%	3109
NA-TTO	AF-ZAF	9906	2%	1136
NA-TTO	NA-USA-CA	8429	2%	1335
NA-TTO	NA-USA-SA	3878	1%	2901
NA-TTO	AS-QAT	15722	3%	716
NA-TTO	EU-PRT	6207	1%	1812
NA-TTO	AS-SGP	19363	4%	581
NA-TTO	NA-MEX	3943	1%	2853
NA-TTO	NA-NIC	3560	1%	3161
NA-TTO	NA-DOM	1394	0%	8071
NA-TTO	SA-CHL	7635	2%	1473

NA-TTO	AF-DZA	7578	2%	1485
NA-TTO	EU-GBR	7104	1%	1584
NA-TTO	AS-IND-WE	15637	3%	719
NA-TTO	NA-USA-HA	10676	2%	1054
EU-SWE	EU-NLD	1790	0%	6284
EU-SWE	AS-TUR	8063	2%	1395
EU-SWE	AS-CHN-SH	21323	4%	528
EU-SWE	SA-ARG	13925	3%	808
EU-SWE	AF-NGA	9410	2%	1196
EU-SWE	AF-EGY	8018	2%	1403
EU-SWE	AS-BGD	16619	3%	677
EU-SWE	EU-ESP	5012	1%	2245
EU-SWE	AF-SEN	6467	1%	1740
EU-SWE	AS-JPN-TO	22732	5%	495
EU-SWE	OC-AUS-WA	19380	4%	581
EU-SWE	NA-USA-SV	7699	2%	1461
EU-SWE	AF-ZAF	13241	3%	850
EU-SWE	NA-USA-CA	16613	3%	677
EU-SWE	NA-USA-SA	10011	2%	1124
EU-SWE	AS-QAT	13580	3%	828
EU-SWE	EU-PRT	3810	1%	2953
EU-SWE	AS-SGP	17221	3%	653
EU-SWE	NA-MEX	10452	2%	1076
EU-SWE	NA-NIC	11744	2%	958
EU-SWE	NA-DOM	8921	2%	1261
EU-SWE	SA-CHL	15819	3%	711
EU-SWE	AF-DZA	5436	1%	2070
EU-SWE	EU-GBR	2699	1%	4168
EU-SWE	AS-IND-WE	13494	3%	834
EU-SWE	NA-USA-HA	18860	4%	596
EU-NLD	AS-TUR	6352	1%	1771
EU-NLD	AS-CHN-SH	19611	4%	574
EU-NLD	SA-ARG	12214	2%	921
EU-NLD	AF-NGA	7698	2%	1461
EU-NLD	AF-EGY	6307	1%	1784
EU-NLD	AS-BGD	14907	3%	755
EU-NLD	EU-ESP	3300	1%	3409
EU-NLD	AF-SEN	4756	1%	2366
EU-NLD	AS-JPN-TO	21020	4%	535
EU-NLD	OC-AUS-WA	17668	4%	637
EU-NLD	NA-USA-SV	6608	1%	1703
EU-NLD	AF-ZAF	11530	2%	976
EU-NLD	NA-USA-CA	15157	3%	742
EU-NLD	NA-USA-SA	8841	2%	1272

EU-NLD	AS-QAT	11868	2%	948
EU-NLD	EU-PRT	2098	0%	5361
EU-NLD	AS-SGP	15509	3%	725
EU-NLD	NA-MEX	9283	2%	1212
EU-NLD	NA-NIC	10287	2%	1094
EU-NLD	NA-DOM	7465	1%	1507
EU-NLD	SA-CHL	14363	3%	783
EU-NLD	AF-DZA	3724	1%	3021
EU-NLD	EU-GBR	987	0%	11395
EU-NLD	AS-IND-WE	11783	2%	955
EU-NLD	NA-USA-HA	17404	3%	646
AS-TUR	AS-CHN-SH	14251	3%	789
AS-TUR	SA-ARG	14118	3%	797
AS-TUR	AF-NGA	9493	2%	1185
AS-TUR	AF-EGY	946	0%	11887
AS-TUR	AS-BGD	9547	2%	1178
AS-TUR	EU-ESP	3326	1%	3382
AS-TUR	AF-SEN	6551	1%	1717
AS-TUR	AS-JPN-TO	15660	3%	718
AS-TUR	OC-AUS-WA	12308	2%	914
AS-TUR	NA-USA-SV	10158	2%	1108
AS-TUR	AF-ZAF	10841	2%	1038
AS-TUR	NA-USA-CA	18074	4%	622
AS-TUR	NA-USA-SA	12150	2%	926
AS-TUR	AS-QAT	6508	1%	1729
AS-TUR	EU-PRT	4280	1%	2629
AS-TUR	AS-SGP	10149	2%	1108
AS-TUR	NA-MEX	12592	3%	893
AS-TUR	NA-NIC	13205	3%	852
AS-TUR	NA-DOM	10382	2%	1084
AS-TUR	SA-CHL	17280	3%	651
AS-TUR	AF-DZA	2628	1%	4281
AS-TUR	EU-GBR	5893	1%	1909
AS-TUR	AS-IND-WE	6422	1%	1752
AS-TUR	NA-USA-HA	20321	4%	554
AS-CHN-SH	SA-ARG	20213	4%	557
AS-CHN-SH	AF-NGA	18953	4%	594
AS-CHN-SH	AF-EGY	13305	3%	846
AS-CHN-SH	AS-BGD	6850	1%	1642
AS-CHN-SH	EU-ESP	16586	3%	678
AS-CHN-SH	AF-SEN	19810	4%	568
AS-CHN-SH	AS-JPN-TO	1849	0%	6085
AS-CHN-SH	OC-AUS-WA	6296	1%	1787
AS-CHN-SH	NA-USA-SV	19801	4%	568

AS-CHN-SH	AF-ZAF	14212	3%	792
AS-CHN-SH	NA-USA-CA	10369	2%	1085
AS-CHN-SH	NA-USA-SA	18868	4%	596
AS-CHN-SH	AS-QAT	10905	2%	1032
AS-CHN-SH	EU-PRT	17540	4%	641
AS-CHN-SH	AS-SGP	4102	1%	2743
AS-CHN-SH	NA-MEX	18887	4%	596
AS-CHN-SH	NA-NIC	15005	3%	750
AS-CHN-SH	NA-DOM	17796	4%	632
AS-CHN-SH	SA-CHL	19599	4%	574
AS-CHN-SH	AF-DZA	15887	3%	708
AS-CHN-SH	EU-GBR	19153	4%	587
AS-CHN-SH	AS-IND-WE	8782	2%	1281
AS-CHN-SH	NA-USA-HA	8411	2%	1338
SA-ARG	AF-NGA	8684	2%	1296
SA-ARG	AF-EGY	14073	3%	799
SA-ARG	AS-BGD	17202	3%	654
SA-ARG	EU-ESP	11067	2%	1017
SA-ARG	AF-SEN	7845	2%	1434
SA-ARG	AS-JPN-TO	19285	4%	583
SA-ARG	OC-AUS-WA	15276	3%	736
SA-ARG	NA-USA-SV	11460	2%	982
SA-ARG	AF-ZAF	6972	1%	1614
SA-ARG	NA-USA-CA	13285	3%	847
SA-ARG	NA-USA-SA	11804	2%	953
SA-ARG	AS-QAT	16195	3%	695
SA-ARG	EU-PRT	10347	2%	1087
SA-ARG	AS-SGP	16918	3%	665
SA-ARG	NA-MEX	11823	2%	952
SA-ARG	NA-NIC	9751	2%	1154
SA-ARG	NA-DOM	9565	2%	1176
SA-ARG	SA-CHL	3968	1%	2835
SA-ARG	AF-DZA	11490	2%	979
SA-ARG	EU-GBR	11753	2%	957
SA-ARG	AS-IND-WE	15608	3%	721
SA-ARG	NA-USA-HA	13678	3%	822
AF-NGA	AF-EGY	9449	2%	1191
AF-NGA	AS-BGD	14972	3%	751
AF-NGA	EU-ESP	6442	1%	1746
AF-NGA	AF-SEN	2943	1%	3823
AF-NGA	AS-JPN-TO	20291	4%	554
AF-NGA	OC-AUS-WA	14044	3%	801
AF-NGA	NA-USA-SV	9501	2%	1184
AF-NGA	AF-ZAF	4741	1%	2373

AF-NGA	NA-USA-CA	15783	3%	713
AF-NGA	NA-USA-SA	10717	2%	1050
AF-NGA	AS-QAT	13964	3%	806
AF-NGA	EU-PRT	5774	1%	1949
AF-NGA	AS-SGP	15134	3%	743
AF-NGA	NA-MEX	11152	2%	1009
AF-NGA	NA-NIC	10914	2%	1031
AF-NGA	NA-DOM	8408	2%	1338
AF-NGA	SA-CHL	12103	2%	930
AF-NGA	AF-DZA	6866	1%	1639
AF-NGA	EU-GBR	7238	1%	1554
AF-NGA	AS-IND-WE	13377	3%	841
AF-NGA	NA-USA-HA	18030	4%	624
AF-EGY	AS-BGD	8600	2%	1308
AF-EGY	EU-ESP	3281	1%	3428
AF-EGY	AF-SEN	6506	1%	1729
AF-EGY	AS-JPN-TO	14713	3%	765
AF-EGY	OC-AUS-WA	11361	2%	990
AF-EGY	NA-USA-SV	10113	2%	1112
AF-EGY	AF-ZAF	9895	2%	1137
AF-EGY	NA-USA-CA	18029	4%	624
AF-EGY	NA-USA-SA	12105	2%	929
AF-EGY	AS-QAT	5562	1%	2023
AF-EGY	EU-PRT	4235	1%	2656
AF-EGY	AS-SGP	9203	2%	1222
AF-EGY	NA-MEX	12547	3%	897
AF-EGY	NA-NIC	13160	3%	855
AF-EGY	NA-DOM	10337	2%	1088
AF-EGY	SA-CHL	17235	3%	653
AF-EGY	AF-DZA	2583	1%	4356
AF-EGY	EU-GBR	5848	1%	1924
AF-EGY	AS-IND-WE	5476	1%	2054
AF-EGY	NA-USA-HA	20276	4%	555
AS-BGD	EU-ESP	11882	2%	947
AS-BGD	AF-SEN	15106	3%	745
AS-BGD	AS-JPN-TO	8259	2%	1362
AS-BGD	OC-AUS-WA	6266	1%	1795
AS-BGD	NA-USA-SV	18713	4%	601
AS-BGD	AF-ZAF	10231	2%	1100
AS-BGD	NA-USA-CA	16613	3%	677
AS-BGD	NA-USA-SA	20706	4%	543
AS-BGD	AS-QAT	6201	1%	1814
AS-BGD	EU-PRT	12835	3%	876
AS-BGD	AS-SGP	2748	1%	4094

AS-BGD	NA-MEX	21147	4%	532
AS-BGD	NA-NIC	21248	4%	529
AS-BGD	NA-DOM	18937	4%	594
AS-BGD	SA-CHL	19654	4%	572
AS-BGD	AF-DZA	11183	2%	1006
AS-BGD	EU-GBR	14448	3%	779
AS-BGD	AS-IND-WE	4077	1%	2759
AS-BGD	NA-USA-HA	14125	3%	796
EU-ESP	AF-SEN	3499	1%	3215
EU-ESP	AS-JPN-TO	17995	4%	625
EU-ESP	OC-AUS-WA	14643	3%	768
EU-ESP	NA-USA-SV	7106	1%	1583
EU-ESP	AF-ZAF	10273	2%	1095
EU-ESP	NA-USA-CA	15023	3%	749
EU-ESP	NA-USA-SA	9099	2%	1236
EU-ESP	AS-QAT	8843	2%	1272
EU-ESP	EU-PRT	1229	0%	9158
EU-ESP	AS-SGP	12484	2%	901
EU-ESP	NA-MEX	9540	2%	1179
EU-ESP	NA-NIC	10153	2%	1108
EU-ESP	NA-DOM	7331	1%	1535
EU-ESP	SA-CHL	14229	3%	791
EU-ESP	AF-DZA	734	0%	15330
EU-ESP	EU-GBR	2841	1%	3959
EU-ESP	AS-IND-WE	8757	2%	1285
EU-ESP	NA-USA-HA	17270	3%	651
AF-SEN	AS-JPN-TO	21219	4%	530
AF-SEN	OC-AUS-WA	16077	3%	700
AF-SEN	NA-USA-SV	6766	1%	1663
AF-SEN	AF-ZAF	6774	1%	1661
AF-SEN	NA-USA-CA	13306	3%	845
AF-SEN	NA-USA-SA	7982	2%	1409
AF-SEN	AS-QAT	12068	2%	932
AF-SEN	EU-PRT	2831	1%	3974
AF-SEN	AS-SGP	15708	3%	716
AF-SEN	NA-MEX	8416	2%	1337
AF-SEN	NA-NIC	8437	2%	1333
AF-SEN	NA-DOM	5673	1%	1983
AF-SEN	SA-CHL	11563	2%	973
AF-SEN	AF-DZA	3923	1%	2868
AF-SEN	EU-GBR	4296	1%	2619
AF-SEN	AS-IND-WE	11982	2%	939
AF-SEN	NA-USA-HA	15553	3%	723
AS-JPN-TO	OC-AUS-WA	7262	1%	1549

AS-JPN-TO	NA-USA-SV	17952	4%	627
AS-JPN-TO	AF-ZAF	15550	3%	723
AS-JPN-TO	NA-USA-CA	8520	2%	1320
AS-JPN-TO	NA-USA-SA	17019	3%	661
AS-JPN-TO	AS-QAT	12314	2%	914
AS-JPN-TO	EU-PRT	18948	4%	594
AS-JPN-TO	AS-SGP	5511	1%	2041
AS-JPN-TO	NA-MEX	17038	3%	660
AS-JPN-TO	NA-NIC	13156	3%	855
AS-JPN-TO	NA-DOM	15947	3%	705
AS-JPN-TO	SA-CHL	18165	4%	619
AS-JPN-TO	AF-DZA	17296	3%	650
AS-JPN-TO	EU-GBR	20561	4%	547
AS-JPN-TO	AS-IND-WE	10190	2%	1104
AS-JPN-TO	NA-USA-HA	6813	1%	1651
OC-AUS-WA	NA-USA-SV	21474	4%	524
OC-AUS-WA	AF-ZAF	9303	2%	1209
OC-AUS-WA	NA-USA-CA	14898	3%	755
OC-AUS-WA	NA-USA-SA	21676	4%	519
OC-AUS-WA	AS-QAT	9097	2%	1237
OC-AUS-WA	EU-PRT	15596	3%	721
OC-AUS-WA	AS-SGP	3518	1%	3198
OC-AUS-WA	NA-MEX	21695	4%	519
OC-AUS-WA	NA-NIC	18686	4%	602
OC-AUS-WA	NA-DOM	20302	4%	554
OC-AUS-WA	SA-CHL	16370	3%	687
OC-AUS-WA	AF-DZA	13944	3%	807
OC-AUS-WA	EU-GBR	17209	3%	654
OC-AUS-WA	AS-IND-WE	6973	1%	1613
OC-AUS-WA	NA-USA-HA	11893	2%	946
NA-USA-SV	AF-ZAF	12805	3%	879
NA-USA-SV	NA-USA-CA	9697	2%	1160
NA-USA-SV	NA-USA-SA	2859	1%	3935
NA-USA-SV	AS-QAT	15675	3%	718
NA-USA-SV	EU-PRT	6005	1%	1873
NA-USA-SV	AS-SGP	19315	4%	582
NA-USA-SV	NA-MEX	3300	1%	3409
NA-USA-SV	NA-NIC	4828	1%	2330
NA-USA-SV	NA-DOM	2629	1%	4278
NA-USA-SV	SA-CHL	8903	2%	1264
NA-USA-SV	AF-DZA	7530	2%	1494
NA-USA-SV	EU-GBR	6032	1%	1865
NA-USA-SV	AS-IND-WE	15589	3%	722
NA-USA-SV	NA-USA-HA	11944	2%	942

AF-ZAF	NA-USA-CA	18236	4%	617
AF-ZAF	NA-USA-SA	13482	3%	834
AF-ZAF	AS-QAT	9223	2%	1220
AF-ZAF	EU-PRT	9605	2%	1171
AF-ZAF	AS-SGP	10393	2%	1082
AF-ZAF	NA-MEX	13713	3%	820
AF-ZAF	NA-NIC	13367	3%	842
AF-ZAF	NA-DOM	10998	2%	1023
AF-ZAF	SA-CHL	9506	2%	1184
AF-ZAF	AF-DZA	10697	2%	1052
AF-ZAF	EU-GBR	11070	2%	1016
AF-ZAF	AS-IND-WE	8636	2%	1303
AF-ZAF	NA-USA-HA	19216	4%	585
NA-USA-CA	NA-USA-SA	8764	2%	1284
NA-USA-CA	AS-QAT	20668	4%	544
NA-USA-CA	EU-PRT	14039	3%	801
NA-USA-CA	AS-SGP	13865	3%	811
NA-USA-CA	NA-MEX	8783	2%	1281
NA-USA-CA	NA-NIC	4901	1%	2295
NA-USA-CA	NA-DOM	7692	2%	1463
NA-USA-CA	SA-CHL	10169	2%	1106
NA-USA-CA	AF-DZA	15447	3%	728
NA-USA-CA	EU-GBR	14601	3%	770
NA-USA-CA	AS-IND-WE	18544	4%	607
NA-USA-CA	NA-USA-HA	3814	1%	2950
NA-USA-SA	AS-QAT	17667	4%	637
NA-USA-SA	EU-PRT	8058	2%	1396
NA-USA-SA	AS-SGP	21308	4%	528
NA-USA-SA	NA-MEX	1412	0%	7966
NA-USA-SA	NA-NIC	3895	1%	2889
NA-USA-SA	NA-DOM	2787	1%	4036
NA-USA-SA	SA-CHL	7970	2%	1412
NA-USA-SA	AF-DZA	9523	2%	1181
NA-USA-SA	EU-GBR	8286	2%	1358
NA-USA-SA	AS-IND-WE	17581	4%	640
NA-USA-SA	NA-USA-HA	11011	2%	1022
AS-QAT	EU-PRT	9797	2%	1148
AS-QAT	AS-SGP	6803	1%	1654
AS-QAT	NA-MEX	18109	4%	621
AS-QAT	NA-NIC	18722	4%	601
AS-QAT	NA-DOM	15899	3%	708
AS-QAT	SA-CHL	18729	4%	601
AS-QAT	AF-DZA	8144	2%	1381
AS-QAT	EU-GBR	11410	2%	986

AS-QAT	AS-IND-WE	2450	0%	4592
AS-QAT	NA-USA-HA	18180	4%	619
EU-PRT	AS-SGP	13438	3%	837
EU-PRT	NA-MEX	8500	2%	1324
EU-PRT	NA-NIC	9170	2%	1227
EU-PRT	NA-DOM	6347	1%	1772
EU-PRT	SA-CHL	13245	3%	849
EU-PRT	AF-DZA	1652	0%	6809
EU-PRT	EU-GBR	1640	0%	6861
EU-PRT	AS-IND-WE	9711	2%	1158
EU-PRT	NA-USA-HA	16286	3%	691
AS-SGP	NA-MEX	21749	4%	517
AS-SGP	NA-NIC	18500	4%	608
AS-SGP	NA-DOM	19540	4%	576
AS-SGP	SA-CHL	19265	4%	584
AS-SGP	AF-DZA	11785	2%	955
AS-SGP	EU-GBR	15050	3%	747
AS-SGP	AS-IND-WE	4680	1%	2404
AS-SGP	NA-USA-HA	11377	2%	989
NA-MEX	NA-NIC	3914	1%	2874
NA-MEX	NA-DOM	2829	1%	3977
NA-MEX	SA-CHL	7990	2%	1408
NA-MEX	AF-DZA	9964	2%	1129
NA-MEX	EU-GBR	8727	2%	1289
NA-MEX	AS-IND-WE	18023	4%	624
NA-MEX	NA-USA-HA	11031	2%	1020
NA-NIC	NA-DOM	2823	1%	3986
NA-NIC	SA-CHL	5995	1%	1877
NA-NIC	AF-DZA	10577	2%	1064
NA-NIC	EU-GBR	9732	2%	1156
NA-NIC	AS-IND-WE	18636	4%	604
NA-NIC	NA-USA-HA	7275	1%	1546
NA-DOM	SA-CHL	6898	1%	1631
NA-DOM	AF-DZA	7755	2%	1451
NA-DOM	EU-GBR	6909	1%	1628
NA-DOM	AS-IND-WE	15813	3%	711
NA-DOM	NA-USA-HA	9939	2%	1132
SA-CHL	AF-DZA	14653	3%	768
SA-CHL	EU-GBR	13807	3%	815
SA-CHL	AS-IND-WE	18142	4%	620
SA-CHL	NA-USA-HA	11442	2%	983
AF-DZA	EU-GBR	3265	1%	3445
AF-DZA	AS-IND-WE	8059	2%	1396
AF-DZA	NA-USA-HA	17694	4%	636

EU-GBR	AS-IND-WE	11324	2%	993
EU-GBR	NA-USA-HA	16848	3%	668
AS-IND-WE	NA-USA-HA	16056	3%	701

TABLE B.0.5 LINEARIZED SHIPPING ROUTE CANDIDATES